IFJ PAN

Report on Research Activities 2011-2013

The Henryk Niewodniczański Institute of Nuclear Physics
Polish Academy of Sciences, Kraków, Poland

Report on research activities 2011–2013

The Henryk Niewodniczański
Institute of Nuclear Physics
Polish Academy of Sciences

Radzikowskiego 152
31–342 Kraków, Poland
http://www.ifj.edu.pl

Phone: +48-12-6628200
Fax: +48-12-6628458
e-mail: dyrektor@ifj.edu.pl

Report on research activities 2011–2013

Edited by
M. Budzanowski, S. Drożdż, B. Fornal, J. Gręboszc,
S. Jadach, M. Jeżabek, E. Łokas, A. Maj, M. Massalska-Arodź,
P. Olko, Z. Sułek, M. Stodulski, J. Turnau, M. Waligórski,
B. Wosiek, U. Woźnicka, W. Zając

Language editing
M.Waligórski

Typesetting
A. Kendziak

Front artwork
J. Gręboszc

June 2014

CONTENTS

INTRODUCTION

The years 2011–2013 will go on record as a very important period in the history of the Henryk Niewodniczański Institute of Nuclear Physics, Polish Academy of Sciences (IFJ PAN). Over this period the fundamental discovery of the Higgs boson was made by ATLAS and CMS collaborations, in experiments performed at CERN's Large Hadron Collider (LHC). Several groups of scientists and technicians from our Institute have significantly contributed to the construction of the LHC machine and of the ATLAS detector. IFJ PAN physicists played a significant role in analyses which led to the historic discovery of this new boson and in providing evidence that all properties of this particle are consistent with predictions of the Standard Model of fundamental interactions. In particular, our scientists were responsible for the analysis of the $\tau^+\tau^-$ decay channel of the Higgs boson. These achievements in basic research were accompanied by successes of other IFJ PAN research teams working together with groups of particle, astroparticle and nuclear physicists at CERN, DESY, KEK and other world-leading research centres.

The Cyclotron Centre at Bronowice (CCB – Centrum Cyklotronowe Bronowice) is a major new project presently under construction at IFJ PAN, to be fully completed in 2015. The CCB is by now a modern nuclear physics research laboratory and will soon become a world-class proton radiotherapy centre, the first one in Poland and one of a few in Europe. In 2013 first experiments were performed at CCB. I am confident that over the coming years, research and proton radiotherapy at CCB will be successfully carried out, further strengthening the role of IFJ PAN as the leading scientific institution in Poland.

The role of IFJ PAN in international and domestic research activities was recently assessed by the Polish Ministry of Science and Higher Education. In 2013 our Institute was awarded the highest A+ rank in this evaluation and categorisation of Polish research institutions performed by the Ministry. The high status of the Polish particle physics community at CERN was also confirmed by the election of Professor Agnieszka Zalewska from IFJ PAN as President of the CERN Council in 2012. IFJ PAN is a member of the Marian Smoluchowski Consortium which has been granted the status of a leading national research centre, KNOW (Krajowy Naukowy Ośrodek Wiodący) over the years 2012–2017.

I invite the Reader of the IFJ PAN Report 2010–2013 to find more detailed information on the activities and accomplishments of our Staff and to share their enthusiasm without which our Institute would not have achieved its leading status in Poland and elsewhere.

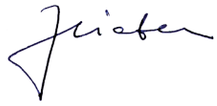

Professor Marek Jeżabek
Director of IFJ PAN

RESEARCH HIGHLIGHTS 2011–2013

I. DIVISION OF PARTICLE AND ASTROPARTICLE PHYSICS

The main area of research covered by our Division are studies of the fundamental constituents of matter and of the forces with which they interact. It is generally accepted that the Standard Model of particle physics successfully represents our present understanding of the world as we see it. Matter is formed of fundamental quarks and leptons which interact via electromagnetic, weak, strong and gravitational forces. The nature of these forces is governed by symmetry and invariance principles. However, the Standard Model is unable to incorporate some well-established features of our Universe, such as the nature of Dark Matter, the matter-antimatter asymmetry, neutrino masses and more. By extending the Standard Model – perhaps by adding new interactions or new fundamental particles, these issues may be resolved.

Astroparticle physics (or particle astrophysics), is a branch of particle physics concerned with elementary particles reaching Earth from the Universe and their relation to astrophysics and cosmology. It is a relatively new field of research positioned at the crossroads of particle physics, astronomy, astrophysics and cosmology. Partly motivated by the historic discovery of neutrino oscillations, this field has rapidly developed in its theoretical and experimental aspects over the last decade. It is aimed at resolving fundamental questions, such as those of the composition of the Universe or of the origin of cosmic rays.

Particle physicists make use of the world's most powerful particle accelerators and experimental facilities to further test the predictions and limits of the Standard Model, and to unveil what lies beyond, thus providing a deeper knowledge and understanding of our world. In the domain of astroparticle studies, physicists are developing new experiments and methods to detect and identify messengers from the Universe, such as ultrahigh-energy cosmic rays or neutrinos. The physicists of our Division contribute significantly to this worldwide effort.

The research groups of our Division actively participate in leading high-energy physics projects carried out by large international collaborations at world-class experimental facilities. These projects, mostly focused on the high-energy frontier, include: the ATLAS and LHCb experiments at the CERN Large Hadron Collider (LHC); the cosmic ray Pierre Auger Project; the Belle-II experiment at SuperKEKB (Tsukuba, Japan); the STAR experiment at the BNL Relativistic Heavy Ion Collider (RHIC); and the future electron-positron collider (ILC and/or CLIC). In the sector of neutrino physics we participate in the T2K experiment at the Japan Proton Accelerator Complex and in the ICARUS experiment at Gran Sasso (Italy). In addition, there are a few projects for which data taking has been completed, but their analysis is still under way, such as the Belle experiment at KEKB, and the H1 and ZEUS experiments at the HERA collider at DESY (Hamburg).

The research carried out in the international **ATLAS experiment** is focused on the physics of elementary particles at the high-energy frontier accessible to the Large Hadron Collider, located at CERN, the world's most powerful accelerator today. The primary aim of these studies is to identify new physics phenomena which may occur in proton-proton and heavy-ion collisions at the highest accelerator energies currently available. The involvement of the research and technical staff of the IFJ PAN in the ATLAS experiment is in several key elements of this experiment, including detector operation, data collection and processing, and data analysis.

The principal goal of the **LHCb experiment** is to study, with unprecedented precision, CP violation phenomena and other rare processes in beauty hadron decays. Apart from delivering data to gain a profound understanding of quark flavour physics in the framework of the Standard Model, the LHCb can probe phenomena beyond the scope of this model. In contrast to the ATLAS and CMS experiments which search for direct manifestations of New Physics, the LHCb activities are oriented towards indirect searches of new phenomena, which can manifest themselves via virtual corrections implemented into the loop diagrams and large CP-violating amplitudes. The Division's LHCb group at IFJ PAN has been involved in the LHCb experiment since 1998. The team has substantially contributed to the design, construction and commissioning of the LHCb's Outer Tracker and participated in software development, particularly in event simulation and event reconstruction algorithms. The group also contributed to the development of the High Level Trigger software.

The Belle experiment is a particle physics experiment conducted at the asymmetric-energy e^+e^- collider KEKB (Tsukuba, Japan), operating primarily at the $\Upsilon(4S)$ $b\bar{b}$ resonance, designed to study CP-violation effects in B meson decays. The universality of the Belle detector has also allowed many other scientific searches, such as extensive studies of rare decays of $B_{(s)}$, $D_{(s)}$ and τ, aimed at seeking effects of physics beyond the Standard Model (SM), and at QCD-oriented measurements, including observations of a number of new particles, such as the $X(3872)$ charmonium-like state and the $h_b(1, 2P)$ bottomonia. Recent measurements from the B factories have revealed discrepancies within the SM predictions. In order to explore such possible hints of new physics with increased precision, both the KEKB accelerator and the Belle detector are being upgraded to become SuperKEKB and Belle II instruments. At the design SuperKEKB luminosity of $8 \times 10^{35}\ \mathrm{cm}^{-2}\mathrm{s}^{-1}$, 50 times as large as the KEKB peak luminosity, a data sample of $50\mathrm{ab}^{-1}$ will be collected in 2023, i.e. about eight years after the commissioning of SuperKEKB. The Krakow group is involved in building important parts of the Belle II spectrometer, such as the silicon detector with pixel and strip components.

The Pierre Auger Observatory studies ultra-high energy cosmic rays, i.e. particles of energies in the EeV range (1 EeV = 10^{18} eV). Extensive air showers of cosmic-ray origin are recorded at the Observatory by applying a hybrid detection technique consisting of an array of particle detectors on the ground and of optical telescopes for detecting the fluorescent light induced by shower particles in the atmosphere. Thanks to this hybrid shower detection system, the Pierre Auger Observatory is able to measure air showers with unprecedented accuracy.

The Tokai to Kamioka (T2K) experiment in Japan is the first of second-generation experiments to study neutrino oscillations using high-power neutrino beams. Two detector stations measure neutrinos from a beam produced by the new high power proton synchrotron at the Japanese Proton Accelerator Research Centre (J-PARC) in Tokai. The "near" detector station, at a distance of 280 m from the target in J-PARC, consisting of ND280 and INGRID detectors, measures neutrinos before their oscillations. The famous SuperKamiokande detector in Kamioka, at a distance of 295 km from the J-PARC accelerator, serves as the distant ("far") detector to measure neutrinos which have undergone oscillations. The near detector station has been built and is operated by a world-wide collaboration, including the group from IFJ PAN. IFJ PAN engineers were responsible for mounting systems of the Side Muon Detector (SMRD) modules and for fixing them inside the ND280 magnet. Data taking with the T2K near and far detectors began in February 2010. Unfortunately, the system was partly damaged by the catastrophic earthquake of 11 March 2011, requiring eight months to re-start the complete acceleration system at J-PARC and the T2K near detectors.

The ICARUS experiment at the Gran Sasso laboratory in Italy began data taking in May 2010. Its detector is based on large Time Projection Chambers (TPC) filled with Liquid Argon (LAr). The detector consists of two cryostats, each of them containing 300 tons of LAr, and is equipped with two TPC's. Due to its fine granularity (3 mm wire pitch in three anode wire planes and probing signal

amplitudes every 400 ns), the ICARUS detector can reach precision in track reconstruction similar to that of the much earlier heavy liquid bubble chambers. The detector is sensitive over a relatively large range of neutrino energies, including atmospheric neutrinos and neutrinos from the CNGS beam, produced at CERN and sent to Gran Sasso over a distance of 730 km. Data taking with the CNGS beam ended in December 2012.

The primary physics task of **the STAR experiment at RHIC accelerator** (Brookhaven National Laboratory, USA) is to study the formation and properties of quark-gluon plasma (QGP). In addition, the ability to collide polarized proton beams at RHIC provides the physicists with a unique opportunity to unravel the spin substructure of nucleons and nuclei, one of the major issues of today's nuclear physics. In 2009 the STAR experiment was fitted with arrays of silicon strip detectors (pp2pp detector) housed within Roman Pots on either side of the interaction point, to be used in polarized proton collision experiments at RHIC. The main focus of attention in the pp2pp project is the search for glueballs in the Double Pomeron Exchange (DPE) process. The program naturally includes many other topics, such as the search for the Odderon, the spin dependence of the elastic and diffractive scattering in polarized pp collisions in the centre-of-mass energy ranges up to 500 GeV and the possibility of new physics of sphaleron production in the DPE. In 2011 a group of physicists affiliated with IFJ PAN, AGH University of Science and Technology and the Cracow University of Technology joined the pp2pp working group of the STAR Collaboration. Its responsibilities include simulation of the RHIC beam line and of the pp2pp detector, determination of luminosity, analysis of the existing pp2pp data and preparation for the second phase of pp2pp project, planned for the year 2014.

The **International Linear Collider (ILC)** is a proposed linear particle accelerator, planned to achieve an initial collision energy of 500 GeV, with the possibility of upgrading it further to 1000 GeV (1 TeV). It is widely expected that at ILC the effects of physics beyond the Standard Model will be observed. In particular, physicists hope to be able to perform precision measurements of the properties of the Higgs boson, recently observed at the LHC (its mass, spin, and interaction strengths), to measure the number, size and shape of any TeV-scale extra dimensions (if they exist) and to investigate the lightest supersymmetric particles, the possible candidates for Dark Matter. IFJ PAN physicists and engineers participate in R&D activities to develop and test the prototype of the luminosity detector, LumiCal. This work is carried out together with the AGH University of Science and Technology (AGH-UST), DESY Zeuthen and Tel Aviv University within the International Forward Calorimetry Collaboration (FCAL) and the Advanced European Infrastructures for Detectors at Accelerator (AIDA) project.

HERA was a particle accelerator at DESY in Hamburg. It began operation in 1992 which terminated in 2007. At HERA, electrons or positrons were collided with protons at the centre-of-mass energy of 318 GeV. The very high energies available at HERA made it possible to probe deep inside the proton to study the structure of its constituents – quarks and gluons. Physicists from IFJ PAN participate in the **H1 and ZEUS experiments** at HERA, both designed to study the photoproduction and deep inelastic scattering on protons.

We participate in the above-mentioned experiments at all stages of their development, commencing with the design and construction of the detectors, through preparation of research programs and active involvement in data analyses, up to on-going maintenance and upgrades of the detector systems. The nature of these activities is of course governed by the current stage of any of these projects.

Running any high-energy experiment requires large computing resources to store and analyse immense volumes of experimental data. Therefore, we are also heavily involved in the global collaboration to link grid infrastructures and computer centres within the WLCG (Worldwide LHC Computing Grid), and in particular in the development of the **Polish Tier 2 in Cracow-CYFRONET** and the local Tier 3 facility at our Institute. Furthermore, the project aimed at overcoming computation limits by employing flexible computing technology, the Cloud Computing **Cracow Cloud 1 Project** (acronym CC1), has been under way since the end of 2009. In multidisciplinary institutes the traditional manner of performing computations is highly ineffective. A computer cluster dedicated to a single research group is typically exploited with rather low efficiency. A private cloud model enables various groups to share computing resources. This can boost the efficiency of exploitation of the infrastructure by a large factor and at the same time reduce maintenance costs. The web site of the CC1 project is located at http://cc1.ifj.edu.pl. The project is financed from the structural resources (Innovative Economy,

National Cohesion Strategy grant, supported by the European Commission and the Polish Ministry of Science and Higher Education). The main goal of the first phase of this project was to develop a fully functional computing system in the form of a private cloud and to make it available to all users at the Institute. The working plan of the second phase was the implementation of a distributed cloud architecture with central management and sharing the computational resources of a large number of distributed computer clusters. The CC1 system provides resources within the Infrastructure as a Service (IaaS) model. Emphasis is on the simplicity of user access, of administrative tasks and of the installation procedure. Self-service access to the system is provided via an intuitive Web interface. The administration module contains a rich set of tools for user management and system configuration.

Physicists of our Division are actively engaged in the **education of students**. Such activities include delivering lectures at various levels of advancement, supervising undergraduate, and graduate research at M.Sc. or Ph.D. levels or training in advanced postgraduate research within our collaborative projects. Over the last two years physicists from our division have supervised a number of graduate students, eight of whom have by now received their Ph.D. degrees in physics. Finally, we should also mention our engagement in the promotion of our Institute, and high-energy physics in general, by organizing and participating in various outreach activities.

The Departments in our Division are closely integrated and cooperate in areas of computing, education, organization of conferences, seminars and outreach events. We also profit from close cooperation with other Divisions of our Institute, especially with the Division of Theoretical Physics, the Division of Nuclear Physics and Strong Interactions (particularly within the international ZEUS experiment) and with the Division of Scientific Equipment and Infrastructure Construction.

The last few years have been remarkably successful for the LHC, marking the machine's first three-year running period ending with the planned Long Shutdown for its further upgrade. The LHC's first run resulted in major achievements, including the discovery of a new particle, which is consistent with the long-sought Higgs boson. The discovery was announced by the ATLAS and CMS collaborations on 4th July 2012. The up-to-date results, based on more data than was available in July 2012, confirm that the new particle is a Higgs boson, a particle associated with the electro-weak symmetry breaking – the mechanism that assigns mass to elementary particles. Furthermore, in November 2013 the ATLAS experiment released preliminary results that show evidence, with a significance of 4.1 standard deviations, that the Higgs boson decays to two tau leptons. This result provides the first observation of the Higgs boson decaying to fermions, and the measured rate for this process is found to be consistent with the rate predicted by the Standard Model. The discovery of the Higgs boson was recognized by the high energy physics community. The 2013 High Energy and Particle Physics Prize was awarded to the ATLAS and CMS collaborations "for the discovery of a Higgs boson, as predicted by the Brout-Englert-Higgs mechanism", and to Michel Della Negra, Peter Jenni, and Tejinder Virdee "for their pioneering and outstanding leadership roles in the making of the ATLAS and CMS experiments". The experimental discovery of the Higgs boson provided the foundation for the 2013 Nobel Prize in physics, awarded to Professors Francois Englert and Peter Higgs: "for the theoretical discovery of a mechanism that contributes to our understanding of the origin of mass of subatomic particles, and which recently was confirmed through the discovery of the predicted fundamental particle, by the ATLAS and CMS experiments at CERN's Large Hadron Collider".

In addition to the discovery of the Higgs particle, the ATLAS experiment has obtained and published many important results, the work in which physicists from our Division played a significant role. The heavy-ion program of the LHC, aimed at understanding matter as it was being created just after the Big Bang, was also pursued with our major contribution to the results from the ATLAS experiment. During the Big Bang, matter and antimatter were created in equal quantities, yet today the Universe is made entirely from matter. The LHCb experiment, another major LHC experiment we participate in, studies the matter-antimatter asymmetry using beauty quarks. It has also the potential to discover new particles, which could make up the Dark Matter. The results obtained by the LHCb experiment from the first LHC run represent, for many of the studied processes, the most precise measurements to date in the domain of heavy quark physics. They show excellent agreement with the predictions of the Standard Model, also for extremely rare processes such as $B^0_s \to \mu\mu$, providing the most restrictive constraints on new physics theories.

In the following, we report in more detail on selected research highlights achieved over the last three years with strong involvement from the staff of our Division in the experiments listed above.

SELECTED RESEARCH HIGHLIGHTS OF THE DIVISION OF PARTICLE AND ASTROPARTICLE PHYSICS

Physicists participating in the ATLAS experiment were actively involved in the **first ATLAS measurement of the pp → γ*/Z → ττ** production cross-sections in p-p collisions at 7 TeV, complementing measurements of the Z boson through the electron and muon decay modes. The decays of Standard Model gauge bosons to τ leptons are important background processes in the search for the SM Higgs boson and for new physics phenomena, thus their production cross-sections need to be measured very precisely. The first measurement of $Z \to \tau\tau$ cross-section was important for the commissioning and validation of τ identification techniques, crucial for the full exploitation of the ATLAS potential in searches for new physics involving τ leptons. The $Z \to \tau\tau$ cross-section was measured separately using four different final states defined by the decay modes of the τ leptons. The distribution of the visible mass (without taking into account neutrinos) for the final state, where one of the τ leptons decays into a muon and the second into hadrons, is shown in **Fig. 1**. Comparison of the individual cross-sections with the combined result is shown in **Fig. 2**. The obtained total combined $Z \to \tau\tau$ production cross-section of 0.97 nb^{-1} is in agreement with next-to-next-to-leading order calculations and other experimental results.

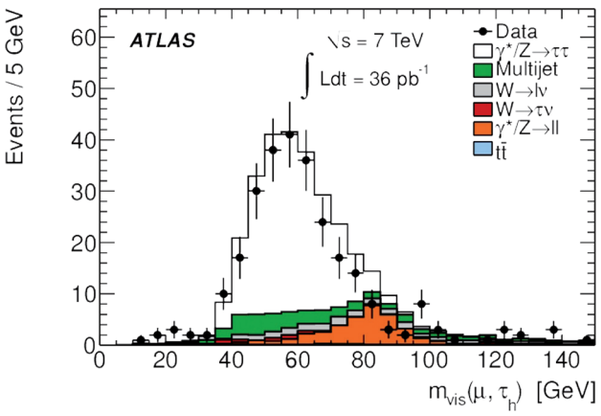

Fig. 1 *Distributions of the visible mass of the combination of the τ candidate and the lepton are shown for the $Z \to \tau_\mu \tau_h$ final state.*

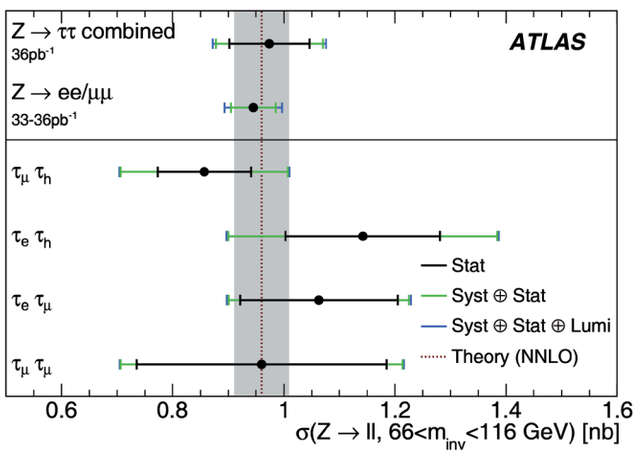

Fig. 2 *Measurements of the individual $Z \to \tau\tau$ cross-section by final state and the combined result.*

Year 2012 saw a spectacular discovery of a new heavy boson at the LHC, announced by both the ATLAS and the CMS collaborations. The observed particle is consistent with the long-sought Higgs particle postulated by the Standard Model. The discovery came from two gold-plated decay channels:

two-photon and four-lepton final states. These decay modes involve elementary bosons, thus confirming the initially proposed Brout-Englert-Higgs mechanism that describes how gauge bosons acquire mass. The Standard Model, however, predicts that fermions also acquire mass through the same mechanism, and consequently the Higgs boson could decay directly to bosons and fermions.

ATLAS has performed a search for the Higgs boson with a mass of about 125 GeV decaying into a pair of τ leptons with a data sample of proton-proton collisions, corresponding to an integrated luminosity of L = 20.3 fb^{-1}, collected with the ATLAS detector at the LHC at a centre-of-mass energy of $\sqrt{s}$ = 8 TeV. Final states in all τ decay combinations (both hadronic and leptonic) are examined. The observed deviation from the background-only hypothesis corresponds to a significance of 4.1 standard deviations, providing the first direct evidence of the Higgs boson decaying to fermions. The measured signal strength parameter μ, which is the ratio of the measured cross-section to that predicted by the Standard Model for mH = 125 GeV, is compatible with the Standard Model expectation. **Fig. 3** shows the comparison of the signal strength parameters measured for different Higgs decay modes.

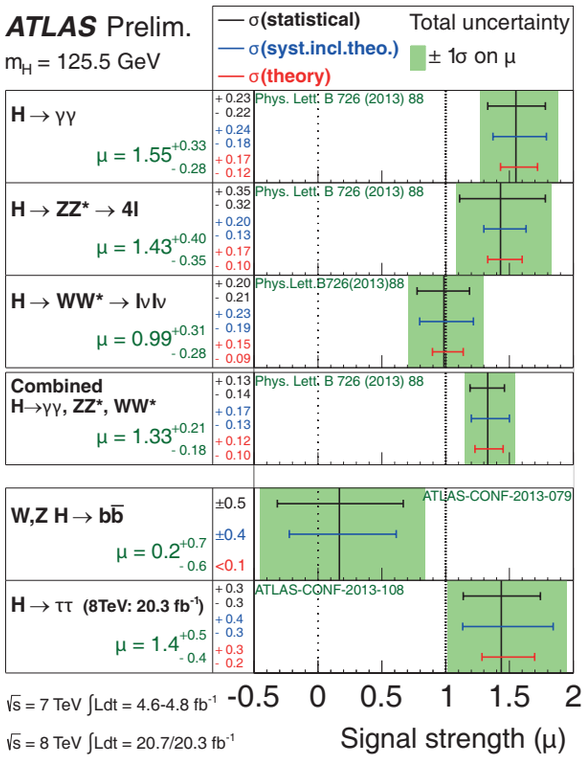

Fig. 3 *Measurements of the signal strength parameter μ in individual decay channels. The measured production strengths are at mH = 125.5 GeV, except for H → ττ which is at mH = 125 GeV.*

The Large Hadron Collider has also opened a new era in heavy-ion physics. The main goal of heavy-ion collisions at relativistic energies is to produce a new state of matter, the hot and dense Quark-Gluon Plasma (QGP), consisting of deconfined quarks, antiquarks and gluons. Since 2010,

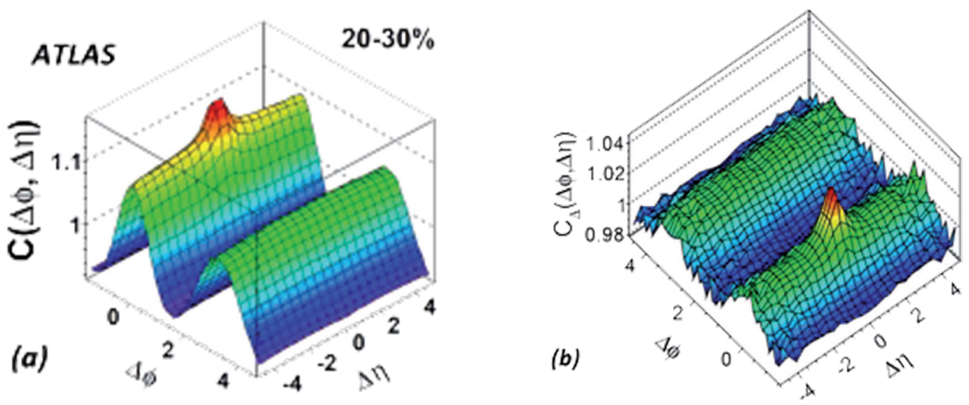

Fig. 4 *Two-dimensional correlation function, C(Δϕ,Δη), for Pb + Pb (a) and p + Pb (b) collisions.*

in the LHC the lead ion (Pb) beams have been accelerated to the largest energies ever obtained in the laboratory. Data samples for Pb + Pb collisions at the centre-of-mass energy of 2.76 TeV per pair of interacting nucleons and proton-lead (p + Pb) collisions at 5.02 TeV, were collected. The ATLAS group from IFJ PAN is strongly involved in the study of heavy-ion phenomena, focusing on **effects related to the collective behaviour of dense and hot matter created in nuclear collisions**. The collective flow of particles leads to a significant anisotropy in the plane perpendicular to the beam direction. This final-state anisotropy can be characterized by coefficients, v_n, of a Fourier decomposition of the azimuthal angle distribution and can also be inferred from the study of particle correlations. Analysis of two-particle correlations as a function of relative azimuthal angle ($\Delta\phi$) and relative pseudorapidity ($\Delta\eta$) in Pb + Pb collisions shows a rich structure, as illustrated in **Fig. 4(a)**. A characteristic long-range structure, extended in $\Delta\eta$ and narrow in $\Delta\phi$, is revealed in addition to the narrow peak due to short-range jet-like correlations. It was shown that the structure in two-particle correlations can be attributed to collective particle flow and described by the interplay of different Fourier coefficients. The small transverse size of the system created in p + Pb collisions is expected to generate a weaker collective flow, if any. However, as shown in **Fig. 4(b)**, the two-particle correlation function measured in p + Pb collisions also indicates the presence of long-range, ridge-like correlations. This observation may suggest that collective flow, the main attribute of the QGP created in the Pb + Pb system, is also present in p + Pb collisions. Additional evidence for the collective flow being present in p + Pb interactions is provided by a direct measurement of the azimuthal anisotropy parameters, v_2, the second harmonic of the Fourier expansion of the particle azimuthal distribution. Transverse momentum dependence of v_2 is shown in **Fig. 5** for p + Pb and Pb + Pb collisions. The large magnitude of v_2 measured in p + Pb interactions and its similarity to Pb + Pb data as well as to hydrodynamic predictions, provide evidence for the importance of collective final-state effects in p + Pb collisions.

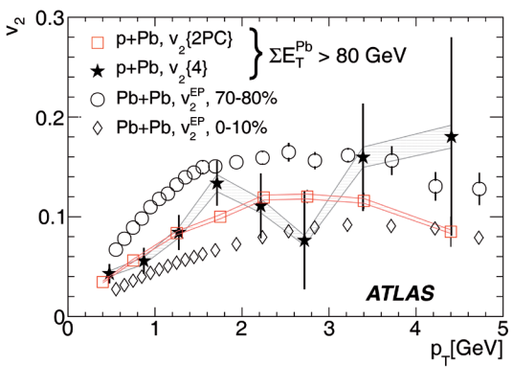

Fig. 5 *Comparison of the transverse momentum dependence of the v_2 coefficient measured in p + Pb collisions with the four-particle cumulants $v_2\{4\}$, and with the two-particle correlation method $v_2\{2PC\}$ to v_2 obtained with the event-plane method for central and peripheral Pb + Pb collisions.*

The ATLAS Collaboration foresees investigations of various processes in which protons are scattered at very small angles and emerge intact from the interaction. Such protons can be registered in the planned **ATLAS Forward Proton (AFP)** detector positioned on both sides of the interaction point at a distance of about 210 m. These detectors will be used in a study of exclusive reactions resulting from the Pomeron or photon exchanges. The two-photon exchange processes deliver a unique opportunity to perform a stringent test of electroweak symmetry breaking – one of the most important and least understood mechanisms. Physicists from IFJ PAN are actively engaged in the **development of selection strategies for rare processes such as exclusive production of heavy boson W+W– pairs**. Measurement of this process could potentially reveal the anomalous quartic gauge boson coupling $\gamma\gamma$WW. The quartic coupling constant a^W_0 is set to zero in the Standard Model but has non-zero values in extra-dimension models. The production rates for lepton pairs originating from various sources, detected in ATLAS central detector and tagged with forward protons in the AFP detectors, are shown in **Fig. 6**. The events origi-

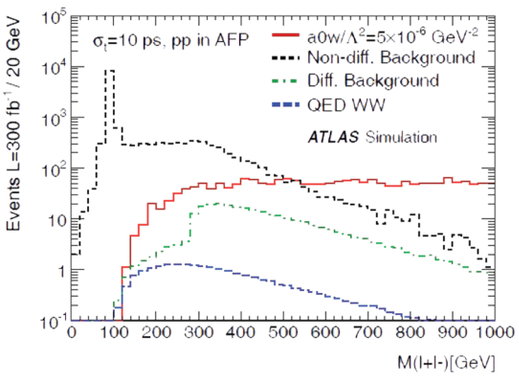

Fig. 6 *Dilepton invariant mass distribution.*

nating from quartic coupling exclusive WW production dominate over background at high dilepton invariant mass. It has been shown that measurements employing AFP detectors can improve the present limits on a^{W}_{0} by four orders of magnitude and have the potential for 5σ discovery at the integrated luminosity of 300 fb^{-1}.

The **LHCb** wide physics program has been carried out on the basis of large samples of high quality data collected over the years 2011 and 2012. Among its recent highlights are: **precise measurement of the Bs oscillation frequency, determination of CP asymmetry in Bs mixing, the first evidence for the $B^0_s \to \mu^+\mu^-$ decay, observation of neutral charmed meson oscillations and extensive searches for lepton flavour violation phenomena**. The measurement of the γ-angle of the unitary triangle from B-decays going through the tree-level processes is of great importance as the precision of this measurement is still poor. The selected signal for one of the decay modes used for the determination of the γ-angle is shown in **Fig. 7**.

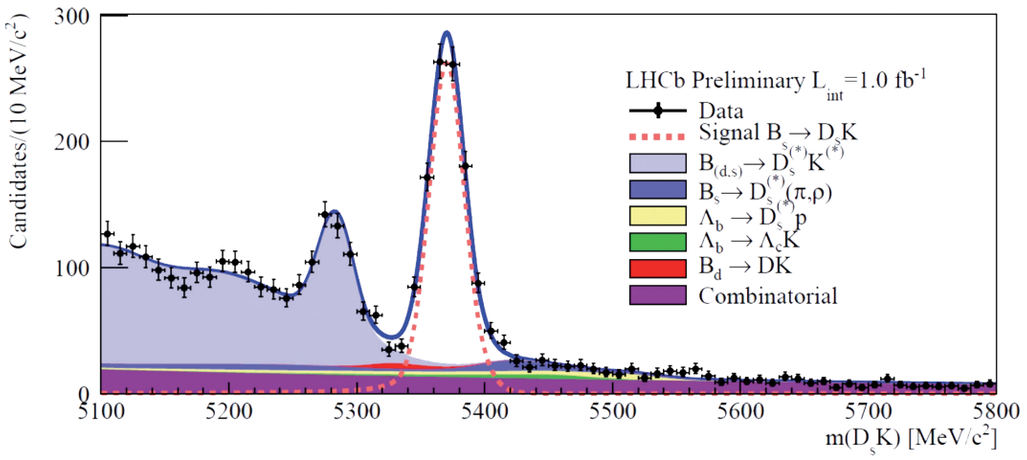

Fig. 7 *Invariant mass spectrum of the $B_s \to D_sK$ candidates.*

Recent measurements from B factories (Belle and BaBar experiments) have revealed discrepancies within the SM predictions, the most outstanding ones being the increased rates of $B^+ \to \tau^+\nu_\tau$ and $B \to D^{(*)}\tau^+\nu_\tau$ reactions, a lower value of the sin $2\varphi_1$ angle of the Unitarity Triangle, and the tension between the Cabibbo-Kobayashi-Maskawa (CKM) matrix element V_{ub} measured inclusively and exclusively from semileptonic transitions $B \to X_u l^+\nu_l$.

In 2012 the Belle experiment updated its studies which are important for understanding electroweak interactions, such as measurements of leptonic decays, $B^+ \to \tau^+\nu_\tau$ and $D_s^+ \to \mu^+\nu_\mu$, $\tau^+\nu_\tau$, performed using improved methods of analysis and a complete Belle data sample.

Among significant new results of the **Belle** experiment one should mention the **study of the two-photon reaction, $e^+e^- \to \gamma\gamma^* e(e) \to \pi^0 e(e)$, shown in Belle-Fig. 8**. The measurement is based on a data sample of 759 fb^{-1} performed in a single-tag mode, where either the recoil electron or positron, denoted in the reaction as *e*, is detected. The $\gamma\gamma^* \to \pi^0$ transition form factor (F) has been measured as a function of four-momentum transfer Q^2, for the kinematical region of 4 GeV^2 < Q^2 < 40 GeV^2, where Q^2 corresponds to the invariant mass squared of a virtual photon γ^*. This measurement offers an important test of QCD in its perturbative approach, in which, as $Q^2 \to \infty$, the $Q^2|F(Q^2)|$ product is expected to approach an asymptotic value proportional to the pion decay constant, f_π. An earlier BaBar measurement revealed a rapid growth of the $Q^2|F(Q^2)|$ with increasing Q^2 values and was thus inconsistent with theory predictions and with results of measurements for other pseudoscalar mesons, η and η′, performed by BaBar. The Belle measurement for the π^0 shows no such increase and confirms

the QCD predictions, as presented in **Fig. 8**. The reasons behind the discrepancy between the Belle and BaBar results are so far unknown.

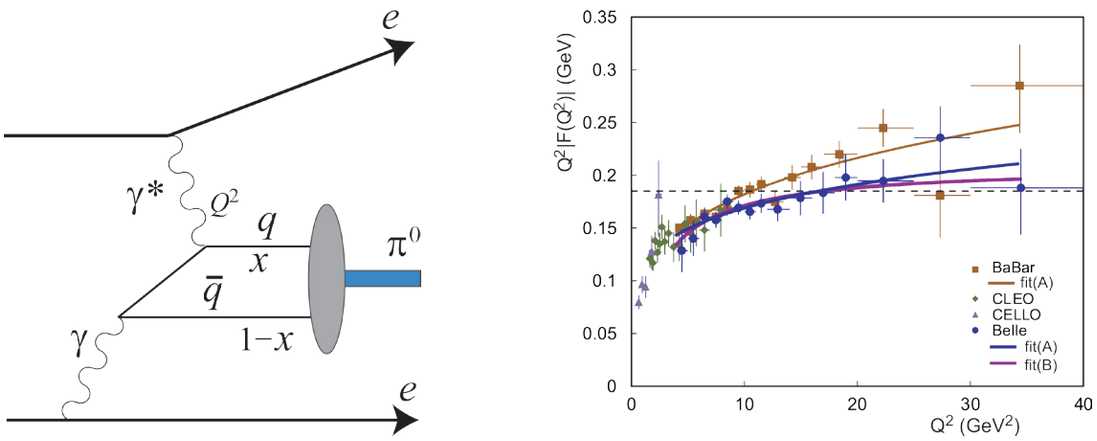

Fig. 8 *Left: The Feynman diagram for* $\gamma\gamma \to \pi^0$ *in* e^+e^- *collisions. Right: Comparison of results for the product* $Q^2|F(Q^2)|$ *for the* π^0 *from different experiments. The dashed line shows the asymptotic prediction from perturbative QCD.*

The large-scale distribution of the arrival directions of ultra-high energy cosmic rays, together with their spectrum and mass composition, are important observables in the search for explanations of the nature and origin of such cosmic rays. If cosmic rays of energies below the "ankle" (spectrum hardening, observed above the energy of about 4 EeV) are of galactic origin, their escape from the Galaxy might generate a dipolar large-scale pattern, as seen from Earth. The amplitude of such a pattern is difficult to predict, as it depends on the assumed galactic magnetic field and the charges of the particles and also on the distribution of sources. Some estimates, even those in which the galactic cosmic rays are mostly heavy nuclei, show that anisotropies at the level of a few percent are nevertheless expected in the EeV range. Even for isotropic extragalactic cosmic rays, a dipole anisotropy may exist due to our motion with respect to the frame of extragalactic isotropy. This so-called Compton-Getting effect has been measured for cosmic rays of much lower energy at the solar frequency, resulting from our motion relative to the frame in which such cosmic rays exhibit no bulk motion. The **Pierre Auger Observatory has improved its experimental limits on dipole anisotropy** as shown in **Fig. 9**. The current limits already exclude the model with an anti-symmetric halo magnetic field (A) and are becoming sensitive to predictions of the symmetric field model (S). These models assume a predominantly heavy composition galactic component at EeV energies, while the scenarios in which galactic protons dominate at these energies would typically predict anisotropies larger than those shown in **Fig. 9**.

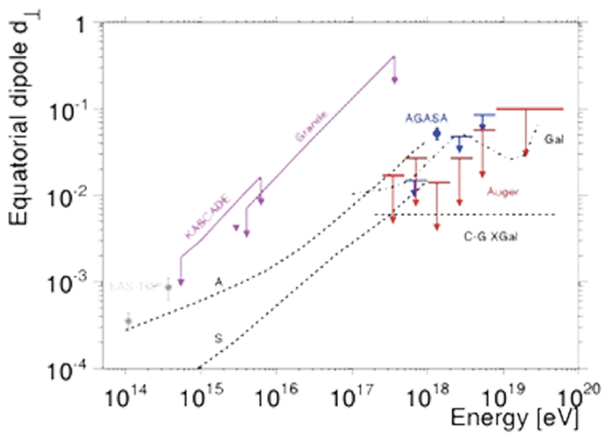

Fig. 9 *Upper limits on the anisotropy amplitude of the first harmonic as a function of energy from Auger and EAS-TOP, AGASA, KASCADE and KASCADE_GRANDE experiments. Predictions are also shown for two galactic field models, one with an anti-symmetric halo magnetic field (A) and another with a symmetric halo (S), together with predictions for the purely galactic origin of cosmic rays (Gal), and predictions from the Compton-Getting effect for an isotropic extragalactic component (C-GXgal).*

Measurements of the proton-air cross-section for particle production at an average centre-of-mass energy per nucleon of 57 TeV, i.e. significantly above the range of the Large Hadron Collider, were made at the Pierre Auger Observatory (Fig. 10). They are based on the depth of shower maximum, X_{max}, i.e. the atmospheric depth at which a shower deposits the maximum energy per unit of mass of atmosphere traversed. The tail of the X_{max} distribution is sensitive to the proton-air cross-section. Using the Glauber model, the proton-proton cross-section can be derived from this measurement to test the hadronic interaction models at the highest energies.

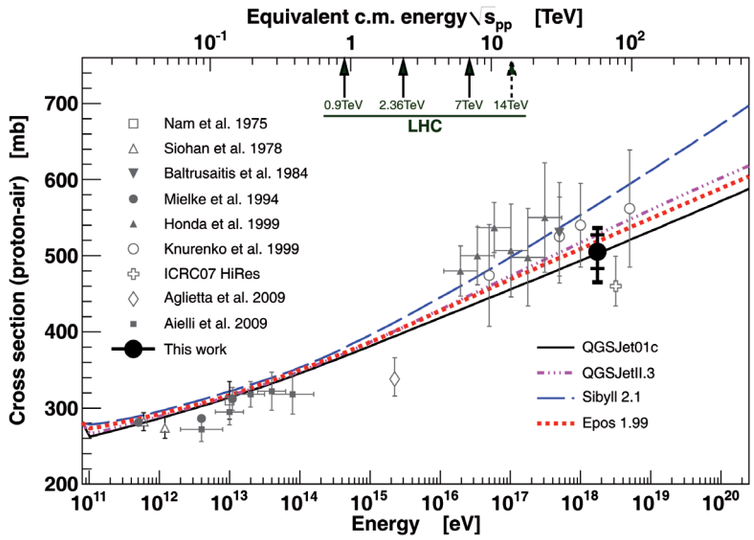

Fig. 10 *Proton-air cross-section for particle production measured by Auger ("This work") compared to other measurements and model predictions. The inner error bars are statistical, while the outer include systematic uncertainties.*

The main goal of the T2K experiment was to measure the unknown oscillation parameter θ_{13}, describing the transition between muon and electron neutrinos. The data collected before the earthquake, corresponding to 1.43×10^{20} protons on target, allowed an indication of this new type of neutrino oscillations to be established. Six events passed all selection criteria for electrons registered at the SuperKamiokande detector. In the three-flavour neutrino oscillation scenario with $|\Delta m_{23}^2| = 2.4 \times 10^{-3}$ eV^2, $\sin^2 2\theta_{23} = 1$ and $\sin^2 2\theta_{13} = 0$, the expected number of such events is 1.5 ± 0.3(syst.). According to this hypothesis, the probability to observe six or more candidate events was 7×10^{-3}, equivalent to 2.5σ significance. **Thus, the T2K experiment provided the first indication of the non-zero value of θ_{13}.** This result, cited already 549 times, heralds new studies of CP violation for neutrinos, which many theorists consider to be a very important element in explaining the observed asymmetry between matter and antimatter in the Universe. The dependences of δ_{CP} on $\sin^2 2\theta_{13}$ are shown in **Fig. 11** for the normal (left) and inverted (right) neutrino mass hierarchy. IFJ PAN physicists have been engaged in the analysis of the $\nu_\mu CC\pi^0$ reaction in the ND280 detector, essential for arriving at a better understanding of neutrino interactions at energies around 1 GeV, and relevant to background studies for the muon neutrino quasi-elastic interactions in this detector, important for oscillation analyses.

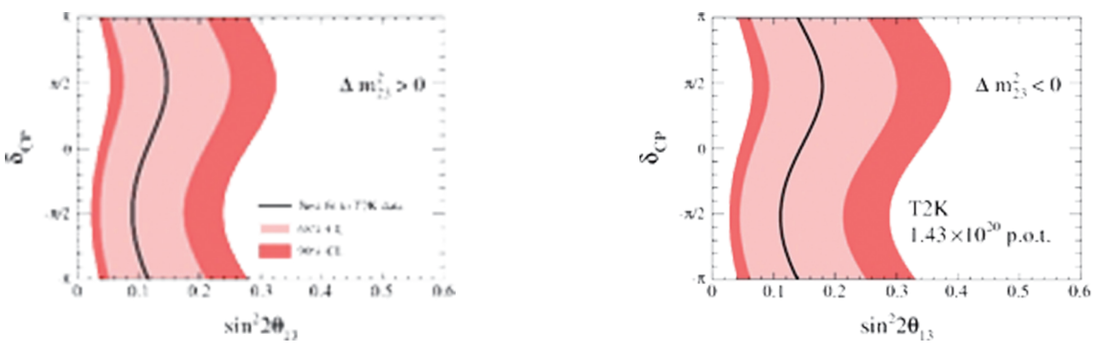

Fig. 11 *The 68% and 90% C.L. regions for $\sin^2 2\theta_{13}$ for each value of δ_{CP}, consistent with the observed number of events in the three-flavour oscillation case for normal (left) and inverted (right)mass hierarchy. The best fit values are shown by solid lines.*

In the ICARUS experiment the large liquid argon detector has for the first time began to take data in the underground laboratory. The data collected by the end of 2012 demonstrated the usefulness of this detector technique for studies of even very complicated high energy neutrino interactions from the CNGS beam. Data analysis was focused on cross-checking the controversial observation of superluminal neutrinos, which had been announced by the OPERA experiment in September 2011. The first result **provided evidence against superluminal neutrinos**, based on the lack of Cherenkov-like radiation foreseen theoretically in such a case. The second cross-check concerned a direct, independent measurement of the neutrino velocity at the CNGS beam with a dedicated time structure. **Fig. 12** shows the comparison between the OPERA and ICARUS measurements obtained with the same beam. The ICARUS result is consistent with the neutrino velocity not exceeding the speed of light. The group from IFJ PAN has been engaged in the analysis of the CNGS neutrino interactions, visual scanning, and in the development of tools for automatic scanning and selections of requested events. This software provides a very efficient and almost background-free selection of neutrino interactions from the CNGS beam. The goal is to use it also for the selection of atmospheric neutrino interactions.

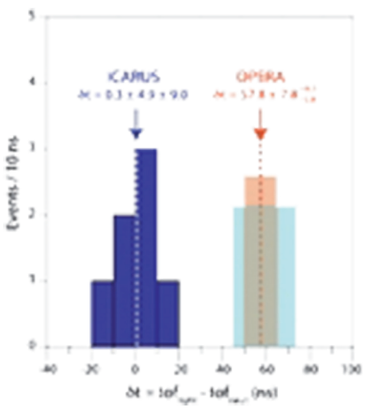

Fig. 12 *Distributions of the difference between the speed of light and the neutrino velocity measured in the ICARUS and OPERA experiments.*

Based on the data collected **in STAR-pp2pp** run in 2009, **the exclusive production of $\pi^+\pi^-$ pairs in the DPE process $pp \to p\pi^+\,\pi^- p$ has been measured**. The $\pi^+\pi^-$ pair is detected in the central detector of STAR, while diffractively scattered protons are tagged in the silicon detectors housed in Roman Pots. In **Fig. 13** the invariant mass spectrum of the centrally produced pions is presented. The exclusivity is proven by the almost negligible like-sign background (red points). This is the first measurement of central diffraction performed using proton tagging in Roman Pots.

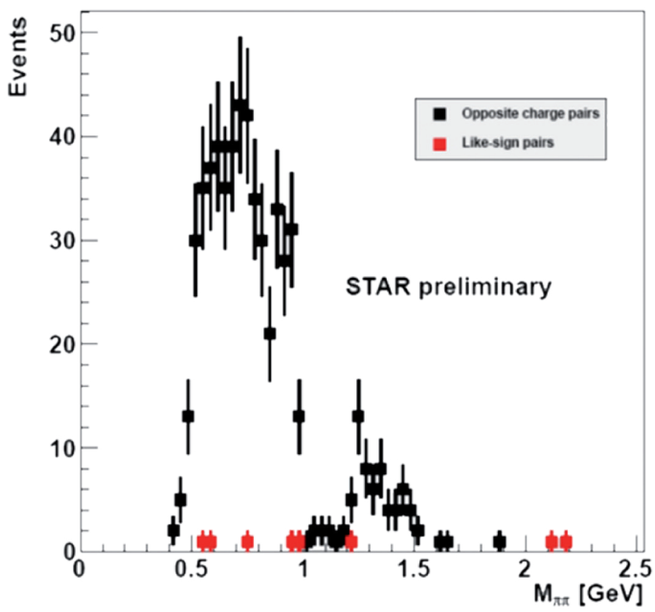

Fig. 13 *Distribution of invariant mass of a π^+ π^- pair produced exclusively in the Double Pomeron Exchange process $pp \to p\pi^+\,\pi^- p$. Red points represent the like-sign background.*

For the last two years the ILC project has been successfully continued and impressive progress on the accelerator technologies has been documented in the Technical Design Report at the end of 2012. Considerable progress was also made in the detector R&D. In 2012 two main detectors at ILC: the International Large Detector (ILD) and the Silicon Detector (SiD) submitted their Detailed Baseline Design (DBD) detector concepts. They represent considerable advances in detectors development made since the original detector design which had been specified in the ILC Letter of Intent. As the DBD Report was prepared, the overall detector design was optimised, basing on extensive simulation studies of the performance of subsystems and on the physics range of the detectors. **Over the period 2011–2012 a modified LumiCal prototype with two layers of silicon sensors, readout electronics and DAQ, was used in test beam measurements** performed using the electron beam at DESY (of energy up to 6 GeV). The readout front-end ASIC used on the dedicated Printed Circuit Board (PCB) was designed and built by AGH-UST. **Fig. 14** shows the LumiCal detector module. The results obtained proved that the complete readout chain comprised of silicon sensors, kapton fanout, front-end ASIC, multichannel ADC ASIC and FPGA-based data concentrator, operated properly under test beam conditions. The signal-to-noise ratios for beam particles, measured by the LumiCal sensors, exceeded 20, as illustrated in **Fig. 15 (Left)**. The features of an electro-magnetic shower observed by placing the silicon sensors under a tungsten absorber **(Fig. 15 Right)** can be reasonably described by Monte Carlo simulations using the GEANT 4 code. These preliminary test beam results were included in the DBD ILD report.

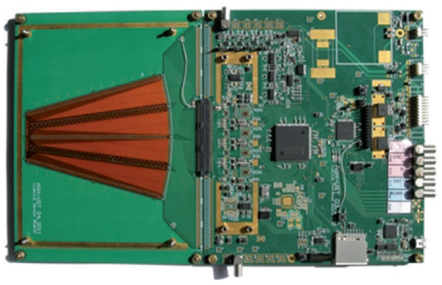

Fig. 14 *The LumiCal readout module with sensors connected.*

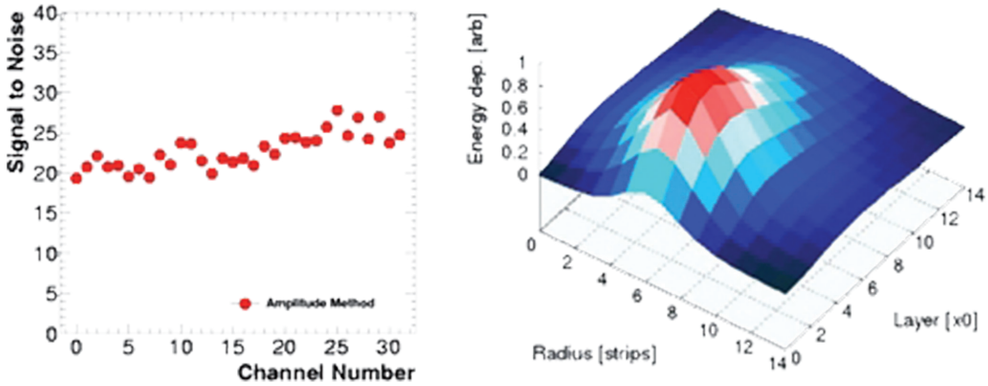

Fig. 15 *Left: The signal-to-noise ratio of all readout channels before calibration. Right: The averaged profile of electromagnetic showers in the LumiCal prototype.*

In 2012 the **H1 Collaboration measured the azimuthal correlation between the most forward jet and the scattered positron in Deep-Inelastic Scattering (DIS)**. This work finalizes H1 studies of hadronic final states in deep inelastic scattering at small parton momentum fractions (Bjorken-x), published over the years, for which physicists from IFJ-PAN provided many essential contributions. Measurements of the hadronic final state in DIS test the validity of an approximate QCD calculation, known as DGLAP, in the kinematic range of small Bjorken-x $\simeq 10^{-4}$. This is the region of high parton densities in the proton, dominated by gluons and sea quarks. This subject has important theoretical and practical aspects (e.g. parton saturation region, multiple parton collisions, QCD calculations for LHC). At the large γp centre-of-mass energy available at small Bjorken-x, the above-mentioned DGLAP approximation is expected to break down together with the transition from parton cascades ordered in transverse momentum, to unordered cascades. In **Fig. 16** the differential forward jet cross-section is shown as a func-

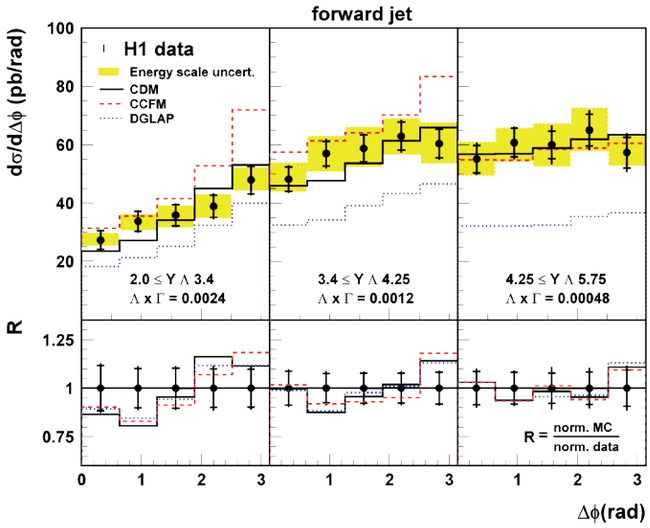

Fig. 16 *Differential forward jet cross-section as a function of the azimuthal angle difference between the most forward jet and scattered positron in three intervals of the variable Y related to −ln(x). The blue, red and black lines correspond to various QCD inspired models with parton emissions ordered or unordered in transverse momentum.*

tion of the azimuthal angle difference between the most forward jet and scattered positron. The shape of this distribution was expected to be different for ordered (DGLAP, dashed blue line) and unordered (CDM, CCFM, black and dashed red lines) cascades. As can be seen in **Fig. 16**, all models describe the shape of the correlation reasonably well, while the absolute normalization of the cross-section requires an unordered parton emission mechanism. This observation, together with the results of the next-to-leading-order QCD calculation, indicates that at HERA energies the DGLAP approximation is still valid. However, higher orders of perturbative series are necessary to correctly predict the forward jet cross-sections.

The experiments at HERA opened a new field of particle physics studies called hard diffraction. Hard diffraction at HERA is an interaction characterized by large transverse momentum transferred to the proton, which nevertheless remains intact. These studies contribute to a better understanding of confinement, a mechanism which maintains quarks and gluons inside hadrons, and of hadron transverse structure. **Recently, the ZEUS Collaboration has studied the exclusive photoproduction reaction $\gamma p \to Y(1S)p$, to measure the exponential slope, b, of the t-dependence of the cross-section**, where t is the squared four-momentum transfer at the proton vertex. **Fig. 17** shows the results of measurements of *b* as a function of the scale $Q^2 + M^2_{VM}$ obtained in this analysis together with other HERA measurements in exclusive vector-meson production and deeply virtual Compton scattering (DVCS). The obtained b value is in agreement with an asymptotic behaviour of this dependence, and is approximately equal to that expected from the size of the proton (b ≈ 4 GeV2) being also consistent with the prediction based on pQCD: b = 3.68 GeV^2. This suggests that the size of the *Y* is small when compared to that of the proton (*b* is related to the sum of the squares of proton and vector-meson radii).

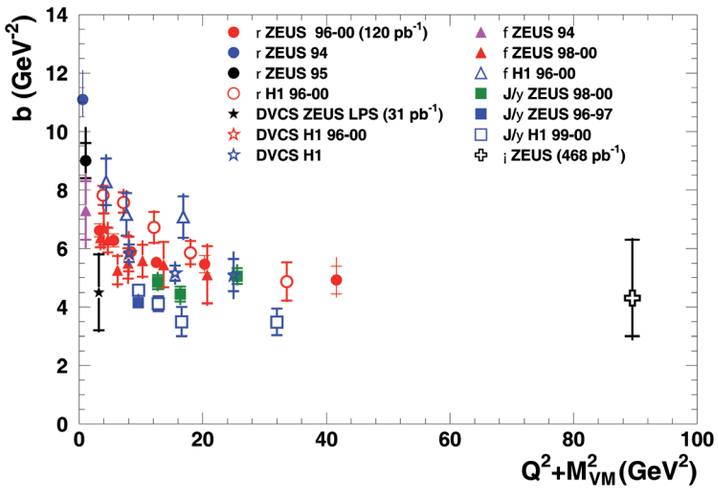

Fig. 17 *Compilation of the different HERA measurements of the slope b as a function of the scale $Q^2 + M^2_{VM}$, where M_{VM} denotes the mass of a vector meson.*

Studies of the inclusive production of neutral strange particles provide information on the fragmentation process in ep collisions and may be very useful in improving constraints on the strange particle fragmentation functions, FFs, which are currently very poorly known. In 2012 the ZEUS Collaboration measured the scaled momentum distributions for strange hadrons K^0_S, Λ and anti-Λ in DIS using an integrated luminosity of 330 pb^{-1}. The scaled momentum is defined as $x_p = 2P^{Breit}/(Q^2)^{1/2}$, where P^{Breit} is the particle momentum in the Breit frame and Q^2 is the photon virtuality. Clear scaling violations are observed in different regions of x_p. **Fig. 18** shows, as an example, the scaled momentum distributions for Λ / anti-Λ as a function of Q^2 in different regions of x_p. The next-to-leading order QCD calculations fail to describe these measurements. Better agreement was found in comparison with CDM and MEPS models based on leading-logarithmic matrix elements plus parton shower and the Lund fragmentation model. As the x_p variable is an estimator of the variable z used in FFs description, measurements of x_p distributions have the potential to further constrain the FFs of quarks, anti-quarks and gluons .

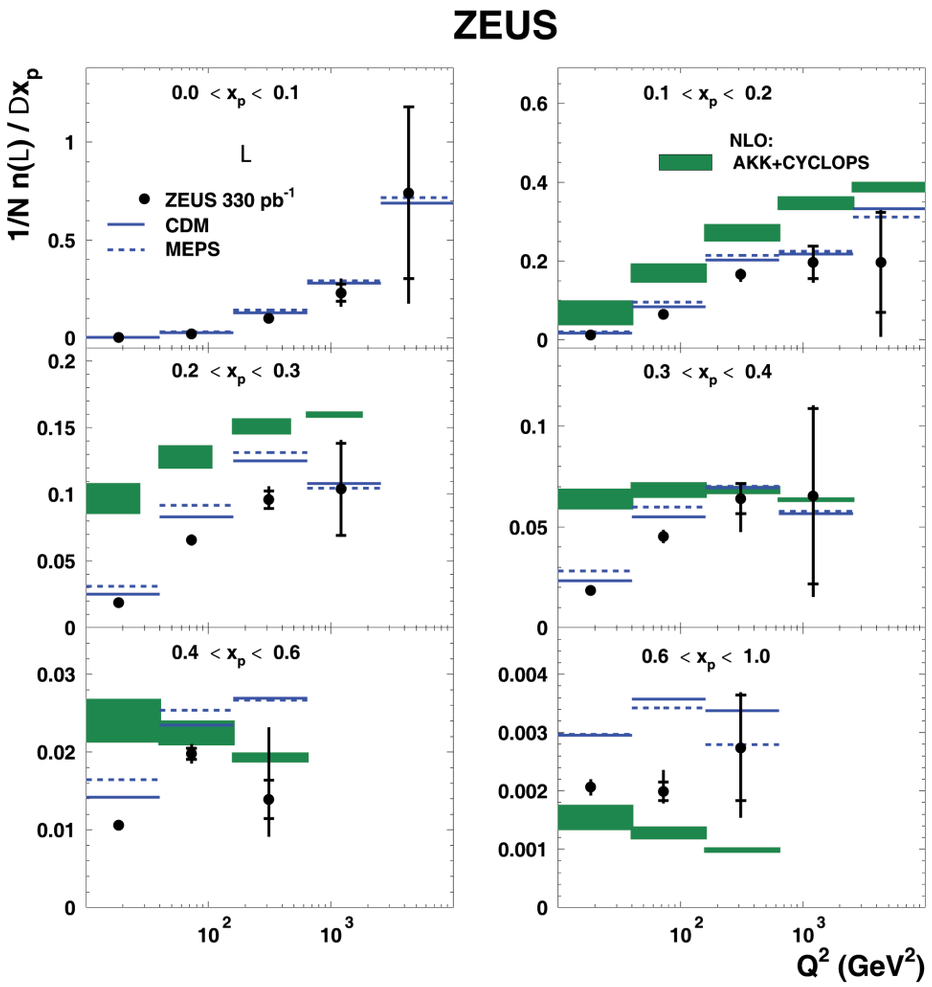

Fig. 18 *Scaled momentum distributions for Λ / anti-Λ particles as a function of Q^2 in different x_p bins.*

At the beginning of 2012 **the stable Cloud Computing – Cracow 1 (CC1) system was launched and extensively used for calculations by various research teams at the Institute and by their collaborators.**

The research reported herein was performed pursuant to internal projects: [102, 103, 104, 105, 106, 107, 108, 109, 113, 114, 205, 504]; [E2, E3, E7, E10, E11, E13, E16, E37, E44]. See Annexes I and IIA.

II. DIVISION OF NUCLEAR PHYSICS AND STRONG INTERACTIONS

Nuclear physics is one of the fundamental areas of science which, through its present technological and computational advances, continues to open new frontiers of discovery and continues to address the most basic questions about the physical universe and its origin. As a matter of fact, 99.9 percent of the mass of all the atoms in the universe originates from the nuclei at their centres, the volumes of which are over trillion times smaller than the atoms themselves. Even though nuclei are incredibly tiny and dense, they are complex structures made of protons and neutrons. In turn, protons and neutrons have an underlying structure of quarks, which are bound by the strong interaction mediated by the force-carrying gluons. This complexity results in countless possible states of nuclei and of nuclear matter, described by different spin or isospin numbers, temperatures and densities. One of the greatest challenges in nuclear physics is to understand the structure of nuclei, and of their constituent protons and neutrons, emerging from such complexity. The scientific activity of the **Division of Nuclear Physics and Strong Interactions** embraces all these topics. Research in experimental and theoretical areas of nuclear physics and strong interactions is carried out in three departments of this Division.

Studies of nuclear structure, aimed at building a coherent picture to explain all properties of nuclei, are carried out in the **Department of the Structure of Atomic Nucleus**. Investigations concerning nuclear reactions and the nature of hadrons – nuclear particles which interact via strong interactions, and the properties of these strong interactions themselves, are pursued in the **Department of Strong Interactions and Mechanism of Nuclear Reactions**. Studies of the physics of strongly interacting matter at extreme energy densities, where a new phase of matter, the quark-gluon plasma, is formed, are the domain of the **Department of Ultrarelativistic Nuclear Physics and Hadron Structure**.

Most of our investigations are carried out through international collaborations, many of which are based around Large Scale Facilities in Europe, such as GSI (Darmstadt, Germany), GANIL (Caen, France), COSY (Jülich, Germany), LNL (Legnaro, Italy) and INP (Orsay, France), and which are supported by the EU's Seventh Framework Programme for Research (for example, ENSAR). A number of projects have also been conducted at other world-leading laboratories: CERN, ANL (Argonne, USA), RIKEN (Tokyo, Japan), or ORNL (Oak Ridge, USA). In many of these research projects, the research staff of our Division plays key roles.

In the following we present a short description of results in the three areas of research conducted in our Division: **nuclear structure, hadronic interactions** and **ultrarelativistic nuclear physics**. Some of the Division's achievements will be described in more detail, including references to specific programmes and to publications in peer-reviewed journals.

NUCLEAR STRUCTURE RESEARCH

The main questions guiding nuclear structure research can be viewed from two general and complementary perspectives: the microscopic perspective, focusing on the motion of individual nucleons moving in a mean field potential created by all the nucleons, which gives rise to the quantum shell structure, and the mesoscopic perspective which focuses on the highly organized complex system exhibiting certain symmetries, regularities, and collective behaviour. In spite of this duality, the two characteristics seem to be intimately related. Presently, one of the major challenges is to investigate and understand how to bridge the gap between these two approaches. It is commonly accepted that in order to gain a more profound understanding of nuclear structure, experimental and theoretical efforts should focus on nuclei localised in the unexplored regions of the nuclear landscape, in terms of their isospin, spin or temperature.

Experimental studies of nuclear structure in our Division have been carried out in various regions of the nuclear chart by performing experiments with radioactive and stable beams, and by combining several experimental techniques, such as discrete gamma-ray spectroscopy, high-energy gamma ray detection and charged particle or heavy-ion scattering.

In one of such experiments, the pygmy dipole resonance (PDR) in the ^{208}Pb nucleus was investigated at LNL by using the ^{17}O + ^{208}Pb reaction at 20 MeV/A and by employing the AGATA Demonstrator array together with a set of the $LaBr_3$ (3"x3") detectors for high-energy gamma-ray measurements. E1 transitions from the PDR decay were identified*.

We proposed and performed two thick-target γ-coincidence experiments using the GAMMASPHERE Ge detector array and a ^{208}Pb ion beam of the ATLAS accelerator at ANL, using ^{208}Pb and ^{238}U targets. Hard-to-reach yrast structures in the two nuclei, ^{207}Tl and ^{210}Bi, were extended up to high-spin, offering a perfect testing ground for realistic shell-model calculations which involve ^{208}Pb core excitations.

Isospin mixing in the hot compound ^{80}Zr nucleus was studied at LNL by measuring and comparing the γ-ray emission from the fusion reactions ^{40}Ca (200 MeV) + ^{40}Ca and ^{37}Cl (153 MeV) + ^{44}Ca. It has been concluded that the isospin mixing width originating from the Coulomb interaction is an intrinsic, temperature-independent property of nuclear structure.

We proposed a method that allowed us to perform discrete gamma-ray spectroscopy studies of states with moderately high spins in neutron-rich nuclei, by employing radioactive beams. The method relies on using the incomplete fusion reactions induced by a radioactive beam on a ^{7}Li target. We successfully tested the method at REX-ISOLDE by using a radioactive ^{98}Rb beam. The main reaction channel, involving transfer of the triton and emission of an alpha particle, ^{7}Li(^{98}Rb,αxn), was associated with evaporation of two neutrons, leading to the ^{99}Sr nucleus in which the known rotational structures were populated.

The data collected earlier with the Cracow Recoil Filter Detector (RFD) coupled to the Ge detector array GASP at LNL, for the reaction ^{40}Ca + ^{32}S, allowed us to measure half-lives in the range of tens to hundreds of femtoseconds in the ^{66}Ge and ^{69}As product nuclei. The Doppler shift attenuation technique was applied. The lifetimes of some states of the negative parity band in ^{66}Ge were extracted and the magnitude of the transition quadrupole moment, Q_t, was determined at approx. 0.9 (2) eb.

Thick-target gamma coincidence data, collected with the GAMMASPHERE gamma-ray array (ANL) for the products of deep-inelastic processes occurring in the ^{48}Ca + ^{238}U, ^{64}Ni + ^{238}U, ^{70}Zn + ^{197}Au, ^{208}Pb, ^{238}U, and ^{76}Ge + ^{238}U reactions, were used to study the structure of neutron-rich species which are hard to access otherwise. The yrast structures in the neutron-rich ^{64,66,68}Ni isotopes, which include the magic nucleus ^{68}Ni with a closed N = 40 neutron subshell, were extended up to high-spin*. Other new findings include:

a) positive-parity level structures above the known $9/2^+$ states in ^{65,67}Cu, based on $p_{3/2}$ protons coupled to negative-parity states in the Ni cores;
b) negative verification of a recently reported 216-ns, 0^+ isomer at 2202 keV in ^{68}Ni;
c) extension of a level scheme built on the previously known 13-μs isomer in ^{67}Ni up to an excitation energy of 5.3 MeV and a tentative spin and parity of $21/2^-$.

Using the gamma-coincidence data from the above-mentioned experiments with GAMMASPHERE, we have demonstrated for the first time that heavy products of deep-inelastic reactions exhibit a significant alignment of their spin. Angular distributions of γ rays from the spin-aligned states of such products offer then an excellent opportunity for making spin-parity assignments to states located in deep-inelastic collisions (DIC) products.

We have also carried out research on the borderline between theory and experiment. For example, competition between fission and evaporation channels in the fusion reactions was modelled by solving the Langevin dynamical equation in 3-dimensional deformation space. The main component of this method is the Potential Energy Surface (PES), which can be obtained from macroscopic models, such as the Finite Range Liquid Drop Model (FRLDM) or the Lublin-Strasbourg Drop (LSD) model. While calculations with PES resulting from these two models give similar results in the heavy mass region, they show noticeable differences in the fission products charge distribution for medium-mass nuclei.

The computer code GEMINI++, which has widely been used to simulate the decay of the compound nucleus by a series of binary decays (charged particle decay and fission fragment emission following heavy-ion fusion reactions), was enhanced by adding the possibility of emission of high-energy gamma rays from the decay of a Giant Dipole Resonance (GDR).

Assessment of the predictive power of nuclear structure models is a very important issue, although rather neglected. We have developed a technique to estimate the predictive power of some nuclear structure theories by applying selected methods of the inverse problem theory*.

The above-described research is strongly linked with work on detector development carried out in the Department. The main activity in this area is related to new multi-detector arrays, PARIS, EXOGAM2 or AGATA, planned to be used in the future European infrastructures, such as SPIRAL2 and FAIR.

The PARIS detector system, proposed and coordinated by the physicists from IFJ PAN, shall combine an energy spin spectrometer, a calorimeter for high-energy photons and a medium-energy resolution detector. To reach this goal, the system was designed to consist of an array of so-called phoswich detectors, arranged in clusters (3"x3" phoswiches). These phoswiches take advantage of state-of-art technology by optically combining $LaBr_3$(Ce) scintillators with more conventional NaI(Tl) scintillators. Advanced GEANT4 simulations were performed within the collaboration and showed that such a two-shell design is well suited for the physics of PARIS. The overall performance (efficiency, energy and time resolution) of the $LaBr_3$-NaI phoswiches was investigated off- and in-beam conditions at several laboratories within the collaboration (Strasbourg, Orsay, Krakow). In addition, substantial work to investigate various electronics scenarios was undertaken. An extensive set of detectors being now available and investigations performed at collaborating laboratories permitted us to reach precise and consistent ideas on the actual capabilities of $LaBr_3$ when coupled to NaI, and to reach tentative recommendations on the accompanying electronics and mechanical construction of this system.

AGATA and EXOGAM2 are state-of-art germanium detector arrays under construction within European collaboration. They are equipped with very fast numeric electronics capable of operation at the highest counting rates. Our group has developed and has been maintaining AGAVA, the VME interface between those detector systems and other ancillary detectors. AGAVA was successfully used to couple AGATA with, among others, the PRISMA mass spectrometer at LNL, Legnaro and the FRS fragment separator at GSI, Darmstadt. These gamma spectroscopy experiments, performed in a framework of a large international collaboration, already resulted in valuable physical results. Moreover, we have contributed to the development of the digitizer board NUMEXO2 that will serve detectors, as for example the PARIS scintillator array, used at the SPIRAL2 radioactive beam facility at GANIL, Caen. Besides integration of the GTS (Global Trigger and Synchronization) functionality directly into the NUMEXO2 board, we have been involved in designing and testing a multipurpose FADC mezzanine card for the digitizer.

INVESTIGATIONS ON HADRONIC INTERACTIONS

Studies of the strong force and of the constituents that make up the internal structure of the proton and the neutron, quarks and gluons, are guided by a few basic questions:

a) How do the internal structural properties of protons and neutrons arise from the behaviour of their constituents?

b) How are those properties reflected in the structure of complex nuclei?

c) Can QCD establish a link between interacting nucleons and the underlying structure of quarks and gluons?

In order to elucidate the above issues, we continued the study of reaction mechanisms and of properties of nuclear matter using heavy ion collisions at low and intermediate energies.

Our groups have been actively participating in three big collaborations: ANKE, WASA and PANDA. Within ANKE collaboration differential cross sections and analyzing powers for the $pp \to pp\pi^0$ reaction were measured at 353 MeV. Similar analysis was done for quasi-free $pn \to pp\pi^-$. Our group participated in a new determination of the mass of the η meson. Cross section has been measured for K^+K^- pair production in proton-proton collisions at 2.83 GeV beam momentum.

Within WASA collaboration we have continued study of the Abashian-Booth-Crowe resonance structure in the double pionic fusion to ^{4}He. A detailed study of the $\eta \to \pi^+\pi^-\pi^0$ decay has been performed. In the last period, experimental investigation of $\pi^0\pi^0$ pair production in proton-proton collisions at T_p = 1400 MeV has been conducted.

Within PANDA collaboration, in frame of preparations to the future experiments, further tests of the detector prototypes and sampling ADCs, as universal tools for data processing, has been carried out.

Introductory studies of synchrotron oscillating effects have been performed in preparation for future measurement of the proton electric dipole moment.

Part of our group was conducting a series of experiments at the Warsaw Cyclotron. This concerns measurements of elastic scattering of ^{20}Ne on ^{16}O and alpha transfer important for astrophysics. Similarly, the ^{12}C(^{11}B,^{15}N)^{8}Be reaction was studied. A measurement of the backscattering of ^{20}Ne on different isotopes has been performed in addition.

Within the S254 experiment at GSI, we have performed an analysis of projectile fragmentation in the reactions of $^{107, 124}$Sn and ^{124}La scattering on Sn at E_{lab} = 600 AMeV. Tests of our detectors by means of heavy ions have been done. We have developed a new algorithm for neutral track analysis in the LAND detector. We have also prepared and conducted ASY-EOS experiment, which concerns studies of symmetry energy term in the equation of state of nuclear matter. The KRATTA detector was prepared and commissioned. The spallation of ^{136}Xe on ^{1}H and ^{12}C was measured at the energy of 1 GeV per nucleon.

The breakup of deuteron on proton and deuteron at the beam energy of 160 MeV has been measured (in KVI Groningen) and analysed in search for effect of three-nucleon forces. The detector BINA has been installed at the Cyclotron Center Bronowice IFJ PAN in Kraków and first experiment is being prepared.

The experiment on neutron electric dipole moment at PSI Villigen entered data taking stage. The experiment makes use of a new source of ultra-cold neutrons from solid deuterium.

Hand-in-hand with experimental developments, theoretical studies have been conducted in our Department.

One of the specialties of our group are exclusive processes in proton-proton collisions. Several new results were obtained in this context. The amplitude for the exclusive $pp \to pp\bar{b}$ reaction was derived. The considered process constitutes a background for exclusive production of the Higgs boson. Several differential distributions have been calculated for the first time. It was shown how to impose cuts in order to improve signal-to-background ratio. Similar analysis was performed for exclusive production of charm.

Differential cross section for $pp \to ppK^+K^-$ was calculated in a Regge model including absorption effects and final state interaction of kaons. A possibility to measure exclusive production of $\chi_c(0)$ meson in the K^+K^- channel was studied for the first time.

The cross sections for exclusive production of omega mesons in proton-proton collisions was calculated for RHIC and LHC energies. The calculation included photoproduction mechanisms (dominating at midrapidities) as well as hadronic bremsstrahlung mechanism (dominating at large rapidities). Also, for the first time in the literature, a calculation of diffractive contribution to the cross section for the $pp \to ppW^+W^-$ reaction were performed. The competition with photon-photon mechanism was assessed. The discussed process is particularly valuable for studying triple and quadrupole gauge boson couplings. Similar analysis was performed for the $pp \to pp\gamma\gamma$ process and results were confronted with recent Tevatron data.

Another topic of interest is inclusive production of heavy quarks, mesons and so-called nonphotonic electrons. A calculation of the $c\bar{c}$ production in proton-proton collisions initiated by photons has been performed, treating photon as a "parton" of the incoming protons. First results were presented. It was suggested that the cross section for the production of two $c\bar{c}$ pairs is the best place to study double-parton scattering. First, the cross sections in the collinear approximation were obtained. It was shown that at the LHC the corresponding cross section is of the same order as the cross section for single pair production. It was discussed how to identify the double parton scattering effects. Similar analysis was performed in the k_t-factorization approach including modern unintegrated gluon distributions. Several correlation observables were calculated and compared with success to the recent LHCb data.

The amplitude for the production of two pairs in single parton scattering ($gg \to c\bar{c}\,c\bar{c}$) was obtained in the high-energy approximation. The corresponding cross sections were calculated and compared to those for double-parton scattering.

Several mechanisms of the two J/Ψ production in proton-proton collisions were considered, including double and single parton scattering. The cross sections were calculated in the k_t-factorization approach.

Another topic of interest is the production of simple final states in ultraperipheral, ultrarelativistic heavy ion collisions. The calculation of heavy quark and heavy antiquark were performed in this context. Several mechanisms, including higher-order pQCD corrections, were considered. Both reactions direct and with resolved photons were included.

An analysis of exclusive production of charmed mesons was performed and the associated cross sections were calculated.

The cross section for the production of heavy quarkonia in photon-nucleus and in ultraperipheral nucleus-nucleus collisions was studied including multipole rescattering of quark-antiquark dipoles in nuclei in the language of perturbative chromodynamics. The predictions for ALICE at LHC were performed.

The cross section for $\gamma\gamma \to J/\psi J/\psi$ was calculated. This elementary cross section is an ingredient for calculating nuclear $AA \to AAJ/\psi J/\psi$ cross section. The calculation was done for the first time and predictions for ALICE at LHC were presented.

The elementary $\gamma\gamma \to \pi\pi$ reaction was studied in great detail. Several perturbative and nonperturbative processes were studied. The total cross section as well as angular distributions were compared with the Belle data. The elementary cross section was used for preparing predictions for ultra-peripheral, ultrarelativistic production of pion pairs for RHIC and LHC.

Calculations of the quark-gluon plasma excitations, corresponding to the scalar and pseudoscalar meson quantum numbers, for different temperatures were performed. Analysis which was performed in the Hard Thermal Loop Approximation leads to a better understanding of the excitations of the quark-gluon plasma in the deconfined phase and is also of relevance for lattice studies. The screening masses of scalar and pseudo-scalar excitations in quark-gluon plasma were calculated. The study of heavy quarkonia in a deconfined quark-gluon plasma with the Bc family of mesons was carried out. With the introduction of this bound state of a charm and a beauty quark, we were able to investigate the behavior of the system at finite temperature, in an energy region between the ψ and the Y states.

We were working in the Rooted Maps Theory, a branch of the Theory of Homology, which is shown to be a powerful tool for investigating the topological properties of Feynman diagrams, related to the single particle propagator in the quantum many-body systems. We were studying the numerical correspondence between the number of this class of Feynman diagrams as a function of perturbative order and the number of rooted maps as a function of the number of edges. Then, we have found topological one-to-one correspondence between some subclass of Feynman diagrams and rooted maps and we have proposed, starting from rooted maps principles, an original definition of the genus of a Feynman diagram.

We have calculated within the Shell Model Embedded in the Continuum (SMEC) the asymptotic normalization coefficients of the one-nucleon overlap integrals for light mirror nuclei with different one-nucleon emission thresholds in A and A-1 systems. In these studies, we tried to disentangle effects of the coupling in mirror overlaps and, hence, establish to which extent one can determine relevant capture reaction cross section based on information obtained from transfer reactions with stable beams. These calculations have covered all nuclei in p and sd shells, especially devoted to radiative proton capture. The critical value of the Sommerfeld parameter (connected to proton separation energy), for which cross section for the radiative capture process becomes minimum, has been established. No such feature was found on the side of neutron radiative capture, where cross sections change monotonically with neutron separation energy.

Another investigations were devoted to establish a relation between threshold phenomena and exceptional point threads for complex extended SMEC Hamiltonian. The exceptional point threads are lines of exceptional points as a function of energy of the system, i.e., the energy of the nucleon in the continuum. The mixing of shell model states of the closed system (SM) in the vicinity of the threshold was analyzed near proton emission threshold to establish the relation between the formation of cluster states, like the Hoyle state in ^{12}C or the Borromean ground state of ^{11}Li. It was found that the key role in near-threshold clustering is played by the so-called aligned state, the eigenstate of SMEC, that captures most of the continuum coupling and, above the decay threshold, exhausts most of the decay width. The collectivity of an

aligned state is a fingerprint of instability in an ensemble of all SM states having the same quantum numbers and coupled to the same decay channel. Quantitatively, manifestations of this instability depend on the strength of the continuum coupling, the density of SM states, and the nature of the decay channel. For large angular momenta and/or charged particle decays, the energy window for the formation of a collective aligned state is pushed by centrifugal and Coulomb barriers above the decay threshold.

A strong nonresonant mechanism of the muonic deuterium molecule ddμ was found. This mechanism greatly influences muon-catalyzed fusion of the two deuterium nuclei, which enables detailed studies of this reaction in the zero-energy limit.

The differential cross sections for cold neutron scattering from imperfect deuterium policrystals were calculated. Such cross sections are necessary for planning effective sources of ultracold neutrons.

Optimal conditions for the laser-spectroscopy measurement of the hyperfine splitting in the 1s state of the muonic hydrogen atom, pμ, were found. The planned experiment will determine the RMS radius of electromagnetic structure of the proton, thus enabling an independent measurement (with respect to the well-known Lamb-shift experiment) of this radius.

The dynamical equations driven by a stable Levy noise are characterised by a divergent variance and it is necessary to introduce a truncation to determine correlation properties of the system. The Langevin equation with the exponentially correlated noise resolves itself to a two-dimensional Fokker-Planck equation which can be solved by a method of characteristics and its solutions also represent the Levy stable distribution. Its width, for a given time, is smaller than for processes in the white noise limit.

The multiplicative noise in the Langevin equation can make the variance finite if interpreted in the Stratonovich sense. Such a process – a generalised Ornstein-Uhlenbeck process – has been applied as a stochastic driving in a dynamical equation. The resulting distributions have the same shape as those of the noise and the tails are steeper than for the Levy stable distribution. The system is characterised by a subdiffusive motion. It has been demonstrated that including a finite inertia essentially modifies the distributions: for a small mass, a white-noise limit corresponds to the Stratonovich interpretation, whereas the distribution tails agree with the Itô interpretation if the mass is very large.

The dynamics becomes more complicated when we introduce a nonlinear deterministic force. The stochastic motion in a bistable, periodically modulated potential was analysed. The mean first passage time was calculated as a function of the multiplicative noise parameter for different values of the stability index and size of the barrier. Dependence of the output amplitude on the noise intensity reveals a pattern typical for the stochastic resonance and its properties, namely the height and position of the peak, depend on the system parameters and on a specific interpretation of the stochastic integral.

If the jumping rate in jumping process depends on the process value, one may observe long-tail distributions and finite correlations; they can assume an arbitrary form, in particular, a power-law. Such a process, a kangaroo process, was considered from the point of view of the transport properties. The stationary solution of the master equation for the case of power-law correlations decays with time, but a simple modification of the process makes the tails stable. Long tails of the distribution are suppressed by long waiting times, due to the variable jumping rate, and the variance becomes finite. It rises with time faster than linearly and the diffusion is anomalously enhanced, in contrast to a process which follows from the superposition of the Ornstein-Uhlenbeck-Levy processes of always divergent variance.

ULTRARELATIVISTIC NUCLEAR PHYSICS AND HADRON STRUCTURE STUDIES

With the advent of the SPS, the Relativistic Heavy Ion Collider (RHIC) and the Large Hadron Collider (LHC), it became possible to create the state of matter which existed a few microseconds after the Big Bang, when the temperature of the universe was several trillion degrees. The properties of such matter can only be investigated in the laboratory, as this information is inaccessible by any conceivable astronomical observations made with telescopes and satellites.

Along these lines of research, hadronic and nuclear reactions at relativistic energies were studied within the NA49, SPS and LHC-ALICE experiments. Although the NA49 experiment completed its data

collection a few years ago, there is still on-going analysis of the rich data taken so far. This includes studies of electromagnetic effects, as well as studies of the production of protons and antiprotons in Pb + Pb collisions at SPS energies.

In 2010, the first LHC data became available. The ALICE experiment collected large samples of pp, PbPb interactions at energies per nucleon pair varying from 0.9, 3.5 and 4 TeV for elementary collisions and 2.76 TeV for nuclear collisions. Also the very first data on pPb interactions at $\sqrt{S}$ = 5.02 TeV were gathered at the end of 2012. We were involved in the gas gain calibration of the ALICE Time Projection Chamber, using the radioactive isotope of ^{83}Kr, and extensively analysed the available data. Of particular interest to us were ultraperipheral and diffractive PbPb interactions and investigation of long-range correlations of charged particles in nuclear collisions.

SELECTED RESEARCH HIGHLIGHTS OF THE DIVISION OF NUCLEAR PHYSICS AND STRONG INTERACTIONS

Pygmy dipole resonances (PDR) are nuclear excitations described as oscillations of neutron excess against proton-neutron core in atomic nuclei. Their importance is in the information they carry on nuclear matter properties, such as symmetry energy. **The PDR**, measured so far using gamma and particle scattering, **has** recently, **for the first time, been investigated** by our group **with the use of heavy ion scattering reaction**. The ^{17}O beam bombarded a ^{208}Pb target at 20 MeV/A. The excited ^{208}Pb nuclei were selected by gating on inelastically scattered ^{17}O nuclei in the energy loss ΔE *versus* total kinetic energy (TKE) histogram (see the **Fig. 1**).

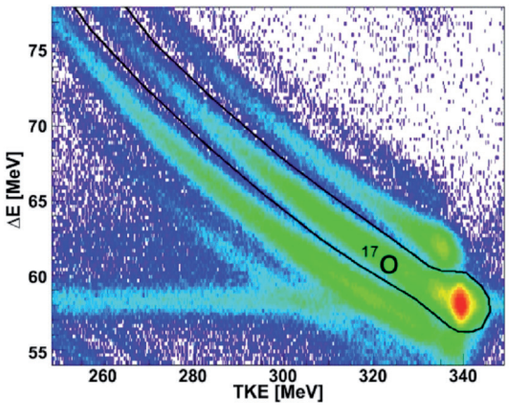

Fig. 1 *Energy loss ΔE versus total kinetic energy (TKE) measured by the silicon detectors of the TRACE array. The beam-scattered events correspond to indicated area.*

The gamma decay of the resonance states excited in ^{208}Pb was measured using $LaBr_3$ (3"x3") detectors and the HPGe AGATA Demonstrator array. Very good energy resolution was obtained for the spectrum collected with the AGATA array. It shows, apart from gamma rays from the decay of low energy excited states, also transitions in the higher energy region corresponding to the PDR. The gamma spectrum measured for ^{208}Pb in the PDR energy region is presented in **Fig. 2**. The most intense of the observed E1 transitions were interpreted as originating from PDR decay based on identification from previous experiments. This confirms the possibility of PDR excitations in experiments with heavy ion inelastic scattering reactions.

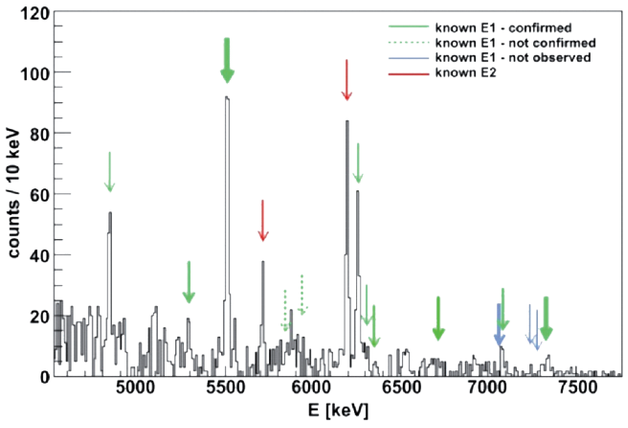

Fig. 2 *The gamma ray spectrum measured in the region of PDR with the AGATA Demonstrator array. Known E1 transitions, identified as PDR decay from ^{208}Pb, are indicated by arrows.*

The validity of the N = 40 subshell closure, established in ^{68}Ni by our group in 1995, has recently been verified in a broad region of neutron-rich nuclei. It turned out that protons above the closed Z = 28 number in Cu and Zn isotopes do not significantly affect the energy gap in the neutron single particle levels, but the N = 40 closure is destroyed rapidly in nuclei below Z = 28 and close-lying Fe isotopes already show

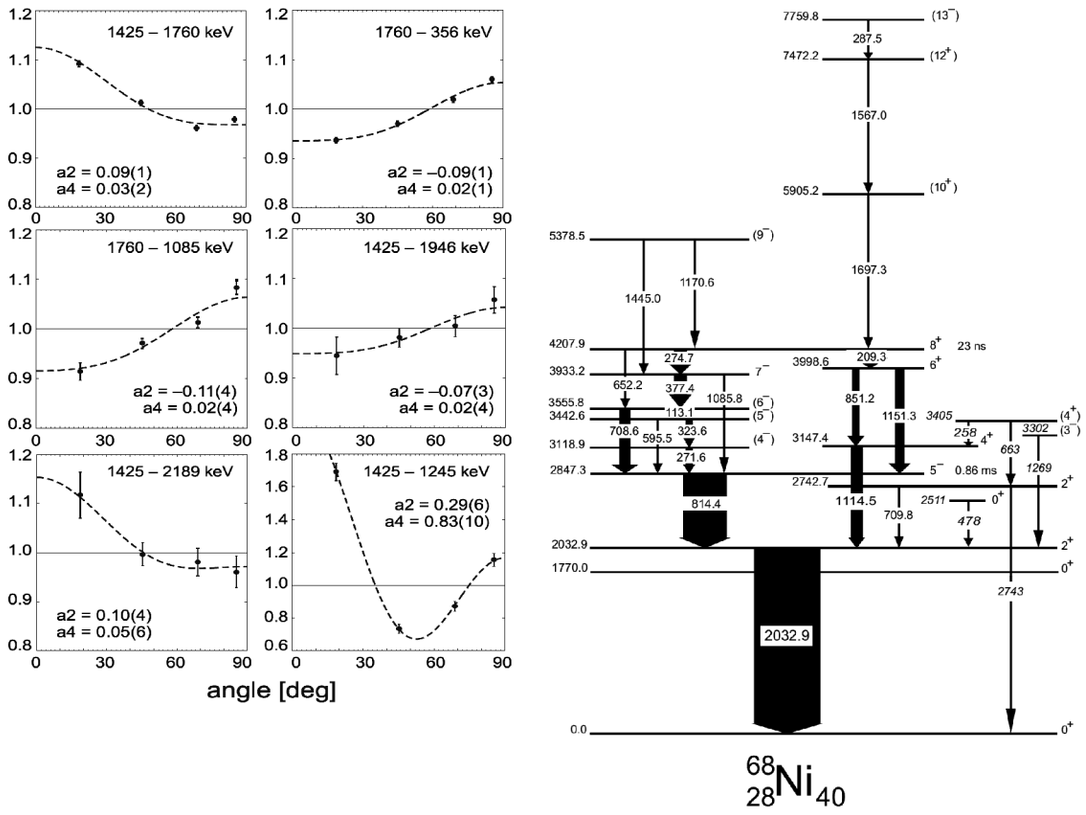

Fig. 3 Left: examples of γ-γ angular-correlation results obtained for ^{66}Ni. The energies of the analyzed transition pairs and the fitting results are indicated in each panel. Right: the ^{68}Ni level scheme established in the present study.

features of deformed nuclei. The clarification of the shell model description in Ni isotopes could be helpful better understanding the observed fast evolution of the structure, since the Z = 28 closed proton shell allows the changes involving pure neutron excitations to be separated. With this aim the data from the ^{238}U + ^{64}Ni experiment performed at the Argonne NL with the Gammasphere array were analysed and **previously inaccessible yrast structures in the neutron-rich ^{64,66,68}Ni isotopes** produced in quasi-elastic and deep-inelastic reactions **were identified**. The high quality of the gamma-coincidence data allowed us to obtain the most complete level schemes for all three isotopes up to about 10 MeV excitation energy. For most of the observed states, unique spin-parity assignments were obtained from the analysis of γ-γ angular correlation and of population intensities. Examples of angular correlation results for ^{66}Ni are displayed in the **Fig. 3 (left)**. The interpretation of level structures involved critical review of all previous experimental information available from earlier studies performed with a variety of nuclear reactions. The ^{68}Ni level scheme, displayed in the **Fig. 3 (right)**, includes the new levels above the 8^+ isomeric state and contains the most complete information established up to now on this doubly-magic nucleus. The shell-model calculations were performed for all three isotopes studied, using two different sets of interaction parameters. The energies of the calculated levels essentially agree with the experimental levels, yet the presently obtained detailed experimental information provides guidance for future theoretical efforts, which should be aimed at substantial improvement of the shell-model description.

Lifetimes of high-spin states in ^{69}As have been measured using Doppler shift attenuation technique. The nucleus of interest was populated in fusion-evaporation reaction ^{40}Ca(^{32}S, 3p)^{69}As at beam energy of 95 MeV. Evaporation residues were detected by the Cracow Recoil Filter Detector (RFD) in coincidence with γ-rays measured with the GASP germanium detector array. For the 1529 and 1923 keV lines, simultaneous fit to the spectra collected at all angles of detection (i.e., 35°, 60°, 72°, 90°, 108°, 120° and 145°) was performed and the resulting χ^2 map for 1529 keV line is shown in the **Fig. 4**. Analysis of the 1529 keV γ-line shape allowed to extract lifetime of 72(−45, +55) fs for the $33/2^+$ state at 7897 keV and, in consquence, transition quadrupole moment $Q_t(K=3/2) = 1.98$ (−0.5, +1.25) eb for that excitation; it also provided the lower limit 1.1 eb for Q_t of the $37/2^+$ state. TRS calculations predict in ^{69}As two positive parity collective structures which might correspond to the experimental "band 3" which includes the two mentioned states. Our results regarding transition quadrupole moment allowed to associate the "band 3" with an yrast, prolate-deformed structure with rather moderate deformation β~0.25, which appears in calculations in the rotational velocity range of 0.9–1.3 MeV.

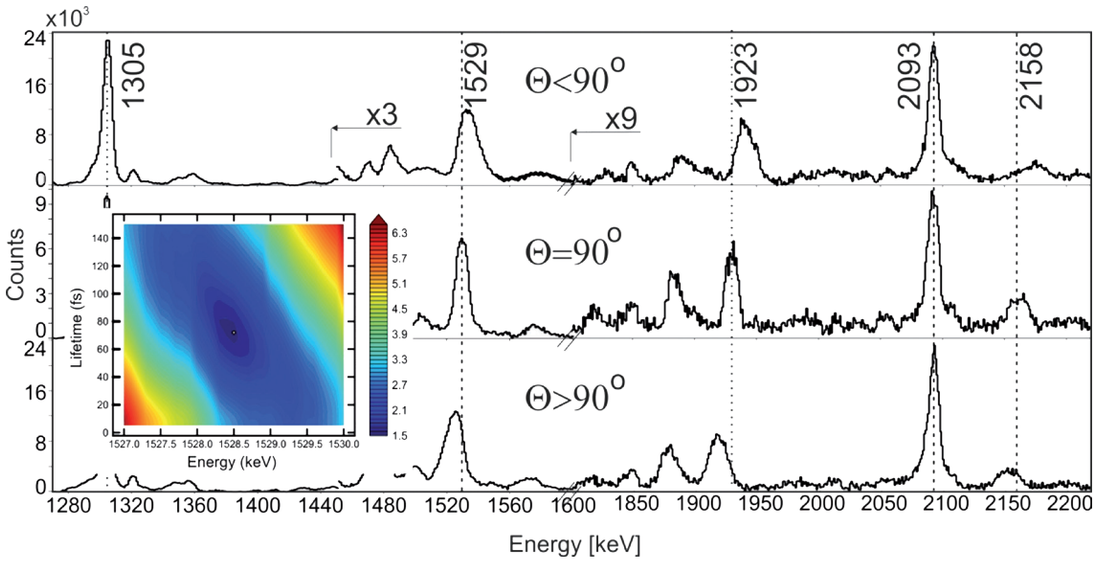

Fig. 4 *Double-coincidence spectra gated with the ^{69}As transitions, registered at forward (upper panel), 90 degree (middle) and backward (lowest) angles with respect to the beam axis. The 1529 keV, 1930 keV and 2158 keV lines corresponding to the consecutive transitions exhibit tails due to very short state lifetimes. For comparison, indicated are the sharp γ-lines at 1305 keV and 2093 keV resulting from excitations with longer lifetimes. The χ^2 map for the 1529 keV transition from the $33/2^+$ state at 7897 keV shows results of simultaneous fit to the spectra recorded at all angles. A minimum is located at E = 1528.5 keV and τ = 72(−45, +55) fs.*

With the rapid development of radioactive isotope beam facilities, theoretical predictions of properties of exotic nuclear species that are yet to be discovered are increasingly in demand. Due to the complicated form of nuclear interaction and its many-body character, the micro- and macroscopic models used for making such predictions are semi-empirical and contain a number of parameters adjusted to experimental data. Until very recently, attention has been paid only to the physical aspects of a model. The *technical* side of the associated parameter estimation problem has not been considered in detail. Therefore, the predictive power of existing models could not be determined since the statistical uncertainties of models parameters were not evaluated, leaving the uncertainty of theoretical predictions mostly unknown.

Our group has been one among the first to notice this serious limitation and began a dedicated **research program to assess the predictive power of nuclear structure models.** To start, we chose

the micro- and macroscopic Skyrme-Hartree-Fock and Woods-Saxon mean field models. By using nonlinear regression techniques and corresponding sensitivity analysis and regression diagnostics, we have shown that estimation of the parameters of the analysed models is an example of ill-posed inverse problem. This significant result indicates that the obtained parameterizations are very sensitive to experimental data used in the fit and to details of minimization procedure applied. Consequently, the optimal values for model parameters cannot be resolved unequivocally. The obtained parameters have very large statistical uncertainties and are correlated with other fitted parameters. This undesirable feature is not easy to recognise without a full statistical analysis. The striking feature is that the same set of experimental data can be described equally well with a number of different parameterizations. This situation occurs for mean field models of nuclear structure, where many different parameterization exist and give equivalent results.

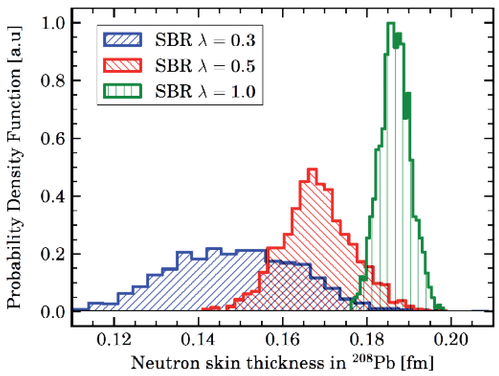

Fig. 5 *The value of neutron skin thickness of ^{208}Pb as predicted by Skyrme-Hartree-Fock model. The predictions are shown for different values of regularization parameter λ. The higher value of λ parameter corresponds to a model in which higher weight is put on a priori information.*

To obtain reliable parameterizations with a determined predictive power we proposed the application of regularization techniques – a standard tool of applied statistics that has never been applied in nuclear structure physics. Results obtained with the methods of Tikhonov regularization and Bayesian Inference method suggests that the inclusion of *a priori* knowledge about the model parameters can significantly increase the predictive power of a model and reduce correlation between the model parameters.

One part of the experimental program of the WASA at COSY collaboration is the **investigation of the ABC (Abashian–Booth–Crowe) effect**. The ABC effect is an enhancement in the s-wave pion–pion invariant mass near threshold seen in inclusive measurements of two pion production in nuclear fusion reactions. New, kinematically complete measurements of the double-pion fusion reaction $dd \rightarrow {}^4\mathrm{He}\pi^0\pi^0$ in the energy range 0.8–1.4 GeV were performed with high statistics. The observables are consistent with a narrow resonance at m = 2.37 GeV + $2m_N$, $\Gamma \approx 160$ MeV. The resonance position is the same as that of the double-pion fusion reaction $pn \rightarrow d\pi^0\pi^0$ (m = 2.37 GeV, $\Gamma \approx 70$ MeV). The increase in the resonance width can be attributed to Fermi motion of the nucleons in the initial and final nuclei. Using the *pn* resonace formation hypothesis, one is able to describe the differential cross sections.

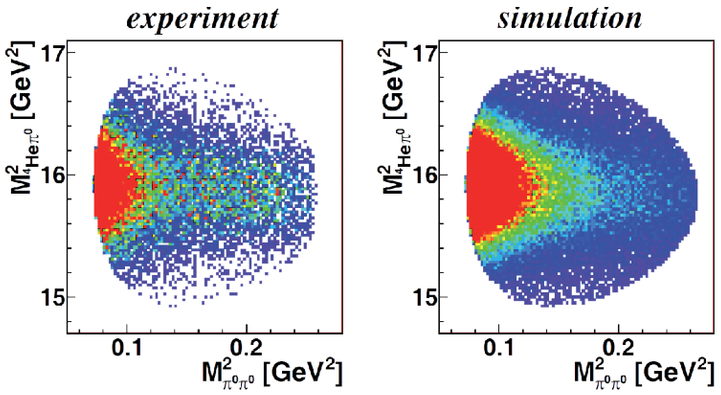

Fig. 6 *Dalitz plot of $M^2{}_{^4\mathrm{He}\pi^0}$ versus $M^2{}_{\pi^0\pi^0}$ at the energy of the peak cross section ($\sqrt{s}$ = 4.24 GeV). Left: experimental data, right: simulation with s-channel pn resonance included.*

A high-precision experiment to determine the η mass was performed **at the COSY–ANKE facility**. The $dp \to {}^3\mathrm{He}\eta$ reaction at low excess energies was used. The η mass was determined only from kinematics by considering the production threshold. To obtain the mass of η with high precision, very accurate determination of the beam momenta is needed. This was achieved by using a polarized deuteron beam and artificial depolarizing spin resonance induced by a horizontal rf magnetic field from a solenoid. Such depolarizing resonance occurs at a well defined frequency. A relative precision of $3{\cdot}10^{-5}$ for values of beam momenta around 3 GeV/c was achieved. Full geometrical acceptance was extensively used for final alignment of the spectrometer by studying 3He final state momenta as a function of the centre-of-mass angles. The obtained value for the eta mass is m_η = (547.873 ± 0.005(stat) ± 0.027(syst)).

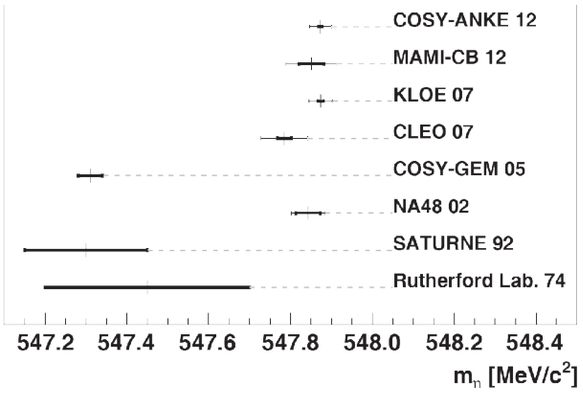

Fig. 7 η *mass obtained by the COSY-ANKE facility in comparison with results of other experiments.*

The cross section for the exclusive production of two pions in ultraperipheral ultrarelativistic heavy ion collisions was calculated in the impact parameter space equivalent photon approximation. Both **the total cross section and angular distributions for the $\gamma\gamma \to \pi^+\pi^-$ reaction were calculated for the first time**. The obtained results are in good agreement with world experimental data in a broad range of $W_{\gamma\gamma}$ energies (see **Fig. 8**). Several mechanisms were identified: nine different s-channel resonances, dipion continuum, pQCD mechanism proposed by Brodsky and Lepage, as well as the handbag mechanism proposed by Diehl, Kroll and Vogt. **Fig. 9** shows the resonance contribution of the $\rho^0(770)$ meson, $\rho^0(1450)$ excited state and γγ fusion in ultraperipheral Pb-Pb collisions at $s_{NN}^{1/2}$ = 3.5 TeV. This calculations demonstrate that the cross section for the $\rho^0(1450)$ resonance is about a factor of 20 smaller than that for $\rho^0(770)$. The exclusive production of ρ^0 meson in γIP and IPγ mechanism is interesting by itself. Our calculations agree with STAR experimental data **(Fig. 10)**. The good agreement allowed us to make first estimate of the double ρ^0 production.

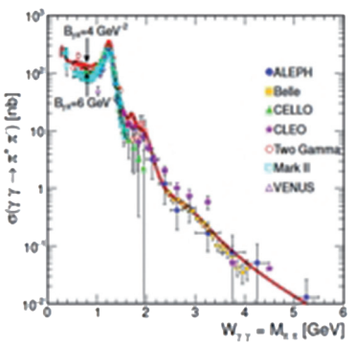

Fig. 8 *The total cross section* $\gamma\gamma \to \pi^+\pi^-$ *for* $|\cos\theta| < 0.6$. *Comparison of our results with experimental data.*

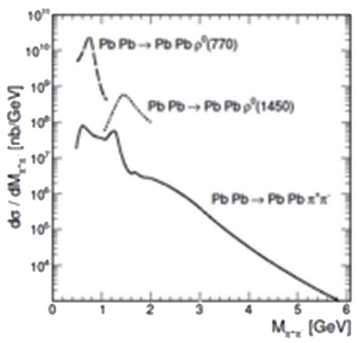

Fig. 9 *Invariant mass distribution of* $\pi^+\pi^-$ *from the decay of* $\rho^0(770)$, $\rho^0(1450)$ *decay and the* γγ *fusion.*

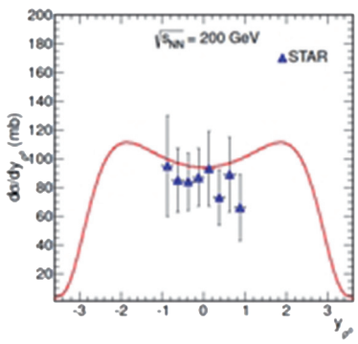

Fig. 10 *Distribution in* ρ^0 *rapidity for single meson production with STAR experimental data.*

We have also considered the **exclusive π^0 meson production in the $pp \to pp\pi^0$ reaction** and presented predictions **for the RHIC and LHC**. The bremsstrahlung contributions dominate at large (forward, backward) rapidities and cross section of the order of mb is predicted, see **Fig. 11** (left panel). This process constitutes diffractive non-resonant background that contributes at small π^0p invariant mass and could be therefore misinterpreted as the Roper resonance. We suggest a search for the odderon contribution at

midrapidity and at $p_{t,\pi} \approx 0.5$ GeV. The bremsstrahlung mechanisms contribute also to the $pp \to p(n\pi^+)$ reaction. Both channels give a sizable contribution to the low-mass single diffractive cross section and must be included in extrapolating the measured experimental single diffractive cross section. The integrated diffractive bremsstrahlung cross section for the exclusive $pp \to pp\gamma$ is only of the order of μb. We considered different mechanisms for the first time in the literature (see **Fig. 11** – right panel).

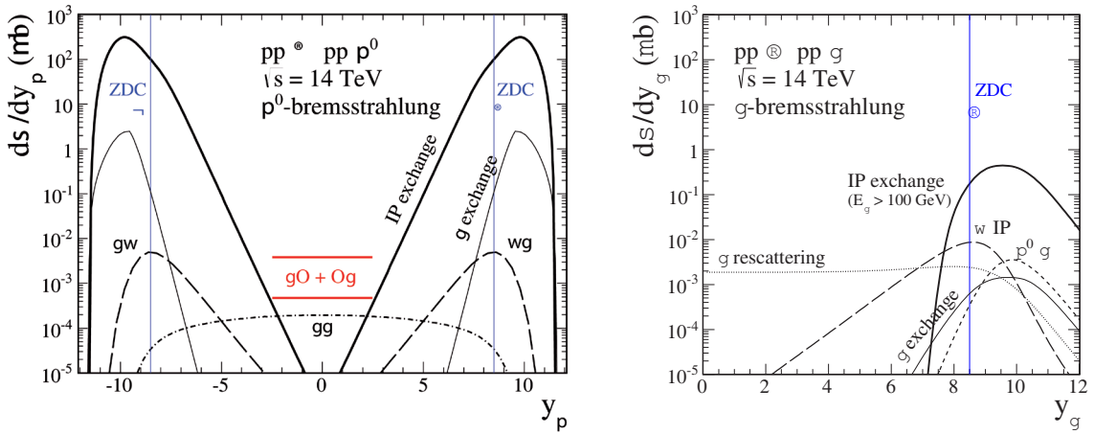

Fig. 11 *The rapidity distribution for $pp \to pp\pi^0$ (left panel) and $pp \to pp\gamma$ (right panel) at c. m. energy $s^{½}$ = 14 TeV. The π^0- and γ-bremsstrahlung mechanisms contribute at large forward and backward rapidity regions. The contributions from other mechanisms are also shown, e.g., the photon-odderon exchange (γO + Oγ) contributes at midrapidity of pions. The lower limit for the CMS ZDC detectors is shown by the vertical lines.*

Analysis of azimuthal anisotropies plays a key role in studies of ultrarelativistic heavy ion collisions presently performed at the SPS (CERN), at RHIC (BNL), and finally at the LHC (CERN). Since the primary nucleon-nucleon collisions are believed to be insensitive to the reaction plane, azimuthal anisotropies may bring information about collective phenomena occurring in the collision. One of the principal observables is the directed flow, $v_1 = \langle \cos(\phi) \rangle$, which provides information on the sideward motion of produced particles.

The **study** which we began in 2012 addresses the problem **of the electromagnetic component of directed flow**. We investigated the influence of electromagnetic repulsion (attraction) of positively (negatively) charged pions by the *spectator systems* on their momentum vectors observed in the final state of the reaction, and on resulting azimuthal anisotropies. An example of the result of our study is presented in **Fig. 12**.

As apparent, the spectator-induced electromagnetic force exerts *a noticeable influence on the directed flow of positive pions*. While our Monte Carlo calculation assumes a fully azimuthally-symmetric initial emission of pions (*i.e.*, no flow induced by the strong interaction before the action of the electromagnetic field), it predicts a well-defined pattern in the rapidity dependence of v1 in the final state of the reaction. In other terms, a purely *electromagnetically-induced directed flow of positive pions* is present in the collision. Our work demonstrates that the magnitude of directed flow induced by this electromagnetic effect can be comparable to values of v_1 observed in experimental data. Moreover, we predict an *electromagnetically-induced splitting of values of v_1* for positive and negative pions. This is indeed observed in the data reported by the STAR experiment from the

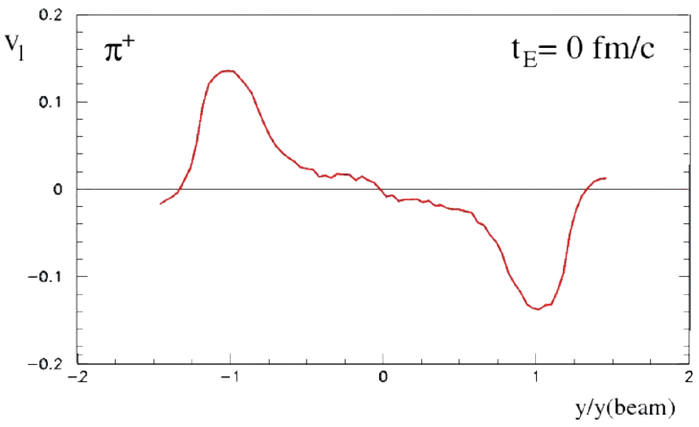

Fig. 12 *Dependence of the electromag-netically-induced directed flow of positively charged pions on the scaled pion rapidity y/y(beam). The simulation assumes the pion emission time t_E equal to zero (immediate pion creation).*

RHIC Beam Energy Scan. Finally, the magnitude of these effects appears to depend on the space-time scenario assumed for the process of pion emission in the course of the collision. Therefore, we conclude that the *electromagnetically-induced directed flow brings new information on the collision dynamics*.

In the so-called ultra-peripheral collisions (UPC) the impact parameter exceeds the sum of the nuclear radii, and, as a consequence, hadronic interactions are strongly suppressed while the strong electromagnetic fields produced by ultra-relativistic heavy ions allow the gamma-gamma and gamma-nucleus processes to be studied. If the photons interact coherently with all nucleons in the heavy ion, the pair transverse momentum of the produced charged tracks is small.

Recently, the ALICE experiment has measured coherent photo-production of J/Ψ at forward rapidities. Here, we report **first results obtained by the ALICE experiment on the cross section of the process $\gamma\gamma \to e^+e^-$** measured in the central rapidity region in Pb-Pb collisions **at $\sqrt{s_{NN}} = 2.76$ TeV**.

For this analysis, we used year 2011Pb-Pb data, representing integrated luminosity of ≈ 22 μb^{-1}. A dedicated UPC trigger was used in order to select events with charged tracks at central rapidity and to veto activity outside of the central rapidity region. Electron particle identification was performed by dE/dx measurement in the time projection chamber.

The cross section $\sigma(\gamma\gamma \to e^+e^-)$ has been measured in two invariant mass intervals, 2.2–2.6 GeV/c^2, and 3.7–10 GeV/c^2, avoiding the region around the J/Ψ resonance, and compared to the prediction of the STARLIGHT MC. In each invariant mass range we have selected events with two oppositely charged electron tracks with pair-p_T < 200 MeV/c and $|\eta_{1,2}| < 0.9$. No like-sign events were found. For the low invariant mass region we obtained 154 ± 11(stat.) + 17-11(sys.) μb, and for the low invariant mass region 91 ± 10(stat.) + 11-8(sys.) μb, this to be compared with the STARLIGHT prediction of 128 μb and 77 μb, respectively.

Fig. 13 shows invariant mass distributions for both invariant mass ranges, while the corresponding pair transverse momentum distributions are shown in **Fig. 14** indicating that STARLIGHT describes the data well.

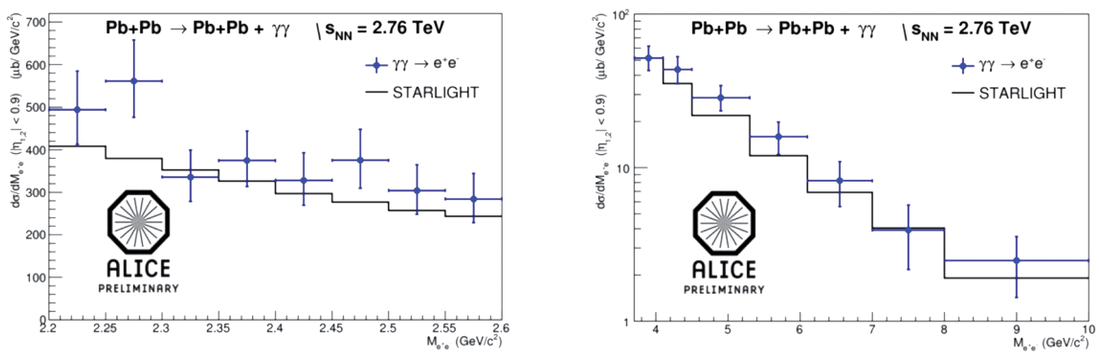

Fig. 13 *$\gamma\gamma \to e^+e^-$ invariant-mass differential cross-sections below (left) and above (right) the J/Ψ resonance, compared to the STARLIGHT prediction. Acceptance and efficiency corrections have been applies to each bin in invariant mass.*

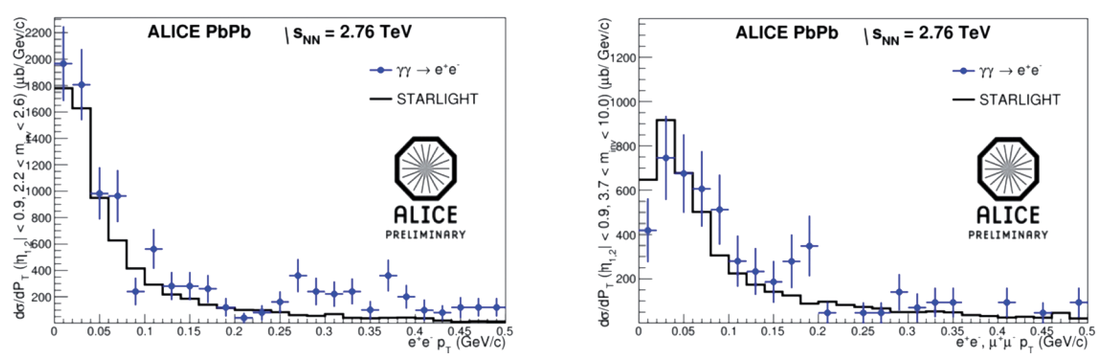

Fig. 14 *$\gamma\gamma \to e^+e^-$ pair-transverse-momentum distributions (containing detector effects) below (left) and above (right) the J/Ψ resonance, compared to the STARLIGHT prediction.*

We have shown that **the production of $c\bar{c}c\bar{c}$ in double-parton scattering** (DPS) offers good opportunity **to study DPS effects**. In the meantime, the LHCb collaboration presented new interesting data for simultaneous production of two charmed mesons of the same flavours.

The double-parton scattering unavoidably leads to the production of pairs of mesons: D_iD_j or $\bar{D}_i\bar{D}_j$. We calculated corresponding production rates for different combinations of charmed mesons as well as some differential distributions. Each step of the applied formalism (factorized Ansatz) is calculated in the kt-factorization approach, i.e., including effectively higher-order QCD corrections. Within large theoretical uncertainties the predicted DPS cross section is fairly similar to the LHCb results. As shown in the figure, rather good agreement has been obtained for transverse momentum distribution of D^0 mesons and D^0D^0 invariant mass distribution.

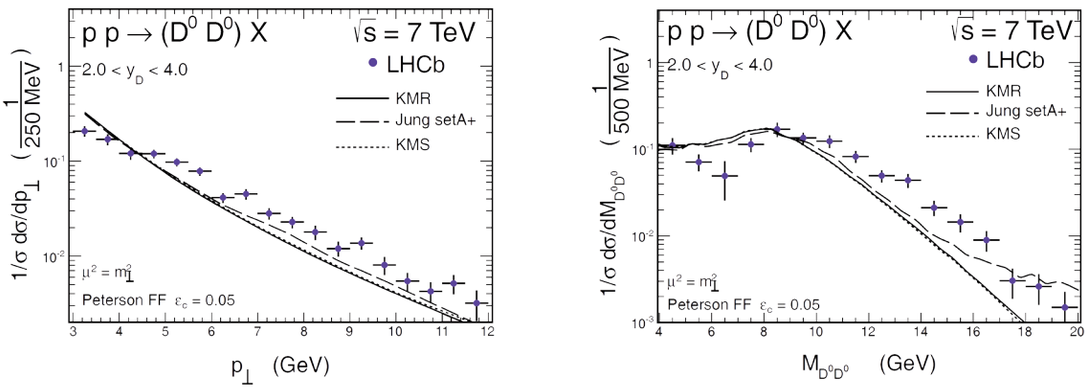

Fig. 15 *Transverse momentum distribution of D^0 mesons from the D^0D^0 pair (left panel) and $M_{D^0D^0}$ invariant mass distribution (right panel) contained in the LHCb kinematical region. The results are obtained with different models of unintegrated gluon distributions.*

Another confirmation of the presence of DPS effects is that their absence leads to a missing contribution to inclusive charmed meson production. The measured inclusive cross sections include events where two D (or two $\bar{D}$) mesons are produced. Therefore, in theoretical predictions, a correction for DPS effects should also be included.

The present study of $c\bar{c}c\bar{c}$ *reaction* in the k_t-factorization approach has shown that this reaction is an extremely good test for the presence of double-parton scattering effects.

Despite the fact the LHC shutdown is not finished yet, the preparation for the next one, scheduled for the 2018, is running. After the second LHC upgrade the luminosity and thus the high collision rate will prevent the effective performance of the ALICE Time Projection Chamber (TPC), which is rather slow detector, with the dead time of 80 μs. In order to secure the continuous detector readout, the replacement of the readout chambers is necessary. The standard proportional chambers are not suitable and the usage of a new technology is required. The best candidate for the new readout chambers are the so-called GEM (Gaseous Electron Multiplier) chambers. In the year 2013, **the extensive studies of GEMs performance including the MC simulations were carried out**. The **Fig. 16** shows, as the example, the dE/dx and the transverse momentum resolutions for GEM chambers for different numbers of the pile-up events. The event pile-up is the phenomenon directly related to the increased LHC luminosity and can affect the detector performance. These results will contribute to the Technical Design Report for the TPC Upgrade.

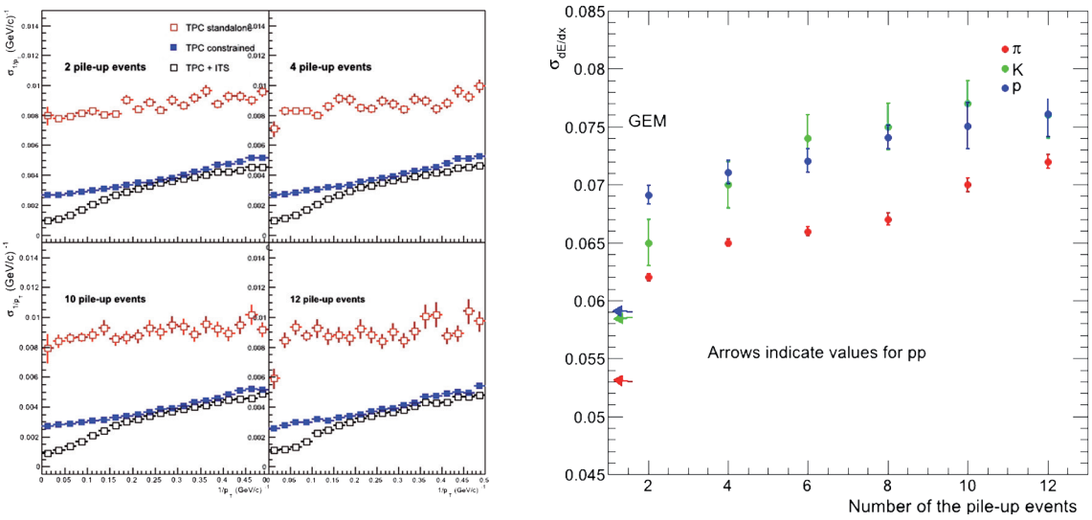

Fig. 16 *$1/p_T$ and dE/dx resolutions for different number of pile-up events in Pb + Pb collisions (simulations).*

In so-called ultra-peripheral collisions (UPC), the impact parameter is exceeding the sum of the nuclear radii, and, as a consequence, hadronic interactions are strongly suppressed, while the strong electro-magnetic fields produced by ultra-relativistic heavy ions allow for the study of gamma-gamma and gamma-nucleus processes. Recently, the ALICE experiment has **measured coherent photo-production of ρ^0 meson in ultra-peripheral Pb + Pb collisions at mid-rapidity at $\sqrt{s}NN = 2.76$ TeV**. For this process there exist a number of model predictions, cf. Fig 2, which differ by almost a factor of two at mid-rapidity. Therefore it is interesting to measure it.

For this analysis, we have used Pb+Pb data collected in 2010. A dedicated UPC trigger was used in order to select events with charged tracks at central rapidity and veto activity outside of the central rapidity region. We have selected events with exactly two oppositely charged pion tracks with pair-p_T < 150 MeV/c. **Fig. 17** shows the invariant mass distribution, corrected for detector acceptance and efficiency.

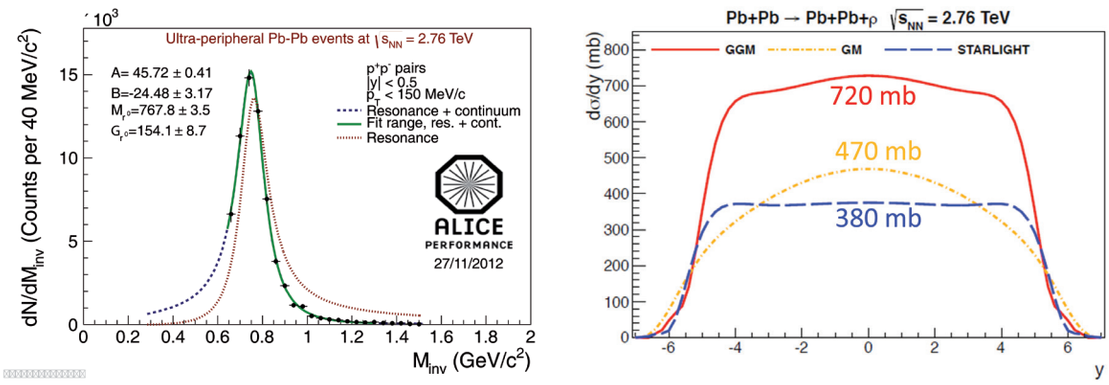

Fig. 17 *Left: ρ^0 invariant-mass spectrum corrected for detector acceptance and efficiency; Right: Model predictions for the cross section of coherent ultra-peripheral photo-production of ρ^0 in Pb+Pb collisions.*

In 2012, we completed the **construction of the KRATTA (Kraków Triple Telescope Array) multi-module array for charged particle detection**, together with its electronic system and dedicated software. We also performed initial data analysis, identification and energy calibration of the data obtained in the

ASY-EOS experiment performed in May 2011 at GSI Darmstadt. Triple telescopes allowed us to measure energies and to perform identification of light charged reaction products in a broad energy range, with a low energy threshold. The system consists of 38 independent, identical, logarithmic telescope modules which can be arranged in various configurations. Thanks to the novel detection technique, application of low-noise electronics, digitization of the pulse shapes and pulse shape analysis, the system is able to perform precise measurements at low and at high energies. The applied pulse shape analysis makes it possible to decompose the measured waveforms into individual, ballistic deficit-free components. The energy thresholds are reduced, resolution is improved and, in particular, background due to the gamma rays, neutrons and secondary reactions of charged particles in the detector material can be treated.

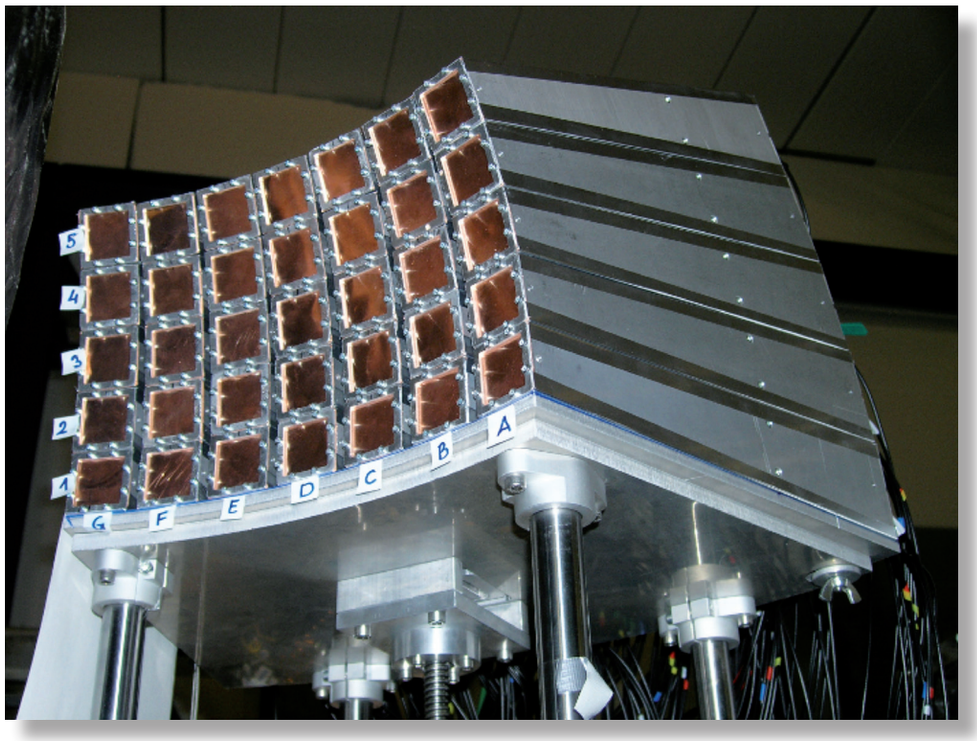

Fig. 18 *The main characteristics of KRATTA:*

- *broad energy range (from ~2.5 do ~260 MeV for protons),*
- *mass identification of charged particles with Z < 7,*
- *solid angle of ~160 msr (~4.5 msr/module for 40 cm distance),*
- *modular design, versatility, portability,*
- *application of three identical, catalog photodiodes for direct detection (Hamamatsu) and of two CsI(Tl, 1500 ppm) crystals as active elements in each module,*
- *application of own design, low noise preamplifiers,*
- *digitization of pulses (15×V1724 CAEN, 100 MHz, 14 bits),*
- *possibility of pulse shape analysis,*
- *stable, remote controlled, own design VH system,*
- *high quality with moderate price.*

In order to perform the final data analysis and model comparison we have developed a software replica of the detection system in the FairRoot environment and adapted the neutron identification procedures in the LAND detector for the needs of ASY-EOS data analysis.

The research reported herein was performed pursuant to internal projects: [201, 202, 203, 204, 207, 208]; [E1, E9, E17, E21, E23, E24, E25, E28, E36, E51, E52, E53]. See Annexes I, IIA and IIB.

III. DIVISION OF CONDENSED MATTER PHYSICS

Materials science is an interdisciplinary field which deals with physical and chemical properties of materials, in the search either for materials with desirable physical properties or in the development of materials able to acquire such properties. Thus, on the one hand, the characteristic features of materials are studied to seek their appropriate applications and, on the other – materials are being developed to suit a particular requirement. Applications of such materials in various areas of technology must necessarily follow from a thorough understanding of their physical properties, hence the basic solid-state or condensed matter physics research component is of key importance in the work of our Department. How important is condensed matter physics to the society may be best illustrated by the transistor, laser, integrated chip or the solar panel, all of which could only be devised with the knowledge of solid-state physics and of materials research. As elements of modern telecommunication, digital technology or supply of energy, they have radically changed our world and our society. Such advances in materials science would not have been possible without quantum mechanics which provided scientists with a deep understanding of the chemical and physical properties of, e.g., semiconductors, superconductors or materials with complex magnetic properties. New synthetic man-made materials, such as polymers, liquid crystals or multicomponent systems exhibit properties which may far exceed those of any material of natural origin. Here, quantum chemistry which applies quantum formalism to large systems, aided by extensive computer modelling and simulations, provides the necessary theoretical background. Developed in parallel are unique technologies of material preparation, such as methods of applying coatings of molecular thickness, controlling the magnetic properties of thin films, of composing layers of materials uniquely doped to modify their conductivity. We are now also able to manufacture and study materials of nanometre dimensions – nanostructures. New fields in solid state physics research have emerged, such as the physics of low-dimension systems, of amorphous materials, of quasicrystals, of granular materials and of soft matter, overlapping not only with other areas of physics research, such as plasma or low-temperature physics, but also with molecular biology or biomedicine. Indeed, with the introduction of thousands of new materials with astonishing properties, our everyday life becomes easier, healthier and more exciting.

In the Division of Condensed Matter Physics most of our research is conducted in our own laboratories on IFJ PAN premises, at the **Department of Structural Research** (Laboratory for Magnetic Studies, Spectroscopic Research Laboratory, Laboratory for Structural Investigations, Positron Annihilation Laboratory, Polarizing Microscopy Laboratory and Calorimetric Laboratory) and at the **Department of Magnetic Resonance Spectroscopy**. *Ab initio* calculations are performed mainly in the **Department of Materials Research by Computers**. Pioneering studies on fast dynamics and phase transitions of molecular crystals using NMR spectrometry and neutron scattering spectroscopy began already at the time the Institute of Nuclear Physics was founded, in close collaboration with research

centres abroad, such as Dubna (then USSR) or Kjeller (Norway). The tradition of close collaboration with leading laboratories abroad is being continued. Today the Departments closely collaborate, with the Laue-Langevin Institute in Grenoble (within a Belgian-Polish-Swedish consortium which we coordinate), the ISIS Rutherford Appleton Laboratory in Oxfordshire, FRMII in Munich, PSI in Villigen, the Helmholtz-Zentrum in Berlin, the Japan Atomic Energy Agency and the Joint Institute of Nuclear Research in Dubna. Our Laboratories also have extensive topical collaborations and exchanges with several research institutions in Poland and abroad, which offer their unique instrumentation and exploit our facilities in joint experiments and studies.

We focus our present studies on properties and processes in novel magnetic compounds, soft materials with tendency to glass formation, low dimensional and confined geometry systems and in materials of geological interest and potential applicability in the environment.

Novel molecule-based magnetic compounds attract much attention as they combine interesting magnetic, electronic and optical properties together with low weight, transparency and chemical sensitivity. Magnetism is an important and still growing area of condensed matter physics. While magnetic moments of atoms, ions or molecules are determined by the rules of quantum mechanics, magnetic properties of real systems are quite diverse and complicated. The reason for the variety of magnetic features is that magnetism is a collective phenomenon, strongly dependent on mutual interactions of an immense number of magnetic centres. Apart from understanding many aspects of magnetism, investigations in this field are aimed at designing so-called functional materials which may be used in modern technology, informatics, electronics or medicine. Switchable systems, the properties of which may be controlled by external stimuli, such as temperature, light, pressure and electric or magnetic fields, are of special interest here. Of interest are also molecular compounds which can reversibly change their ordering temperature T_c and their coercive field H_c upon hydration/dehydration processes (magnetic sponges) or on sorption/desorption of various guest molecules.

Soft matter, a term coined by Pierre-Gilles de Gennes, encompasses a broad range of organic materials, such as polymers, plastic crystals, liquid crystals, colloids, amphiphiles and gels, exhibiting phases of various long range ordering of molecules and multiscale dynamics. We study substances (in bulk and enclosed in cavities) of relatively flexible molecules, often interconnected by hydrogen bonds, forming liquid-like and solid-like phases. Our goal is to identify polymorphism of solid state and/or liquid state, and to characterize phase transitions found as well as changes of their molecular motions which follow after cooling/heating cycles or on pressure growth. This is accomplished by a wealth of experimental techniques, looking at molecular structure, interactions and dynamics, to reveal the complex interplay among them. We focus on understanding of the crystallization vs. vitrification pattern in phases of various degrees of long range order.

Molecules confined in nanoscale cages represent a particularly interesting system for investigation by means of nuclear magnetic resonance and dielectric relaxation methods. New kinds of dynamics are detected, such as collective motions and those typical for the gas phase, liquid-like layers or partially immobilized molecules. In some cases a new thermodynamic phase appears and a tendency to glass formation. Theoretical analyses point to new phenomena, such as supersonic and subsonic surface waves which require experimental confirmation.

Materials of geological interest and potential applicability are also studied at our Division. We use theoretical calculations and experimental methods to understand the features of some minerals important for power generation and for chemical industry, and those found in Earth's mantle. Our goal is also to investigate molecular systems of potential applicability in molecular spintronics, in hydrogen storage or for reduction of CO_2 in the environment.

SELECTED RESEARCH HIGHLIGHTS OF THE DIVISION OF CONDENSED MATTER PHYSICS

Deformation of the Mn_2-$C_4H_4N_2$-[$Nb(CN)_8$] crystal structure, caused by dehydration or external pressure leads to strengthening of ferrimagnetic interactions between Mn and Nb centres. Together with our colleagues at the Jagiellonian University, we investigated the family of molecular compounds based on the octacyanido building block $[M(CN)_8]^{n-}$ (M = Nb^{IV}, Mo^{V} or W^{V}), forming Me_2-L-[$Nb(CN)_8$] networks, where Me = Mn, Fe or Ni and L stands for nonmagnetic organic ligand. That type of a ligand was found to significantly affect the structure and the overall behaviour of the material. The compound with L = $C_4H_4N_2$ turned out to be exceptionally interesting, as it showed two-step magnetic sponge behaviour. Structural transformations provoked by dehydration in Mn_2-$C_4H_4N_2$-[$Nb(CN)_8$] bring about an increase in the magnetic ordering temperature T_c from 43 K for the as-synthesized sample, through 68 K for the partially dehydrated, and up to 98 K for the unhydrous phase. The characteristic features of all three phases are ferrimagnetism, zero coercivity field and the sharpness of the magnetic transition. We also observed an increase in the magnetic ordering temperature on applying external pressure, with T_c increasing from 43 K to 51 K under 0.57 GPa.

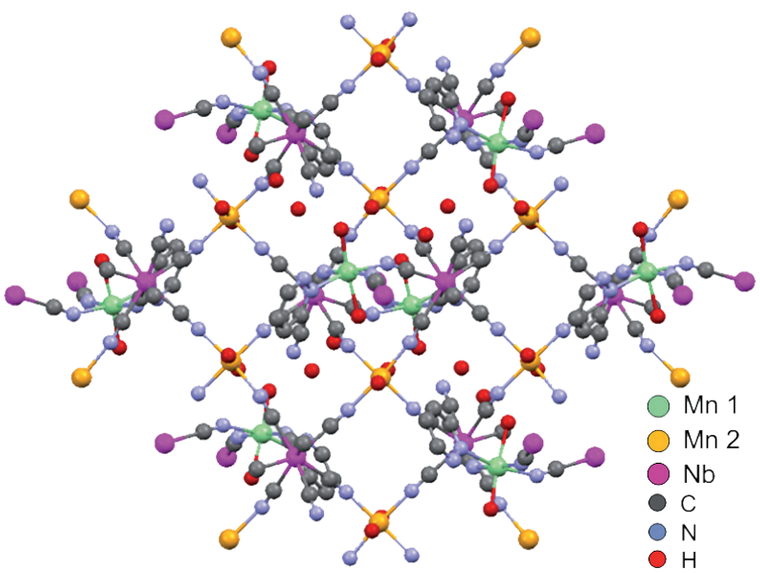

Fig. 1 *Structure of the Mn_2-$C_4H_4N_2$-[$Nb(CN)_8$] molecular network.*

The parameter n(T) describing the magnetocaloric effect (MCE) in the magnetic sponge according to $\Delta S \sim (\Delta H)^n$, turned out to be consistent with the mean field model and corresponded to β and γ critical exponents obtained from magnetization data. We have determined and analysed the MCE in all three phases of the Mn_2-$C_4H_4N_2$-[$Nb(CN)_8$] magnetic sponge. This was the first study of MCE in the ordered molecular magnet other than the popular Prussian blue analogues and moreover the first for a switchable one. The maximum entropy changes ΔS_{max}, detected for $\mu_0\Delta H$ = 5 T were equal to 5.36 J $mol^{-1}K^{-1}$ at T = 43 K (for phase **1**), 3.33 J $mol^{-1}K^{-1}$ at 68 K for the dehydrated (phase **2**) and 3.38 J $mol^{-1}K^{-1}$ at 98 K for the anhydrous phase (phase **3**). It is worth noting that the decrease of ΔS by a factor of 0.6 observed for phases **2** and **3** in comparison to **1** corresponded to the downshift of the AC susceptibility of these phases. Because MCE is an intrinsic thermodynamic property, its value and dependence on magnetic field should be related to other magnetic characteristics of the material. Magnetization measurements, carried out with the aim to determine the entropy changes, were also used to extract critical exponents. Due to the magnetic sponge behaviour, pressure dependence of T_c and the significant value of MCE, the Mn_2-$C_4H_4N_2$-[$Nb(CN)_8$] compound may be regarded as an example of a multifunctional molecular material.

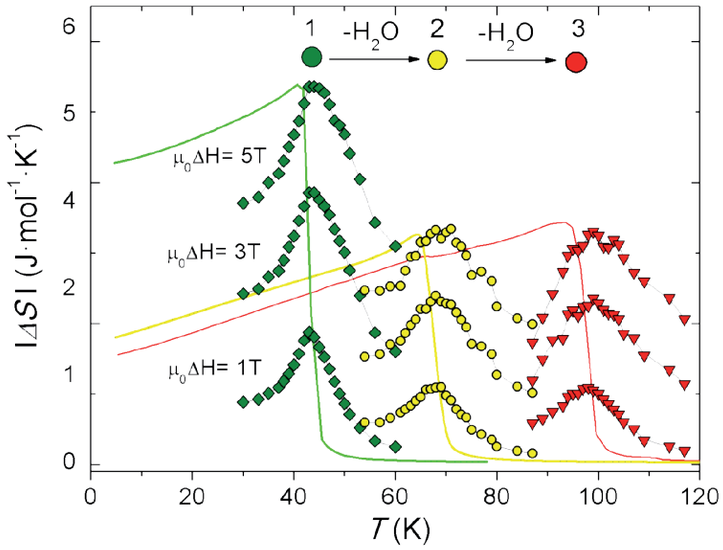

Fig. 2 *Magnetocaloric effect in the Mn_2-$C_4H_4N_2$-$[Nb(CN)_8]$ magnetic sponge expressed as the magnetic entropy change ΔS of phase 1, 2 and 3 for $\mu_0\Delta H$ = 1, 3, and 5 T. Solid lines show AC susceptibility for appropriate phases.*

Evolution of the magnetic structure from the spiral through the conical up to the ferromagnetic phase in an external field has been revealed for the semiconducting $ZnCr_2Se_4$ spinel doped with Ce. $ZnCr_2Se_4$ is a matrix for various diluted systems, where effects of site disorder, lattice frustration and random distribution of spin interactions create novel potential applications in spin-based electronic technology. Despite the presence of strong ferromagnetic interactions, the compound orders antiferromagnetically at T_N = 20K, showing a complex spin configuration. We dealt with single crystalline samples of $ZnCr_2Se_4$ doped with nonmagnetic Al, Ga, In and magnetic Ce. From the measurements of magnetic field dependence of AC susceptibility, two characteristic critical fields have been determined: H_{c1} related to the metamagnetic threshold, where the simple spin spiral transforms into conical magnetic structure, and H_{c2}, at which the conical magnetic structure transforms into the ferromagnetic phase. Based on the temperature dependence of H_{c1} and H_{c2}, the phase diagram of a spin system has been concluded. The broad maxima in AC susceptibility observed at $T_m > T_N$ are due to ferromagnetic fluctuations which appear at a strong enough magnetic field.

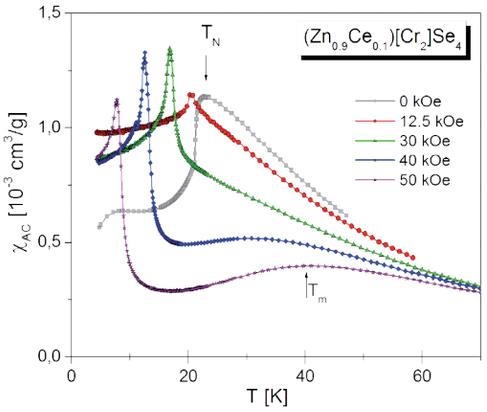

Fig. 3 *AC magnetic susceptibility at different external magnetic fields for $(Zn_{0.9}Ce_{0.1})[Cr_2]Se_4$.*

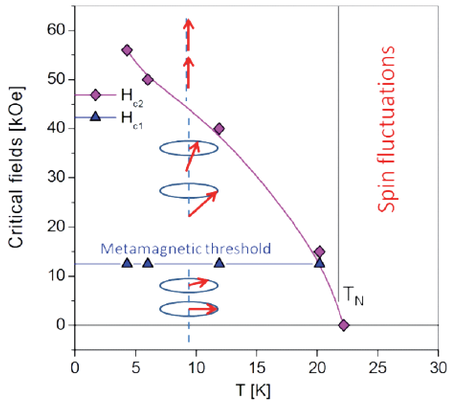

Fig. 4 *Phase diagram of $(Zn_{0.9}Ce_{0.1})[Cr_2]Se_4$ determined from the temperature dependence of critical fields H_{c1} and H_{c2}.*

We have analysed the properties of the quasi-1-dimensional molecular system $\{[Cu(dien)]_4[W(CN)_8]\}[W(CN)_8]_2$ with a nontrivial and complex topology, whose main structural element is a chain of spin ½ centre. Between the chains there is a regular network of isolated octacyanotungstate ions $[W(CN)_8]^3$. To obtain zero-field susceptibility of the chain segment, a semi-classical analytical approach was employed, where only one, namely the spin of the W^V ion, out of five spins ½ of the chain unit WCu_4 was treated as a classical commuting variable. The calculation of the field-dependence of the magnetization was performed by replacing the same spin with the Ising variable and applying the standard transfer matrix technique. The fits to experimental data were performed independently for susceptibility and magnetization. A relatively large ferromagnetic coupling (+4 to +7 cm^{-1}) was found within the chain, alternating with a small antiferromagnetic coupling (–1 to –0.6 cm^{-1}). A sizable antiferromagnetic interaction (–0.4 to –0.1 cm^{-1}) between the chain segments and the off-chain $[W(CN)_8]^{3-}$ ions was determined using the molecular field approximation. The magnetic properties of the family of other quasi 1-dimensional molecular compounds, $[MnR_4TPP][TCNE]$ (TPP – tetraphenylporphyrin, TCNE – tetracyanoethylene, R – functional group), were discussed and reviewed. Special attention was paid to magnetic relaxation and distribution of relaxation times, investigated by means of the AC susceptibility technique with or without external magnetic field. It was found that **slow relaxation, adequate in isolated single chain magnets (SCM) appears also in quasi 1-dimensional systems which show transition to long-range magnetic ordering**. Such slow relaxation becomes evident on application of an external magnetic field.

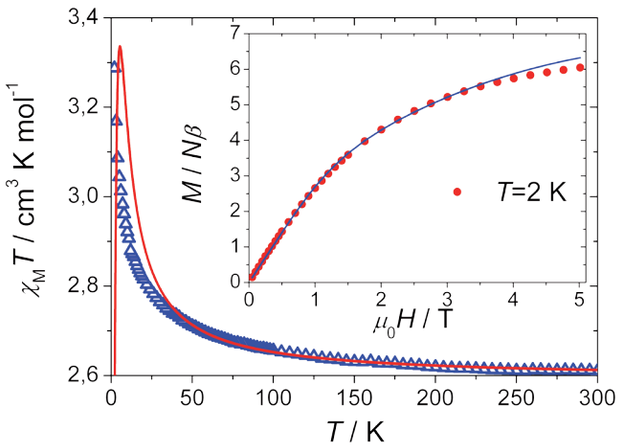

Fig. 5 *Experimental (symbols) and computed (lines) data for susceptibility and temperature product and for magnetization (inset) of the* $\{[Cu(dien)]_4[W(CN)_8]\}[W(CN)_8]_2$ *molecular chain.*

The critical behavior of three-dimensional molecule-based magnet $\{[Fe^{II}(pirazol)_4]_2[Nb^{IV}(CN)_8]\cdot 4H_2O\}_n$ **(FeNb) was studied with ac magnetometry and positive muon spin rotation in zero external magnetic field (ZF-μSR).** Characteristic oscillations observed in asymmetry spectra at temperatures below 8 K confirm the presence of quasistatic local magnetic field at muon stopping sites and hence indicate a long range magnetic order in agreement with the ac susceptibility measurements. Thermal dependence of internal magnetic field at the muon stopping site was examined, providing values of the static exponent β = 0.42(3) and the dynamic exponent w = 0.33(2). The β parameter corroborates value of static exponent γ = 1.38(8) obtained via ac magnetometry, suggesting that the FeNb belongs to the 3D Heisenberg universality class. Value of the exponent w close to 0.328 points towards the antiferromagnetic coupling between the magnetic moments of the compound.

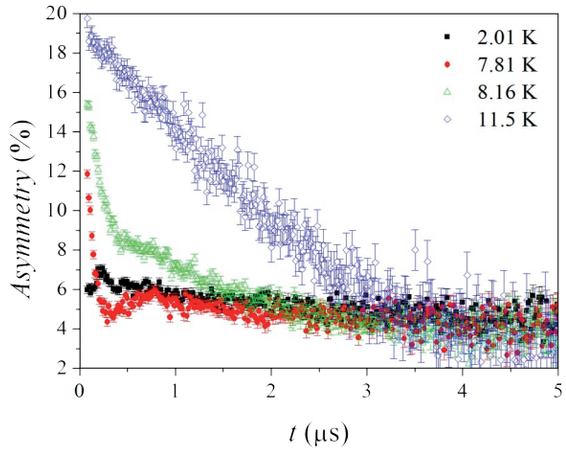

Fig. 6 *ZF-μSR asymmetry at temperatures below (full symbols), and above (empty symbols) transition temperature.*

Calorimetric studies of five liquid crystalline materials allowed us to identify the phase diagrams and complex dynamics. Interestingly, for nematic, smectic B and E and for orientationally (ODIC) and conformationally (CONDIS) disordered metastable crystalline phases, a tendency to glass formation was found, instead of ordered phase crystallization. Thermodynamic parameters and low temperature features of glasses with partial long range order of molecules and a conventional amorphous glass of isotropic liquid were compared. In the X-ray diffraction pattern of glass of smectic B (and of smectic E) a slightly disturbed hexagonal (orthorhombic) arrangement of molecules in the smectic layers was found. Besides, we regard the anomaly found in the temperature dependence of layer thickness as an additional signature of glass transition. For liquid crystalline material 4CFPB of fluorinated molecules, investigation of the influence of higher pressure on dynamics was performed up to 300 MPa using the dielectric relaxation method. In the isobaric experiment, vitrification of nematic phase occurred and reorientations of molecules around short axes, precession (both of superarrhenius type) and intra-molecular motions (Arrhenius-type relaxation) were identified. In the isothermal experiment a new liquid-like smectic phase was found with local motions not visible. For the main structural relaxation a single master curve of dielectric absorption at various temperatures and pressures was found. Changes of textures with temperature observed in polarizing microscopy were used to illustrate nematic phase vitrification and crystallization processes as well as transformation between crystalline phases of various order. Studies of chiral and non-chiral cyanobiphenyls, performed using the quasi-elastic neutron scattering method, allowed us to show the existence of reorientation of whole molecules around their long molecular axis and of diffusive motion of the terminal chains in both isotropic and nematic liquid phases. For branched molecules chain mobility was reduced. Dynamics of heptyl isotiocyanatobiphenyl liquid crystal with smectic E phase was studied in elongated nano-pores of 4–10 nm diameter using dielectric spectroscopy. It was found that, due to the influence of the pore surface, librational motions of molecules close to the pore walls appear and smectic E-phase ordering was imposed by short-range molecular arrangements. We found that pore size affected the molecular dynamics.

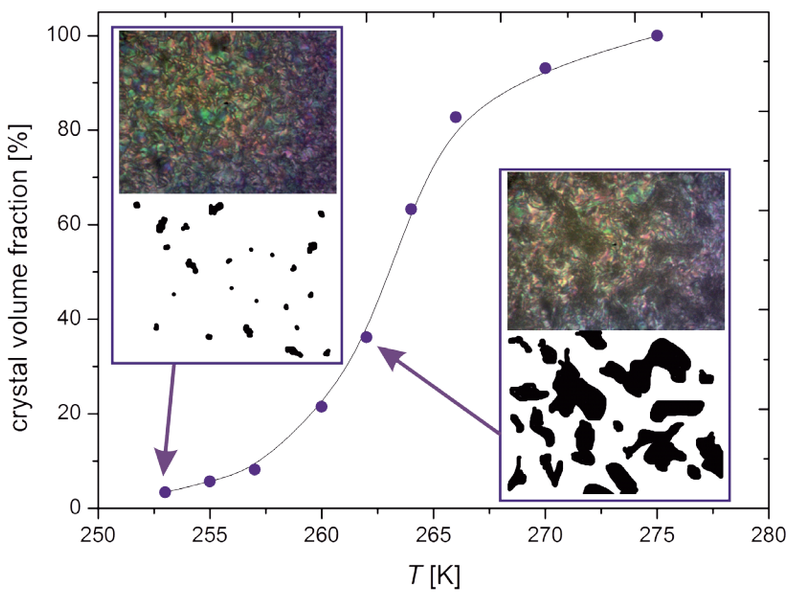

Fig. 7 *Crystal growth in the nematic phase of 4CFPB.*

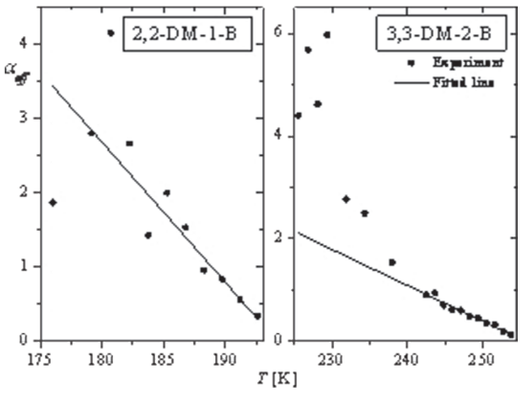

Fig. 8 *Experimental points (filled circles) and theoretical fitted lines of effective exponents α_{eff} as functions of temperature.*

The dependence of the specific heat on temperature for isomers of neohexanol 2,2-dimethylbutan-1-ol and 3,3-dimethylbutan-2-ol ($C_6H_{13}OH$ – 2,2-DM-1-B and 3,3-DM-2-B, respectively), ferroelectric pentakis methylammoniumundeca-chlorodibismuthate(III) ($[CH_3NH_3]_5Bi_2Cl_{11}$ – MAPCB) and liquid crystal 4-propyl-4'-thiocyanato-1,1'-biphenyl ($C_{15}H_{15}CNS$ – 3TCB) were analysed within the Landau-type expansion of the free energy density function. The conclusion is that in order to reproduce polymorphism of these substances one needs to deal with temperature dependent coefficients and exponents α_{eff} below the phase transitions. The transitions between the ODIC phases in 2,2-DM-1-B and 3,3-DM-2-B, and between the different crystalline phases of MAPCB and 3TCB occurred to be of the isomorphic type. Moreover, the values of the effective exponents point to a strong first order phase transition between the fully ordered crystalline phase and isotropic liquid, and to a very weak first order phase transition for melting of the ODIC phase.

Dynamics of whole molecules, hydrogen groups and hydrogen bonded clusters was found in plastic phases of 2,3 dimethylbutan-2-ol (the isomer of neohexanol) using the dielectric relaxation method. No tendency to glass formation, observed for all other isomers, was traced. Influence of the number of molecules in a cluster on vibrational spectra was shown – vibrations of OH bonds calculated for tetramers give the best agreement with IR and neutron scattering experimental spectra. For clusters of larger size the strength of OH bonding appears to be higher.

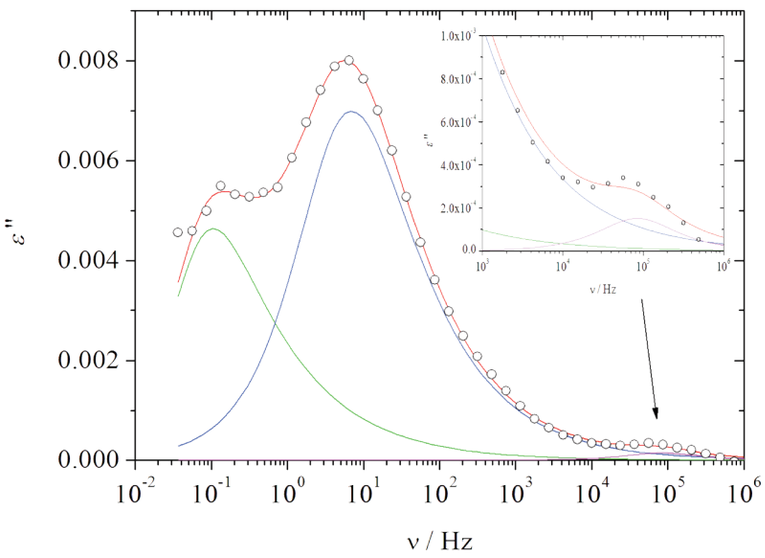

Fig. 9 *Complex dynamics in 2,3 dimethylbutan-2-ol as seen by dielectric spectroscopy.*

2D IR spectroscopy correlation analysis was used to elucidate the influence of the inter- and intramolecular interactions on conformational changes in phase transitions of the 4-bromobenzylidene 4'-alkyloxyanilines (nBBAA n = 4–12). First it was found that in the smectic A and the smectic B phases the molecules have the same conformational freedom as in the isotropic phase. For substances with n equal 4 and 5 the isotropic-smectic B transition starts by ordering of the phenyl rings rather than the alkyloxy chains. For substances with n = 6–12 along the isotropic – smecticA – smectic B transitions the molecules reorient faster and faster thanks to better organization of the alkyloxy chains.

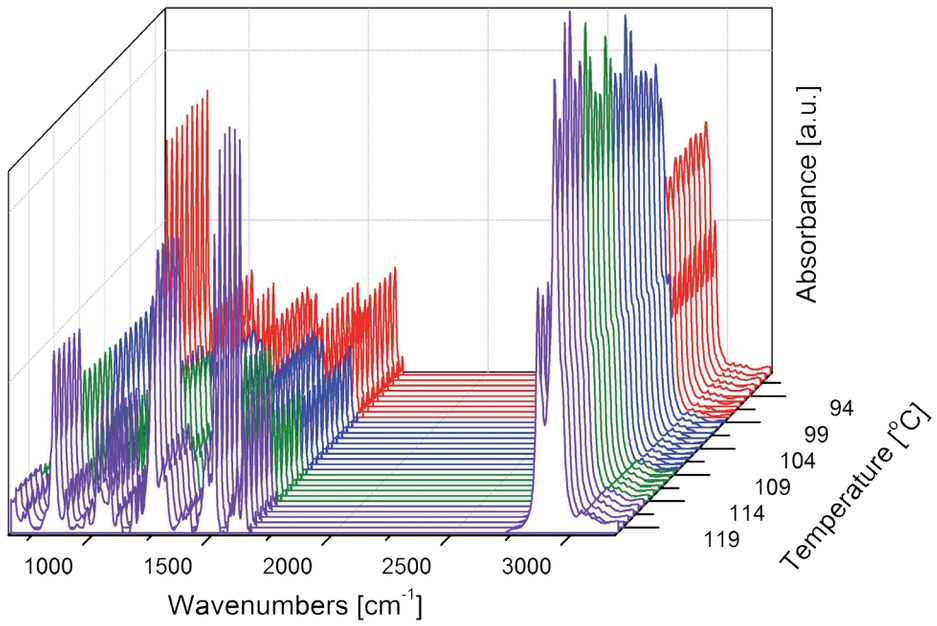

Fig. 10 *Temperature changes of the IR spectra for 4-bromobenzylideno-4'-dodecyloxyaniline in isotropic phase (violet) and SmA (green), SmB (blue) and crystalline (red) phases.*

Short-range order in otherwise disordered or partially ordered matter is now a well-established feature of soft matter. **DFT calculations proved that atactic polystyrene interactions of local dipole moments and π–π coupling between aromatic rings are responsible for diffuse neutron scattering peaks**. Now it is becoming evident that this type of interaction brings about a specific configuration in hydrogen-bonded chains of resorcinol as well as texture formation in 9OSBchol. This study, eventually aimed at finding bent-core (banana-type) mesogens of potential interest for industry, has been undertaken in order to understand the influence of local ordering interactions on the polymorphism of these substances and their mixtures.

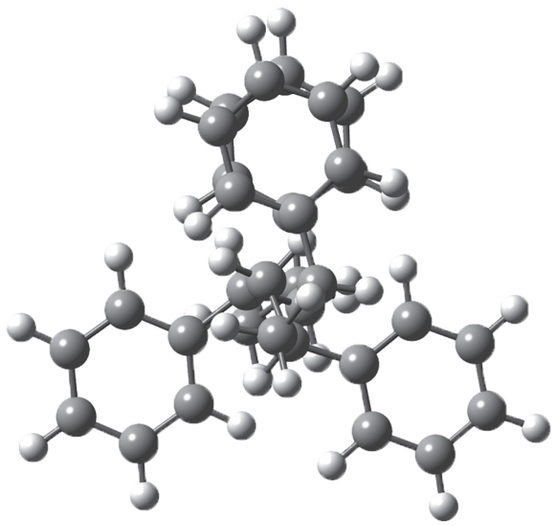

Fig. 11 *Local arrangement in the atactic polystyrene along the chain axis.*

When nano-pores in an elastic medium are cavities with curved surfaces, the inner surface turns out to support a number of surface leaky waves: supersonic and subsonic which do not occur for flat surfaces. In particular, the shear-horizontal surface wave, which is a skimming wave on a flat surface,

transforms to a supersonic resonance at large enough wavelengths emerging from the bulk band to become a subsonic surface leaky wave, of lifetime increasing with increasing wave vector. To reveal the physical significance of such leaky waves we studied the response of the systems to an external perturbation with the corresponding complex frequency. **Theoretical analysis of surface leaky waves has shown that the ratio of the response to the perturbation tends to infinity, while the response itself exhibits a maximum, which may be of importance in practical realisations.**

For D_2, CD_4 and CD_3OD molecules confined in nanoscale zeolite cages, transition from translational diffusion to isotropic reorientation was found to be the main mechanism of relaxation, as shown in the analysis of deuteron NMR spin-lattice relaxation. Other molecules, such as D_2O, ND_3, and $(CD_3)_2CO$ strongly bonded – both mutually and to the zeolite framework – exhibit a much more restricted diffusion. We detected the formation of methanol-d_4 trimers confined in zeolite NaX and NaY cages on loading 172 and 112 molecules per unit cell, respectively. This conclusion was based on observing different relaxation rates for methyl and hydroxyl deuterons undergoing common dynamics. Assumption of intramolecular rotation of methyl groups and fixed positions of hydrogen bonded hydroxyl deuterons in methyl trimmers results in relaxation rates observed experimentally. A change in the slope of the temperature dependence of both relaxation rates indicates a transition from relaxation dominated by translational motion to a prevailing contribution of reorientation at 240K. Methanol molecules become localized on adsorption centres at 169.5K and 153.8K for NaX and NaY, respectively as indicated by extreme broadening of the deuteron NMR spectra. The transition temperature, higher for NaX, indicates the dominating role of the hydrogen bonding to framework oxygen atoms. NMR spectra are consistent in general with the model in which molecules are bonded at two positions: horizontal (methanol oxygen bonded to sodium cation) and vertical (hydrogen bonding of hydroxyl deuteron of methanol to zeolite framework oxygen). Mobility of single molecules, thus no trimers, was observed for lower loading (86 molecules/uc) in NaX. Direct transition from translation to localization was observed at 190 K.

High-resolution solid-state NMR spectroscopy using the Magic Angle Spinning (MAS) technique is used to study new materials for potential applications in chemical industry and power generation. By measuring internal nuclear interaction, such as dipolar and quadrupolar couplings, as well as chemical shifts, the method provided us unique information about the local environment of atoms. This includes the symmetry of the occupied site, coordination, and the nature of chemical bonds. The projects focus on new synthetic heterogeneous catalysers**,** based on zeolites, mesoporous, and layered materials, modified by incorporation of catalytically active species. Structural effects are investigated in parallel with the changes of catalytic efficiency and selectivity. Introduction of novel catalytic materials is of crucial importance in designing new processes for Green Chemistry and Clean Energy**.** Apart from these crystalline materials, novel oxide glasses and other amorphous materials are studied. Particularly important are biologically active glasses, which can be used as fertilizers. **By a careful choice of the matrix content the speed of dissolution into the soil may be controlled.** Another group of mixed oxide glasses modified by some rare earth ions is being studied for their potential application in optoelectronics

***Ab initio* studies of $LiFeSi_2O_6$ revealed the existence of the phonon soft mode** at the zone boundary point Z of the high-temperature phase, which is responsible for the crystal instability and structural phase transition. Pyroxenes belong to a wide group of minerals of the general formula $AMSi_2O_6$, where A is a mono- or divalent alkali metal (Li,Na) and M is di- or trivalent metal. They can be found in the Earth's crust and in the upper mantle up to the depth of 400 km, in the meteorites, and also in lunar and Martian rocks. The presence of transition metal atoms leads to diverse magnetic properties observed in this class of materials. Some pyroxenes also exhibit multiferroic behaviour showing a non-zero electric polarization induced by an external magnetic field. At room temperature, $LiFeSi_2O_6$ crystallizes in the monoclinic C2/c symmetry. The crystal structure is built of edge-sharing FeO_6 octahedra forming zigzag chains running along the c direction and separated by SiO_4 tetrahedra. The crystal transforms into a monoclinic $P2_1/c$ structure in a phase transition observed at T = 228 K. In agreement with diffraction analysis, the largest changes induced by the soft mode are connected with displacements of oxygen atoms which induce distortion of the Si–O chains and reduce the Li coordination from six to five.

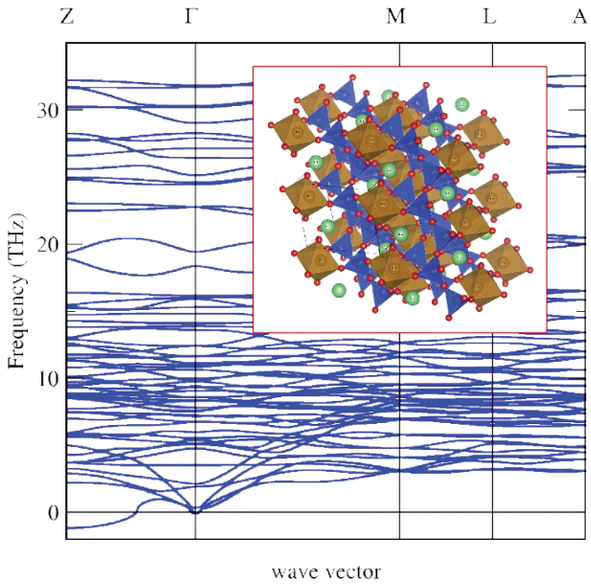

Fig. 12 *Phonon dispersion curves and the crystal structure of* $LiFeSi_2O_6$.

Based on a comparison to the phonon spectrum of $NaFeSi_2O_6$ (aegirine) measured at ambient conditions, **evidence was found of correspondence between the boson peak observed in glasses and the van Hove singularity in crystals.** Calculations of the phonon spectrum enabled us to interpret the experimental studies of the glass phases of sodium silicate of similar composition ($NaFeSi_2O_{8.5}$) conducted by Alexandr Chumakov from ESRF and co-workers. This study shed new light on the long-standing problem of anomalous enhancement of heat capacity at low temperatures in glasses. Measurement of the pressure dependence of the low-energy part of phonon density of states using nuclear inelastic scattering revealed the shift of the maximum, called the boson peak, to higher energies. As demonstrated by *ab initio* calculations, the van Hove singularity arises due to transverse acoustic phonon modes, connected mainly with iron atoms. In a detailed study we found that the number of states measured around the boson peak is exactly the same as the number of the acoustic degrees of freedom in the crystal. Therefore, the increased heat capacity observed in glasses is not induced by additional vibrational states but is due to the shift of vibrational states to lower energies which can be efficiently activated at lower temperatures.

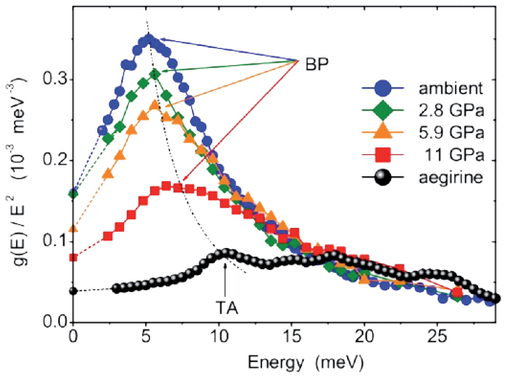

Fig. 13 *Phonon spectra of the* $NaFeSi_2O_{8.5}$ *glass normalized by energy squared at various external pressures.*

Intensive development of molecular spintronics and the design of molecular analogues of the inorganic spintronic structures are motivated by the relatively easy production of molecule–based magnets in the form of thin films (mostly cyanido– bridged coordination networks) and by longer spin-relaxation times than those characterising metallic systems. In our analysis of surface and magnetic properties of an electrochemically deposited $Cr_3[Cr(CN)_6]_2$ film, **a strong correlation between the small roughness of the surface and the high values of the coercive field was found.** Atomic Force Microscopy and the Magnetooptical Kerr Effect were applied in these measurements, indicating the particle-size effect observed earlier in other molecule-based materials. In thinner films, of narrower non uniform size distribution of crystallites and smaller concentration of impurities, larger coercivity and squareness in their hysteresis were seen. Light reflected from the thickest film shows significant depolarization due to multiple reflections from the non-uniform layer thickness.

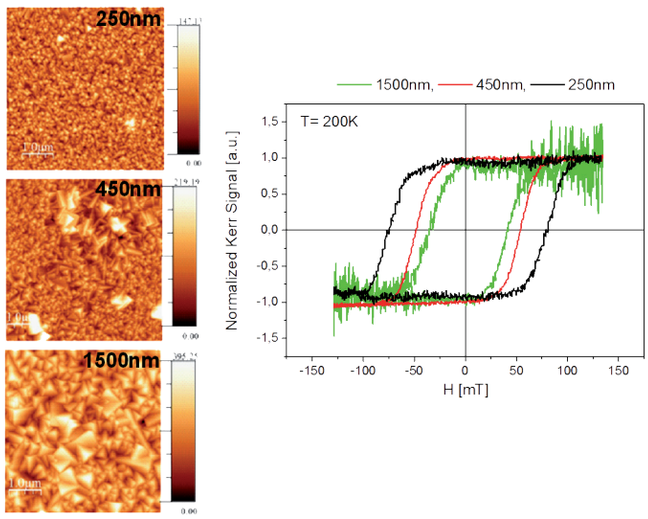

Fig. 14 *AFM topography images of the surface of $Cr_3[Cr(CN)_6]_2$ thin films of different thickness and normalized MOKE hysteresis loops obtained for these films in polar configuration.*

Efforts are made to apply positron annihilation techniques as a non-destructive method of evaluation of metals and alloys in mechanical engineering applications. In particular, this concerns dramatic structural modification of the material near the sliding surface, caused by plastic deformation or fatigue due to defects created by friction and wear. **In samples of stainless steel 1.4301 (EN), defects in the form of edge dislocations decorated by vacancies were identified**, induced by dry sliding in the pin-on-disk tribotester **(Fig. 15 a)**. A SEM micrograph of the worn surface with laminated flat debris, as shown in the **Fig. 15 b**, indicated the delamination wear mechanism. The **Fig. 15 c** presents the results of positron annihilation measurements, i.e. the so-called S-parameter depth dependence which reflects the changes of the defect concentration with depth from the worn surface of the sample after sliding it with a load of 150 N. The microhardness profile is also depicted. In this case the revealed defect profile induced by dry sliding extended to 400 μm under the worn surface diminishing exponentially with depth. The microhardness profile exhibits a much shorter range and a steep decrease in the 5 μm thick layer of the worn surface.

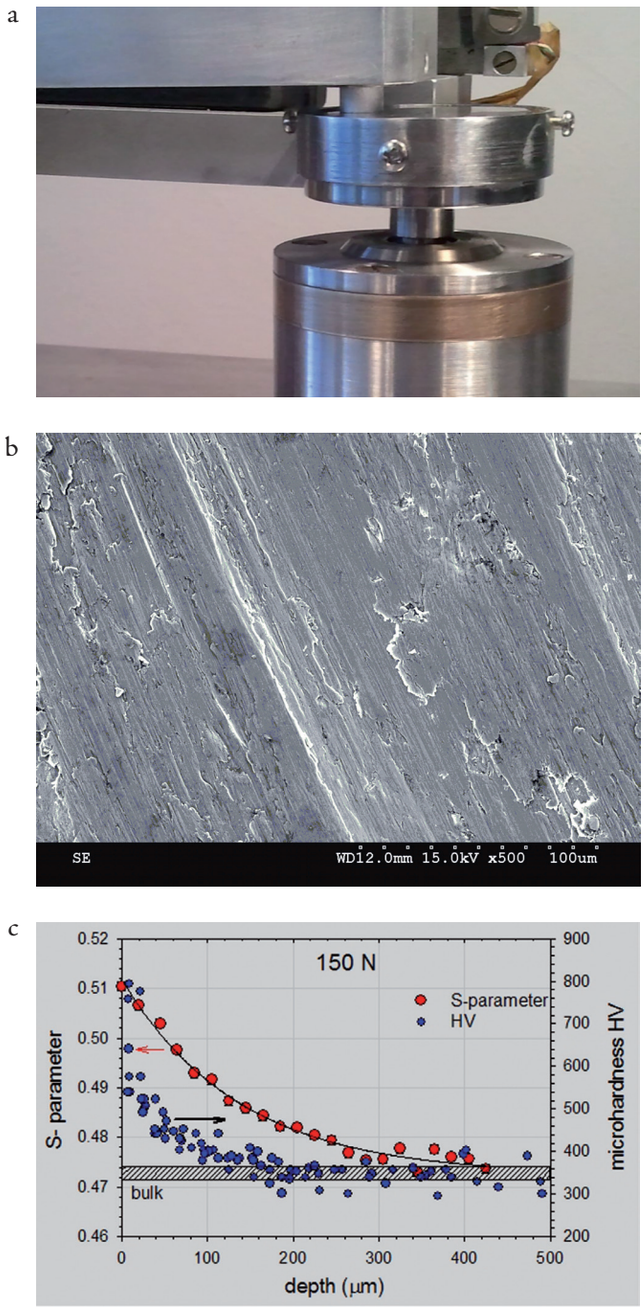

Fig. 15 *Pin-on-disk tribotester (a), SEM micrograph of the worn surface (b), S-parameter and microhardness profiles (c).*

Hydrogen is viewed as one of the important energy carriers of this century and believed to be the future fuel. **A general phase diagram for RMn_2H_x hydrides (R: Tb, Gd, Dy, Ho, Er and Nd) was constructed** thanks to systematic detailed structural studies. The issue of hydrogen storage makes the studies of physical properties of metal hydrides, such as RMn_2H_x systems a very topical subject. The RMn_2 compounds exhibit a complex interaction of the R- and 3d-metal sublattices (the first is described within the localized moment model while the other as an essentially itinerant – electron system). Due to various distances between the nearest Mn atoms, the Mn sublattice can be nonmagnetic, the Mn atoms can carry stable magnetic moments or the Mn moments are close to the instability limit, and magnetic ordering temperature of RMn_2 compounds falls in the range 14 K÷ 105 K. The RMn_2 compounds can easily absorb a large amount of hydrogen at interstitial tetrahedral sites. This leads to an increase of the cell volume (even up to 30 %) and of the magnetic ordering temperature from below 100 K up to (200 ÷ 400) K, which depend on the hydrogen concentration. Structural transformations and magnetic transitions are also observed.

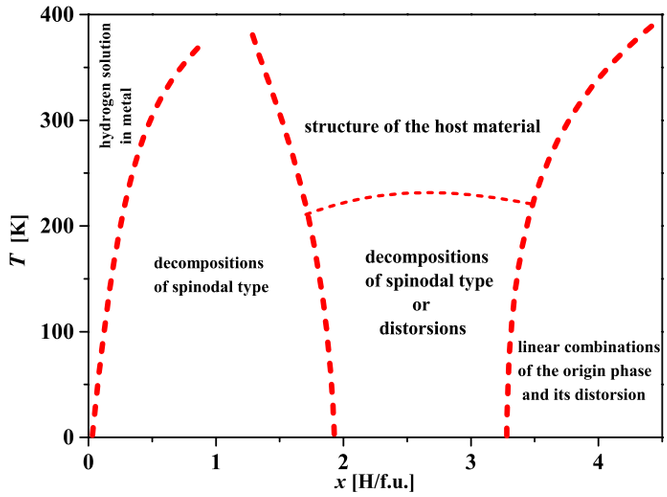

Fig. 16 *General phase diagram for RMn_2H_x hydrides.*

Social and political aspects have recently stimulated research towards developing efficient methods for CO_2 reduction. Among such methods, those which involve novel materials and processes, such as mineral carbonation, are especially suited for theoretical investigation. Additionally, the dry processes of CO_2 absorption combined with reversible chemical transformations are very attractive because of their high carbon dioxide capacity and simplicity. For example, dawsonite ($NaAlCO_3(OH)_2$) is a mineral composed of sodium aluminium carbonate hydroxide, thus it contains only cheap and abundant elements: alumina (Al_2O_3); sodium oxide (Na_2O); CO_2 and water (H_2O). Within dawsonites, the alkali metal cation can be substituted by Na, K, or other elements or by molecular groups such as NH_4. While chemical methods of transformation between alumina and dawsonites in liquid solution are well known, the dry process of potassium substituted dawsonite formation under pressure of 10 bar of equimolar mixture of CO_2 and steam (H_2O) and at temperatures below 573 K, was reported only recently. The simplicity of such a transformation makes it interesting as a method for carbon dioxide capture, however the mechanism of this transformation remains unknown. Since the actual process of CO_2 capture and storage by dawsonites is rather complex, a hierarchical understanding approach from the stability of the bulk material to the surface properties and potential reaction catalyst is necessary for each reaction step. At the first step, the differences between dawsonites with different alkali metal cation need to be understood. Theoretical studies of Na, K, and NH_4 dawsonite structural properties by means of density functional theory (DFT) calculations provide us, besides structural parameters, with the basic spectroscopic fingerprints of compounds to be observed by means of IR and Raman spectra, electronic structure, and elastic properties. **Our analysis confirms the *Imma* and *Cmcm* ground state structures for Na- and K-dawsonites, while the *Pnma* symmetry for the NH_4-dawsonite has been proposed** (the previously reported *Cmcm* crystal configuration appears to be unstable with respect to atomic vibrations). However, calculations indicated the possibility of NH_4 disorder at elevated temperatures. The estimated formation enthalpy provides the following stability order: K-dawsonite > Na-dawsonite > NH_4-dawsonite, matching the previous thermal analyses and empirical observations of stability of aqueous solutions. The three dawsonites considered are strongly ionic systems that have similar electronic properties with a band gap ranging from E_g = 5.3 eV for $NaAlCO_3(OH)_2$ to E_g = 5.5 eV for $NH_4AlCO_3(OH)_2$. A small variation of the charge on the CO_3 group appears. The vibrational spectra show considerable similarities between compounds where, besides lattice modes, the localized bands related to CO_3 at ≈ 1500 cm^{-1} and to OH at ≈ 3400 cm^{-1} can be distinguished. However, the potassium substituted dawsonite is elastically the least stable and has either a very anisotropic bulk modulus or high stiffness along the *b* lattice direction. The next step in understanding properties of dawsonites as carbon dioxide storage media concerns their surface properties. Upon calculations of the surface energy the equilibrium crystal shape was determined. The depicted Wulff shape of the small crystallite of Na-dawsonite provides its atomistic morphology, directly corresponding to this observed via electron microscopy methods.

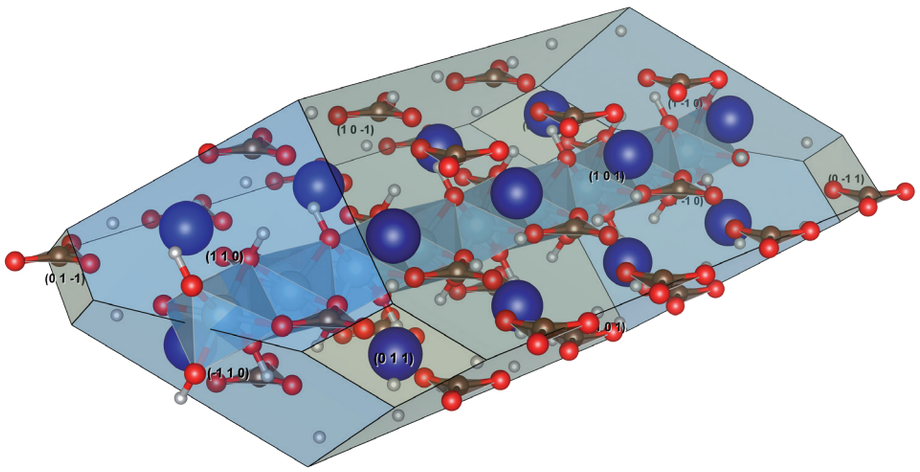

Fig. 17 *The Wulff construction of the equilibrium nano-crystallite of $NaAlCO_3(OH)_2$. The sodium atoms are blue; oxygen is red; carbon is brown. The exposed crystal facets are marked in the figure.*

DFT results indicate that **Li_4SiO_4 is a good candidate for being a high-temperature CO_2 sorbent with potential application in postcombustion capture technology**. Lithium silicates are widely used in lithium batteries due to their better energy per unit weight, high melting point, and high lithium ion conductivity. In recent years, lithium silicates have found another possible application: as CO_2 sorbents to counter global warming. Capture of CO_2 from high-temperature gases can be achieved through the reversible reaction: $Li_4SiO_4 + CO_2 \leftrightarrow Li_2SiO_3 + Li_2CO_3$ (reaction 1). First-principles methods based on DFT have been applied to investigate the electronic and dynamical properties of Li_4SiO_4 in the monoclinic and triclinic phases. In order to study CO_2 capture properties, the thermodynamic characteristics of reaction (1) have been evaluated on the base of total energies and phonon density of states obtained for both phases of Li_4SiO_4. In the figure we present the contour plot of the calculated chemical potential (ΔG) versus temperature and the CO_2 pressure for the CO_2 capture reactions. For each reaction, the curves corresponding to $\Delta G = 0$ separate the region with $\Delta G < 0$ (upper curves), where the sorbents absorb CO_2, and with $\Delta G > 0$ (lower curves), where CO_2 is released and the reverse reaction regenerates the sorbents.

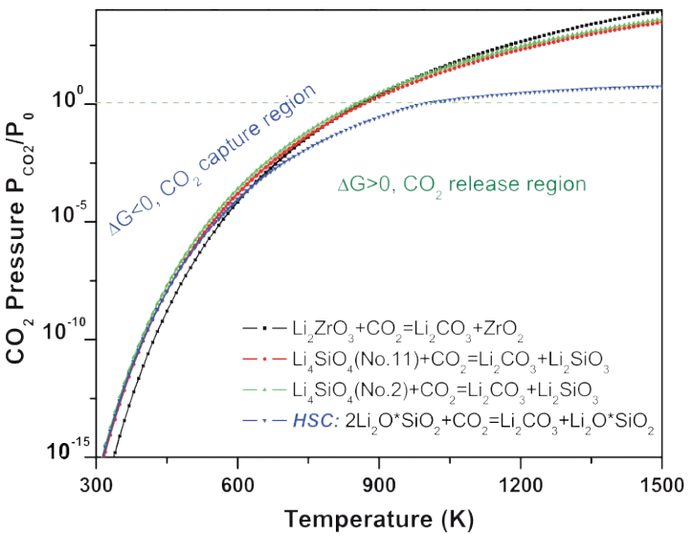

Fig. 18 *The relationship of the chemical potential and CO_2 pressure versus temperature for the reaction of Li_4SiO_4 with CO_2, compared to reactions of other known sorbents.*

The research reported herein was performed pursuant to internal projects: [301, 302, 303, 304]; [E19, E20, E31, E45, E49]. See Annexes I, IIB.

IV. DIVISION OF THEORETICAL PHYSICS

The scientific activity in the Division of Theoretical Physics concerns a broad range of fundamental issues addressed at understanding the structure and dynamics of the Universe at all scales, from the smallest up to the largest possible. Being part of the global scientific community, most of our research is conducted within international collaborations located at major research centres, such as CERN, DESY, JINR Dubna, Budker Institute of Nuclear Physics, NCSR Democritos, DAPHNIA Saclay, LAPP Annecy, BNL Berkely, ENEA Frascati, INRIA Rocquencourt, NCNR Santiago de Compostela and a number of universities: of Aachen, Hamburg and Potsdam in Germany; Pierre et Marie Curie (Paris VI), Denis Diderot (Paris VII) and Paris-Nord (Paris XIII) in France; Baylor, Penn State and Southern Methodist in the USA; of Castilla La Mancha, Granada and Valencia in Spain; of Birmingham and Liverpool in the UK; the Central China Normal and Hangzou Normal in China; of Nagoya in Japan and of Coimbra in Portugal. The related scientific topics may be grouped within the following categories:

- Hard processes, parton densities and Monte Carlo
- Heavy-ion and quark-gluon plasma physics
- Heavy and light meson decays and interactions
- Single atoms and multiparticle systems
- Theoretical astrophysics
- Complex systems theory
- Mathematical physics

Some of our results, grouped within the above list of general topics, are presented below.

HARD PROCESSES, PARTON DENSITIES AND MONTE CARLO

The next-to-leading order (NLO) double-real-parton distributions for QCD evolution kernels have been calculated in the standard collinear scheme and in a new, modified collinear scheme for the Non-Singlet case. These distributions were used to construct fully unintegrated partonic distributions. The structure of singularities of these distributions was analysed. In particular, for diagrams with internal collinear singularities, soft counterterms which have an identical structure of singularities were constructed. These counterterms are useful both in combining real and virtual contributions as well as in the construction of stochastic algorithms and as a component of weights which include NLO corrections in the Monte Carlo simulation. The differences between NLO evolution kernels in MS factorization scheme and in the new scheme proposed, called the Monte Carlo scheme, have been investigated for the Non-Singlet evolution and partly for the Singlet evolution in the case of double-real emission.

The universality of the new factorization scheme has been discussed at length. In its construction, detailed knowledge of the soft limit of real gluon emission within NLO kernels was instrumental. It enabled the construction of a positive and numerically stable Monte Carlo NLO weight to be imposed on the LO distributions.

A new method has been proposed of including the NLO corrections to the hard process matched with two LO-type parton showers for W/Z heavy boson production and for the DIS process. The new solution is an alternative to the existing projects MC@NLO and POWHEG, and has certain advantages: it is simple in formulation; it uses positive Monte Carlo weights; it does not need the complicated "vetoed shower" nor "truncated shower" methods. These advantages are achieved thanks to the modification of the factorization scheme and to introduction of a new implementation of the LO parton shower.

Three prototype solutions of the problem of including the NLO corrections to the multiparton stochastic simulation, which describes the evolution of hadron quark densities (the Non-Singlet part), have been proposed. This is a novel result as, for the first time, Monte Carlo simulation of the partonic cascade ("ladder") has been proposed at the NLO level. In the future this solution will be used to construct the complete parton shower programs describing W/Z and Higgs production at the Large Hadron Collider (LHC) including the complete NLO QCD corrections.

Final-state interactions are of great importance in the phenomenology of high energy physics. In the years 2011–2012 significant extension of the on-going projects in the domain of phenomenology of W, Z, H bosons and tau leptons was achieved. The main documentation and older publications related to the TAUOLA and PHOTOS projects have been cited 683 and 560 times, of which 154 and 131 citations were recorded within the last 2 years (according to the Inspire-HEP database). Documentation of TAUOLA C++, which was published in 2012, has already been cited 68 times.

The substantial progress of the phenomenological projects for final-state interactions in the last 2 years, apart from introduction of changes in the programming language, has resulted in the development of: (1) new parameterizations of hadronic currents for the tau decay, based on Resonance Chiral Lagrangians; (2) new tools used for spin analysis of tau leptons in the decay of electroweak bosons at LHC; (3) exact first-order matrix elements for bremsstrahlung in Z and W decays, which were carefully studied.

The developed techniques were used by the experimental collaborations at the Tevatron and LHC in the most precise ever measurement of the W mass or for the Higgs boson discovery. A total of 20 papers or conference presentations were related to this activity. Currently on-going is the productive cooperation with Belle and BaBar experiments.

At LHC energies, the so called *high-energy factorization* formalism can be applied, whereby a reaction can be described as a convolution of *unintegrated gluon densities* and *hard matrix elements*. Unlike in the more common collinear factorization, the matrix elements are defined with the incoming gluons being *off-shell*. The last issue constitutes a challenge in consistently defining the matrix elements, in particular with respect to *gauge invariance*. These difficulties have however been overcome and a formulation for matrix elements with off-shell initial-state gluons was developed. It applies to a wide range of processes, and can be readily used in explicit calculations. The framework has been implemented into a numerical computer program and proved its computational potential through the calculation of high-multiplicity benchmark processes.

As mentioned above, theoretical calculations concern not only matrix elements, but also parton densities, which correspond to solutions of certain *evolution equations*. With the advent of the LHC

the last are needed in a form which allows for studies to be performed of exclusive processes and *gluon saturation*. So far, equations formulated in the high energy factorization did not allow for that. New evolution equations have been formulated which allow for the study of the properties of a dense system of partons probed with a hard projectile. A numerical method to solve nonlinear evolution equations for exclusive processes has been developed and a new Monte Carlo solution for the linearized version of the new equations has been provided. The method was implemented in the form of a dedicated set of numerical programs, which will be further transformed into a numerical tool for general use. An important contribution in the search for saturation effects has been made in collaboration with researchers from Durham University. Using the high energy factorization framework and the Balitsky-Kovchegov equation further support in favour of the hypothesis of existence of nonlinear effects in the proton structure data has been provided. The calculation based on the nonlinear equation turns out to describe a much wider range of data than the linear and collinear frameworks. Furthermore, predictions for saturation effects in di-jet production in proton-lead collisions have been provided.

The nonlinear Balitsky-Kovchegov equation at small x has been solved numerically. Comparison of the calculations with the inclusive data from HERA on the structure functions F2 and FL has been performed. Complete theoretical analysis of the azimuthal angular correlation of two-hadron productions in the forward dAu collisions at RHIC in the saturation formalism has also been performed, giving very good agreement with experimental data. Future experiments of di-hadron correlations in pA collisions at both RHIC and LHC, and in eA collisions at the planned electron-ion collider, shall lead to better understanding of the strong interaction dynamics in the saturation regime. Forward correlations between the lepton-pair and associated hadrons in Drell-Yan process in pA collisions have been studied numerically. Forward correlations between the lepton-pair and associated hadron in Drell-Yan process at RHIC and LHC were calculated using the modified Golec-Biernat-Wüsthoff model.

The physics programme and the design of a new collider for particle and nuclear physics, the Large Hadron Electron Collider (LHeC) in which a newly built electron beam of 60 GeV, up to possibly 140 GeV, energy would collide with the intense hadron beams of the LHC, have been developed. Compared to HERA, the kinematic range covered is extended by a factor of twenty in the negative four-momentum squared, and in the inverse Bjorken x, while with the design luminosity of $10^{33}\,\mathrm{cm}^{-2}\,\mathrm{s}^{-1}$ the LHeC is expected to exceed the integrated HERA luminosity by two orders of magnitude. The physics programme is devoted to exploration of the energy frontier, complementing the LHC and its discovery potential for physics beyond the Standard Model.

The effects of the saturation boundary on small-x evolution at the next-to-leading order accuracy and beyond have been investigated. Re-summation of the higher order corrections was needed for the nonlinear evolution. It has been shown that the double diffractive electroweak vector boson production in the pp collisions at the LHC is an ideal probe of QCD-based mechanisms of diffraction. Assuming the resolved Pomeron model with flavour symmetric parton distributions, the W production asymmetry in rapidity equals exactly zero. In other approaches, such as the soft colour interaction model in which soft gluon exchanges are responsible for diffraction, the asymmetry is non-zero and equal to that in the inclusive W production. This effect can be tested at the LHC. Motivated by the regime of QCD explored nowadays at LHC, where both the total energy of collision and momenta transfers are high, evolution equations of high energy factorization have been investigated.

HEAVY-ION AND QUARK-GLUON PLASMA PHYSICS

The viscous relativistic hydrodynamic model in 2 + 1D is applied to heavy-ion collisions at LHC energies giving a good description of the elliptic flow and interferometry radii. The presence of large pressure asymmetry at the early stage of the collision could be observed in the direct flow of emitted particles, while other observables are not sensitive to this asymmetry. Fluctuations of the fireball lead to a decorrelation of the directions of particle emission at different rapidities, which could be measured.

A major advance has been achieved with the development of a fully 3 + 1D relativistic viscous hydrodynamic code, with a realistic equation of state based on recent lattice QCD data. The model predicts transverse momentum spectra of identified particles in good agreement with experimental data. Most importantly, the code can be applied event-by-event using fluctuating initial densities generated in the Glauber Monte-Carlo model. The model predicts the presence of collective elliptic and

triangular flow in p-Pb collisions at the LHC and strong directed flow in Cu-Au interactions at RHIC. Fluctuations of the size of the initial fireball lead to fluctuations of the transverse momentum of emitted particles, which explains the experimental observations. The effects of local charge conservation at freeze-out induce azimuthal and pseudorapidity correlations, also in agreement with experiment. The influence of the "wounding profile" in the framework of the Glauber model to the early phase of the relativistic heavy-ion collisions is being examined. A realistic profile, obtained from the differential elastic cross section via the optical theorem, leads to larger initial-state fluctuations in the system.

Leading-order QCD evolution from the low quark-model scale to higher lattice scales has been carried out. Also evaluated were several lowest-order generalized transversity form factors, accessible from the recent lattice QCD calculations. These form factors agree properly with the lattice data, supporting spontaneously broken chiral symmetry as the key element also in the evaluation of the transversity observables.

We examined the systematics of radial and angular-momentum Regge trajectories of light nonstrange qq-states listed in the 2011 edition of the Particle Data tables. The obtained values for the parameters show that strict universality of the radial and angular-momentum slopes does not hold in the light nonstrange sector.

Due to the rapid longitudinal expansion of the quark-gluon plasma produced in relativistic heavy ion collisions, large momentum-space anisotropies are generated. The magnitude of these anisotropies can be so large as to violate the central assumption of standard viscous hydrodynamical treatments which linearize around an isotropic background. In order to better describe the early-time dynamics of the quark gluon plasma, expansion around a locally anisotropic background which results in a dynamical framework called anisotropic hydrodynamics is being considered.

We have also contributed towards the application of the Colour Glass Condensate (CGC) framework to shed some light on the thermalisation problem of quark-gluon plasma, which takes place in the collision of heavy ions. Within the typical hydrodynamic description, the large amount of entropy that is needed at the early stage of the collision, requires justification. The CGS framework allowed us to introduce a well-founded definition of entropy which appears to be capable of introducing a substantial contribution to the final amount of entropy produced.

HEAVY AND LIGHT MESON DECAYS AND INTERACTIONS

Studies of CP violation and of final state interactions in charged B-meson decays into three charged kaons or pions have been pursued in collaboration with the LPNHE Laboratory in Paris. Studies of Dalitz plot for the $D0$ meson decays into $K_0^s\pi^+\pi^-$ have been elaborated. The heavy-meson decay amplitudes are constructed in the QCD factorization framework. Unitarity plays an important role in constraining the number of free parameters required in the description of experimental data obtained in B-meson factories.

The relative size of two independent penguin amplitudes has been studied using the data on the $B^+ \to \pi^+K^{*0}$, and $B^+ \to K^+\overline{K}^{*0}$ decays. A Regge phenomenology-based estimate of SU(3) breaking in the final quark-pair-creating hadronization process was discussed. The results agree with earlier studies of $B^+ \to \pi^+K^0$, $K^+\overline{K}^0$ decays, thus confirming that the ratio C/T of the `true' tree amplitudes is small and of the order of 0.2. We have noted that antiparticles may be interpreted in macroscopic terms using the language of nonrelativistic phase space, without explicit consideration of the concepts of time and of its reversal.

It has been pointed out that antiparticles may be interpreted in macroscopic terms using the language of nonrelativistic phase space, without explicit consideration of the concept of time and its reversal. We have demonstrated that the phase-space approach leads also to the emergence of internal quantum numbers of weak isospin, weak hypercharge and colour, together with the Gell-Mann-Nishijima relation, while simultaneously offering a preonless version of the Harari-Shupe rishon model. Finally, it has been shown that the approach entails the emergence of string-like mesonic and baryonic states, providing a very interesting alternative view on the unobservability of quarks.

Koide's Z3-symmetric parametrisation of charged lepton masses has been extended to quarks. The Brannen-Rosen observation that a certain phase parameter δL appearing in this parametrisation is experimentally indistinguishable from 2/9 was generalized: quark masses at the low-energy scale (at $\mu = 1$ GeV^2) are characterized by $\delta U = \delta L/3 = 2/27$ and $\delta D = 2\delta L/3 = 4/27$.

Apart from the recently derived GKPY dispersion relations for the pion-pion S and P-wave amplitudes, other relations, also with one subtraction and with imposed crossing symmetry, have been derived for the D and F partial waves. First numerical fits to the GKPY equations delivered very precise and unitary parameterizations of the S, P, D and F partial wave amplitudes up to about 20 GeV. We began to apply the GKPY relations in practice, to test other parameterizations.

Model-independent analysis of the pp → pp and pp → KK data below 1.8 GeV has been applied to test results for the f0(980) resonance obtained in fits of these two kinds of data. Significant differences between these results have been found and analysed.

SINGLE ATOMS AND MULTIPARTICLE SYSTEMS

The process of energy dissipation by dispersion, which is the key mechanism of relaxation of excited states into equilibrium static configurations on unbounded domains, has been investigated. In spite of its importance, the mathematical understanding of this phenomenon is still rather vague. For better insight, good toy-models of dissipation processes need to be examined. To this end, a modified wave map model in 3 + 1 dimensions was used. The modification affects the domain of maps (exterior of a ball of radius r = 1 was analysed). For such model there exists a set of linearly stable static solutions – end states of relaxation process. Quasinormal modes – states vanishing at r = 1 and satisfying the outgoing wave conditions for r → ∞, were determined. Their fundamental (i.e. least damped) mode is expected to govern the intermediate asymptotics of relaxation.

We studied the dynamics close to the blow-up threshold in the nonlinear Klein-Gordon model with on-line focusing power-law nonlinearity. In this model there exist analytically known unstable static solutions S(x), which play an important role in threshold dynamics. We formulated a precise quantitative description of asymptotic dynamics using a combination of analytical and numerical methods. Analytical equations for the asymptotic behaviour of linearized perturbations around S were derived and used to solve the dynamical equation with fine tuning of the initial data the borderline between blow-up and global regularity. This threshold dynamics is well approximated by linearized dynamics around S. The most interesting feature of this solution is its dependence on the power of nonlinearity resulting from the change of spectral properties of the linearized operator around S with changing power of nonlinearity.

An algebraic approach was elaborated to describe the shape transition of two-fermion systems, confined in a three-dimensional axially symmetric parabolic potential, in an external magnetic field. New symmetries of this system arise for particles moving in a mean magnetic field, related to the scaling of effective mass and the magnitude of the magnetic field. Explicit algebraic expressions were derived in terms of parameters of this system and of the magnetic field strength, in order to trace such transitions in the classical limit.

Heterogeneous clusters composed of Xe and Ar noble gas atoms for which chemical-bond effects can be neglected, were studied theoretically. The effects of the cluster composition on ionization dynamics, and on electronic damage in particular, were discussed in detail.

High-resolution structural analysis of single particles sprayed from an aqueous solution into the laser beam has been undertaken, to study coherent diffractive imaging using x-ray free-electron lasers (XFELs). Diffraction images are recorded from randomly oriented objects, covered by a layer of water. We analysed theoretically how the thickness of the covering water layer influences the structural and orientation information contained in the recorded diffraction images. This study has implications for planned experiments using single-particle imaging with XFELs.

Limitations of continuum models for coherent diffraction imaging (CDI) of single molecules at atomic resolution were studied. We derived a universal formula to calculate scattered intensities (including both elastic and inelastic scattering) from the estimates obtained with a single-particle continuum model under conditions typical for CDI studies.

We obtained predictions of modification of ionization thresholds and rates of some photo-induced processes in carbon irradiated by an X-ray free-electron laser pulse. We extended the Hartree-Fock-Slater model to include electron screening and ion correlation effects induced by external charges, obtaining model-predicted modifications of orbital energies and photo-absorption cross sections due to plasma formation.

THEORETICAL ASTROPHYSICS

In our study of galaxy models we addressed the problem of the influence of large-scale magnetic fields on galactic rotation, using the spiral galaxies NGC 891 and NGC 253 as examples. Based on the available data we determined the column mass density and the resulting mass-to-light ratio in the framework of the global disk model. We discussed factors that may influence the rotation of matter in these galaxies and calculated how they could affect the profile of the local mass-to-light ratio, focusing mainly on the possible effect of magnetic fields on the motion of the ionized gas. Next, within a simple finite-width disk model, we showed that the amount of mass seen through gravitational micro-lensing measurements inside the region R < 8kpc in our Galaxy, is consistent with the dynamical mass evaluated from the galactic rotation, after subtracting the gas contribution. Since micro-lensing detects compact objects only, this result suggests that the hypothetical non-baryonic mass component may be negligible in this region. We also estimated the lower bound for the Galaxy mass, basing on the radial motions of remote velocity tracers (halo external compact objects). In the point-mass approximation (justified by the hypothesis of absence of any extended massive dark matter halo) we studied motions of tracers exterior to a sphere of 20 kpc radius, far beyond the main concentration of luminous mass components. We solved the Jeans problem with a generic phase-space distribution function without any simplifying assumptions constraining the functional dependence of various secondary quantities, such as the flattening of the velocity ellipsoid. Our distribution function is a spherically symmetric collection of confocal elliptic orbits with various energies and eccentricities which we called the Keplerian ensemble. We found that while there is no obvious upper bound for the Galaxy mass based on the motion of external halo objects, there is a sharp lower bound. In particular, we found that a low mass of $2.4*10^{11}$ of solar masses, comparable with the dynamical mass inferred from the Galaxy rotation curve in the global thin disk model, is consistent with the observed radial motion of halo objects and that this motion does not necessarily indicate that total Galaxy mass is much larger than that visible.

We studied the collisions of non-magnetised and weakly magnetised nonrelativistic plasmas with parameters applicable to the conditions at young supernova remnants, using Particle-In-Cell computer plasma simulations. In two colliding plasma slabs of different densities, two different shocks and a contact discontinuity are formed. We demonstrated that while nonrelativistic shocks in both non-magnetised and magnetised plasmas can be mediated by short-wave Weibel-type instabilities known from relativistic systems, the efficiency of shock formation processes is higher if a large-scale parallel magnetic field is present. Downstream of the forward and reverse shocks electrons remain close to equipartition with ions and their distributions are generally isotropic. The efficacy of particle pre-acceleration, required for injection into Fermi-type shock acceleration, is low.

COMPLEX SYSTEMS THEORY

We studied the hierarchical structure of complex systems at various levels of their organization. The term 'complex systems' refers to a new scientific paradigm according to which full comprehension of such systems demands a holistic approach, at all underlying scales. In our view, to study the effects of the typically nonlinear interactions among elements of such systems in microscale, which lead to mutual dynamic correlations between such elements and to the appearance of constructive patterns of macroscopic activity. To study these aspects and mechanisms of relations of such systems with the environment, are major issues in the science of complexity and are thus of great interest to our Theory Division. All living organisms and all processes through which they interrelate are obvious examples of complexity. Consequently, the concept of complexity appears relevant not only from the perspective of "hard" sciences, but may also be relevant to biology, economy or social sciences. Nowadays, even in the domain of arts and literature the theory of complex systems is gaining recognition as a creative source of cognitive inspiration. This paradigm then justifies the interest of our Theory Division in issues related to the dynamics of financial markets, to quantitative linguistics and music and in selected topics related to the manner in which the human brain operates.

There exist many scientific arguments to support the statement that real complexity is situated just at the border between regularity and chaos. A multitude of related quantitative characteristics indicate a hierarchical organization of structures which thus emerge. The most meaningful of those

characteristics are the scale-free-laws and their geometrical counterparts – the fractals – objects the appearance of which is similar at any level of their magnification. Therefore, multiscaling points to the general direction in which the most essential properties of complexity may be grasped quantitatively. The presence of self-similar, or more generally self-affine, forms and patterns of activity in the systems commonly considered as complex, seems to suggest the existence of a single underlying and universal law which governs the principles of Nature's organization. Moreover, traces of self-similarity, ubiquitous in Nature, indicate that its architecture may be based on a programme which – in proportion to the complexity perceived – is comparatively simple. Identification of such a law is considered to be the ultimate aim of the science of complexity.

From an empirical point of view, complex systems are typically represented by huge ensembles of data. In order to optimally describe their multiscaling characteristics these data are analysed using advanced procedures of multifractal analysis and their cross-correlation variants. As a supplementary element of methodology the issue of multiscaling is studied in the appropriate representations of complex networks and quantified in terms of the corresponding network characteristics. Using such a methodological approach, we studied the financial markets, identifying in particular the anomalous and exotic effect of negative fractal dimensions of the foreign exchange market (Forex). We have now significantly extended our research of complex systems to natural languages and music. Natural language is an evolving system, the present structure of which is the product of a long history of self-organization. Like in many other self-organized natural systems, the observables associated with language, such as written texts or spoken messages, reveal complex dynamics. Language samples are not amorphous mixtures of symbols (letters, phonemes, morphemes, words, etc.) but rather represent a highly organized sequence in which particular symbols are ordered according to specific rules, most of which are defined by grammar. Accordingly, quantitative analysis of language samples shows interesting scaling effects that in some cases even demand a mutliscaling description. The interdisciplinary character of fractal geometry is not restricted only to science, but may also be valid in arts. Indeed, if art is treated as some reflection of reality, certain interesting fractal features might be discerned. For example, music, from the perspective of spectral analysis, imitates natural processes called pink noise. Music itself may be considered to be a sequence of tones or sounds ordered in a way which is pleasant to listen to. This definition offers the possibility of treating music as a time series and investigating it by means of advanced methods of multifractal analysis, which is currently under way at the Theory Division.

As a significant extension of the multifractal formalism we introduced a novel algorithm – Multifractal Cross-Correlation Analysis (MFCCA) – that constitutes a consistent extension of the Detrended Cross-Correlation Analysis (DCCA) and is able to properly identify and quantify subtle characteristics of multifractal cross-correlations between two time series. Our motivation for introducing this algorithm is that the already existing methods have at best serious limitations for most of the signals describing complex natural processes and often indicate multifractal cross-correlations when there are none. The principal component of the present extension is proper incorporation of the sign of fluctuations to their generalized moments. Furthermore, we presented a broad analysis of the model fractal stochastic processes as well as of the real-world signals and show that MFCCA is a robust and at the same time a selective tool, and therefore allows for a reliable quantification of the cross-correlative structure of analyzed processes. In particular, it allows one to identify the boundaries of the multifractal scaling and to analyze a relation between the generalized Hurst exponent and the multifractal scaling exponent. This relation provides information about character of potential multifractality in cross-correlations and thus enables a deeper insight into dynamics of the analyzed processes than allowed by any other related method available so far. By using examples of time series from stock market, we have shown that financial fluctuations typically cross-correlate multifractally only for relatively large fluctuations, whereas small fluctuations remain mutually independent even at maximum of such cross-correlations. Finally, we indicated possible utility of MFCCA to study the effects of time-lagged cross-correlations.

MATHEMATICAL PHYSICS

Interest in Lévy stable probability distributions, being a subset of the so-called "heavy-tailed" probability distributions, stems from their ubiquitous applications both in physics and in other fields,

such as statistics, econophysics, geology, or biophysics. Our research has been focused around applications of integral transforms to find the exact and explicit form of the Lévy stable laws and, thereafter, to employ them to solve the Fokker-Planck equation with time-independent coefficients. These solutions encompass the so-called one-sided Lévy distribution, $g(\alpha; x)$, $(0 < \alpha < 1)$, the characteristic function of which is given by the Laplace transform, and the so-called two-sided Lévy stable distribution $g(\alpha, \beta; x)$, $(0 < \alpha < 1, |\beta| \leq \alpha$ or $1 < \alpha \leq 2, |\beta| \leq 2 - \alpha)$, the characteristic function of which is related to the Fourier transform. We introduced a new type of integral transform, the so-called Lévy transform, whose kernel is defined via the one-sided Lévy stable distribution. Using the Lévy laws we arrived at a complete construction of an evolution operator method to solve the 1-dimensional Fokker-Planck equation with time-independent coefficients.

In the theory of generalized coherent states (GCS) resolution of the identity, expressing the completeness of these states, is usually considered to be the most important property. Understanding this condition has been the subject of our interest for a long time, both from the mathematical and physics points of view. Inspired by the seminal paper of V. Bargmann published in 1961, we considered the reproducing kernel Hilbert space formalism (which in fact underlies all standard approaches to the theory of coherent states) to be a basic element of the construction and not an *ad hoc* stated and devoid of deeper meaning consequence of the resolution of identity. This enabled us to put aside the measure context involved in the resolution of unity while still maintaining the crucial properties of the notion of coherent states.

Our motivation to study geometric models of relativistic particles with spin was to understand the non-uniqueness in the motion encountered for the fundamental relativistic rotator described by a Lagrangian determined by the requirement that the invariant mass and spin are separately fixed parameters. The same Lagrangian can be obtained (and is uniquely singled out from among other dynamical systems with the configuration space $R^3 \times S^2$) by the requirement that the Hessian should be singular. This structural property cannot be removed and, unlike for other dynamical systems with the configuration space $R^3 \times S^2$, a secondary constraint appears for the consistency of the Hessian singularity with the interaction term. Moreover, it imposes an unphysical limitation on the initial conditions and admissible motions. This suggests that the minimal coupling principle may be inadequate for particle models with separately fixed mass and spin except for some special field configurations. The singularity of motion can be easily understood at the constrained Hamiltonian level. We showed how to obtain hamiltonization of a family of relativistic rotators by direct application of the Dirac procedure for constrained systems. The unexpected result of such an approach is that a genuine physical observable, namely the rapidity in the centre of momentum frame, becomes a gauge variable. The same strange conclusion can be drawn for a family of dynamical systems larger than the relativistic rotator. Performing the 'constrained hamiltonization' of a quite generic family of geometric models of particles with spin we found that if the Casimir mass and spin are set to be separately fixed parameters, then, as a rule, the models lead to indeterminate motion. These paradoxes suggest that for a consistent description of spinning particles with separately fixed mass and spin (which resembles quantum particles rather than macroscopic bodies) something more general than a world line concept should be used and that the interaction with external fields should not be arbitrary but should obey the unusual gauge freedom.

SELECTED RESEARCH HIGHLIGHTS OF THE DIVISION OF THEORETICAL PHYSICS

To establish a unified framework for proton-proton and proton-lead collisions at LHC, unintegrated gluon densities accounting for saturation and applicable over a wide range of transversal momentum, need to be known. To this aim, the Theory Division researchers formulated a new, resummed form of the Balitski-Kovchegov equation. Such an **evolution equation, with coherence and nonlinearity**, sums up classes of Feynman diagrams which are ordered over the parton angle of emission, thus becoming a nonlinear generalization of the Catani-Ciafaloni-Fiorani-Marchesini equation. Its nonlinearity originates in the double convolution of the triple pomeron vertex with gluon densities, as shown in **Fig. 1**. Interestingly, in this result the nonlinear term itself does not need to be resummed since it is non-singular, and resummation of the linear parts affects the nonlinear term in a simple multiplicative manner. An equation which generalizes the resumed equation to account for colour coherence has also been proposed.

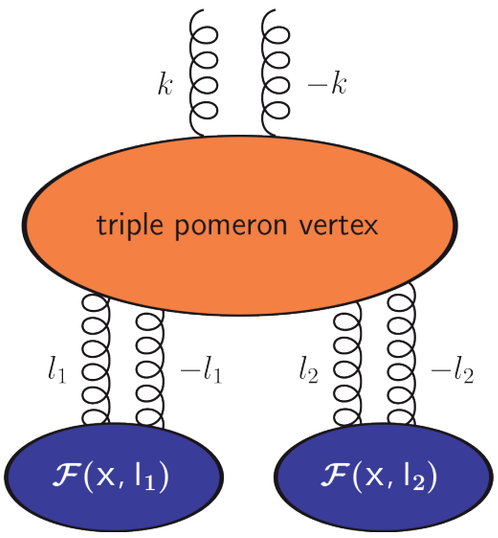

Fig. 1 *Triple pomeron vertex leading to nonlinearity.*

Solving nonlinear evolution equations is a highly nontrivial task. Nevertheless, an effective algorithm has been constructed and tested. The solutions, providing gluon densities, can be used to analyse hard processes where gluon saturation effects are taken into account.

An example of a practical application of this nonlinear evolution is shown in **Fig. 2**, where calculations for transverse momentum spectra of the forward jets in proton-proton collisions at LHC are compared to CMS data. The plot shows that the data favour nonlinear rather than linear evolution.

Recent studies of relativistic heavy-ion collisions focus on correlations, expecting that more details of the underlying early-stage dynamics will be revealed in these objects. The most studied case is the two-dimensional two-particle correlation function in relative azimuth (Df) and pseudorapidity (Dh), which typically displays a central peak and two ridge structures, as shown in **Fig. 3**. While the mechanism of formation of these structures based on collective flow of the strongly-interacting quark-gluon plasma has been known for some time, the fall-off of the near-side ridge (i.e. that close to Df = 0) with |Dh| was a mystery. We were able to solve it by showing that the nature of this phenomenon is due to local conservation of the electric charge at hadronization. Indeed, if a pair of opposite-charge hadrons is formed in a moving fluid element, its motion is collimated. Since hydrodynamic expansion leads to flow, together with **charge balancing**, it provides the necessary mechanism explaining the shape of the ridge. Moreover, the correlation function exhibits a dependence on the relative sign

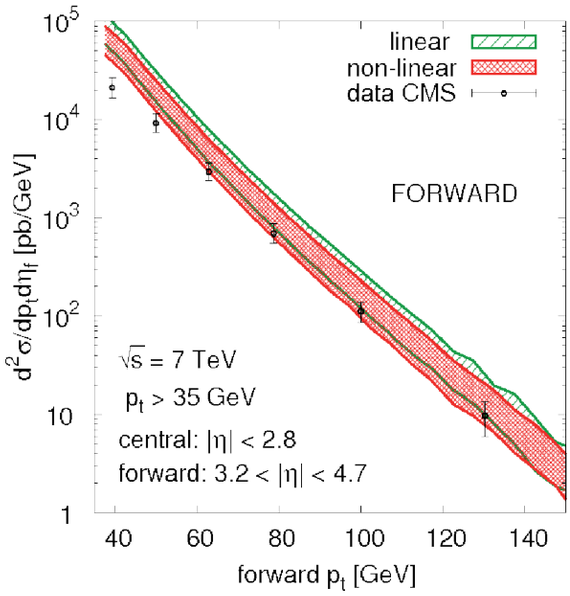

Fig. 2 *Comparison of nonlinear and linear evolution for transverse momentum spectra of forward jets in proton-proton collisions at the LHC.*

of particles in the pair: balancing **and the resulting fall-off** occur only for particles of opposite signs, while the near-side ridge for the same-sign particles remains flat. These features, observed experimentally, are reproduced in our simulation, as shown in **Fig. 3**.

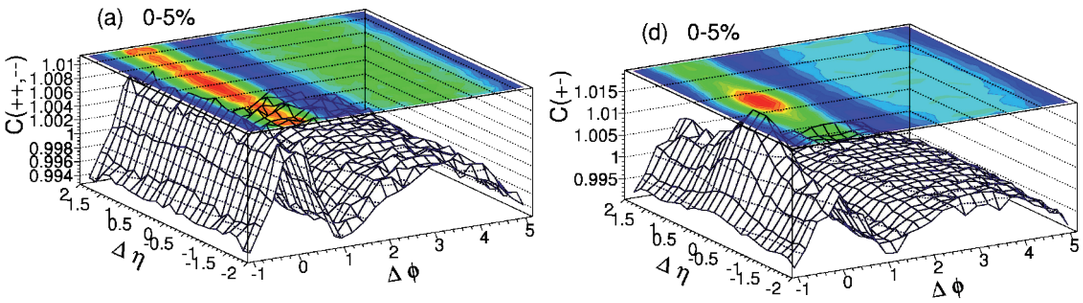

Fig. 3 *The two-particle correlation function obtained by 3 + 1 D viscous event-by-event hydrodynamic simulations for the most central Au + Au collisions at the highest RHIC energies: (a) same-sign particles and (d) opposite-sign particles in the pair.*

Our findings strongly support the collective, hydrodynamic picture of relativistic heavy-ion collisions dynamics.

Recently derived once-subtracted dispersion relations with imposed crossing symmetry condition for pp → pp interactions (the so-called GKPY equations) were used for the **determination, with exceptional accuracy, of pole parameters of the f0(500) and f0(980) resonances**. Together with the well-known Roy equations with two subtractions, they allowed us to construct a very demanding and efficient tool to examine pp amplitudes in the effective two pion mass range from threshold to about 1.1 GeV. In order to perform the test of crossing symmetry in the S and P-partial waves, a set of model-independent unitary amplitudes in all significant partial waves – S, P, D and F was constructed up to 1.42 GeV. Over the higher energy region, up to around 20 GeV, Regge parameterizations were used.

Analytic continuation of the S-wave amplitude to the complex energy plane resulted in poles related to those resonances occurring at $457\ ^{+14}_{-13} - i279^{+11}_{-7}$ MeV and at $996 +/- 7 - i25^{+10}_{-6}$ MeV, respectively. Basing on these results, significant changes have been introduced in the section of Particle Data Tables 2012 (PDG2012) concerning light scalar mesons, correcting previous editions of Particle Data Tables (PDG2010).

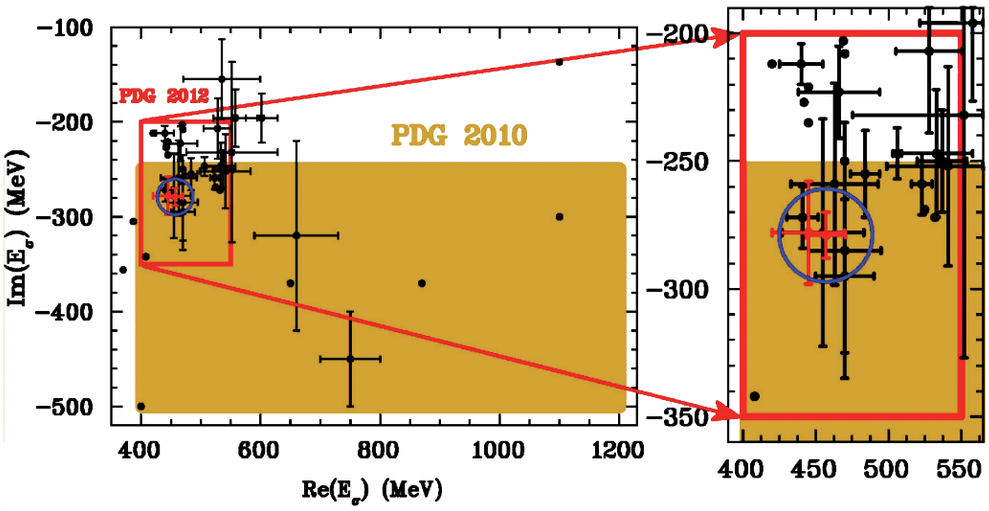

Fig. 4 *Positions of poles (black dots) related to the f0(500), cited in PDG2010, energy* $E_\sigma = \sqrt{s_\sigma}$ *. The large rectangle represents uncertainties in mass and half-width of the f0(500) in PDG2010. The smaller rectangle on the left-hand-side of the figure indicates the magnified area on the right drawing and shows uncertainties in mass and half-width of the f0(500) in PDG2012 (marked in red). Poles calculated using the GKPY and Roy equations lie within the blue circles.*

The H.E.S.S. (High Energy Stereoscopic System) collaboration in which IFJ PAN researchers participate, is involved in gamma-ray detection from a number of galactic and extragalactic sources. In 2012 the H.E.S.S. telescope array **discovered** high-energy **gamma-ray emission from the pulsar wind nebula** (PWN) N157B. Located in the Large Magellanic Cloud galaxy at a distance of 48 kpc, this is the most distant gamma-ray-emitting PWN ever detected, being the first individual stellar extragalactic TeV gamma-ray source. The pulsar PSR J0537−6910 which powers the PWN is the most energetic pulsar known. Detection of a PWN at such a large distance is possible due to the high spin-down power of the pulsar and also due to strong infrared-photon fields emitted from nearby sources. These serve as additional targets for inverse Compton up-scattering by relativistic electrons and positrons to TeV photon energies. If the pulsar emission is provided mainly at the cost of its rotational energy loss, then the pulsar's birth period would be shorter than the shortest birth period ever derived for a pulsar, unless spinning up by a companion star in a binary system is assumed. The estimated mass of the progenitor star of at least 15 solar masses is close to the limit for black hole formation in supernova explosion. This places the pulsar PSR J0537−6910 at the upper mass limit for neutron star production.

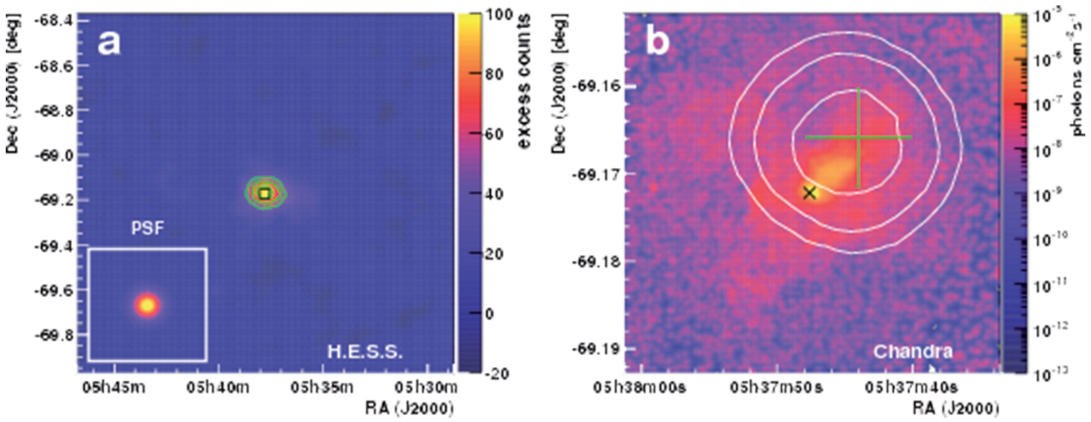

Fig. 5 *Gamma-ray and X-ray view of N157B. a) Image of the TeV gamma-ray excess obtained with H.E.S.S. The instrument's point-spread function is shown in the inset. The green contour lines denote 6, 9, and 12σ statistical significance and the black box outlines the region shown in the X-ray image. b) X-ray image from Chandra X-ray Observatory (0.8–8 keV) with white contours denoting regions of 68%, 95%, and 99% confidence limits for the position of the gamma-ray source. The position of the pulsar PSRJ0537−6910 is indicated by a black cross. The green cross marks the best-fitted position and the systematic uncertainty in pointing of the H.E.S.S. telescopes.*

The Cherenkov Telescope Array (CTA) is the biggest astronomical project dedicated to observations of very high-energy gamma rays in the energy range from about 20 GeV up to more than 100 TeV. Two observatories (or arrays) will be built, one placed in each of the Northern and Southern Hemispheres, so that the whole sky is covered. Each array will be composed of 50–100 Cherenkov telescopes. To sample the gamma rays in the wide energy range three different telescope types will be constructed: Small-Size Telescopes (SSTs) with 4 m diameter reflector, 12 m diameter Mid-Size Telescopes (MSTs) and 23 m diameter Large-Size Telescopes (LSTs).

The array of small-size telescopes will be dedicated to observations of the most extreme gamma-ray sources emitting in energies up to 300 TeV. This energy range has been unavailable so far for current instruments of gamma-ray astronomy, but it is very important for understanding the cosmic ray acceleration processes. The main limitation for observations at highest energies is due to a much smaller fluxes of high-energy photons compared to the less energetic ones. Because of that the SST array composed of several tens of telescopes will cover an area of several kilometers square, in order to achieve the sensitivity which is sufficient for the observations to be performed.

The team of engineers and scientists from the Institute of Nuclear Physics PAS has designed and built the prototype mechanical structure and drive system of the Small-Size Telescope. The telescope has a focal length of 5.6 m, 4 m diameter reflector, and will be equipped with a novel fully digital camera based on silicon photomultipliers. The latter is currently being developed by other institutions of the Polish Consortium of the CTA Project and the cooperating team from the University of Geneva. The full telescope prototype – with the camera, mirrors, and auxiliary systems – will be ready for first observations at the end of 2014 (see **Fig. 2**, page 83).

Grammatical rules together with the information content of a message impose relations on the symbols, which can conveniently be expressed in the form of networks. Such **linguistic networks appear to reveal novel aspects of complexity**. If words are considered as the building blocks of language samples, a network can be constructed by associating the words with nodes and the relations among them with edges. The simplest relation that can be studied in this manner is adjacency: if two words are direct neighbours in any place in a sample, they are connected with an edge. Even such a straightforward choice of a network representation of texts leads to the formation of a complex network structure. Topological details depend on the text sample, but the overall picture seems to be universal: adjacency network is strongly non-democratic with a clear hierarchy of hubs, characterized by a large number of edges, surrounded by clouds of peripheral nodes with one or at most a few edges. This is documented in the upper panels of **Fig. 6** for two examples of English literary works: *Finnegans Wake* by James Joyce and *Pride and Prejudice* by Jane Austen, but the same can be said about texts written in other languages (e.g., in Polish). There are texts that are characterized by a clear power-law distribution of node degrees and there are some in which such a structure is less evident (bottom left panel of **Fig. 6**).

From the topological perspective, as important as the structure of a "mature" network, is also the process of network formation, i.e., how does the network topology change as new edges are added. In the case of scale-free networks, the standard mechanism of network growth is preferential attachment. However, adjacency networks grow according to a different mechanism in which growth of the number of nodes is substantially constrained by the so-called Heaps law. The resulting networks may thus be considered as being of a new type, the topology of which has not yet been considered. One of the properties of such networks can be observed in bottom right panel of Figure, presenting the average shortest path length (APL) as a function of network size (number of nodes N). Despite the hierarchical structure of associated networks, their APL behaves differently than does the APL of scale-free networks (in the last, APL(N)~log(N)). Networks of this new type will be further studied.

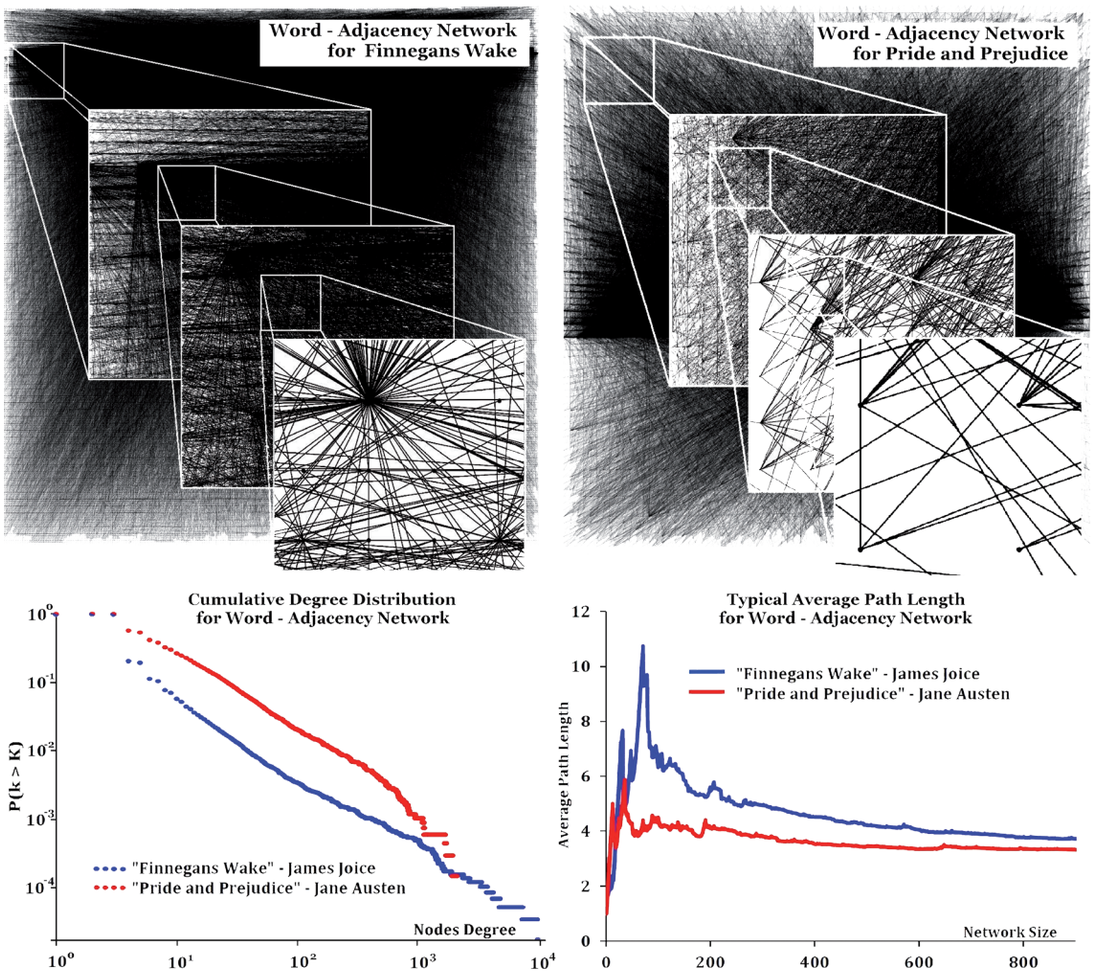

Fig. 6 *Topology of word adjacency networks created for Finnegans Wake by James Joyce and Pride and Prejudice by Jane Austen. Nodes correspond to words and edges connect pairs of neighbouring words (top). Distributions of node degrees (bottom left) and functional dependence of average shortest path length on number of nodes (bottom right) is shown for the same two texts.*

A Study of multiscaling in musical compositions was based on analysis of 160 pieces of music of six popular genres: classical music, pop music, rock, hard rock, jazz, and electronic music. All the analysed pieces were written in WAV format. In this format the varying amplitude of the sound wave V(t) is encoded by a 16-bit stream sampled with 44,1 kHz frequency. After encoding, the amplitude V(t) was expressed by a time series of length depending on the temporal length of a given piece of music (several million points, on average). Multifractal Detrended Fluctuation Analysis (MFDFA) was used to calculate fractal dimensions ($f(\alpha)$) and Hoelder exponents (α) for individual components of a signal decomposed with respect to the size of fluctuations. In **Fig. 6**, we present a typical example of such a multifractal spectrum. The multifractal strength is a quantity which describes the richness of multifractality, i.e., how diverse are values of the Hoelder exponents in a data set. It can be estimated by the width of the parabola-like shaped $f(\alpha)$: $\Delta\alpha = \alpha_{max} - \alpha_{min}$.

In **Fig. 7** we present a collection of all the calculated widths of $f(\alpha)$. Vertical lines separate different music genres and each piece is represented by a single horizontal line. The years placed in the **Fig. 8** stand for the period of artistic creativity or year of release. Interestingly, the largest multifractal strength $\Delta\alpha$ and hence the richest multifractal structure appear in pop music. Moreover, the most variable multifractal spectra widths characterize also pop ($0.5 < \Delta\alpha < 2.8$), rock ($0.5 < \Delta\alpha < 2.1$) and hard rock ($0.51 < \Delta\alpha < 2.15$) music. This variability of multifractal properties suggests that the pieces belonging to these genres markedly differ within that genre. Much more consistent from this point of view are pieces of classical music, jazz and electronic music. It is worth noting, that in the case of Fryderyk Chopin's music, the later the pieces were created, the more complicated on average is their multifractal structure (but not the variability of $\Delta\alpha$). One may therefore tentatively conclude that it is the richness of multifractal forms which makes the distinction between popular music and the more refined, less popular and more "classic" musical genres.

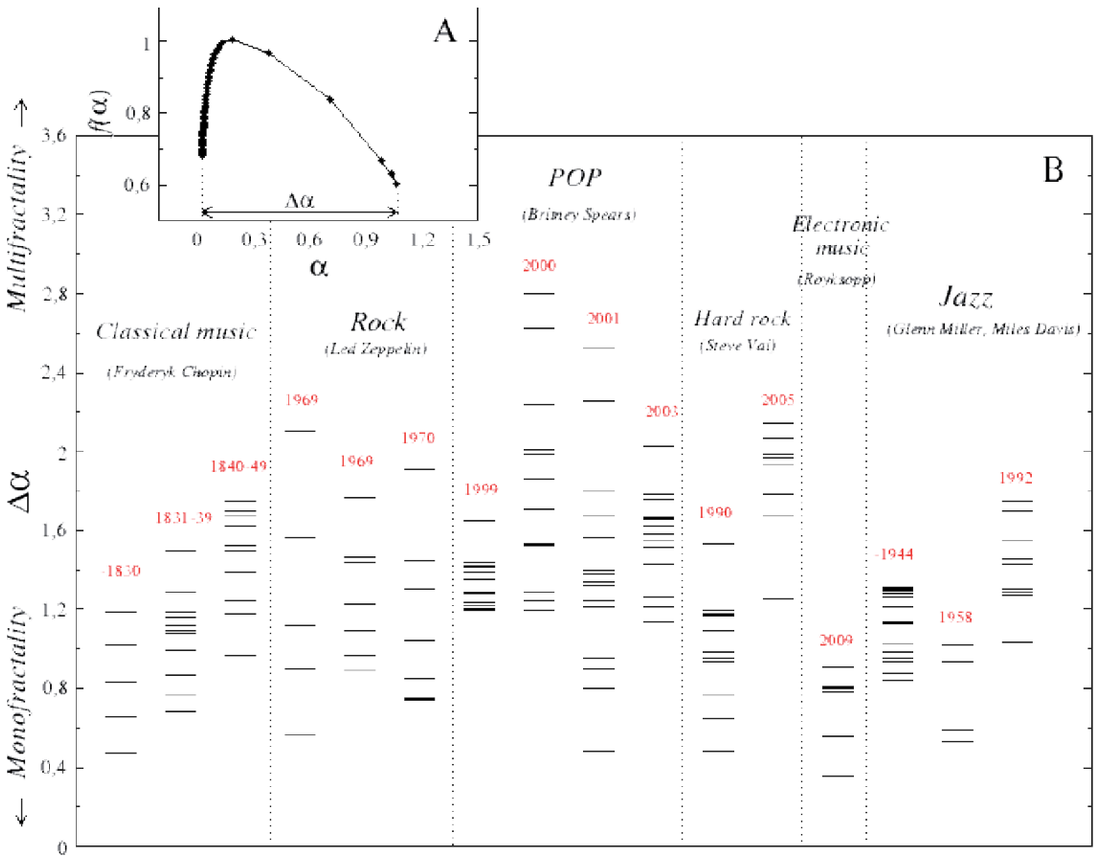

Fig. 7 *A) Example of a multifractal spectrum $f(\alpha)$ of a music piece. B) Values of $\Delta\alpha$ calculated for every analysed piece of music (short horizontal lines). Columns correspond to individual artists, period of their career, or year of issue of piece. Dotted vertical lines separate different music genres.*

Interest in toy models of **quantum** phenomena – such as the **Cube model of a qubit** presented here – stems from the simplicity of classical concepts they are built on. Besides intuitive insights, they also provide us with a convenient tool for studying the distinctive features of quantum theory. Recent research shows that many phenomena typically associated with strictly quantum mechanical effects have their classical analogues. These results suggest that quantum states can be seen as states of knowledge and a considerable effort is presently under way to understand the possible ψ-*epistemic* reconstructions of the theory. Here, we focus our attention on a single qubit for which a simple discrete system is able to faithfully reproduce the characteristic quantum-like behaviour of a certain nontrivial subset of states of a qubit. In the model we explicitly describe what constitutes a measurement and how the system can be transformed, thereby restricting the agent's ability to gain information about the system. We show that the agent's account of the system is fully equivalent to a constrained version of a qubit, corresponding to the convex hull of eigenstates of Pauli operators, Clifford transformations and Pauli observables.

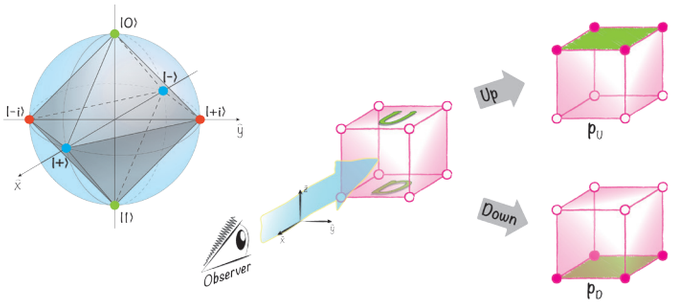

Fig. 8 *On the left, an octahedron inscribed in the Bloch ball representing states faithfully reproduced by the toy model. On the right, an observer performing a basic measurement may distinguish only between the upper U and the lower L faces of the cube, respectively.*

The research reported herein was performed pursuant to internal projects: [110, 111, 112, 115, 206, 401]; [E16, E18, E27]. See Annexes I, IIB.

V. DIVISION OF APPLIED PHYSICS AND INTERDISCIPLINARY RESEARCH

The main scientific activity of the Division is in the areas of life and health, energy and environmental hazards, and in studies of physical properties of low-dimensional materials. Most of research is performed in our own laboratories. The Division is composed of eight Departments which are generally organized around their advanced research tools available at the Institute.

The **Department of Applied Spectroscopy** (since 2012 renamed as the **Department of Experimental Physics of Complex Systems**) is engaged in interdisciplinary studies in the fields of biology, medicine and protection of the environment, carried out using ion, X-ray and synchrotron radiation microprobes. The main research tool is the HVEC KN-3000 Van de Graaff (VdG) accelerator, equipped with an ion microprobe, able to deliver a 3 MeV proton beam focused to a spot of 7 μm diameter in vacuum and 15 μm in air. The microprobe setup is the only such facility in Poland. Extensive trace element analysis is performed using PIXE, PIGE, and RBS beam techniques, and by SR-FTIR, XANES, and EXAFS methods, using synchrotron radiation. All these techniques are applied in biology, ecology, medicine, agriculture and geology. To obtain synchrotron radiation microprobes we collaborate with LNF, NSLS, ANKA, SOLEIL, and HASYLAB institutes. Our studies in the fields of biology, geology and medicine (radiation biology, in particular), as well as in materials science are carried out with the use of our X-ray microprobe. Research methods include computer microtomography, XRF and Total Reflection XRF, microcrystalography, and targeted irradiation of mammalian cell compartments. Our nanoscale biomedical studies are carried out using atomic force microscopy integrated with optical and fluorescence microscopes. Atomic force microscopy (AFM) enables measurements of mechanical properties to be performed for individual cells in conditions close to natural. The AFM technique has found numerous applications in different research areas, such as biophysics or medical sciences.

The **Department of Materials Science** applies nuclear and non-nuclear methods to study condensed matter. Our research covers a wide spectrum of topics related to thin films, coatings and structure of intermetallic compounds and alloys. Various methods, such as molecular beam epitaxy, laser ablation, ion beam sputtering, dual ion beam-assisted deposition, chemical vapour deposition or chemical synthesis are used to develop new materials. These materials are fabricated using micro- or nanopatterning with direct laser interference lithography, nanosphere lithography or with nanopore alumina templates. In our research we are able to apply classic solid state-physics methods (magnetoresistance measurements, SQUID magnetometry, X-ray diffraction), spectroscopy and microscopy (Raman spectroscopy, Auger spectroscopy, atomic/magnetic force microscopy, electron microscopy) and to combine them with nuclear analytical techniques

such RBS, NRA, ERDA measurements, using our VdG accelerator and local probe methods, such as Conversion Electron Mössbauer Spectroscopy or the Perturbed Angular Correlation technique.

The **Department of Radiation Transport Physics** is mainly engaged in theoretical, experimental and computational aspects of neutron and gamma-ray transport physics. The Department is a member of the Euratom – IPPLM Association which coordinates fusion research related to the International Thermonuclear Experimental Reactor (ITER) programme. The Department is engaged in developing neutron and ion diagnostic methods for the needs of thermonuclear devices: tokamaks (JET, ITER) and stellarators (Wendelstein 7-X). The Department is equipped with a 14 MeV pulsed neutron generator with a tritium target and a double-module nanosecond source of 2.45 MeV fast neutrons generated in Plasma-Focus devices from a high electric current discharge in gaseous deuterium. The Department is also engaged in research to counter illicit trafficking of materials by applying neutron detection methods, and in projects concerning nuclear borehole geophysics.

The **Department of Radiation and Environmental Biology** studies biomarkers associated with the alteration of the DNA repair process, and the corresponding radiation hazard. A retrospective biological dosimetry laboratory has been established in this Department for rapid evaluation of radiation exposure, where classic cytogenetic, molecular cytogenetic – fluorescence in situ hybridization (FISH) and the alkaline version of single cell gel electrophoresis (SCGE) methods are applied for diagnostic and research purposes.

The **Department of Magnetic Resonance Imaging** is an interdisciplinary laboratory dedicated to biomedical and materials research and to developing new MRI techniques. Our main MRI research system is based on a Bruker Biospec 9.4T horizontal magnet equipped with a number of dedicated probe heads, including the CryoProbe™, and also with advanced animal monitoring and control systems. This equipment was purchased with partial EU funding and is used predominantly for interdisciplinary biomedical studies *in vitro* or *in vivo* using animal models. Another 4.7 T MR imaging system equipped with an USP-4 compatible probe head is used for dissolution studies of pharmaceuticals in different encapsulations. In combination with an ergometer, MR is used for dynamic exercise studies on human extremities. Apart from biomedical applications of MR, dedicated actively shielded gradient coils and RF probes are also being designed and developed at this Department.

In the **Department of Nuclear Physical Chemistry** measurements of plutonium, americium, uranium, thorium, polonium, ^{90}Sr, ^{63}Ni, ^{7}Be, ^{99}Tc and ^{137}Cs in various environmental samples are performed. The main equipment consists of low background, high resolution (germanium) gamma-ray spectrometers, semiconductor alpha-ray spectrometers and liquid scintillator spectrometer. From 1990 onwards, the Laboratory has participated in the national monitoring network for radioactive contamination organized by the Polish National Atomic Agency (PAA) and the Central Laboratory for Radiation Protection. Air filters are exposed and measured every week to assess the activity of

gamma-emitters in the aerosols. The detection limit of this system is below 1 μBq/m^3. Since 2007 the Department is also part of the global scientific network of laboratories conducting similar measurements, coordinated by the University of Tenerife, Spain). Apart from alpha-spectrometry, mass spectrometry has also been introduced as a measurement technique, in collaboration with the Institute of Geological Sciences of the Polish Academy of Sciences. Germanium detectors are designed, produced and regenerated in the Department's workshop. The leader of the germanium detector group has developed a new method of obtaining germanium detectors of low electrical capacity which enable low-energy gamma radiation to be detected.

The **Department of Radiation Physics and Dosimetry** is involved mainly in solid state dosimetry research, and in particular in the development of new methods of dose measurements and the development of new types of detectors of ionizing radiation for applications in medical physics and radiation protection. The Department specialises in thermoluminescent (TL) dosimetry. Its staff has over 30 years of experience in development, manufacture and application of TL detectors in radiation protection, environmental monitoring and clinical dosimetry. Luminescence methods and detectors for dosimetry are being developed. TL detectors produced in the Department's laboratory have also been applied in the dosimetry of cosmic radiation. Unique two – dimensional (2D) TL dosimetry systems have been developed and constructed in the Department for clinical applications in medical physics.

Current research in the **Department of Physicochemistry of Ecosystems** is focused on the analysis of trace compounds in air and in water, by means of chromatographic methods. Results of these investigations are applied in medical diagnostics, environmental physics and in hydrogeology. Some of these methods, based on gas chromatography, have been originally developed in the Department. Gas chromatographs (Agilent Technologies, Shimadzu, Fisons) equipped with a range of detectors for example mass spectrometer, thermal conductivity detector or electron capture detector, are used in the Department.

ENERGY AND CIVILIZATION HAZARDS

To assess the civilization hazards related to energy production, widely ranging methods are applied. Neutron transport physics is applied to thermonuclear plasma diagnostics in the future sources of energy-thermonuclear reactors based on tokamak or stellarator principles. Methods based on neutron transport physics are being developed for applications in geophysical prospecting of hydrocarbons, the conventional source of energy. The related civilization hazards are studied in terms of the health impact of natural and man-made radioactivity in the environment (via individual and environmental dosimetry) over a wide range of doses, or over different migration pathways of radionuclides in the environment. Levels of greenhouse gases are monitored as well as pollution of the environment by toxic trace elements, including carcinogens. Environmental markers (e.g. noble gases, CFCs and SF_6 as hydrological markers) are studied. Methods of identifying radioactive sources and illicit trafficking of hazardous materials are being developed using neutron detection techniques. The technology of improving the properties of water by magnetic treatment is also being developed.

Two working packages of the Strategic Research Project "Technologies supporting the development of safe nuclear power", financed by the National Centre for Research and Development (NCBiR) are carried out by the IFJ PAN, mainly in Division V. This Project covers issues of nuclear safety, environmental protection, and radioactive waste management related to the national programme of developing nuclear energy in Poland. A separate task, concerning fusion energy research, within the project: „Research and development of techniques for controlled thermonuclear fusion" is carried out by an IFJ PAN – coordinated consortium of five Polish institutions. Research on the use of the thermonuclear fusion reaction as a new energy source is a global challenge for the scientific community. The on-going project gives the Polish fusion research community an opportunity to contribute within the EU ITER project, which is expected to demonstrate that fusion can be used to generate electrical power. This project involves elements of research and development of measurement methods for fusion diagnostics, development of material technologies, and strengthening the Polish research infrastructure engaged in experiments related to controlled thermonuclear fusion. The **Department of Radiation Transport Physics** is deeply involved in the EU ITER project. A new Laboratory equipped with pulsed 14 and 2.4 MeV neutron sources has been organised at IFJ PAN to develop diagnostic systems for fusion energy production.

Studies of civilization hazards and other issues due to changes in the environment are carried out mainly at the **Department of Nuclear Physical Chemistry** and at the **Department of Physicochemistry of Ecosystems**.

On March 11, 2011 the great east-Japan earthquake and tsunami led to severe damage to three of the six nuclear reactors on the site of the Fukushima-Daiichi Nuclear Power Station. First signs of this accident were detected in Europe a few days later when the radioactive cloud flowing across the Pacific and towards North America reached Europe. At the **Department of Nuclear Physical Chemistry** traces of this nuclear accident were first measured in the air in the morning of March 24, in air filters exposed since March 21st, 2011. The presence of ^{131}I, ^{132}I, ^{129m}Te, ^{132}Te, ^{134}Cs, ^{136}Cs and ^{137}Cs was established. Some of our results have already been published in a joint report of the European air-monitoring network. Measurable concentrations of caesium (above the detection limit) were observed two days after enhanced iodine levels were measured. Maximum activities of ^{131}I, ^{134}Cs and ^{137}Cs in aerosols were observed on March 29th. Our laboratory was the only one in Poland and one of the few in Europe where not only the aerosol but also the gaseous fractions of ^{131}I in the air could be measured. The time profile of ^{131}I in gaseous and aerosol fractions is presented in **Fig. 3**. The ratio of activity in the aerosol fraction ^{131}I to the gaseous fraction changed with time, being almost equal to 1 at maximum activity, and next decreased to below 1:10 in mid-April. It is evident from our results that the doses to people at such remote locations as Poland, due to the Fukushima cloud, are completely negligible – being in the range of a few nano-Sv (while doses to Polish citizens due to the Chernobyl accident were a thousand times higher – fractions of mSv – but still very small).

Natural and man-made radioactivity and the contribution of potentially harmful chemical elements in the environment are studied in our Division. Several of our projects concern radioactivity in the environment over polar regions of Spitsbergen and the Antarctic.

Chlorofluorocarbons (CFCs), used in the manufacture of aerosol sprays, solvents, refrigerants, or as foaming agents in packing materials, contribute to ozone depletion in the stratosphere. The CFCs and sulphur hexafluoride SF_6 contribute to the greenhouse effect. Their concentrations in the atmosphere are at ppt levels. At our **Physicochemistry of Ecosystems Departments** for almost 15 years we have continuously measured CFCs and SF_6 concentrations over the urban area of Kraków, using a system of gas chromatography. The long-term data collected by our urban-area monitoring station, unique in Central Europe, are referenced against data from the "clean" station at Mace Head (Ireland, 53° N, 10° W), of lattitude close to that of Kraków (50° N, 19° E). Based on these data, implementation of the Montreal Protocol (adopted in the Polish law), has been monitored.

An assessment of the natural status of the environment at locations planned to become potential sites for nuclear power stations in Poland is mandatory. An important element of this evaluation is the status of groundwaters. Measurements of concentrations of anthropogenic gasses (SF_6, freons: F-11, F-12) offer the possibility of dating "young" waters (up to 50 years) in hydrogeological investigations. We are able to measure concentrations of SF_6, F-11, and F-12 using chromatographic methods at detection levels (LOD) of 0.06 fmol/l H_2O, 2.1 pg/l H_2O and 1.2 pg/l H_2O, respectively. On the other hand, the concentration of He is a perfect marker for dating "old" ground-waters of ages ranging between a hundred and ten thousand years. We are able to measure helium concentrations at a detection level of $1.2 \cdot 10^{-8}$ cm^3 STP/cm^3 H_2O.

Of similar nature are studies of physical properties of geological and environmental samples, carried out using our nuclear and X-ray microprobes at the **Department of Applied Spectroscopy**. We are able to evaluate the elemental content and its distribution in a sample by detecting induced X-rays and back-scattered or transmitted ions, using μ-PIXE, μ-RBS or STIM techniques. We are also able to evaluate the porosity, specific surface area, tortuosity and hydraulic permeability of samples by means of computed X-ray micro-tomography. Such studies are of interest over a wide range of applications, e.g. in geochronology or in fluid flow parameters through porous media, extremely important in oil prospecting.

LIFE AND HEALTH RESEARCH

Important areas of our life and health research are medical physics and dosimetry, proton radiotherapy and biomedical applications (effects of radiation on cells in vitro and in vivo, such as generation of mutations, chromosome aberrations or DNA damage, as well as variation of mechanical properties of cell membranes, such as their deformability or rigidity). This research is carried out using a wide range of methods: nuclear spectroscopy, magnetic resonance imaging (MRI), atomic force microscopy (AFM), gas chromatography, fluorescence in situ hybridization (FISH), single-cell gel electrophoresis (the Comet assay) and by synchrotron radiation-based techniques.

Basic and applied research in biomedicine and radiobiology is carried out in the **Department of Applied Spectroscopy** where micro-focused ion, X-ray, and synchrotron radiation beams are applied, together with studies of the distribution of oxidation states of sulphur, transition metals and trace elements in pathological cells and tissues. Elemental analysis is carried out by means of SR-XRF, PIXE, PIGE, RBS and STIM techniques while the chemical microstructure of samples is studied using EXAFS, XANES, SR-FTIR, and Raman methods.

Research on the mechanical properties of living cells in their native environment is also carried out at the **Department of Applied Spectroscopy** using atomic force microscopy (AFM). The AFM technique is able to determine the mechanical properties of cancerous cells in order to develop a method for diagnosing changes resulting from cancerous transformation or other pathological manifestations in cells. This research is performed in collaboration with the Chair of Medical Biochemistry of the Jagiellonian University and with the Ecole Polytechnique Federale de Lausanne in Switzerland.

Studies of post-irradiation DNA damage and repair processes and of chromosomal aberrations as a function of environmental, diagnostic, therapeutic, professional or accidental exposures (retrospective biological dosimetry), and of the related health risks, are performed at **the Department of Radiation and Environmental Biology**. The Department also studies individual radiosensitivity of patients with prostate

cancer or with benign prostatic hyperplasia, applying the FISH technique. DNA damage, sensitivity and rate of lymphocyte repair have also been investigated by single-cell gel electrophoresis. Also, to explore the dependence on LET of ionizing radiation of the DNA repair process *via* homologous recombination (HR), dose-response relationships for sister chromatid exchanges (SCE) were investigated.

Nuclear magnetic resonance imaging (MRI) is a powerful technique in biomedical research. The **Department of Magnetic Resonance Imaging** is involved in preclinical investigations of pharmaceutics to avert pathological changes in cardiovascular and neurological systems, using animal models. Investigations of diastolic and systolic heart function failures in Transgenic Mice, MR diffusion tensor imaging (DTI) of of spinal cord injury in a rat model, and MRI and MRS studies of brain diseases in animal models, have been performed. Molecular imaging approaches to better detect pathologies have also been undertaken. USP4-compatible MRI studies of the dissolution of controlled release pharmaceutic dosage forms, and 31P MRS studies of human muscles under dynamic exercise conditions are also being performed.

The **Department of Nuclear Physical Chemistry** where radionuclides for medical applications are being developed (e.g., isolation of ^{211}At to obtain new radiopharmaceuticals) and activation analyses are conducted using our AIC-144 cyclotron, contribute significantly to our *Life and Health research*. The Department collaborates with Voxel Company in developing ^{66}Ga as a PET radionuclide. A set-up with a rotating probe holder was constructed and initial activations using beams of charged particles were conducted. A whole-body spectrometer with a XIX-th century steel shield and a large scintillation detector, obtained from the University Hospital of Łódź, was installed at IFJ PAN and further equipped with two germanium detectors and NIM electronics, to be used in cases of accidental exposures and for research.

The presence of specific volatile compounds in air exhaled by patients may be exploited for diagnostic purposes. An elevation in the concentration of sulphur compounds in exhaled breath is observed in paradentosis, halitosis, liver failure, lung cancer, or allograft rejection. Amines are present in the breath of renal failure or trimethylaminuria patients. Measurements of amine concentrations in breath samples may be useful in the early diagnosis of renal failure or in monitoring the process of dialysis. The **Department of Physicochemistry of Ecosystems** has developed methods of measuring concentrations of sulphur compounds (H_2S, COS, CH_3SH, C_2H_5SH, $(CH_3)_2S$) and of aliphatic amines ($(CH_3)_2NH$, $(CH_3)_3N$) in exhaled air using gas chromatography and has also developed special procedures for collection and storage of breath samples.

The **Department of Radiation Physics and Dosimetry** has significantly contributed to the European "Matroshka" space radiation dosimetry project organized by the European Space Agency. Within this project, a humanoid phantom representing the human body was exposed in space outside the International Space Station (ISS) for 1.5 years, in order to measure organ doses, which would be experienced by astronauts in space. At several locations within this phantom, representing different internal human organs, over 3000 miniature lithium fluoride thermoluminescent detectors (mostly produced at the IFJ PAN) were placed and read out at this Department after recovering the phantom to Earth.

PHYSICAL PROPERTIES OF LOW-DIMENSIONAL MATERIALS

*The research activities in the field of low-dimensional materials, carried out in the **Department of Materials Science**, are focused primarily on solid state effects due to the small scale of dimensions, surfaces and interfaces of samples. Studies concentrate in two areas: (i) magnetic ultrathin films and nanostructures, with emphasis on perpendicular magnetic anisotropy and (ii) carbon and diamond coatings for biomedicine. We perform basic research on potentially applicable magnetic materials and biomaterials, such as specific coatings, thin films, nanostructures, nanoparticles and coatings of thicknesses ranging between a few tens to thousands of nanometers. We are particularly interested in relationships between the change of structural properties and growth type of materials on the one hand, and on their magnetic, transport and thermoluminescent properties on the other.*

The main part of our research is devoted to the rapidly developing field of spintronics, and to such important effects as Giant Magnetoresistance, perpendicular magnetic anisotropy, and to exchange-bias.

Our present work concerns studies of the magnetic properties and structure of FePd thin films improved by alloy admixtures patterned with nanosphere lithography. To better understand phenomena at nanoscale range, control is required of the properties of the material and of processes at the atomic scale, which can be achieved using local nuclear probe techniques. Here, application of Conversion Electron Mössbauer spectroscopy is of particular importance in providing information about the transformation of Cu-doped Fe/Pd multilayers deposited on nanospheres into the FePd L10 magnetic alloy. Changes of structural and magnetic properties of non-epitaxial Cu-doped FePd thin films induced by pulsed laser irradiation is a new concept which has not yet been applied in studies of the L10 multilayer-alloy transformation system. We expect to gain insight into the L10-phase ordering mechanisms and to the origin of magnetocrystalline anisotropy present in the investigated alloy. Apart from nanosphere and direct laser interference lithography we are currently exploring other patterning methods. Within our group, we invented a new method of chemical synthesis of anodized alumina substrates which will now be used as substrates for nanostructuring of the FePdCu alloy.

Magnetic particles, studied by the **Department of Materials Science**, find many applications in magnetic resonance imaging, cancer therapy, or delivery and separation of pharmaceutics. To pursue their unique properties and functions, α-Fe2O3/ Fe3O4 composite particles are fabricated by laser irradiation of colloid solutions. The size and composition of these particles can be controlled by varying the fluence or irradiation time of the laser beam.

Optimization of growth conditions during deposition of diamond coatings by the microwave plasma-enhanced chemical vapour deposition method, allowed us to obtain polycrystalline diamond films of high purity with good and reproducible thermoluminescent properties, applicable in TL-based clinical dosimetry of ionizing radiation in radiotherapy. Development of these diamonds as active detectors and dosimeters of ionising radiation is currently under way.

Ion beam deposition methods were used to prepare carbon coatings doped with metals (Ti, Ir, Pt) on polymer substrates for applications in hip and heart endoprotheses. A special method for homogeneously depositing carbon coatings on 3-dimensional elements was developed, resulting in perfect biocompatibility and very good mechanical strength of elements of the endoprotheses.

In our collaborative research efforts in the area of magnetic alloys we have been aided by our long-standing and fruitful cooperation with the Chemnitz Technical University and Karlsruhe Institute of Technology. Our Materials Science Department also closely collaborates with other academic institutions in Poland (AGH – University of Science and Technology, Jagiellonian University, Institute of Metallurgy and Materials Science Polish Academy of Sciences, University of Rzeszów) and abroad: the Ukraine (Sumy State University), Belarus (Belarussian State University) and Belgium (Hasselt University).

SELECTED RESEARCH HIGHLIGHTS OF THE APPLIED PHYSICS AND INTERDISCIPLINARY RESEARCH

The European Atomic Energy Community (Euratom) programme of research on controlled thermonuclear fusion has been continued for many years. It is aimed at building a tokamak-based thermonuclear power plant where the deuterium-tritium (D-T) burning plasma will produce energy from the fusion reaction. One of the key issues within this programme is to develop suitable detectors for thermonuclear plasma diagnostics. Only detectors resistant to high particle fluxes and high temperatures are suitable for this purpose. **Synthetic high purity monocrystalline diamonds, scCVD, are good candidates for ion and neutron spectrometry in the harsh environment of a thermonuclear fusion reactor.**

The spectrometric properties of a scCVD diamond detectors of 50 μm thickness and active area diameter of 2 mm were tested using the AMR33 triple alpha isotope source (^{239}Pu, ^{241}Am, ^{244}Cm, energies at ~5.5 MeV) and a ^{212}Bi + ^{212}Po source (energies 6.0 and 8.7 MeV). Much better results were achieved than those obtained using a typical silicon detector. The scCVD detectors were also investigated using mono-energetic ion beams from the Van de Graaff accelerator. The geometry for Rutherford backscattering spectrometry was used to obtain better energy resolution and to decrease the high particle flux of helium ions, protons and deuterons of energies between 0.5 and 2.1 MeV. The obtained calibration curve is linear over the whole range of energies of ions used in these experiments. Therefore, **we expect to be able to apply diamond detectors for spectrometry diagnostics of "escaping" alpha-particles of maximum energy 3.5 MeV in a magnetic confinement plasma device.**

A further issue is with the performance of the diamond detector in the mixed radiation field of the tokamak. Our 14 MeV neutron generator was used as a source of particles from the D-T reaction, to simulate the neutron and alpha particle fluxes in the hot plasma of the tokamak. The ^{3}H(d,n)^{4}He, ^{2}H(d,p)^{3}H, and ^{3}He(d,p)^{4}He nuclear reactions also occur in the tritium target. Using our diamond detectors of different construction, we are currently measuring the energetic spectra of these mixed fields in a high flux deuteron beam in order to find their best configuration for tokamak applications.

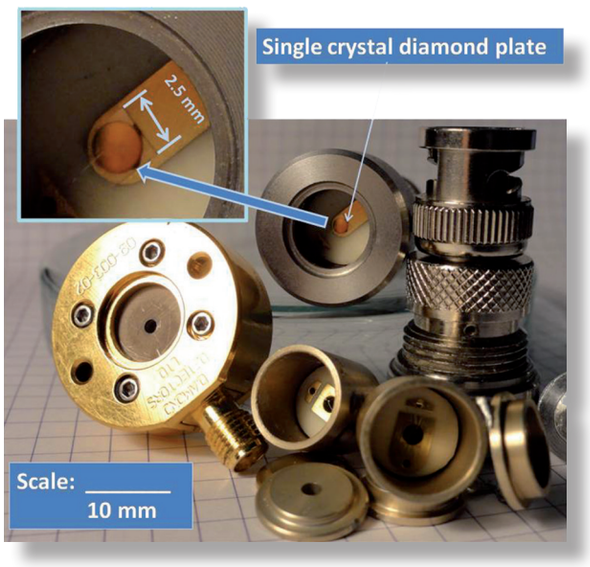

Fig. 1 *scDVD diamond detectors of 2.5 x 2.5 mm^2 size in various holders, for tokamak applications.*

Within the national research project "Technologies supporting the development of safe nuclear power" in the part concerning nuclear power radioactive waste management, **we have proposed the reduction of radioactive waste by radiochemical methods** applying short-lived radioisotopes obtained using our AIC-144 cyclotron. We obtained short-lived radioisotopes (^{90}Sr, ^{129}I, ^{134,135,137}Cs) as analogues of long-lived radionuclides or stable isotopes of metals of the platinum group (Pd and Rh) present in spent nuclear fuel. **We developed radiochemical methods for selective separation of these radioisotopes from cyclotron-irradiated targets.** The technique of ion exchange chromatography was used to extract Pd radioisotopes, of reversed-phase chro-

matography to extract ^{82,85}Sr and of thermo-chromatography to extract ^{124,126}I. We also combined some of our currently used analytical procedures to determine the presence of ^{99}Tc, ^{63}Ni and ^{237}Np in environmental samples. Within this national project, we are currently working on the detection of noble radioactive gases.

The Whole Body Spectrometer (WBS) at the Institute of Nuclear Physics (IFJ PAN), one of only two such instruments now operating in Poland, is able to perform whole-body gamma-spectrometry (Fig. 2). Our whole body spectrometer began operation at the end of February 2011. It is used to monitor natural or accidental intakes of radioactive contamination in the human body, such as intakes of radiation workers at IFJ PAN, of medical staff who work in the field of nuclear medicine, or in persons exposed as a result of an accident in which radioactive materials are released to the environment. **The Fukushima accident which followed the earthquake and tsunami of 11 March 2011 gave us the first opportunity to use our WBS (Fig. 3).** We were able to study assess the body burden of a few Polish citizens who visited Japan at the time of the Fukushima accident. Although a clear signal from the Fukushima fallout could be observed in persons who returned from Japan, their calculated doses are negligible. During 2012 several measurements were performed of nuclear medicine workers exposed to ^{131}I or ^{99m}Tc. We are currently improving the calibration of our WBS to account for differences in body shape.

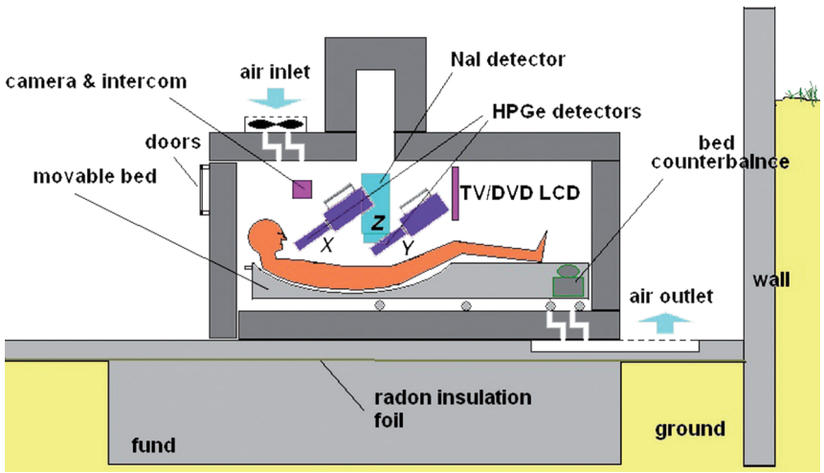

Fig. 2 *Overall design of the Whole Body Spectrometer (X,Y – detectors HPGe, Z – NaI).*

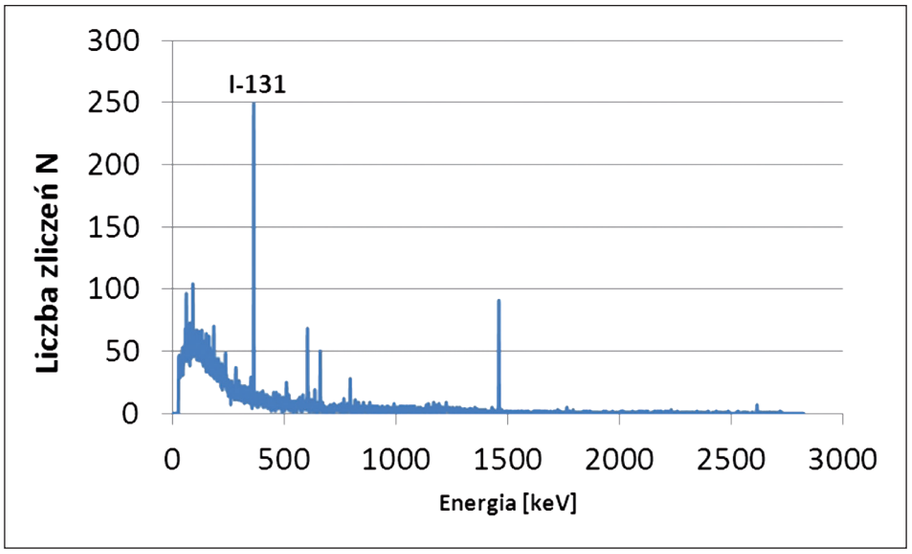

Fig. 3 *Gamma spectrum of a person who returned from Japan to Poland after the Fukushima accident. While the ^{40}K activity is normal, enhanced activity of the caesium and iodine isotopes is related to radioactive releases from the Fukushima nuclear power station. The resulting body burden is negligible.*

Retrospective radiation dosimetry, a new field of interest of the **Department of Radiation Physics and Dosimetry**, allows a rapid dose assessment using luminescent techniques of individuals potentially overexposed during a radiological accident. For this purpose various objects may be used as personal fortuitous dosimeters. Especially mobile phones are good candidates as they are carried by a large part of the population and their parts (display glasses, resistors, etc.) were found to show luminescent properties. In 2013, we took part in a large scale EURADOS intercomparison on **application of mobile phone resistors for retrospective dosimetry**, which involved twelve laboratories from eleven European countries and one institute from the USA. Our team reconstructed by the optically stimulated method the unknown nominal doses, which were 0.3, 1.7 and 3.3 Gy, with the best accuracy among all participants.

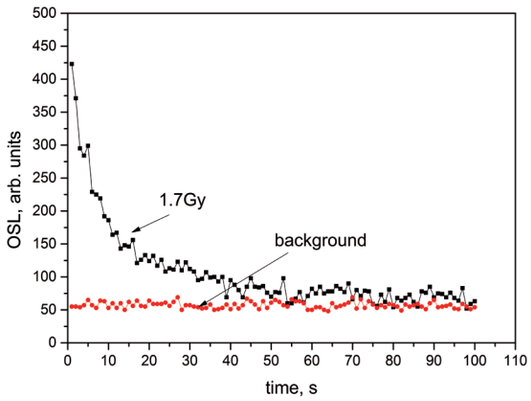

Fig. 4 *OSL signal of resistors irradiated with a dose of 1.7Gy.*

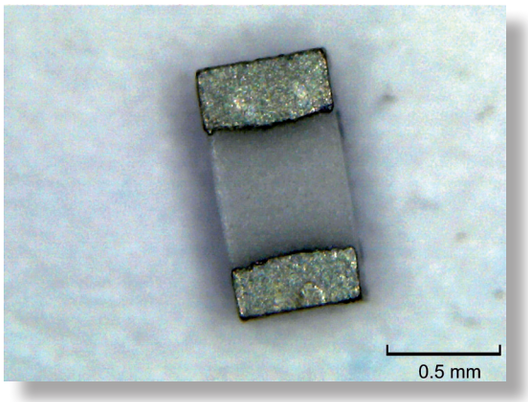

Fig. 5 *A resistor dismounted from a mobile phone.*

Analysis of the response of biological systems after doses of ionising radiation at the cellular level may provide information on the effects of natural and man-made radiation on the human organism, of relevance to natural or medical exposures. Such studies performed using cancer cell line cultures may also be relevant in cancer radiotherapy. **At the IFJ PAN we irradiate cells in culture using a unique in-house developed X-ray microprobe system.** The X-ray microprobe is based on an open-type X-ray source with a microfocusing system, delivering a source spot of about 3 μm in diameter. To evaluate the dose in such a special configuration (~0.65 Gy per second deposited in a cell of 10 μm in diameter), the GEANT4 code, extended by low energy data libraries (PENELOPE, LIVERMORE) and a toolkit for simulating interactions of radiation with biological systems at the cellular and DNA levels (GEANT4DNA), were applied.

In our experiments we used PC3 human prostate cancer cells. A population of about 10^5 cells in 4 μl medium was seeded and irradiated after 16-18 hours through a thin Mylar foil. During the cell irradiation procedure the medium was removed and the sample previewed by an optical microscope under precision step motor control. Using dedicated control software which includes image recognition algorithms, a precise dose of X-rays was then delivered to each cell, in one-by-one or in raster modes of irradiation. After irradiation at different time periods, necrotic and apoptotic cells were visualized and analysed under a fluorescence microscope. **After completing the pilot and test experiments, the microprobe has been validated for routine irradiation experiments.**

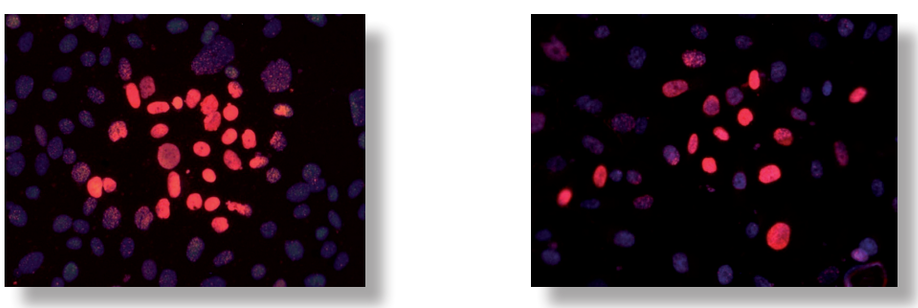

Fig. 6 *DSB damage (red spots) is visualised in irradiated PC3 cells (60 Gy per cell, average cell size ~30 μm). Left: 30 minutes after irradiation in raster mode; Right: partial recovery seven hours after irradiation (much fewer red-stained cells in the same area).*

Radiotherapy plays an important role in the treatment of many types of cancer. In the current search for methods that would maximize the efficiency of therapy and minimize the side effects and any further health risk, **we compared variability in the individual susceptibility to the induction of aberrations in chromosome 1 in the lymphocytes of prostate cancer patients (PC) by a challenging dose and compared it against individuals with benign prostatic hyperplasia (BPH)**. Peripheral blood lymphocytes were used as the biological material. To assess cellular radiosensitivity, X-rays were applied to induce DNA damage. In chromosome 1 three chromosomal regions predisposing to hereditary prostate cancer (HPC1, PCAP, CAPB) are suggested. To validate the role of these regions in family predisposition to prostate cancer, we applied region – specific probes: 1q22-31, 1q43-44 and 1p36. We also evaluated the presence of changes in cells not treated with X-rays, in subgroups stratified according to information on the occurrence of cancer in the immediate family (CIF factor). We showed that of the whole spectrum of aberrations which may be analysed using the FISH technique **(Fig. 7)**, acentric fragments appear to be a specific aberration detected in response to a challenging treatment in cases of prostate cancer, they could thus become a biomarker of radiosensitivity to radiation therapy. Moreover, **our studies suggest that to estimate individual susceptibility to radiation, it is sufficient to analyse only acentric fragments, thus significantly reducing the extent of analysis and its cost**.

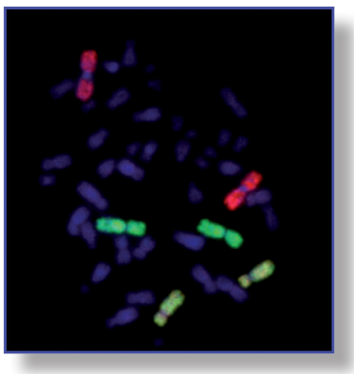

Fig. 7 *A representative example of normal metaphase spread detected by fluorescence in situ hybridization (FISH) using whole chromosome paints. Chromosome pairs 1 are painted red, 2 – green and 4 – yellow.*

Iodine-131 is used in nuclear medicine for diagnostic and therapeutic purposes. **Internal exposure to radioiodine can lead to cellular DNA damage not only in the target thyroid cells but also in peripheral blood lymphocytes. The aim of our study was to evaluate the biological effect of exposure at low** (average ^{131}I activity 2.8 ± 0.8 MBq) **and higher** (average ^{131}I activity 486.4 ± 71.9 MBq) **doses of ^{131}I, based on the frequency of chromosome aberrations** (CAS) in 27 patients diagnosed and next treated for hyperthyroidism with ^{131}I. Results from cytogenetic studies with chromosome aberrations (CA) assay in lymphocytes collected from patients 5 weeks after therapeutic ^{131}I administration have revealed, after the standardization, per applied ^{131}I activity, a high variability of the levels of cytogenetic damage, and a significant increase in the average frequency of dicentrics and rings (4.9 ± 0.8) compared to respective frequencies evaluated in these patients prior to therapy (1.69 ± 0.2, $p < 0.0002$).

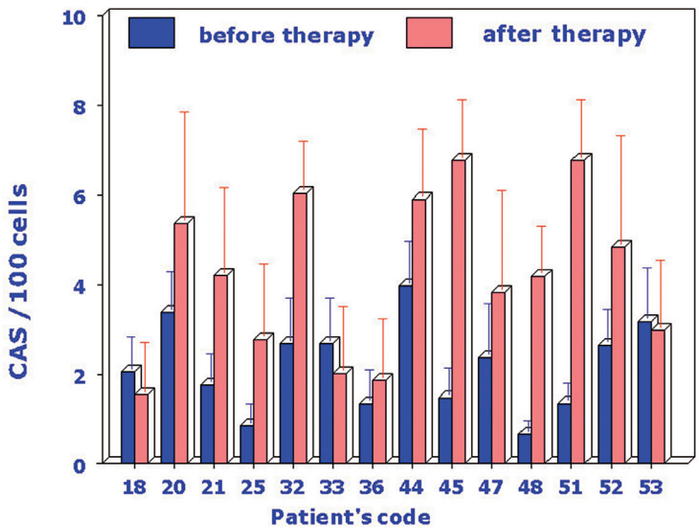

Fig. 8 *Frequencies of chromosome aberrations (CAS), per delivered ^{131}I activity in patients before and 5 weeks after ^{131}I radiotherapy.*

DNA damage due to ionizing radiation was also studied with **Tip Enhanced Raman Scattering (TERS)** allowing for the molecular structure study with the spatial resolution below 20 nm. The molecular structure of individual **Double Strand Breaks (DSBs) was experimentally verified and characterised for the first time ever by TERS** with a top-down configuration and reflective substrate. The topography of the pUC18 plasmid fixed on mica surface was imaged by AFM tip and then chosen strands were analysed by TERS using green laser beam **(Fig. 9)**. Based on spectral interpretation it was found that DSBs result from cleavage at the 3'- and 5'- bonds of the deoxyribose unit upon exposure to UVC radiation. The observation of P-O-H and methyl/methylene deformation modes enhanced in the TERS spectra proved that strand fragments are hydrogen-terminated at the lesion, indicating the action of free radicals during photon exposure. This research was performed in collaboration with Centre for Biospectroscopy, Monash University. The results were published in prestigious journal Angewandte Chemie.

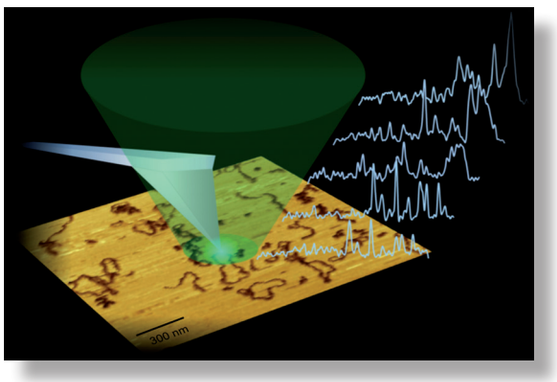

Fig. 9 *The schematic idea of TERS technique performed on DNA strands fixed on mica surface showing the AFM tip, green laser beam focused on braked DNA end, and some typical DNA TERS spectra.*

As shown in our previous studies **the cell Young's modulus, as determined by atomic force microscopy (AFM), could be useful as a marker of cell malignancy. The current question when applying AFM in medical diagnostics is not its methodological capability to detect cell malignancy but its diagnostic usefulness in in cases where cancerous cells are mixed with normal cells**. To address this issue, cancer cell recognition was performed for human melanoma (WM115 & WM266-4) and bladder (HCV29 & T24) cell lines. Each cell line was cultured either separately or as a mixture of two corresponding cell types, i.e. HCV29 together with T24 cells and WM155 with WM266-4 cells. In both cases, **AFM-based elasticity measurements have shown that the Young's moduli, determined for a mixture of cells, are grouped around two values which correspond to moduli measured for each cell line separately. This may prove the usefulness of diagnostic application of the AFM technique with Young's modulus of the cell as a marker**.

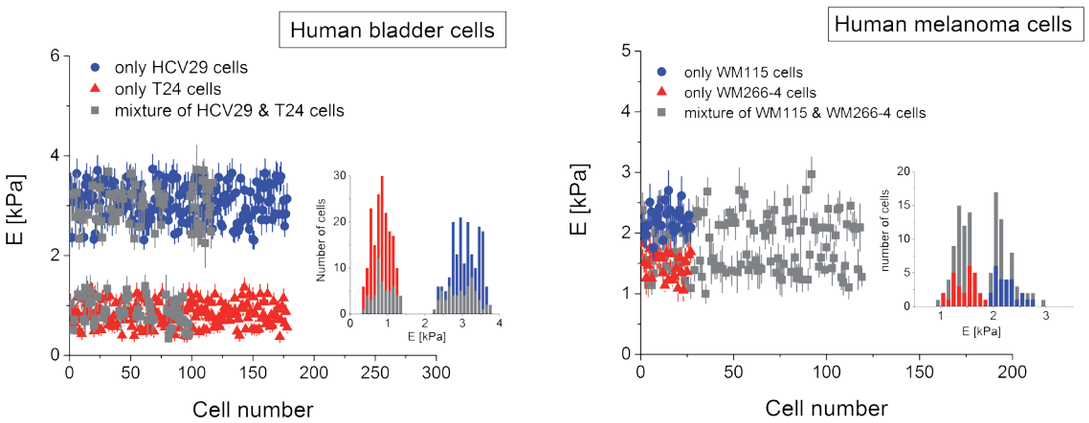

Fig. 10 *Young's modulus in individual cells, established by Atomic Force Microscopy, of human bladder and melanoma cells measured separately (blue and red points) and in cell mixtures (grey points). Each point denotes the mean value of the Young's modulus of a single cell, with its standard deviation. Insets: distributions of elastic moduli showing good separation between the corresponding cell lines.*

Applying focused beam of synchrotron radiation we were **studying prostate cancer disease by investigating individual cells and tissues to obtain 2D maps of the content of different sulfur forms** together with the microscopic image. Our studies, based on **X-ray Absorption Spectroscpy (XAS)**, are focused on determination of sulfur chemical species occurring in prostate cancer cell lines and tissue. Sulfur has a particularly rich biochemistry and fills a number of important roles in structure, catalysis, and metabolism in all organisms, thus it may play an important role in cancer initiation and/or progression. We performed our experiments at synchrotron radiation sources ANKA (Karlsruhe Institute of Technology, Germany) and SLS (Paul Scherrer Institute, Switzerland), which makes it possible to study elements with very low concetration and with high spatial resolution.

Our results showed that in case of prostate cells and tissue sulfur is present in two main chemical forms – reduced and oxidized. It was established that cell lines from different metastasis, which may differ from each other both morphologically and biochemically, had different ratios of these two sulfur species and, compared to non-cancerous cells, higher content of oxidized sulfur forms. These findings may confirm the hypothesis of changes in redox balance due to oxidation stress in case of carcinogenesis.

Moreover, for **the first time we determine the distribution of different chemical forms of sulfur in chosen areas of prostate cancer tissue**. Obtained results revealed that the dominant form of sulfur in tissue is reduced one, sulfur in intermediate oxidation state is on trace level and the oxidized form is present mainly in interstitial part **(Fig. 11)**.

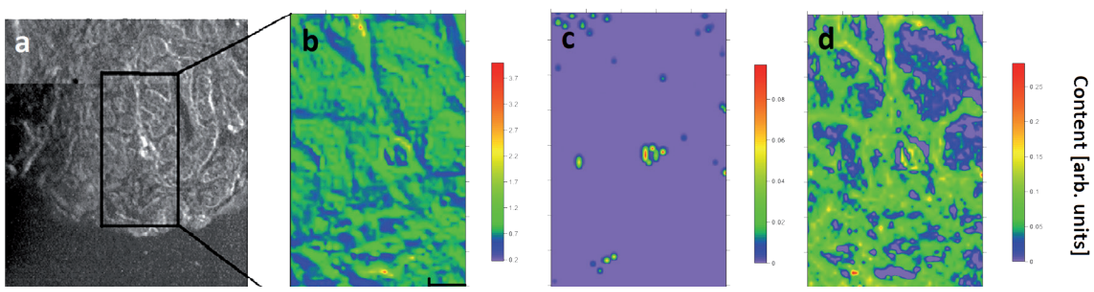

Fig. 11 *2D maps of the content of different sulfur forms together with the microscopic image (a) obtained during experiment; b.) reduced sulfur form, c.) sulfur with intermediate oxidation state, d.) oxidized sulfur form.*

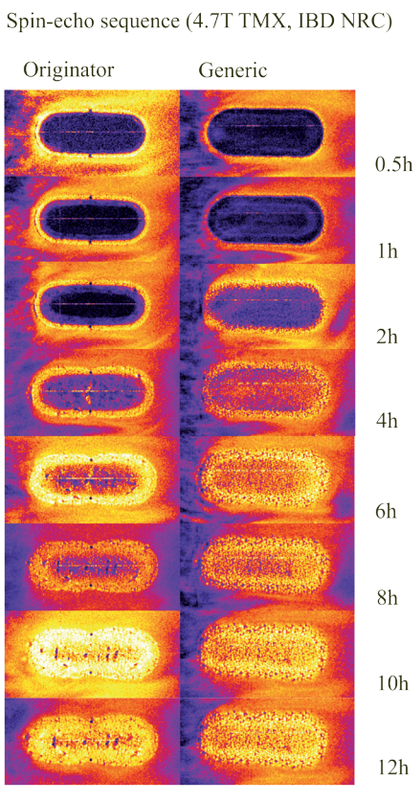

Magnetic Resonance Imaging (MRI) and micro computed tomography (μCT) can serve as complementary techniques applied in life and health research. The form of drug administration and subsequent drug dissolution are important factors in pharmacotherapy. **We evaluated NMR-based multimodal characteristics of dissolution of originator and of generic QbD (Quality by Design) - controlled pharmaceutical tablets.**

We performed the following investigations:

- MRI in USP apparatus 4 was performed using 4.7T TMX (NRC IBD, Canada) for 12 hours to assess the evolution of the hydrating matrix **(Fig. 12)**.
- Parametric images (T2 and proton density) were obtained on samples removed from the dissolution apparatus at 2h of hydration, using the 9.4T Bruker Biospec MR scanner and the BLIP_MODES pulse sequence.
- μCT imaging was performed using the Benchtop 160 CT Xi (Nikon Metrology Inc.) after 2h of hydration in the flow-through cell **(Fig. 13)**.

Fig. 12 *MR images of hydration of the originator and generic dosage forms.*

The original dosage form was a commercial "Seroquel Prolong" (AstraZeneca) compressed HPMC tablet containing 400mg quetiapine fumarate as an active/drug substance and excipients. The generic dosage form was developed according to pharmaceutical QbD (Quality by Design). Both were compared using several complementary methods:

Significant differences in matrix morphology and its temporal evolution were detected. A region of lower intensity in MR images obtained by spin-echo technique in the outer part of the interface layer was observed in the generic formulation. μCT imaging allowed us to correlate MR signal attenuation with micro-pore structure formation. We conclude that designing a generic formulation solely on the basis of dissolution profiles can lead to potential pitfalls. Our proposed method can offer guidelines for redesigning the generic formulations and can be implemented in QbD.

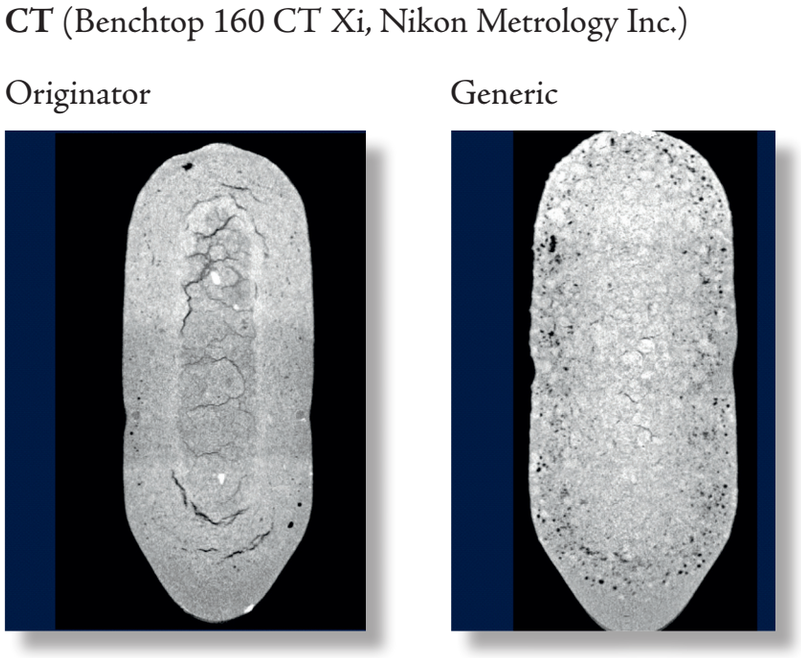

Fig. 13 *μCT images after 2h hydration of originator and generic dosage forms.*

We applied the MRI technique in vivo to characterise Cardiac Response to a Low and High Dose of Dobutamine in a Mouse Model of Dilated Cardiomyopathy.

Assessment of the left ventricular ejection function (LVEF) in response to dobutamine under echocardiography monitoring is a standard diagnostic test widely used in cardiovascular patients to detect myocardial viability or ischemia and to determine the risk of subsequent cardiovascular events. We assessed the cardiac response to low (0.15–0.5 mg/kg i.p.) and high (1.5–20 mg/kg i.p.) doses of dobutamine in Tgμq*44 mice with dilated cardiomyopathy at the stage of advanced heart failure. Inotropic, lusitropic, and chronotropic response to β1-adrenergic stimulation was assessed using the cine magnetic resonance imaging (MRI) protocol based on electrocardiogram (ECG)-triggered bright-blood images of one mid-ventricular short-axis slice.

In wild type mice (FVB) increasing doses of dobutamine resulted in subsequent increase in the left ventricular function and heart rate acceleration, but significant inotropic, lusitropic, and chronotropic cardiac response was observed only after high doses of dobutamine, which is typical. In the Tgμq*44 mice low doses of dobutamine significantly increased the inotropic and lusitropic cardiac performance without chronotropic changes. An increased heart rate was observed only after high doses of dobutamine, but then inotropic and lusitropic cardiac functional reserve was lost. **We developed an MRI stress test protocol based on a low and high dose of dobutamine-induced response, which may be useful in revealing alteration in the cardiac function of mice with heart failure.**

We applied a high resolution 3D MRI technique using Bruker BioSpec 9.4T imaging system for obtaining T1/T2* magnetic resonance images of the postmortem opossum brain collected with the isotropic resolution of 50 um. This work was done as a part of the study aimed to provide a multimodal

stereotactic template of the Monodelphis opossum brain to enhance usefulness of this species as a convenient model in neurobiological research.

The gray short-tailed opossum (Monodelphis domestica) in an increasingly popular laboratory animal due to the early stage of development of its newborns, which makes this species particularly useful in developmental and comparative neurobiology. However, while a number of studies were performed on the opossum brain, still, a consistent and comprehensive neuroanatomical reference is not available.

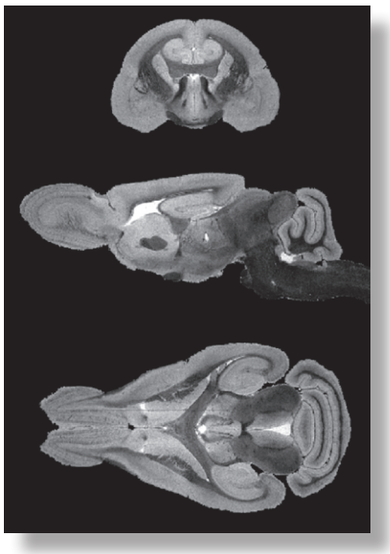

Fig. 14 *Three orthogonal cross-sections through 3D MRI of the post-mortem opossum brain.*

We have recently developed a new method of discriminating between different radiation modalities in mixed radiation fields by exploiting the specific luminescent properties of lithium fluoride (LiF), routinely used in thermoluminescent (TL) dosimetry. LiF detectors can be used as luminescent dosimeters by stimulating them by increasing their temperature (up to 400 ˚C) or by light (of 460 nm wavelength) during their readout. TL processes and light-induced photoluminescent (PL) effects are connected with different types of trapping centres and are not related to each other. They also show different TL-light efficiency after different radiation modalities. This offers the possibility of discriminating between radiation modalities using a single LiF detector, if combined TL and PL measurements are performed. **The PL HELIOS-2 reader, optimized for TL stimulation with blue light and measurement of green light emission, recently developed at IFJ PAN together with the Jan Dlugosz University in Częstochowa, is a useful tool for discrimination between radiation modalities using photoluminescent dosimetry.**

The high-dose high-temperature thermoluminescence of LiF:Mg,Cu,P (the so-called peak "B") is a new effect discovered at the Department of Radiation Physics and Dosimetry over the recent years. To further understand this phenomenon, thermoluminescent emission spectra were measured over the dose range 1 kGy to 280 kGy and temperature range 50 ˚C to 550 ˚C, in collaboration with Delft University of Technology (Netherlands). We studied the emission bands in the spectrum. The emission spectrum of peak "B" was found not to be dependent on dose, unlike the remaining peaks in the glow-curve. **We intend to apply high-temperature TL in high-dose dosimetry at CERN and in nuclear fusion studies.**

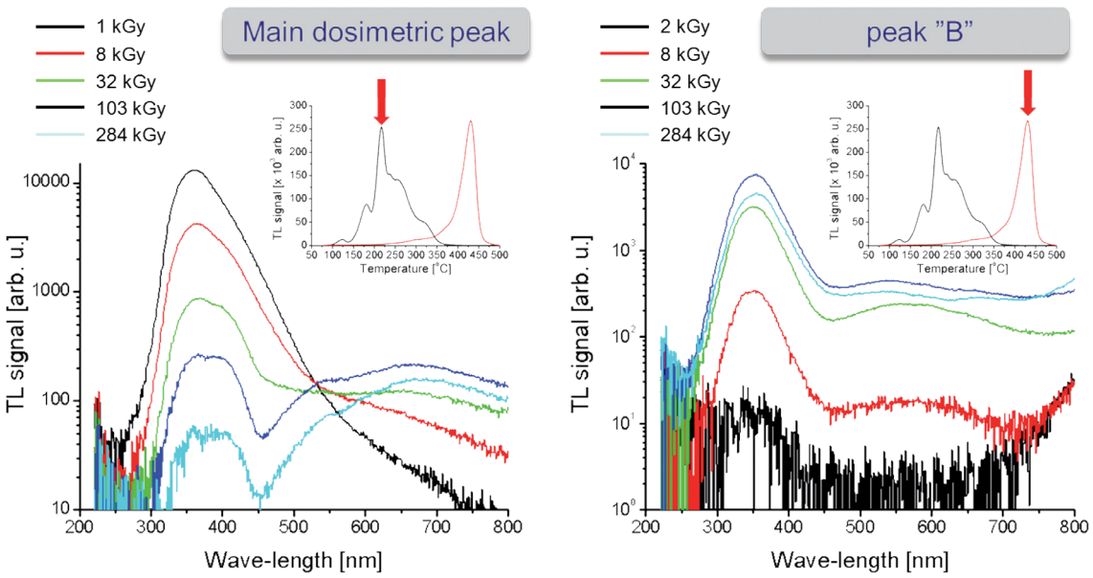

Fig. 15 *Evolution of MCP-N TL emission spectra with increasing dose of gamma radiation. Left: spectra of the main dosimetric peak; Right: spectra of "peak B". The respective thermoluminescent glow-curves are shown as insets.*

For several years the Department of Radiation Physics and Dosimetry has participated in **measurements of radiation doses in space**. Within the DOSIS ESA project, the cosmic-origin doses were measured inside the European module Columbus of the International Space Station (ISS), using thermoluminescent and nuclear track-etched detectors. **Miniature lithium fluoride thermoluminescent detectors (mostly produced at the IFJ PAN) were used in these measurements.** Within two other experiments, EXPOSE-E and EXPOSE-R, these detectors were also exposed to cosmic radiation together with biological samples on special platforms mounted outside the ISS. **In the year 2011 the long-term space project MATROSHKA to determine the dose distribution within a human phantom, due to cosmic radiation, using IFJ PAN-produced TL detectors, was completed.**

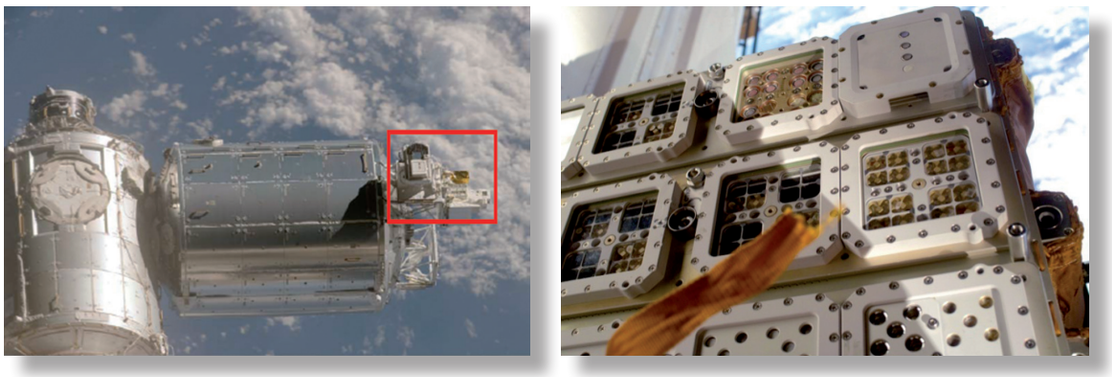

Fig. 16 *The external European Technology Exposure Facility (EuTEF) platform mounted outside the International Space Station (ISS). A close-up of the EuTEF platform with the EXPOSE-E experiment hardware containing biological samples, thermoluminescent and track detectors is shown in the right-hand-side photograph.*

In the year 2011, a **facility for growing single crystals using the Micro-Pulling-Down method (MPD)**, considered as a reversal of the well-known Czochralski method, **was launched at the IFJ PAN in Kraków. This is the second facility of this type in Poland**. The setup consists of a 20 kW generator and a Cyberstar induction furnace, where temperatures above 2100 °C can be achieved. The system is used to grow crystals of luminophors in the form of thin fibres or rods with a diameter up to about 4 mm.

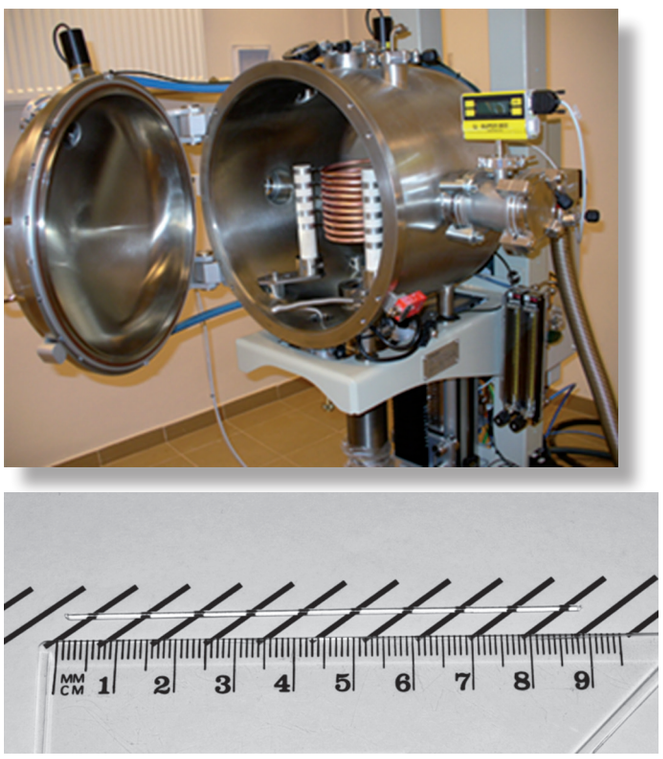

Fig. 17 *The Micro-Pulling-Down facility and the first rod (a single LiF crystal) grown using this system.*

This **relatively new technique of crystal growing enables single crystals to be grown quite rapidly (within a few hours)**. For this reason it is perfectly suited for our materials research: development of luminophors with specific features, optimization of growth conditions, doping, etc. The **MPD system will be used to grow crystals for studies of stimulated luminescence and for applications in radiation dosimetry**.

The remarkable properties of diamonds, such as human soft tissue equivalence, non-toxicity and

their wide energy gap (5.5 eV) make them extremely suitable for applications in clinical dosimetry of ionising radiation. Material properties of diamond coatings were investigated in terms of their thermoluminescent (TL) properties. Diamond films were deposited using the microwave plasma-enhanced chemical vapour deposition (MV CVD) method at different growth conditions, various gas composition mixtures and substrate temperatures. Modulation of the deposition process parameters strongly affected the morphology and structure of polycrystalline diamonds, determining their thermoluminescent properties. Raman spectra of two samples prepared at different temperatures demonstrated the narrow 1332 cm^{-1} diamond line and, for a lower deposition temperature, also a broad D peak of disordered graphite centred at 1370 cm^{-1}. Increase of the deposition temperature resulted in higher dissociation of H, causing sp^2 bonds to be etched faster than sp^3 bonds, and also changing diamond grain sizes. To study their thermoluminescence response, diamond samples were irradiated with γ- and β-rays over the dose range 5–80 Gy. **The CVD diamond samples deposited at different growth conditions showed various shapes of thermoluminescence glow curves**, consisting either of a single dosimetric peak or of a convolution of two or more overlapping peaks, but **in all cases their sensitivity to ionising radiation was very high**.

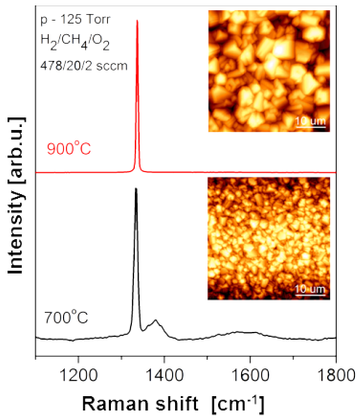

Fig. 18 *Raman spectra and Atomic Force Microscopy images of polycrystalline diamond coatings deposited by MW CVD at different conditions.*

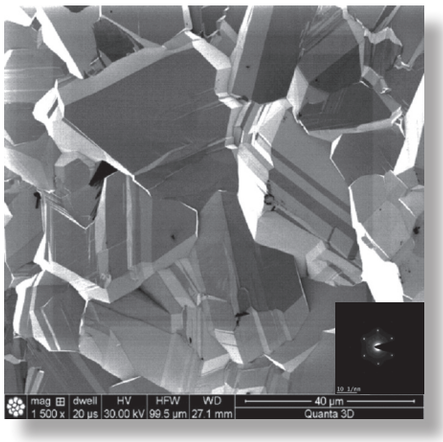

Fig. 19 *Scanning electron microscopy image of polycrystalline diamond coating. The diffraction pattern (inset) shows perfect crystalline diamond structure.*

Arctic ecosystems are vulnerable to radioactive and other contamination. **The recent "nuclear renaissance" further stimulates studies of the deposition of man-made radionuclides in the environment.** We systematically studied the presence of artificial radionuclides (^{137}Cs, Pu and ^{241}Am) in peat and soil samples from the High Arctic environment, due to airborne sources. Samples were collected from remote areas poorly investigated up to now, i.e. five regions of Spitsbergen (Hornsund, Bellsund, Isfjorden, Billefjorden and Ny Ålesund), representing both maritime and more continental locations and extending across three degrees of latitude. Radionuclide levels and activity ratios of ^{238}Pu/$^{239+240}$Pu, ^{241}Am/$^{239+240}$Pu, $^{239+240}$Pu/^{137}Cs were determined by gamma and alpha spectrometry. Additionally, the atomic ratios of ^{240}Pu/^{239}Pu were assessed by ICPMS (collaboration with the University of Northern Arizona, Flagstaff and ING PAN, Kraków). **The measured activities and atomic ratios indicate global fallout as the dominant source** of the studied radionuclides. **In some samples contamination from the nuclear testing site at Novaya Zemlya was identified**. We also evaluated levels of natural radionuclides (^{210}Pb, U, Th and Ra) in soils, sediments, fluvioglacial deposits and peats. An important finding was that radionuclide levels are not related to soil properties (pH, organic carbon content, grain size and mineral composition). Therefore, Arctic soils can preserve information on the past fluxes of airborne radionuclides.

Fig. 20 *Gathering samples in the proglacial zone of a glacier in Spitsbergen.*

Current research in the area of breath analysis confirm that composition of exhaled air gives valuable information about biochemical processes in the body and offers new possibilities for non-invasive medical diagnostics. The development of chromatographic methods and preconcentration techniques enables to detect different volatile organic compounds (VOC) in human breath. Some of them could be applied as markers of different diseases. Gas chromatograph (Agilent 6890NGC) coupled with mass spectrometer detector (5975MSD) is used in our laboratory. The technique of a thermal desorption has been applied to enrich gaseous samples.

Our studies are focused on the exploration of markers of chronic disorders in which oxidative stress plays especial role. Among our interests are diabetes, nephropathies and atherosclerosis (the main cause of cardiovascular complications).

The studies on breath composition carried out among patients suffering from chronic kidney diseases (CKD) have delivered especially promising results. Trimethylamine (TMA), proposed earlier as potential marker of renal disorders, was detected in the breath of all patients with CKD in the range of 1.76 to 38.02 ppb.

Additionally TMA decrease and isoprene increase during hemodialysis (HD) were noticed. The strong decrease of TMA concentration during HD (from 60% to almost 100 %) and observed statistically significant correlation with decreasing urea changes ($p = 0.004$) indicated that TMA could be good parameter of dialysis efficiency. Observed increasing tendency of isoprene concentration in breath during dialysis did not indicate clear dependency with typical blood parameters characteristic for renal insufficiency. The hydrocarbons (propane, butane pentane, methylated hydrocarbons) detected in breath can be potential markers of oxidative stress. Other compounds detected in breath of CKD patient are marked on exemplary chromatogram **(Fig. 21)**.

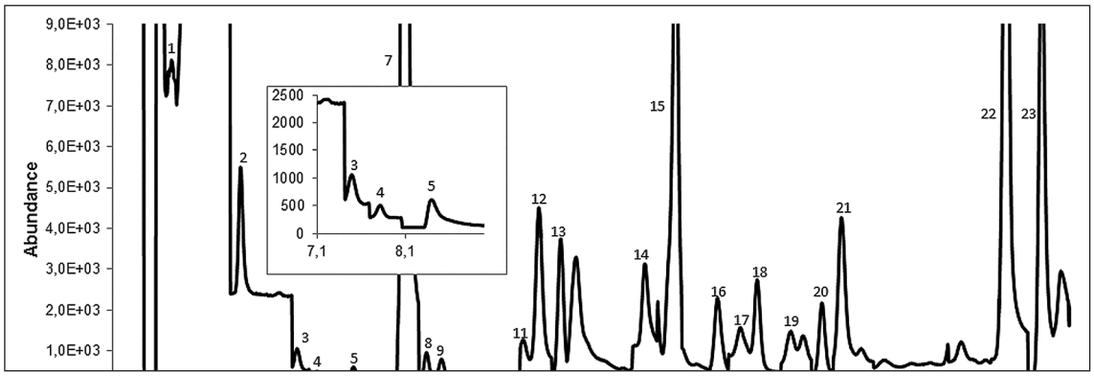

Fig. 21 *Chromatogram of exhaled air sample of CKD patient: 1 – carbonyl sulfide, 2 – propane, 3 – butane, 4 – methanethiol, 5 – trimethylamine, 6 – ethanol, 7 – acetonitryle, 8 – 2-propanal, 9 – acetone, 10 – alcohol isopropyl 11 – pentane, 12 – isoprene, 13 – dimethyl sulfide, 14 – carbon disulfide, 15 – acetic acid, 16 – 2,3-butanedione, 17 – 2-methylpentane, 18 – 2-methylpropanal, 19 – 2-methylfuran, 20 – 3-methylpentane, 21 – hexane, 22 – propanoic acid, 23 – benzene. Additionally signals of 3 – butane, 4 – methanethiol and 5 – trimethylamine, are visible on cutting of chromatogram.*

To aid in selecting the best method of treating technological water to reduce the environmental impact of oil production, we measured the phase composition of deposits from an oil plant sedimentation tank.

The X-ray diffraction pattern of the sediment powder with results of its analysis are presented in **Fig. 22**. In the spectrum one can distinguish iron compounds (magnetite – Fe_3O_4, goethite – α-FeOOH, lepidocrocite – γ-FeOOH, siderite – $Fe(CO)_3$), iron-sulphur compounds (mackinawite – FeS, stoichiometric FeS, greigite – Fe_3S_4) and other compounds such as aragonite/calcite – $CaCO_3$, anorthite – $CaAl_2Si_2O_8$, quartz – SiO_2 and barium sulphate $Ba(SO_3)_{0.3}(SO_4)_{0.7}$. The Mössbauer spectrum with subspectra and the component fraction in the inset, are shown in **Fig. 23**. The magnetic components were assigned to ferrimagnetic magnetite Fe_3O_4 (B_{hf} = 48.4 T – green spectrum and B_{hf} = 45.0 T – cyan spectrum) and iron sulphide such as antiferromagnetic, stoichiometric FeS or ferrimagnetic greigite Fe_3S_4 (B_{hf} = 29.9 T – yellow spectrum). The doublet (blue spectrum) with fraction equal to 25% may represent paramagnetic lepidocrocite γ-FeOOH, diamagnetic pyrite FeS_2, antiferromagnetic

goethite α-FeOOH or paramagnetic siderite $FeCO_3$ however the considerably smaller value of QS may suggest a significant doping level or vacancy concentration. It may also be related to superparamagnetic particles of iron oxide or hydroxide particles smaller than 10 nm. The single line (red spectrum) appearing with the largest fraction (35%) corresponds to Fe atoms in nonmagnetic surrounding and may be interpreted as iron-doped illite or as superparamagnetic particles.

The high concentration of magnetic components of the deposit suggests that **installation of the magnetic device designed at the IFJ PAN would be useful in enhancing the water cleaning processes via** coagulation, sedimentation and filtration.

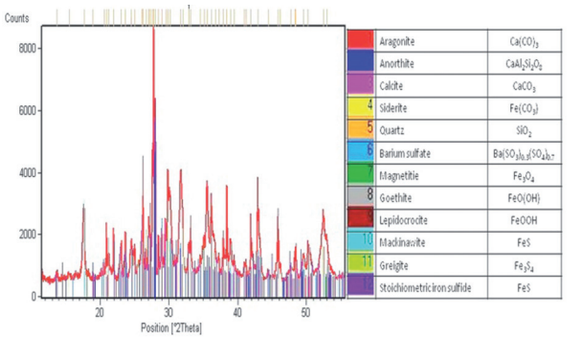

Fig. 22 *X-ray diffraction pattern of deposits from an oil plant sedimentation tank.*

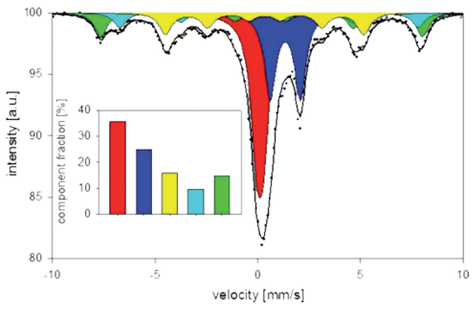

Fig. 23 *Mossbauer spectrum with subspectra. Inset shows the component fraction.*

The magnetic properties of multilayers such as **antiferromagnetic coupling and the giant magnetoresistance (GMR) effect – discovered in Fe/Cr systems– depend on the structural properties of multilayers and especially on interface roughness**. An accurate picture of interfacial roughness is necessary to know its effect on the magnetic properties of multilayers, and the atomic processes that occur on the surface during layer growth. The novel approach of interface roughness modification in Fe/Cr multilayers is the addition of small amount of impurities, known as surfactants. We studied the effect of Bi and In surfactant on interface roughness and on the value of magnetoresistance in Fe/Cr multilayers. The selected structure modifiers belong to different surfactant families, and affect the interface structure differently. Introduction of these impurities resulted in an enhancement of interfacial roughness seen by conversion electron Mössbauer spectroscopy. These changes were attributed to segregation of surfactants to the surface, as demonstrated by Auger electron spectroscopy. Increase of interface roughness did not affect the magnetic coupling of Fe, which preserved its antiferromagnetic arrangement even in the sample with very rough interfaces. At the same time, increase of interface roughness was found to enhance the GMR.

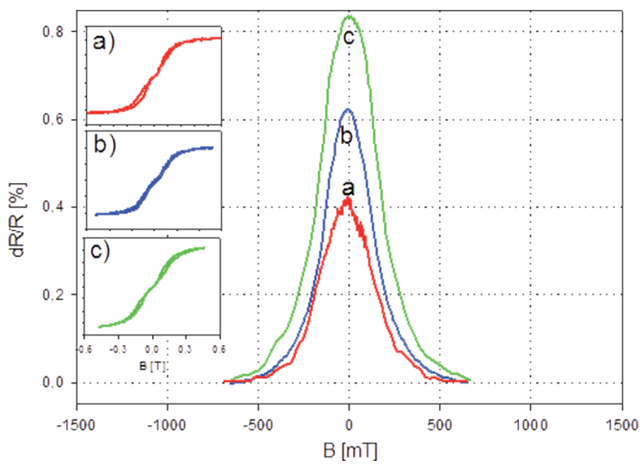

Fig. 24 *Magnetoresistance and hysteresis loops at room temperature of the Fe/Cr multilayer (a) and the Fe/Cr multilayer doped with Bi (b) and In (c) surfactants.*

FePd alloys with its strong magnetic anisotropy are good candidates as bit patterned media used to record data in an uniform array of magnetic cells. Here we fabricated thin FePd alloy films using an innovative solution of thin film deposition on ordered arrays of silica nanoparticles, and we studied the structure and magnetic anisotropy associated with the nanostructure size and thickness of the magnetic layer. Formation of the $L1_0$ phase, responsible for perpendicular magnetic anisotropy in FePd alloys, can be achieved by annealing the Fe\Pd multilayers at temperatures above 600 °C. In order to decrease the temperature of the alloy formation a non-magnetic admixture, such as Cu, can be applied. Cu\Fe\Pd multilayers of 10 nm thickness were nanopatterned by film deposition on templates of 100 nm and 50 nm self-assembled silica nanobeads, followed by annealing, which led to the creation of well-ordered arrays of isolated alloy nanoislands seen in Scanning Electron Microscope images. Local probe conversion electron Mössbauer spectroscopy measurements confirmed the transition from superparamagnetic multilayers to FePdCu magnetic alloys **on top of** the nanobeads. The islands consist of nanocrystalline $L1_0$ FePdCu phase, and the value of ordering parameter, crystallite size **and** texture do not depend on the size of nanospheres.

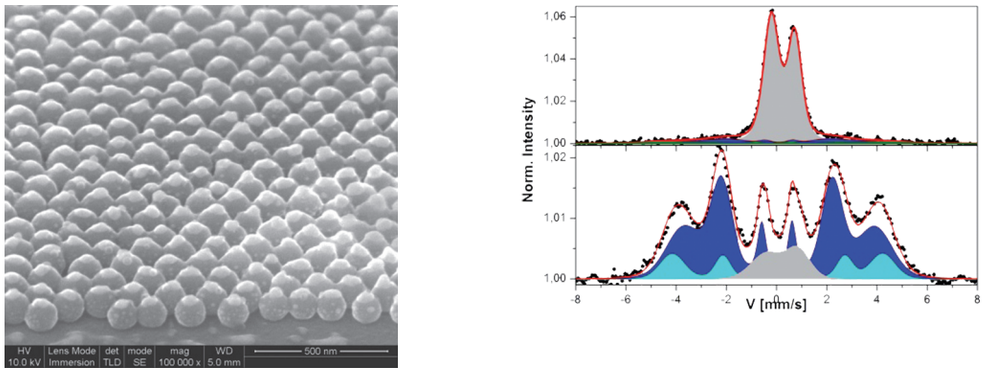

Fig. 25 *Scanning Electron Microscopy image of a self-assembled SiO2 nanoparticle array covered with FePdCu alloy. Conversion electron Mössbauer spectra of Cu/Fe/Pd multilayers (top) and FePdCu alloy (bottom).*

The research reported herein was performed pursuant to internal projects: [402, 403, 404, 405, 406, 407, 408, 409, 411, 503]; [E5, E6, E14, E15, E29, E30, E32, E50]. See Annexes I, IIB.

VI. DIVISION OF SCIENTIFIC EQUIPMENT AND INFRASTRUCTURE CONSTRUCTION (DAI)

Over the years 2011–2013 DAI engineers and technicians have participated in many local and international projects:

- design of the Small Size Telescope (SST) and of composite mirrors for the CTA (Cherenkov Telescope Array) project;
- providing engineering and mechanical support for the proton ocular cancer radiotherapy facilities at IFJ PAN;
- supervision and assembly of the bus bar system powering the superconducting coils of the W7-X stellarator at MPIPP Greifswald;
- preparation of acceptance tests and performing them for components of XFEL at DESY in Hamburg;
- involvement in shutdown and consolidation activities of the Large Hadron Collider at CERN in Genève (concerning the accelerator itself and the ATLAS detector);
- providing engineering support for the ITER project, in Barcelona and Frascati.

More detailed descriptions of some of these activities are given below.

DAI has been involved in the **Cherenkov Telescope Array** (CTA) project since 2008. From the very beginning of this project DAI was involved in two areas: design of the Davis–Cotton (D-C) telescope structures and developing prototypes of the composite mirrors.

In 2010 DAI developed a complete design of the Small Size Telescope (SST) structure with a mirror dish of 6 m diameter. The CTA collaboration changed its technical specifications twice during 2011–2012. Each time, DAI went through the full design process to develop structures to incorporate mirror dishes of diameters 7.6 m and 4.0 m. The design process included structural optimization, strain-stress analysis under static and dynamic loads, modal analysis and cost estimation.

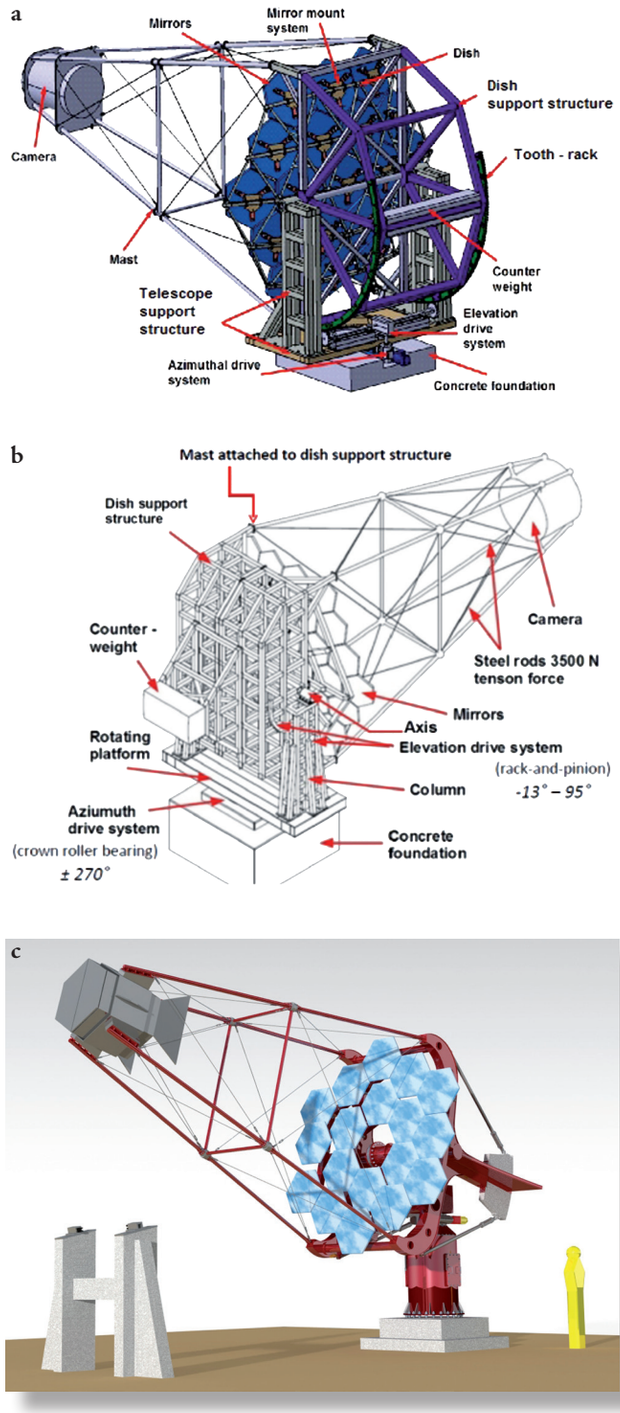

Fig. 1 *Three D-C SST structures designed at IFJ PAN, of diameters: 6 m (a), 7.6 m (b), 4 m (c).*

Various types of **drive systems** of the elevation and azimuth axes were considered. The first two structures were driven by conventional pinion-rack gears, with a hydraulic drive system also taken into account at the beginning. The last structure is driven by two identical twin warm gears. The D-C SST structure with 4.0 m mirror dish diameter was manufactured by the Polish company PONAR Żywiec and has been installed at IFJ PAN in 2013. The structure will be equipped with mirrors and with a prototype segment of the digital camera, and tested at IFJ PAN in 2014.

Fig. 2 **The** *4 m diameter D-C SST structure installed at IFJ PAN.*

Two prototypes of **open-structure mirrors** of 7.6 m diameter were built for the D-C SST. The hexagonal mirrors are of size 0.78 m (flat-to-flat) and of concavity radius 23 m. The R&D process also included ANSYS® simulations. The mirror weighs only 16.6 kg, much less than a glass one, which has a great impact on the construction of the whole telescope and on its price. The mirrors were built and pre-tested at DAI. The prototype mirrors were tested in several CTA laboratories. Test results were presented during the SST Mirror Review in September 2012. The results were encouraging enough for the referees to recommend that IFJ PAN build nine prototype mirrors for the D-C Medium Size Telescope (MST). Technology limitations prevent the manufacture of such mirrors for the D-C SST prototype telescope of 4 m diameter.

The size of the MST mirror is 1.2 m (flat-to-flat) and the concavity radius is 32 m. In 2013, ten mirrors were built for the MST prototype developed in Zeuten, Germany. Some of these mirrors are mounted on the prototype while the rest are undergoing tests at the CTA laboratories. Preliminary results confirm the optical performance of the DAI mirrors to be very good.

Fig. 3 *Front and back sides of the MST mirrors (left and central); DAI mirrors mounted on the MST prototype (right).*

Since the first days of the development of the **ocular hadron radiotherapy facility** using the proton beam from the AIC-144cyclotron, DAI played a major role. Over the years 2011–2013 the DAI staff was involved in the following design and manufacturing activities:

- development of a device for rapid cut-off of the proton beam (the so-called beam shutter) – a new version was manufactured after some proposed modifications;
- construction of supports for the beam line end in the therapy room;
- construction of adjustable supports for x-ray units;
- construction of holders for digital x-ray recorders (so-called flat panels);
- manufacture of a set of polyethylene shields for patient protection against neutron radiation;
- digital machining of a set of range discriminators (so-called propellers), and beam collimators, manufactured individually for every patient (15 patients);
- manufacture of a set of eye phantoms to verify eye therapy plans.

Several elements of the proton ocular beam line have also been adapted and duplicated for the new radiotherapy facility, presently under construction at the Cyclotron Centre Bronowice (CCB) of IFJ PAN.

Fig. 4 *Setup for proton ocular radiotherapy: beam forming bench and x-ray tube on an adjustable support.*

Stellarator Wendelstein 7-X (W7-X) is a device dedicated for the study of very hot deuterium plasma in conditions close to ignition of nuclear fusion (density equivalent to the pressure of 2 Bars and temperature around 100 million degrees). This device is currently being assembled at the Max Planck Institute for Plasma Physics in Greifswald, Germany. The in-kind contribution of IFJ PAN to the W7-X project is the assembly of so-called bus bars – superconducting cables connecting 70 coils, constituting a magnetic trap for the plasma.

While the theoretical principles of stellarators are as old as tokamaks, only nowadays do we have tools for constructing them. This is because modelling of the shape of magnetic field and design of coils and the whole structure is possible only with the aid of very advanced three-dimensional computing techniques. The W7-X stellarator is a large and heavy device weighting almost 750 tons, of some 15 m diameter and a height of 5 m. Fortunately, it was designed with 5-fold symmetry, so it can be split into 5 almost identical modules, each consisting of two sub-modules. Each module has 14 coils, with 24 bus bars to connect them, and also for connection with neighbouring modules. The external aluminium jacket of each bus bar serves as a liquid helium cooling channel, so all electrical connections of extremely low resistance must also be vacuum-tight.

The complete work package for bus bar assembly is divided into several sub-packages:

1. Bus bar pre-assembly. Bus bars of 5-19 m lengths were manufactured at the Forschung Zentrum Jülich. They were bended to pre-defined 3-D shapes and covered with a multilayer composite

isolation. Only the last 1,5 m from both ends of each bus bar were not isolated for *in situ* final adjustment to the coil end terminal. At the beginning 95 holders are installed, half of them within 1,5 mm radial deviation from their design positions. Then all bus bars are installed on the module with the greatest care and without any tension. To make manipulation with a long, rigid and fragile bus bar less risky, they have been suspended from several large helium balloons. Finally, positions of connections and all supports and clamps are marked on the bus bars.

2. Preparation of bus bar ends. A length of about 40 cm of the aluminium jacked is dismantled, a special adapter is welded to the jacked in a marked position and leak tested, 243 superconducting wires are arranged into 81 twisted triplets and tinned, while the remainder of the bare cable and adapter are covered with composite isolation. Next the isolation is tested in a local vacuum chamber under high voltage (so called Paschen test, avalanche discharge).
3. Final installation of all bus bars on the module. All holders are fixed with a torque, additional clamps are assembled between holders for further compensation of electrodynamic forces.
4. Electrical connection of the bus bars to the coils. That connection, the so called joint, must have a very low resistance of below 6 nano-ohms, must be very stable and leak-tight while liquid helium coolant is to flow through it. Bus bar adapters are welded to the joint body, superconducting triplets are soldered in 81 pairs, then very tight clamped. After welding the joint housing and leak testing, the whole assembly is covered with isolation and then connections of the additional quench protection cables are made (so-called QD boxes). The whole isolation is tested in the local vacuum chamber and then joints are fixed to the module structure.
5. Electrical connections between modules. On completing the installation of bus bars and helium piping, the assembled module is mounted in an outer vacuum shell and transported to its final position where it is connected to neighbouring modules. As part of that phase, electrical connection of the bus bars and QD cables of adjacent modules is made, in a way very similar to that described in point 4.

The work described above was performed by the bus bar team (occasionally up to 40 persons), mainly technicians from IFJ PAN, occasionally assisted by a few German technicians over periods of very intensive work on several modules in parallel and when two working shifts were required. Work was supervised by 2-4 engineers from IFJ PAN. Their duties were to coordinate the work within the planned schedule and according to approved procedures, to develop or improve the assembly technology and tooling, to train the personnel, to record work completed in relevant documents and to act as a first stage of the quality assurance system.

The bus bar work package began in May 2008 with Module 5. Modules were prepared in the order: 5-1-4-2-3. Over the years 20011-2012 we continued our work with bus bars within the following scope:

- 2011 – final check of Module 2, searching for possible conflicts between different components and eliminating them;
- 2011 – final installation of bus bars on Module 3, connecting them to coils and insulation of connections (28 joints), final check before transport to the machine foundation;
- 2011 – completion of 8 bus bar connections (joints) between modules 5 and 1 (Module Separation Plane MSP 5-1);
- 2011 – mechanical and electrical works with 10 joints on MSP 4-5, 1-st part of their insulation;
- 2011 – preparation works on MSP 1-2;
- 2012 – completion of joint insulation on MSP 4-5, final assembly;
- 2012 – completion of 10 joints on MSP 1-2, 8 joints on MPS 2-3 and 8 joints on MSP 3-4.

In December 2012 the bus bar package was completed, as agreed between MPIPP Greifswald and IFJ PAN Kraków. Works with stellarator W7-X are continued, commissioning is foreseen for middle of 2014 and first experiments will start in 2015. The physics community is eagerly awaiting this advance in the knowledge of plasma behaviour and control. Another aspect is in the search for new materials for use in the construction of plasma reactors. Stellarators could provide a very interesting alternative to tokamaks and may significantly contribute to the future of thermonuclear power generation.

Fig. 5 *Final installation of bus bars on Module 3 of the Stellarator Wendelstein 7-X.*

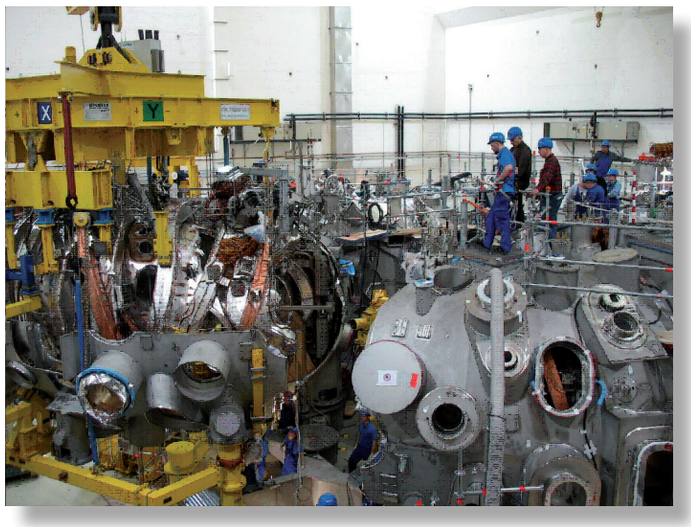

Fig. 6 Transport of Module 3 to the Stellarator Wendelstein 7-X machine foundation.

Fig. 7 *Insulation of QD boxes of the Stellarator Wendelstein 7-X.*

Fig. 8 *Finished joints with QD boxes of non planar coils on the MSP 5-1 segment of the Stellarator Wendelstein 7-X.*

DAI continues its work within the **European X-ray Free Electron Laser (XFEL)** project at DESY, as the Polish in-kind contribution to this project. IFJ PAN is responsible for preparation and execution of acceptance tests of 103 cold magnets, 840 superconducting cavities and 103 whole accelerator cryomodules on the facility location provided by DESY. The activities are split into two phases, the preparatory phase (2010–2012) and series tests (2013–2015).

During the preparatory phase, DAI engineers and physicists, together with DESY groups, elaborated the scope of the tests and executed training tests of the pre-series magnets, cavities and cryomodules. Training tests of the cold magnets were performed on the final test-stands while the training tests of both the cavities and cryomodules – on the temporary ones.

Tests of the series of cold magnets began in August 2012 and are being continued according to schedule. Tests of the series cavities and of cryomodules are delayed. The final test-stands for the cavities and the cryomodules in the Accelerator Module Test Facility (AMTF) hall are not yet fully operational. The first cryostat for the cavity tests was commissioned in January 2013 and the second one in May 2013. Only one of three test benches for the cryomodule tests has been made available in December 2013. The tests of the series cavities began in the summer of 2013. The tests of the series cryomodules will start in 2014.

Fig. 9 *Three cryomodule test benches at AMTF hall under construction.*

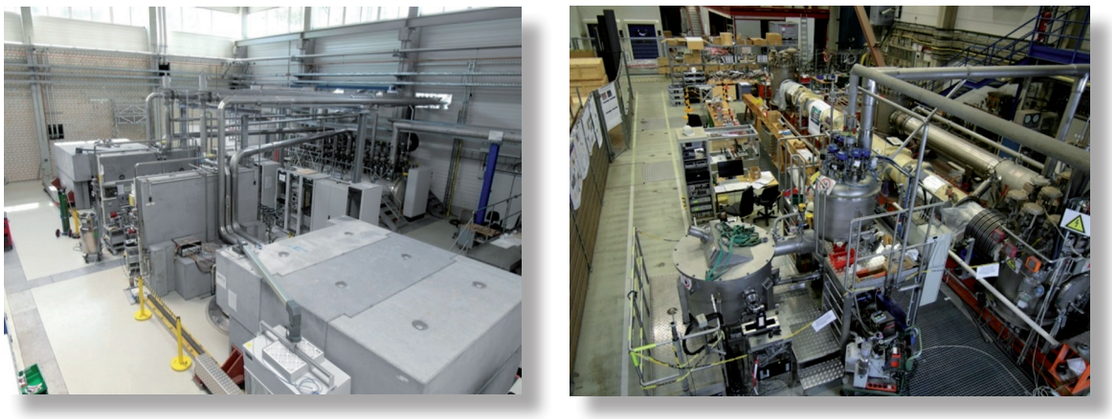

Fig. 10 *Two vertical cryostats in AMTF hall (left); The cold magnet test-stand (right).*

DAI engineers and physicists are also involved in creating a data base for the tested components, and writing documentation and test procedures. It is the responsibility of DESY to develop the measurement software, however, DAI engineers often support the DESY staff in that area whenever the need arises.

Fig. 11 *Test of a warm quadruple magnet and a screenshot of measurements performed.*

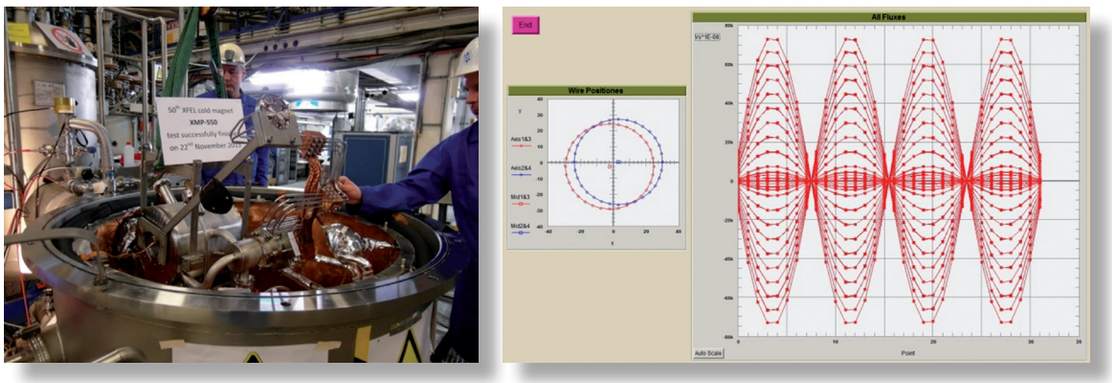

Fig. 12 *Removal of 50th XFEL quadrupole magnet XMP-S50 from the cryostat after successful cold test (left); results of measurement of stretched wire harmonics at cold (right).*

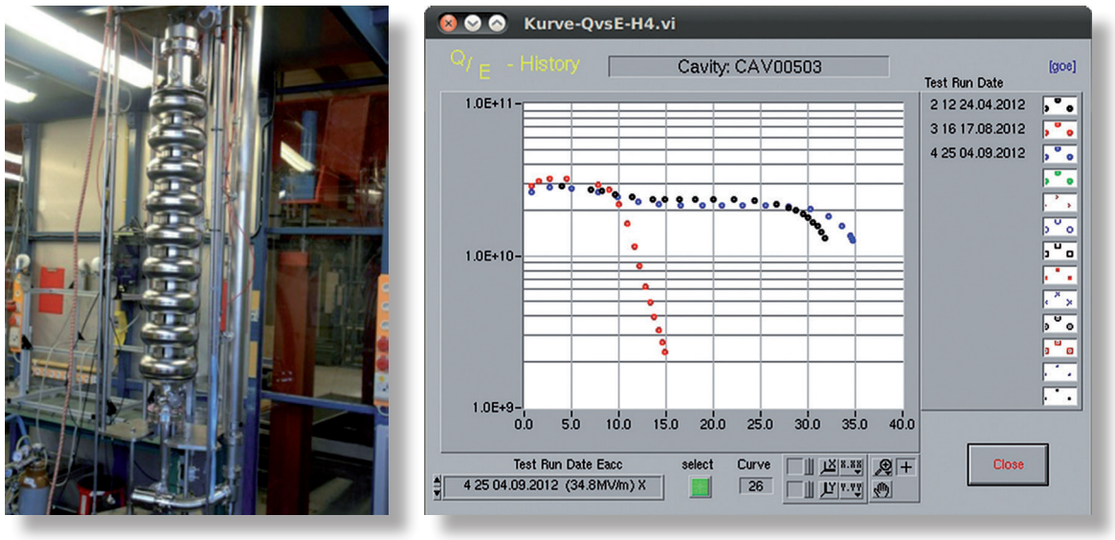

Fig. 13 *Test of a superconducting accelerating cavity on a temporary test-stand (left); results of measurements of E, Q0-factor, and radiation (right).*

Fig. 14 *Superconducting cavities in the preparation area of the AMTF hall (left); connection of cavity vacuum pipes to the insert in clean room conditions in the AMTF hall (right).*

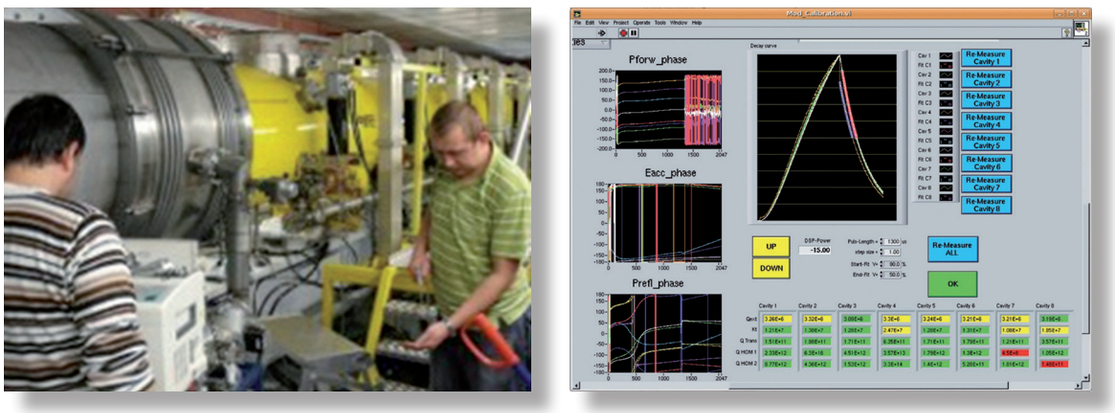

Fig. 15 *Leak test of a cryomodule on the temporary test-stand (left); a snap shot of the cryomodule RF test (right).*

Fig. 16 *Preparation of cryomodules for cold tests on the temporary test-stand (left) and on the final test-stand (right).*

The following operations were performed over the years 2011–2013:

- Learning the test process and executing training tests for the cold magnets, the cavities and the cryomodules;
- Training in preparation of the cavity/cryomodule tests: installation and dismantling, vacuum pumping, tightness tests, cool-down and warm-up processes;
- Performing independent tests of pre-series cold magnets (3), cavities (42) and prototype cryomodules (3);
- Preparation of the organization scheme for execution of the cavity/cryomodule tests in the AMTF hall;
- Write-up of test procedures for existing test-stands (cold magnet tests – 7 procedures, cavity tests – 18 procedures and cryomodule tests – 146 procedures);
- Preparation of necessary documents such as: Quality Plans, Risk Assessment, Working Instructions, Inspection, Testing and Non-conformity forms etc;
- Completion of tests of 53 series cold magnets;
- Completion of tests of 162 series cavities;
- Performing tests of 2 pre-series cryomodules;
- Design and creation of a data base for the tested components: cold magnets, cavities and cryomodules.

DAI has also continued its contribution to the **shutdown and consolidation of the Large Hadron Collider** at CERN in Genève. In the preparation phase (2011-12) our engineers developed an upgrade of the TP4 measurement system, a basic tool for Electrical Quality Assurance of the superconducting circuits. The main components of the system are two high precision digital multi-meters, a high precision power supply, a gain phase analyser, a high voltage insulation tester and the so-called TP4 crate for routing signals between the measurement instruments and the device under test. All instruments are mounted on a trolley which can be easily moved within the LHC tunnel.

The new TP4 system has a thermally stabilized current path with specially selected current relays and four 1-of- 84 signal multiplexers. The upgrade led to an improvement of system stability (by introducing a thermostat with feed-forward functionality), of its precision (by simplifying and better shielding the signal paths) and to better overall reliability. Another element of the hardware upgrade was to change the gain phase analyser type and to replace the single digital multi-meter by two better suited multi-meters. Finally, within the upgrade, the number of measurement systems was increased from 4 to 8. The new TP4 systems have been equipped with sets of measurement cables used for connection to the LHC superconducting circuits.

Along with improvement of the hardware, the software was also upgraded. All measurement software applications were adapted to the new hardware and optimized. New functions were added, such as the measurement of the turn-on voltage of the magnet protecting diodes. All eight upgraded TP4 systems were commissioned, new measurements were introduced and the procedures were revised and approved.

DAI has taken part in the consolidation phase of the collider since January 2013. Involved were over 30 engineers, physicists and technicians from IFJ PAN, grouped into two teams, the ELectrical Quality Assurance Team (ELQA) and the InterConnection Inspection Team (ICIT), working in the LHC tunnel.

The responsibility of the ELQA Team includes:

1. Electrical measurements and qualification of all superconducting circuits and magnets of the LHC before and after the consolidation works. The measurements are performed on the complete circuits when they are in cryogenic (1,9 K) state and at room temperature. Qualification of each circuit consists of low voltage DC and AC measurements and high voltage insulation test.

Fig. 17 *ELQA measurements in the LHC tunnel.*

2. Monitoring of the electrical parameters of the LHC superconducting circuits during the Superconducting Magnets and Circuits Consolidation (SMACC) project. Every day the ELQA team performs measurements of the resistance and the insulation quality of all circuits affected by the consolidation works. Any errors not detected at this stage of works could lead to a serious delay of the LHC restart.
3. Electrical checks after replacement of the LHC magnets and other elements. Replacement of 19 superconducting magnets during the consolidation campaign caused redoing of about 1700 superconducting connections. The ELQA team has to check the correctness of each redone connection before welding of the wires and again after the wires are welded.
4. Follow-up of the nonconformities discovered during the measurements.
5. Daily maintenance of the measurement system, both hardware equipment and software – the reliability of the system is very essential for coping with the enormous number of measurements within the scheduled requirements.

6. Handling of the measurement data and maintenance of the ELQA measurement database. All the measurement systems automatically send measurement data to the central database composed of over 100 tables, storing currently almost 100 000 000 records.

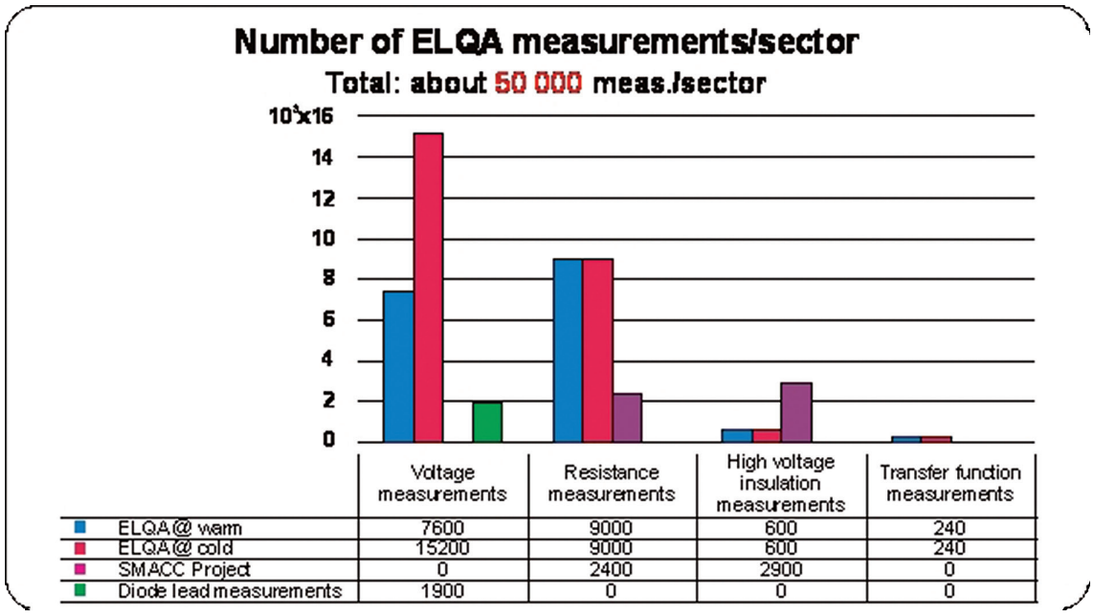

Fig. 18 *Total number of discreet measurements performed by IFJ PAN teams in one LHC sector in 2013.*

7. Design and fabrication of new measurement systems, e.g. Diode Lead Measurement system. The salvage operation of the LHC at full energy requires that diode lead resistance must not exceed 10 μΩ at room temperature.
8. Participation in upgrade of the instrumentation of the superconducting circuits.
9. The ELQA team was heavily involved in the design of the current transformers (CT) for the LHC quench protection system and in the design and production of the CT tester. The tester was later delivered to the producer of current transformers. Results of tests are being analyzed by the ELQA team.

Fig. 19 *Tester of current transformers.*

In September 2013 the Polish Minister of Science and Higher Education, Mrs Barbara Kudrycka, visited CERN and the Polish groups involved in the LHC experiments and LHC operation. She also met with members of the ELQA team and was informed about their work.

Fig. 20 *Visit of the Minister of Science and Higher Education, Mrs Barbara Kudrycka, Genève, September 4th 2013. (Photo copyright: CERN, Maximilien Brice).*

Responsibility of the Interconnection Inspection Team includes:

1. Supervision of opening and closure of interconnections (IC) between superconducting magnets.
2. Evaluation of the overall state of ICs after opening, inspection and protection of beam line bellows.
3. Inspection of the beam line bellows and installation of their final protections just after all activities are completed and the IC is ready for closure.
4. Endoscopy of the beam lines every time they are opened.
5. Writing-up and follow-up non-conformity reports.

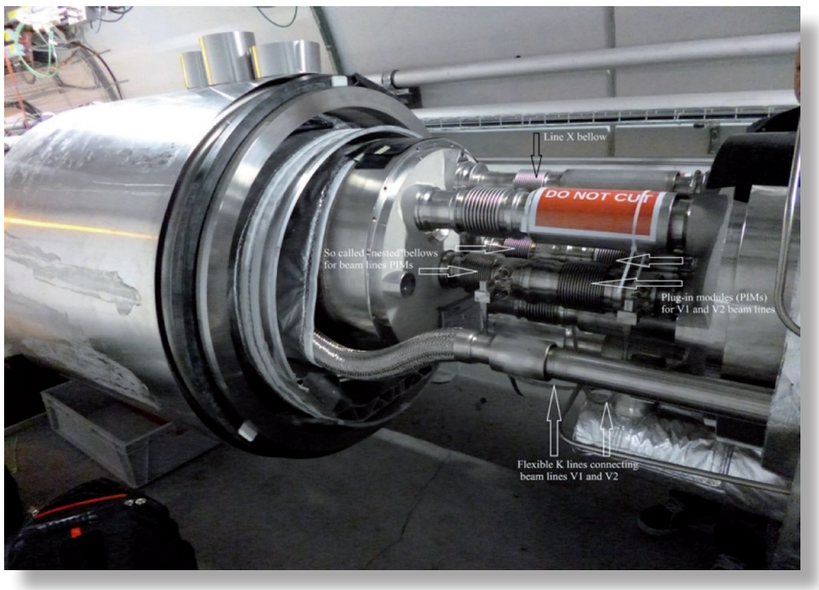

Fig. 21 *Opened IC with specific points of interest to ICIT indicated.*

During 2013 the Interconnection Inspection Team:

- supervised the opening of almost 1700 interconnections;
- evaluated and inspected them just after opening;
- inspected above 500 ICs prior to their closure;
- supervised closures of almost 500 ICs;
- performed endoscopic inspections of about 170 beam lines;
- wrote up over 150 Non Conformity Reports.

Fig. 22 *Examples of mechanical damage to the Plug-in-modules resulting in their exchange: deformed beam line bellows (left) and electrical contact strips protruding into the aperture (right).*

Another case of involvement of DAI in international projects is its participation in the **ITER project**. A Finite Element Method analysis of some components was performed. The dynamic behaviour of the Tokamak Machine, the Vacuum Vessel and the First Wall of the Blanket Module, subjected to seismic or electro-magnetic loads, was assessed by applying the response spectrum method or by full transient dynamic analysis. The work was completed in 2013.

Currently, DAI is involved in the planning phase of the project "Diagnostics Design and Development: the Radial Neutron Camera (RNC) and Radial Gamma-Ray Spectrometer (RGRS)". The project is being carried out by a consortium consisting of six European institutions including IFJ PAN, and shall be completed in 2016.

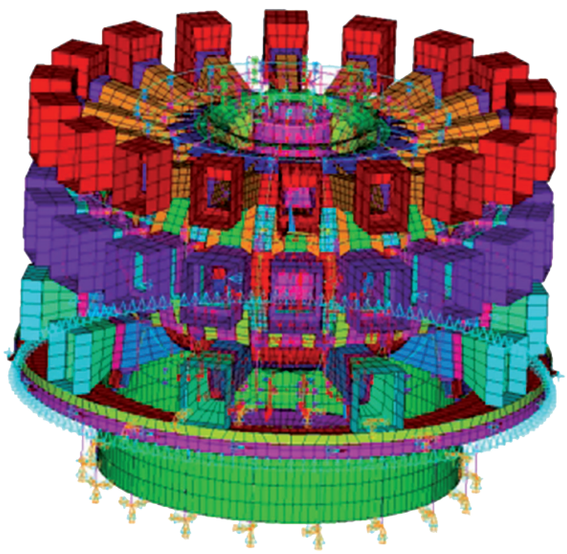

Fig. 23 *ANSYS model of the ITER tokamak.*

The research reported herein was performed pursuant to internal projects: [501]; [E12, E34; E35, E38, E39, E40, E41, E42, E43]. See Annexes I, IIB.

VII. DIVISION OF THE BRONOWICE CYCLOTRON CENTRE

The Bronowice Cyclotron Centre (in Polish – *Centrum Cyklotronowe Bronowice*, CCB) is a part of the Institute of Nuclear Physics of the Polish Academy of Sciences (IFJ PAN) and also a leading member of the National Centre of Hadron Radiotherapy (NCRH), formed in 2006 as a Polish national consortium of several research institutions collaborating in the development of ion radiotherapy in Poland. The activities of the CCB are focused around two cyclotrons now operating at IFJ PAN: the in-house developed AIC-144 isochronous cyclotron which accelerates protons to an energy of 60 MeV, and the recently purchased Proteus C-235 cyclotron, produced by Ion Beam Applications (IBA, Belgium) which accelerates protons to a maximum energy of 230 MeV. The Proteus C-235 is also an isochronous cyclotron with a conventional magnet, but equipped with a degrader and energy selector which allows the proton beam energy to be varied continuously over the energy range 70 – 230 MeV. The reason for choosing this type of cyclotron was to be able to apply its proton beams in cancer radiotherapy and in basic intermediate-energy nuclear physics. Currently, the Proteus C-235 in the most powerful accelerator in Poland. The 60 MeV proton beam from the AIC-144 cyclotron is currently used to irradiate patients with cancer of their eyeball – the first proton radiotherapy facility to operate in Poland. In line with the aim to develop at CCB IFJ PAN a proton cancer radiotherapy facility able to irradiate patients with tumours at all sites using the full energy of the Proteus C-235 cyclotron, a rotating arm for the proton beam (gantry) and a scanning beam nozzle have also been purchased from IBA, soon to be accompanied by a second gantry, making CCB with its physical and medical infrastructure, a fully-equipped proton radiotherapy facility able to treat patients by the year 2015 or 2016.

The Henryk Niewodniczański Institute of Nuclear Physics has had a long tradition of applying its cyclotrons to cancer radiotherapy. Its first Soviet-made U-120 cyclotron which produced a 24 MeV alpha-particles and 12 MeV deuteron beams, installed at IFJ in 1958, was adapted around 1975 to supply a collimated fast neutron beam from deuterons on a thick beryllium target for neutron radiotherapy. Over the years 1976–1994 some 550 patients of the Centre of Oncology in Kraków with head-and-neck and breast cancers were treated at IFJ using this beam. At the end of 80's the U-120 was replaced by the AIC-144 cyclotron, designed at IFJ PAN, and between 2008 and 2010 this cyclotron was also adapted for proton radiotherapy to develop an ocular proton irradiation facility. The beam delivery system and the treatment room facility were constructed at IFJ PAN by its engineers, technicians and software developers. On February 18, 2011 proton irradiation of the first two patients with ocular melanoma began at IFJ PAN, the first such proton radiotherapy treatment in Central Europe. In this clinical endeavour the team of IFJ PAN physicists and engineers collaborated for several years with medical doctors – radiotherapy specialists and medical physicists at the Centre of Oncology in Krakow and

with specialists in ophthalmology at the Department of Ophthalmology and Ophthalmic Oncology (Collegium Medicum of the Jagiellonian University – CMUJ).

Currently, under contract from the National Health Fund (NFZ) with the University Hospital in Krakow, ocular melanoma patients of the CMUJ Department of Ophthalmology are being irradiated with protons at IFJ PAN on a regular basis. At the same time, the newly installed Proteus C-235 cyclotron has produced its first proton beam, the degrader and energy selector are undergoing tests and the first gantry is being installed. The new building has been erected to house the Proteus C-325 cyclotron, the gantry and medical infrastructure, and its physical and medical equipment are under installation. An extension to this building, to house the second gantry, is being designed. We expect the proton radiotherapy complex to be able to irradiate patients with tumours at all sites by the years 2015–2016, and the second ocular radiotherapy facility to receive its first ocular patients by 2015. Meanwhile, research in nuclear and radiation physics, medical physics, dosimetry and radiobiology is under way, in line with the development of the proton beam facilities at CCB. We believe that developing CCB – a well-equipped proton radiotherapy installation at a nuclear physics research laboratory such as the IFJ PAN, and not at a hospital, offers us the unique possibility of combining cutting-edge proton radiotherapy with strong expertise in accelerator physics and with extensive basic research capability in hadron radiotherapy, nuclear physics, radiation physics, clinical dosimetry, medical physics, radiobiology, microdosimetry, and materials engineering.

Over the years 2007–2013, Poland, as a new member of European Union received about 60 billion Euro towards its infrastructure reconstruction programme. In 2006 the National Centre of Hadron Radiotherapy (NCRH), a consortium of 14 major universities, technical universities, medical schools and oncology centres to develop modern infrastructure for hadron radiotherapy in Poland, was established. The NCRH is coordinated by IFJ PAN. Over the years 2007–2013, within the NCRH, IFJ PAN successfully applied to receive about 45 M€ (85% from EU structural funds, 15% from the Polish government) towards the purchase and installation of the Proteus C-235 cyclotron and gantry with a scanning beam nozzle. Recently, financing for a second gantry was also secured. This is the highest single infrastructure investment at IFJ PAN in its history of over 50 years. Active involvement of senior physicists and medical doctors within the NCRH consortium and of the IFJ PAN administration in preparing the tenders and resolving the complicated legal issues of EU "Innovative Economy" Structural Fund projects, were key to this success.

Currently, the CCB team at IFJ PAN includes about 60 scientists, medical doctors, engineers, technicians, and Ph.D. students. The Bronowice Cyclotron Centre consists of the Medical Physics Department, the Proton Radiotherapy Group, The Department of Radiation Physics and Dosimetry, the Independent Gantry Laboratory and the Departments of the AIC-144 and Proteus C-235 Cyclotrons. The first three Departments and the Gantry Laboratory are research units, coordinating their work with the AIC-144 and Proteus C-235 Departments in technical development and engineering. Basic research in intermediate-energy nuclear physics at CCB is coordinated by the Division of Nuclear Physics and Strong Interactions within a Polish consortium of nuclear physics research institutions, also led by IFJ PAN.

THE CYCLOTRONS AT CCB

The AIC-144 Cyclotron

The AIC-144 cyclotron is an isochronous cyclotron designed and constructed at IFJ in the early 90's to accelerate light ions (protons, deuterons and alpha particles) for research in nuclear physics. Its design, with a single dee, is unconventional. This cyclotron was used until 2010 mainly for the production of rare radioactive isotopes for scientific purposes. Later, its construction was optimised to produce a 60 MeV proton beam at a current of 80 nA, stable to within ± 5%, for purposes of proton radiotherapy.

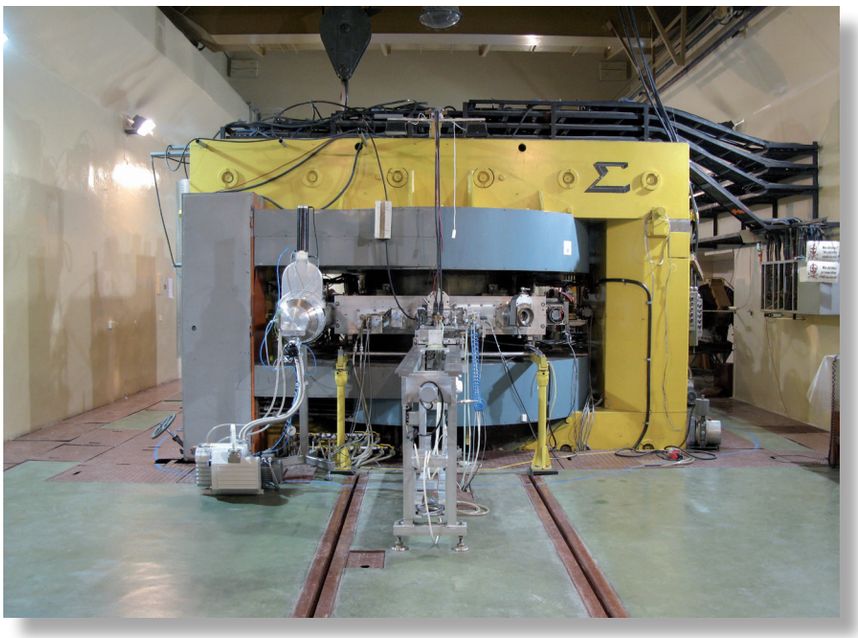

Fig. 1 *The AIC-144 cyclotron. The main magnet, magnet coils, vacuum vessel, RF supply and ion source (centre) are visible.*

The AIC-144 cyclotron is currently used mainly for ocular proton radiotherapy and for production of proton-based radioisotopes, for research purposes. Apart from radiotherapy, the horizontal proton beam supplied to the patient irradiation hall is also used by the CCB teams for research and development experiments in radiation physics, dosimetry, medical physics and radiobiology.

The AIC-144 cyclotron is operated by the AIC-144 Department engineering team of 13 accelerator engineers, technicians and support personnel, closely collaborating with scientist and engineers of all other CCB units and of IFJ PAN laboratories.

The Proteus C-235 Cyclotron

The Proteus C-325 cyclotron was designed and produced by IBA (Ion Beam Applications S.A., Belgium) specifically for medical applications. It is an isochronous cyclotron with a compact conventional magnet, able to accelerate protons to an energy of 230 MeV. Protons of this energy have a range of some 30 cm in water which and are thus able to reach all tumour locations in a radiotherapy patient. An energy degrader and selector, allowing the beam energy to be downgraded continuously to 70 MeV, with intensities up to 600 nA, is an integral part of this installation. The Proteus C-235 cyclotron with its energy selector was installed in its new building at IFJ PAN on May 11, 2012. The rotating arm (gantry) has also been installed and is currently undergoing completion.

The basic parameters of the Proteus C-235 cyclotron are as follows: weight-220 tons, outer magnet yoke diameter – 4,34 m, magnetic field – up to 3.1 T, maximum current in the main coil magnet – 800 A, operating frequency – 106 MHz, radially-dependent dee voltage amplitude 50-100 kV, PIG-type internal source, extraction efficiency – 70%, external beam current at 1 MeV – 230 – 300 nA, total operating power consumption – 1.3 MW.

The Proteus C-325 Cyclotron Department which maintains and operates this cyclotron consists of six engineers and technicians.

Fig. 2 *The Proteus C-235 cyclotron installed at the IFJ PAN. A part of the energy degrader and selector is also visible.*

The variable energy beams of the Proteus C-235 cyclotron are directed to the physics experimental hall and to the new eye treatment room. A 230 MeV beam is directed to the gantry. The new building which houses this cyclotron also includes a medical area, a patient treatment area and additional space for the preparation of physical and radiobiological experiments. The layout of the cyclotron part of the CCB building and its overall external architecture are shown below.

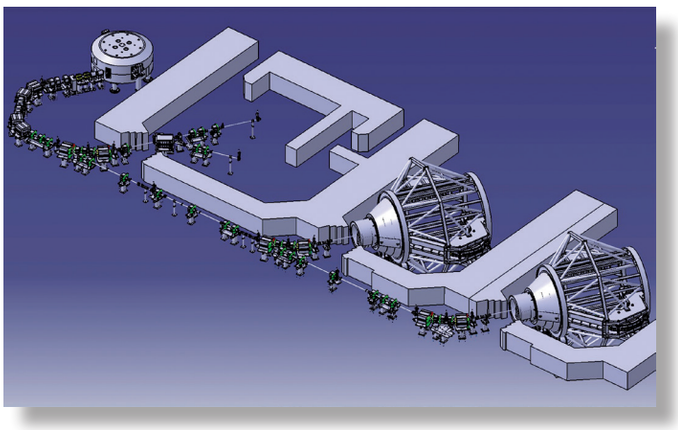

Fig. 3 *Layout of the Proteus C-235 cyclotron part of the CCB building, showing the cyclotron, energy degrader and beam lines supplying to the research and ocular radiotherapy areas. The gantries are at lower right.*

Fig. 4 *Overall view of the completed CCB building (April 2014).*

The Gantry and Scanning Beam Nozzle

The rotating arm (gantry), also designed and supplied by IBA, is a huge construction weighing some 150 tons and a diameter of 11 meters carrying beam magnets to achieve a vertically rotating position of the 230 MeV proton beam. The gantry can be oriented at any direction within 360 degrees to a precision of below 1 mm in the patient's body. The scanning beam nozzle is a highly advanced instrument which allows proton beams of varying initial energy to be precisely directed towards pre-selected locations within the patient's body using a dedicated magnetic field computer-controlled system. This allows one to suitably extend the region of the dose maximum (Bragg peak) of the proton beam, achieving full coverage of the irradiated tumour volume in the patient. The gantry was delivered to the IFJ PAN in June 2013. An overall view of the gantry, its principle of operation, and a view of the patient irradiation facility using the gantry and the beam scanning nozzle, are shown below. We expect the gantry and scanning beam nozzle to be fully operational by the end of 2015.

The gantry and beam scanning system is developed and managed by a team of five highly skilled specialists in engineering, computer science and medical physics of the Independent Gantry Laboratory.

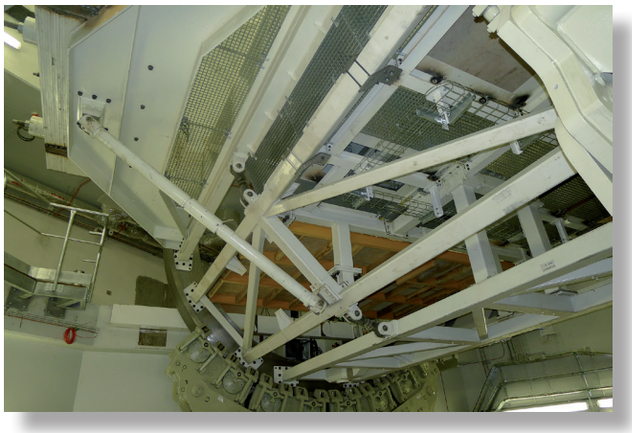

Fig. 5 *Mechanical assembly of the first gantry at IFJ PAN.*

Fig. 6 *Waiting room for the children at the medical area of the CCB building.*

Fig. 7 *View of the patient irradiation facility showing the gantry and the scanning beam nozzle (April 2014).*

AIC-144 – BASED OCULAR RADIOTHERAPY FACILITY AT CCB

Development of the AIC-144 cyclotron-based proton ocular radiotherapy facility

The basic advantage of proton radiotherapy is in its exceptional sub-millimetre accuracy, unattainable by conventional radiotherapy using external photon beams. The proton ocular radiotherapy facility has been in-house developed at IFJ PAN in cooperation with the Department of Ophthalmology and Ophthalmic Oncology of the Medical College of the Jagiellonian University, and with the Krakow Branch of the Maria Skłodowska-Curie Memorial Institute Centre of Oncology. In developing and performing ocular proton radiotherapy we closely collaborated with experts abroad, including Germany (Charité – Universitätsmedizin HZB, Berlin), the UK (Clatterbridge Centre of Oncology), Russia (Joint Institute for Nuclear Research, Dubna) and Italy (CATANA, Catania).

The 60 MeV proton beam is produced by the AIC-144 cyclotron which had been optimised for this purpose in 2008. Over the years 2008–2011 an optical beam line was designed and constructed in-house at the IFJ PAN. The proton beam from the cyclotron is delivered to the therapy room where it is suitably formed and monitored. The facility is equipped with several in-house – developed beam forming elements. The beam line allows a small tumour volume in a patient's eyeball to be repeatedly irradiated at dose rates of 0.25–1.0 Gy/s. The beam range (in water, 90% at the distal edge) is 28.3 mm, the distal fall-off (90%–10%) is 0.75 mm and lateral penumbrae measured in air (90%–10%) do not exceed 1.3 mm. These parameters are in line or exceed other ocular radiotherapy centres worldwide.

After a medical review of the ocular patient and surgical placement of fiducial markers on the patient's eyeball at the Department of Ophthalmology, an individual therapy plan is prepared for each patient at IFJ PAN, using a Varian Medical Systems Eclipse Ocular Proton Planning system, and approved by a specialist in radiotherapy from the Centre of Oncology. The input beam energy is then precisely matched for the individual patient by a wedge filter. Passive spreading of the Bragg peak is achieved by rotating wedge modulators also individually designed and machined for each patient. Beam dose is precisely and continuously monitored by PTW beam monitors and a four-segment ionization chamber. The patient is immobilised and positioned to a precision of 0.1 mm in a Schär Engineering AG eye therapy chair. Precise positioning of the patient's eyeball, basing on the images of fiducial markers and patient's cooperation, is achieved by a Varian RAD-14 Diamond X-ray system and a Kodak "Point of Care" CR-260 digital radiography system. The beam control system and the autonomous safety system are based on National Instruments hardware and on in-house developed dedicated software, using the LabView platform. A NetView Thermo dosimetric system, with a FHT762 WENDI II neutron monitor and a FHT191N/TL gamma dose rate monitor evaluate the ambient dose inside the therapy room, in terms of H*(10). FHT751 BIOREM neutron monitors and FZH 621G-L14-10 gamma dose rate monitors monitor the H*(10) dose in selected areas outside the therapy room.

Fig. 8 *Overall view of the proton eye treatment room at the AIC-144 cyclotron.*

Fig. 9 *Preparation for treatment of one of the first ocular patients at CCB, February 2011.*

The first two patients were treated at our ocular radiotherapy facility at CCB in February 2011, making the CCB at IFJ PAN the first ocular proton radiotherapy centre to operate in Poland and in Central Europe. By the end of 2012 experimental radiotherapy was performed on 15 patients. From January 2013 onwards patients will be treated under regular contract of the University Hospital in Krakow with the National Health Fund.

RESEARCH PROJECTS AT CCB

Nuclear Physics research projects at CCB

The proton beam of the Proteus C-235 cyclotron at CCB, equipped with a dedicated energy selector, will be able to deliver a fairly monoenergetic beam of protons over the energy range between 70 MeV and 230 MeV, and to deliver stable proton beams of currents ranging between 1 nA and 500 nA. An experimental hall for nuclear physics research has been built specifically for basic research in the areas of nuclear physics, radiobiology, dosimetry and medical physics.

Nuclear physics research projects in these areas are currently under way at CCB, carried out by a research consortium led by IFJ PAN researchers of the Division of Nuclear Physics and Strong Interactions and of other Divisions of the IFJ PAN. The current research topics are:

- dynamics of a few-nucleon systems and physics of nuclear clusters, aimed at delivering new insights into the nucleon-nucleon interaction,
- measurements of collective, high-energy excitations in nuclei (e.g., giant nuclear resonances) in yet unexplored regions of excitation energy and spin,
- high resolution gamma-ray spectroscopy of nuclei produced in the process of proton-induced fission and spallation,
- tests of elements of modern detection systems under construction, for large-scale nuclear physics facilities in Europe (SPIRAL2, FAIR),
- development of new dosimetry methods for of proton beam diagnostics, using state-of-art active and passive detectors,
- development of new treatment planning systems for hadron radiotherapy.

The CCB will also be used as an education and training centre. In particular, it will provide to the PhD and undergraduate students with an excellent opportunity to participate in advanced experiments using a wide range of proton beams.

The first physical experiment at CCB using protons delivered from the newly installed Proteus C-235 cyclotron was performed in March 2013. The aim of this pilot measurement was to **test a response of** different **new generation scintillator detectors to protons** of energy ranging from 70 up to 230 MeV. More than 30 physicists from abroad (Italy, France, Germany, Spain, Japan, Romania, Hungary and Turkey), as well as the groups from Krakow and Warsaw, involved in the PARIS and CALIFA collaborations in the framework of the European NuPNet- GANAS network, have participated in the test.

The novel scintillator crystals based on Cerium-doped Lanthanum: as $LaBr_3$:Ce or $LaCl_3$:Ce attract many attention as a new material for nuclear radiation detectors. These crystals reveal very high light output and fast scintillation response, therefore are much superior to conventional scintillators as concerns energy and time resolution. Lanthanum Halides are considered very promising for building large spectrometers and calorimeters for gamma rays and charge particles, as for example PARIS and CALIFA, being prepared respectively for the SPIRAL2 at GANIL and NUSTAR/R3B at FAIR projects. Such large international projects as SPIRAL2 and FAIR require that all scientific equipment is fully tested and evaluated prior to being installed in the future radioactive beams. The facility offered by the Cyclotron Center Bronowice at IFJ PAN (CCB), that is a high quality (medical grade) proton beam with a possibility of quick energy and intensity alteration provides an excellent opportunity to perform such tests.

The experimental setup and the results are shown in the **Fig. 10**. A proton beam of a selected energy was scattered into air on a 23 mg/cm^2 thick titanium foil mounted at the exit of the beam line. Several detectors brought by the collaborating parties were exposed to protons in the same time.

The IFJ PAN group have tested a $LaBr_3$:Ce detector placed at the angles of 5° and 20° with respect to the beam axis. The detector consisted of a 2" x 2" x 2" $LaBr_3$:Ce crystal (BriLanCe380^{TM}) supplied by Saint Gobain Crystals and Detectors, hermetically sealed in an aluminum can with a glass window coupled to a photomultiplier tube Photonics XP3292B. In future set of such detectors will constitute an inner shell of the PARIS calorimeter. Output signals from both the dynode and the anode were collected using either analog or digital electronics.

In **Fig. 11** we show proton spectra measured at energies varying from 70 MeV – the minimum energy available from the accelerator, up to 140 MeV – the maximum energy that can be fully deposited

in the detector volume. The spectra are normalized to have the same height of the peak due to proton elastic scattering. Beside the peak one also observes a background from inelastic scattering, increasing with rising beam energies. The detector performance can be still improved by optimizing the readout electronics, however these first results obtained in beam are already very promising for possible applications of the novel scintillator detectors for high-energy proton spectroscopy.

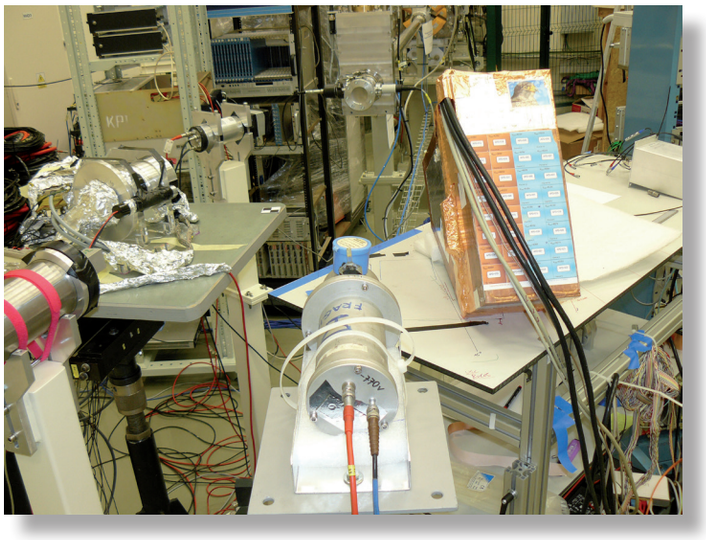

Fig. 10 *Experimental setup.*

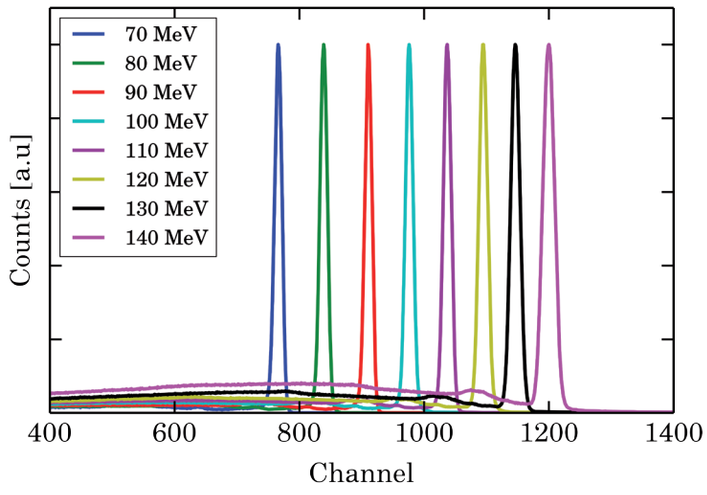

Fig. 11 *Proton spectra of scattered beam at energies varying from 70 MeV to 140 MeV, measured in 2"x2" LaBr3 detector.*

BINA (Big Instrument for Nuclear Reaction Analysis) **detector**, constructed and used for some years at KVI Groningen, **has been brought to Krakow and installed in experimental hall of Cyclotron Center Bronowice**, with the aim of continue the research program of completing the nuclear data base used in searches for three-nucleon force effects in nuclear interactions.

First in-beam tests at the new location have been performed delivering valuable informations about both, the condition of the detection setup after complicated process of migration, and the quality of proton beam delivered by the proton cyclotron Proteus C-235. Obtained data proved satisfactory performance of both scintillator hodoscopes allowing for unambiguous particle identification and precise energy reconstruction of all detected protons and deuterons in relevant range of phase-space (see the figure). However measured width of the horizontal beam distribution at the target position and beam

related halo, suggest the need of farther beam development, which are planned for the first half of the year 2014. Full operational readiness of the detector, as well as first measurements of breakup reaction are planned for the second half of 2014.

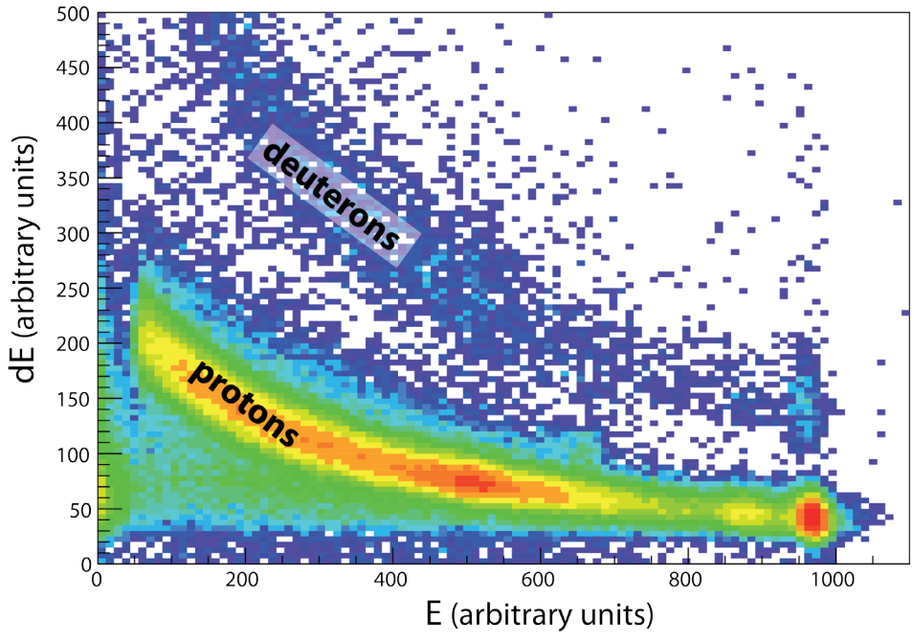

Fig. 12 *BINA particle identification spectrum. Plotted are energy losses versus total energy of detected particles. Proton and deuteron bands are clearly visible.*

Efficiency of luminescent detectors for the measurement of the proton dose of cosmic radiation in the Earth's orbit and in the dosimetry of proton beams

The aim of this research project is to determine the efficiency of relative luminescence detection (mainly thermoluminescent, TLD) of protons and its dependence on proton energy.

Relative efficiency of luminescence (REL) is defined as the ratio of intensities of emitted luminescence light, per unit dose, for a given type of radiation, to the same dose of reference gamma radiation (Cs-137 or Co-60 gamma-rays). REL is known to depend on ionisation density, as represented by the Linear Energy Transfer (LET) of densely ionising radiation. For weakly ionizing radiation (gamma rays, X-rays, electrons) REL is typically constant, and usually, above about 100 keV, RE = 1. For densely ionising radiation REL typically decreases with increasing LET, to values ranging between 0.05 and 0.5 at LET values around several hundred keV/um in water, depending of the type of detector.

Contradictory experimental data on REL have been reported. In a number of publications, REL of some thermoluminescence (TL) detectors (including lithium fluoride doped with magnesium and titanium, LiF: Mg, Ti) after doses of light ions (H and He, of LET < 5 keV/um, corresponding to protons of energy above 10 MeV He and heavier ions of energies above 50 MeV/n), has been reported to exceed one, even by up to 30%. On the other hand, at least as many published results show REL for protons to be equal to one, or lower. The proposed research project will attempt to resolve this issue by a systematic study of proton REL for several TL detectors and its dependence of proton energy or other factors that may affect this value.

The main result of this project will be achievement – for the first time – of a large systematic collection of reliable data on the REL of various luminescent detectors and on its dependence on proton energy and dose. Collection of such data will allow us to better understand the trapping and recombination processes which govern the phenomena thermo-and opto-luminescence in materials irradiated by ions. We will use this knowledge to improve the accuracy of dose measurements in such important applications as space and clinical dosimetry of external proton fields.

Development of a therapy planning system for carbon radiotherapy, based on the Cellular Track Structure radiobiological model

In ion beam therapy planning, enhanced radiobiological effectiveness (RBE) of ions in the Spread Out Bragg Peak (SOBP) region has to be correctly accounted for, unlike in conventional photon beam radiotherapy where uniform dose distribution over the target implies uniform cancer cell inactivation. We developed an algorithm of a one-dimensional kernel of a treatment planning system (TPS) for carbon ions, consisting of radiobiology and physical beam transport components. In the radiobiology component, Katz's track structure theory (TST) of cellular survival is applied, after validating its physical assumptions and improving some of its aspects.

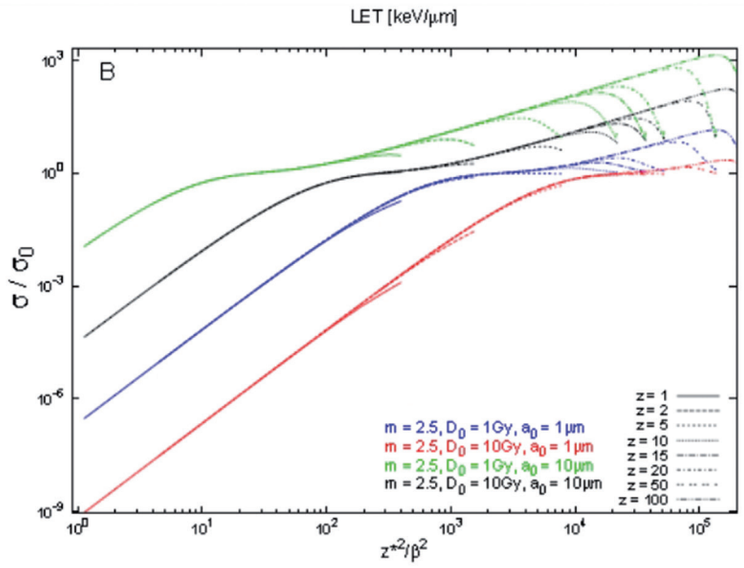

Fig. 13 *Example of scaling of the activation cross-section values in Katz's Cellular Track Structure Theory radiobiological model to a saturation value, by the use of the squared ratio of effective ion charge and its relative velocity, over a range of ion energies and model parameters. Calculations were performed using an optimised formula to describe the radial distribution of dose around the path of an ion at any given ion energy.*

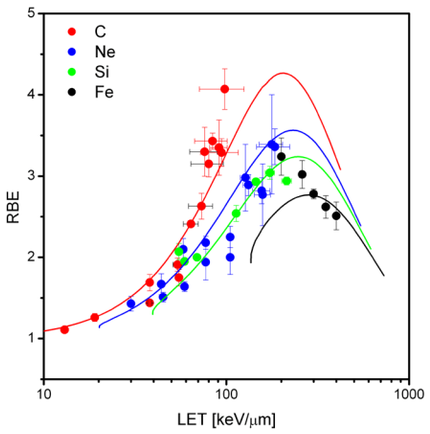

Fig. 14 *Experimentally measured and model-calculated dependences or Relative Biological Effectiveness (RBE) of normal human skin fibroblasts (HSF) at 10% survival, vs. ion LET, for carbon, neon, silicon and iron ions.*

The Katz TST radiobiological model offers fast and accurate predictions of cell survival in mixed fields of the primary carbon ions and of their secondary fragments. The physical beam model component is based on available tabularized data, prepared by Monte Carlo simulations of a carbon beam SOBP. Both components of our TPS kernel are combined within an inverse-planning optimization tool, allowing the entrance energy-fluence spectra of the carbon ion beam to be selected in order to achieve a pre-assumed (flat) depth-survival profile over the target region.

We have successfully benchmarked our TPS kernel against a published data set of CHO (Chinese Hamster Ovary) in-vitro cell survival curves after carbon ion irradiation. Our TPS kernel could be

expanded to a realistic 3-dimensional TPS, also for proton radiotherapy. Application of Katz's radiobiological model offers an alternative to the presently used ion planning systems based on the Local Effect Model (LEM), due to the robustness and simplicity of the Katz model and to the efficient computational techniques applied. The source coding is open within a generally accessible library of codes.

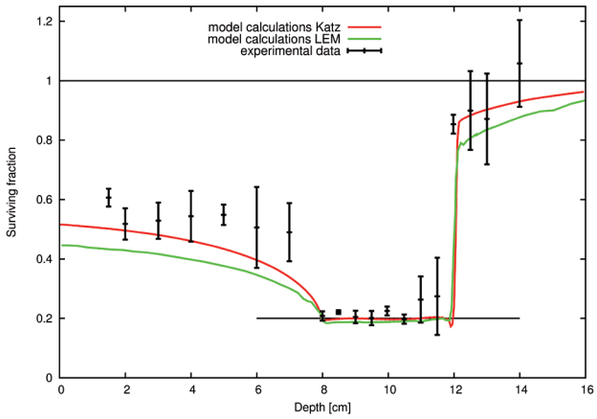

Fig. 15 *Survival of Chinese Hamster Ovary (CHO) cells vs depth: results of calculations using the dose optimization algorithm of the developed kernel of a treatment planning system which applies the scaled Katz model, compared with results of Local Effect Model (LEM) calculations and experimental data.*

RESEARCH AND DEVELOPMENT PROJECTS AT CCB

Reduction of undesired patient doses in eye treatment

The procedure of preparation and delivery of proton beams for treating ocular patients leads to undesired secondary scattered radiation received by the patient. This undesired patient dose should be reduced to the extent possible, for regulatory reasons and as a possible cause of secondary cancer induction in healthy tissues of the irradiated patient. Within a research and development (R&D) project carried out at CCB, the design of the eye treatment facility at IFJ PAN was optimised to reduce patient doses, in particular due to neutrons. This optimization was performed in several steps. First, the ranges of parameters of the proton beam fulfilling clinical requirements, were established. At dose rates between 0.25 Gy/s and 0.45 Gy/s at the reference point, the dose fraction of 13.6 Gy may be delivered in under 60 seconds. Assuming such conditions, a quantitative analysis of the secondary radiation field was performed, basing on results of field measurements and of numerical calculations using the MCNPX Monte Carlo code. Having estimated the equivalent doses to the patient from this secondary radiation (predominantly from neutrons and gamma rays), a suitable shielding system was proposed and implemented. The efficiency of this shielding system was then re-evaluated by MC calculations and by direct measurements. Evaluation of patient exposure was performed using several techniques. Organ doses were measured in an anthropomorphic RANDO phantom mimicking the patient's position during irradiation. MTS-6 and MTS-7 thermoluminescence detectors and CR-39 track detectors were placed inside this phantom and simulated ocular radiotherapy of the phantom performed. The relevant environmental dose rate levels were determined using a He-3 Wendi 2 gauge for the neutron field and an FHT-192 ionization chamber for gamma-rays. Additionally, the MCNPX v.2.5.0 Monte Carlo code and the mathematical Adam phantom were applied to cross-check the results of these measurement, with good agreement found. The ambient dose equivalent per unit therapeutic dose, H*(10)/D, was reduced to below 2 microSv/Gy and the total value of undesired patient exposure from scattered X-rays and neutrons was found not to exceed 1 mSv per entire treatment course.

Evaluation of undesired patient doses in MegaVolt X-ray radiotherapy

Due to the application of modern radiotherapy techniques, the effectiveness of radiotherapy increases, but secondary cancer occurrence might also increase in the future, due to irradiation of healthy tissues by undesired radiation fields. The IFJ PAN has contributed to the activities of the European Radiation Dosimetry Group (EURADOS) by performing a systematic study of undesired (non-target) patient doses in radiotherapy and the related risks of secondary malignancy.

In experiments involving the application of Volumetric Modulated Arc Therapy (VMAT), Tomotherapy, Intensity Modulated Radiotherapy (IMRT), 5-field Conformal Radiotherapy (CRT) and 4-field CRT radiotherapy techniques, we applied type MTS-7 thermoluminescence (TL) detectors to measure doses of scattered X-rays and from secondary γ-radiation in a rectangular water phantom and in an anthropomorphic BOMAB-like phantom. We confirmed that TL dosimetry is suitable for measuring scattered X-rays and secondary γ radiation over a broad photon beam energy spectrum and a dose range of several mGy to several Gy. The response of MTS-7 to the scattered radiation favourably compared with the response of reference dosimeters and of other luminescence detectors. The experiments confirmed that patients treated with conformal radiation therapy are exposed to higher doses of radiation over areas remote from the target volume in comparison with conventional radiotherapy. Comparison of measured doses with doses calculated in the treatment planning systems has shown that some therapy planning systems may underestimate the expected dose values outside the target, even by factors of up to 2.

The Proton Beam Imaging System (ProBimS)

A high-resolution system for imaging the transverse fluence distribution of a 60 MeV proton beam is under development at CCB IFJ PAN, as an R&D project. This system will serve for quality assurance purposes in a proton ocular treatment facility. For the proton beam to be applicable in clinical radiotherapy the precise localization and repeatability of its physical parameters are essential and, in particular, accurate measurements of the dose distribution along the beam range and across the beam axis, at different beam depths, are required. The core elements of the ProBimS under development are a scintillation detector to convert the ionisation from protons in the beam to visible light, a front-laminated mirror and a high-resolution CCD camera. To avoid radiation damage to the CCD sensor, the light from the scintillator is reflected by a glass mirror towards the CCD camera. The prototype system consists of a highly efficient DuPont 000128 scintillator (typically used in X-ray image converters), with maximum quantum efficiency covering the optimum wavelength range of the CCD camera (of type ATIK 383, with a 3362x2537 pixel matrix). The light image of the beam is viewed and further processed by dedicated software. To achieve a relatively high temporal resolution, a data acquisition system based on the standard USB transfer is employed. The acquired images undergo detailed analysis in order to extract the physical and geometry parameters of the beam. Software for image analysis has been in-house developed within the MATLAB programming environment. The specific functions and algorithms are then transferred to the Nuclear Instruments LabView environment. Initial tests of the prototype version of the ProBimS system have shown it to be useful in rapid evaluation of transversal proton beam profiles.

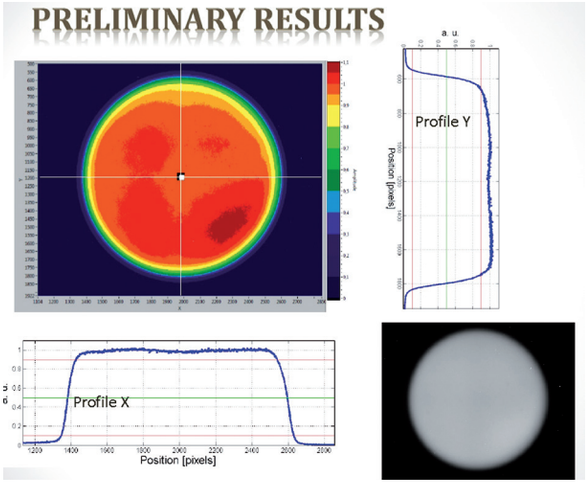

Fig. 16 *An example of a transverse proton beam dose profile measured by the prototype ProBimS system.*

EPR/alanine dosimetry for ion beam radiotherapy

EPR/alanine dosimetry is a well-established method for measuring high radiation doses, based on determining the concentration of free radicals in amino acid L-α–alanine (CH3-CH(NH2)-COOH) induced by ionising radiation. The concentration of these radicals trapped in the crystal structure of alanine is proportional to dose absorbed in the alanine detector. The main goal of this R&D project is to provide the ability to perform dose measurements, based on alanine dosimetry, for quality assurance (QA) purposes in proton radiotherapy procedures performed at CCB. The EPR spectrometry laboratory at IFJ PAN uses a Bruker ESP300 spectrometer, upgraded by a new cooling system and a module for digital data acquisition. Several types of alanine dosimeters (foils, rods and pellets and in-house-manufactured detectors) have been tested in AIC-144 proton beams. The response of alanine detectors has been investigated at different depths within a pristine proton beam and over the Spread Out Bragg Peak region. Measurements of efficiency of alanine detectors, relative to Co-60 doses, were performed with alanine films and calculated using SRIM and MCNPX Monte Carlo codes. The relative efficiency per absorbed dose for protons, in track-segment mode of irradiatoion, was found to be fairly independent on proton energy above 10 MeV, which makes this detector suitable for the desired QA purposes.

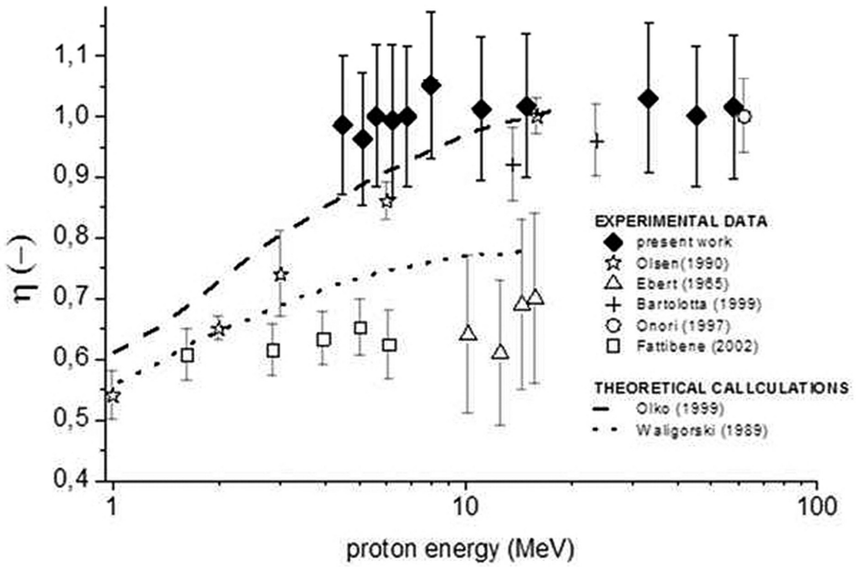

Fig. 17 *Measured values of relative effectiveness of alanine foil vs. track segment energy of protons in a pristine proton beam, and model predictions.*

Alanine detectors will be used for Quality Control of the therapeutic proton beam and of patient irradiation. Due to the non-destructive read-out of the alanine dosemeter it will be possible to record cumulatively the dose received by the patient after each fraction and to maintain a permanent record of the total dose received by the target volume (tumour) in the patient. This project is partly supported by the Polish Science Foundation and by EU structural funds.

Development of two-dimensional thermoluminescent dosimetry (2D TL)

Application of current radiotherapy techniques leads to dose distributions featuring high dose gradients, therefore 2-D imaging of dose distributions offers many advantages over the traditional dose measurement at a given point. This is of particular importance in ion beam radiotherapy where "geographical error", i.e. inaccurate positioning of the dose distribution outside the target volume, may

lead to severe complications in the healthy tissues surrounding the target volume, due to the high doses involved. Two-dimensional, thermoluminescent dosimetry techniques (2D TL) have been developed at IFJ PAN over several years, offering a valuable tool for modern clinical dosimetry. This technique relies on large-area (up to 20 x 20 cm^2) TL foils, consisting of TL powder (based on LiF or $CaSO_4$) sintered into a polymer base by an in-house-developed method, and on large-area TL readers which use a CCD camera to view the TL light emitted on heating the 2D TL foil. Two such readers were developed at IFJ PAN – a laboratory reader able to read 5 x 5 cm^2 foils and a clinical reader which is able to read foils of dimensions up to 20 x 20 cm^2. Dedicated software to control the reader operation and image analysis (FlatView) has also been in-house developed. We believe that the developed 2D TL technique will find many applications in clinical dosimetry and industry, to complement other 2D detectors, such as photographic film, portal imaging systems or dye film detectors. The particular advantages of 2D TL dosimetry are the re-usability of TL foils, their flexibility and water-resistance, and the possibility to pre-calibrate the TL foil in terms of absorbed dose prior to its application.

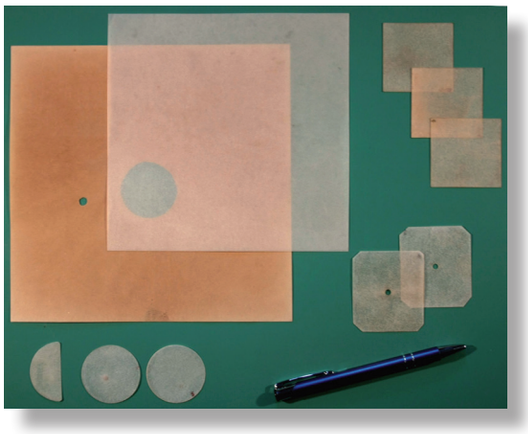

Fig. 18 *Samples of 2D TL foils produced at IFJ PAN.*

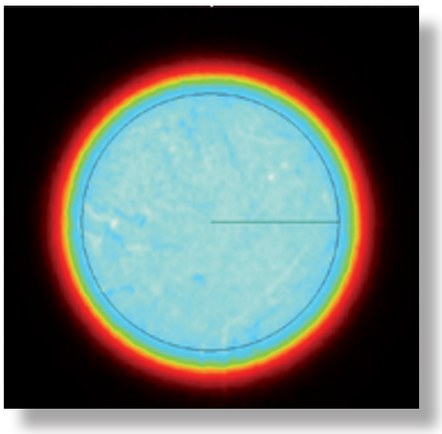

Fig. 19 *Image of a transverse proton beam dose profile, measured at CCB using a 2D TL foil.*

The research reported herein was performed pursuant to internal projects: [410, 412, 413, 502, 505]; [E4, E8, E22, E26, E33, E46, E47, E48]. See Annexes I, IIB.

VIII. ACCREDITED LABORATORIES

Within the Institute of Nuclear Physics PAN, four Accredited Laboratories are in operation. Their accreditation, from the Polish Centre for Accreditation (www.pca.gov.pl), covers the PN-EN-ISO/IEC 17025:2005 laboratory measurement standard. Within the requirements of this standard, a broad spectrum of measurements and expert evaluations are available for outside customers, in the general field of dosimetry of ionizing radiation. More specifically, the laboratories perform calibration of instruments used in dosimetry, spectroscopy and spectrometry of ionizing radiation and perform measurements of the concentration of man-made and natural radioisotopes in gaseous (atmospheric air), solid or liquid samples.

Laboratory for Calibration of Dosimetry Instruments – NLW (www.wzorcowanie.ifj.edu.pl)

This laboratory performs calibration of radiation survey meters in terms of air kerma rate and in terms of radiation protection units, using ^{137}Cs γ-rays. Calibration is also performed in terms of surface emission (^{239}Pu and ^{241}Am α-particles and ^{90}Sr/^{90}Y, ^{36}Cl and ^{14}C β-particles). Individual and environmental dosemeters are calibrated in terms of kerma in air, $H_P(10)$ and $H_P(0.07)$. The laboratory is equipped with a gamma-ray irradiator containing three, remotely interchangeable ^{137}Cs sources, of activities 1.96 TBq, 25 GBq and 250 MBq. Using this irradiator and a 7 m-long calibration bench, it is possible to obtain calibrated dose rates ranging between 1 μGy/h and 1 Gy/h. Each year the laboratory calibrates about 800 survey meters for customers from all regions of Poland.

Laboratory of Individual and Environmental Dosimetry – NLD (www.dawki.ifj.edu.pl)

This Laboratory of Individual and Environmental Dosimetry (LADIS) performs, as a complete service, measurements of individual and environmental doses using the thermoluminescence method developed at IFJ in 60's. The majority of these measurement services concern individual dosimetry for radiation workers exposed to ionising radiation (measurements of Hp(10) , Hp(0,07), Hp(3)) and measurements of K_{air} in environmental monitoring (Fig 1). Currently, LADIS performs over 45 000 measurements yearly for individual radiation workers and at locations in working or natural environment, for over 7000 institutions in Poland. The Laboratory also offers, as a service, Quality Control tests of medical X-ray equipment for radiography, fluoroscopy, mammography, for dental and panoramic dental systems and for computed tomography units. Research in these areas is also carried out in the Laboratory, currently within two research projects.

Laboratory of Radiometric Expertise – NLR (www.radon.ifj.edu.pl)

The research activity of this Laboratory is focused on the following main fields: physics of natural radioisotopes, identification and ultra-sensitive measurements of gamma isotopes in environmental samples, investigations of ^{222}Rn diffusion processes, measurements radon and thoron concentration, and calculation and modelling of dose in the environment. The Laboratory participated in four research grants on radon survey technologies to support the development of nuclear power in Poland. The Laboratory offers a wide range of certified measurement techniques for evaluating environmental radioactivity: measurements of concentration of natural gamma isotopes (^{226}Ra, ^{228}Th, ^{40}K) in solid samples using low-background gamma spectroscopy, measurements of radon ^{222}Rn concentration in liquid samples using alpha spectroscopy, measurements of radon ^{222}Rn concentration (indoor, outdoor and in soil gas) using alpha spectroscopy and using CR-39 track detectors. The Laboratory also uses the CHIMERA Lab - a mobile laboratory vehicle (Fig 2.), the equipment of which was covered by European Union funds. This mobile unit is able to perform measurements of outdoor gamma dose rates, to perform *in-situ* gamma spectrometry in the environment and to measure radon concentration in air and in water. Such measurements are relevant to the development of nuclear energy in Poland.

Laboratory of Radioactivity Analyses – LAP (www.lap.ifj.edu.pl)

This Laboratory grew from the experience gained in research on environmental radioactivity. Within its accreditation, this Laboratory offers measurements of gamma emitters, among them ^{137}Cs, ^{134}Cs and all isotopes of plutonium in various materials. Being the first, it is currently the only laboratory in Poland to be accredited to perform analyses of plutonium radioisotopes. The Laboratory has four low-background gamma-ray spectrometers with germanium detectors and alpha spectrometers with semiconductor detectors. The main task of this laboratory is to support and maintain the high credibility of measurements performed by the Polish state monitoring system.

Fig. 1 *Typical placement of an individual dosimeter used for evaluating the $H_p(10)$ dose equivalent, in mSv.*

Fig. 2 *The mobile CHIMERA radiometry laboratory and its basic equipment for measuring radon concentration, dose rates in the environment and for performing* in situ *spectrometry.*

The research reported herein was performed pursuant to internal projects: [409, 410]; [E54]. See Annexes I, IIB.

IX. INTERNATIONAL POST-GRADUATE STUDY COURSE

HEAD: TADEUSZ LESIAK, PROF.

Doctoral studies at the Institute of Nuclear Physics were launched in 1984. In December 2013 we celebrated the 30th anniversary of the Course's activity (see photograph). Over the current academic year (2013/14), 62 students are attending, among whom two are from the Ukraine, one is from Belarus and one from Iran. We co-operate closely with the Tadeusz Kościuszko Cracow University of Technology, the Pedagogical University of Cracow, and with the University of Rzeszów. Also, since 2009, we have collaborated with the AGH University of Science and Technology and the Haber Institute of Catalysis and Surface Chemistry of the Polish Academy of Sciences within the PhD-level education project *"Interdisciplinary PhD Studies: Advanced Materials for Modern Technology and Future Energy Production"*, supported by the EU Operational Programme Human Capital. In the framework of this project 15 PhD students are completing their theses at our Institute.

Prospective candidates must be university graduates with an M. Sc. degree in Physics or with a M. Eng. degree in a physics-related discipline of applied science. Candidates are recruited each year. Available subjects of study cover all areas of research performed at our Institute: theoretical and experimental investigations of fundamental interactions (Nuclear and High Energy Physics), theoretical and experimental investigations of condensed matter, atomic physics, astrophysics, foundations of physical theories and mathematical methods of physics, dynamic systems in studies of complex phenomena in nature, computer modelling of structural and dynamical properties of condensed matter, physical methods in investigations of polymers, biological and biomedical applications of Magnetic Resonance Imaging and other tomography methods, development of radioisotopes for biomedical sciences, application of radiation in medical diagnostics and therapy, ultra-sensitive detection methods in biology, materials science and environmental studies, ion implementation in the preparation of new materials. The Ph. D. course takes four years.

During the past 30 years of activity, we have granted Ph.D. degrees in physics to over 160 young scientists (47 in the years 2011-2013). To name a few of the most outstanding results, let us mention: searches for instantons in deep inelastic scattering (Paweł Sopicki), studies of diffraction with the Atlas detector at the LHC (Rafał Staszewski and Maciej Trzebiński), description of collective phenomena at early stages of relativistic heavy-ion collisions (Radosław Ryblewski), studies of the predictive power of nuclear structure models (Bartłomiej Szpak), properties of molecular magnets, molecular thin films and magnetic nanoparticles (Magdalena Fitta) or out-of-field dosimetry in proton radiotherapy (Liliana Stolarczyk). Two of these PhD theses (of Rafał Staszewski and Maciej Trzebiński) were co-directed in the framework of Polish-French programme *thèse en cotutelle*.

In 2013 our Institute of Nuclear Physics was awarded the prestigious title of the most pro-PhD student scientific institution of the Polish Academy of Sciences. Among other honours, two of our graduates were beneficiaries of the START programme of the of Foundation for Polish Science; Katarzyna Pogoda was awarded a **Fulbright Foundation** fellowship; Marcin Chrząszcz was awarded with a "diamond grant" of the Polish Ministry of Science and Higher Education and a Polish-Swiss Scientific Exchange Programme fellowship; Michał Krupiński came third in the Polish Famelab Competition. In the last three years 40 students received special grants to prepare their PhD theses, awarded by the Polish Ministry of Science and Higher Education, the National Science Centre and the National Centre of Research and Development.

Fig. 1 *A group of PhD students with authorities of their mother institutions, supervisors and tutors, celebrating the thirtieth anniversary of PhD Sudies at IFJ PAN.*

X. OUTREACH ACTIVITIES – PROMOTION AND EDUCATION IN SCIENCE

In the years 2011–2013 the Institute of Nuclear Physics PAN continued its outreach activities by promotion of science and education of the general public about the Institute's research areas. Our main outreach objectives are:

- to educate different societal groups in the general area of physics and about the latest advances in science, in a comprehensive but accessible manner,
- to promote the research topics pursued at our Institute,
- to stimulate and develop an interest in physics among young people.

In 2012, the Institute of Nuclear Physics was awarded the prestigious "Populariser of Science 2012" national prize by the Ministry of Science and Higher Education and the Polish Press Agency, in the category of scientific institutions.

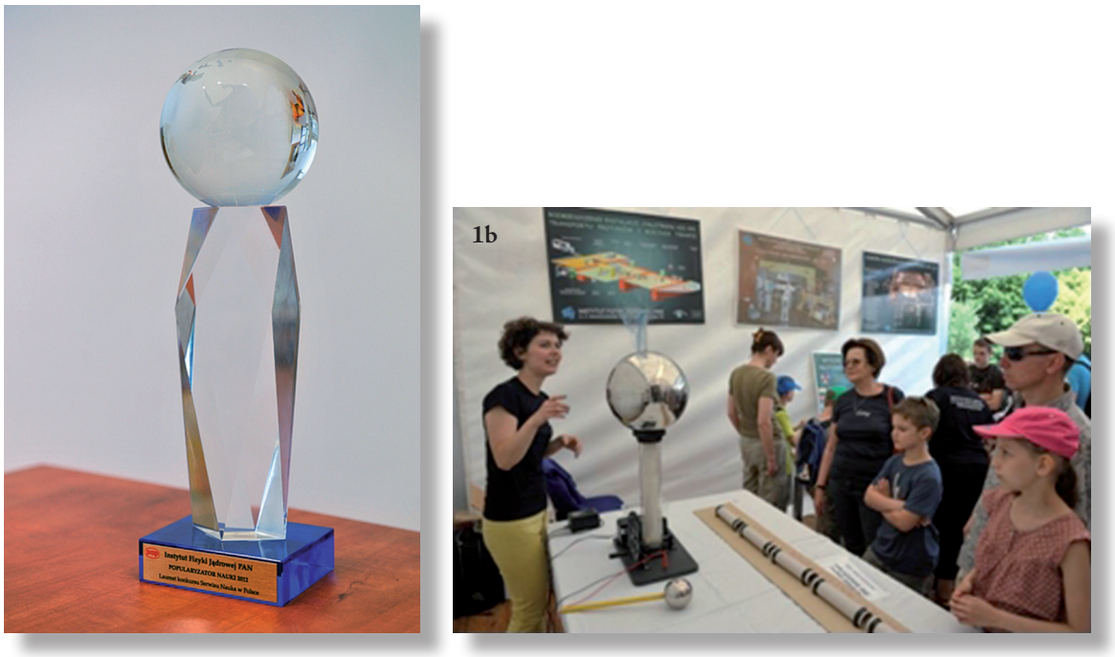

Fig. 1 *Crystal Ball – Award for the best "Populariser of Science 2012" (1a). Katarzyna Byk demonstrates simple electrostatics experiments at the Warsaw Science Picnic Festival, 2013 (1b).*

Among our outreach activities in the years 2011–2013 were:

- creation of a dedicated website "On the trail of the Mysteries of Nature" devoted entirely to popularising science,
- active participation in lectures and demonstrations at regular yearly events co-organized with other scientific institutions:
  - » Science Festival in Krakow,
  - » Małopolska Researcher's Night,
  - » Warsaw Science Picnic of the Polish Radio and the Copernicus Science Centre.
- several visits to selected laboratories of our Institute by small groups of university, secondary and high school students were arranged throughout the year. We had over 1700 such visitors over the last three years.
- every year the Institute financially supported the Kraków and Małopolska Competition in Physics and Astronomy for secondary and high school students.

- in collaboration with the International Particle Physics Outreach Group and CERN, each year we organised an International Workshop on Particle Physics for high school students ("International Master Classes – Hands on Particle Physics") for about 100 participants.
- we took part in the implementation of the e-Academy of the Future, a competence development programme for teachers and school children, with particular emphasis on mathematics and natural sciences.
- we participated in the INTERBLOK Social Educational Society project, a curriculum block of mathematics, natural sciences and computer science at high school level,
- our research staff were invited to lecture on popular science by various organizations and associations (including the Children's University, the National Natural Science Workshops Children's Fund, the Centre for Civic Education, PAU Cafe Scientific Association of Physics demonstrators, etc.),
- our research staff gave interviews on TV, in the radio, over the Internet and published popular articles on physics phenomena.

Each year, we pay particular attention to prepare an interesting programme for the "Małopolska Researcher's Night" event. At the Institute premises we organised a popular programme "Science in the open air and behind closed doors ". In tents, situated in the green areas of the Institute, the latest achievements of our Institute in five major areas: Particle and Astroparticle Physics, Nuclear Physics and Strong Interactions, Condensed Matter Physics, Theoretical Physics and Applications of Physics and Interdisciplinary Research were presented with very good attendance and often enthusiastic response of our visitors.

Within the "Małopolska Researcher's Night", visits to our most interesting laboratories were possible. The participants could also communicate with experiments conducted at the Large Hadron Collider (LHC) at CERN, using a special telebridge prepared for the occasion. Visitors could also attend special lectures, demonstrations and panel discussions with our experts.

In 2013, a premiere theatre, film and interactive show was presented, directed by Dr Jerzy Gręboszand entitled: "Physics – The Largest Spectacle of the Universe".

Every year, the "Małopolska Researcher's Night" gathers over 1000 visitors at our Institute, most of whom enthusiastically respond to our outreach programme of that event.

Over the years 2011–2013 the outreach efforts of our science educators have been acknowledged on several occasions:

Michał Krupiński, Ph. D. Eng., placed third in the FameLab in Poland competition – edition 2012. Fame Lab is an International Competition set up in 2005 to support and encourage those working in science and engineering to use the skills they learn to communicate their work to society. It is now held in 20 countries across Europe, Asia, Africa and the United States.

Piotr Konieczny, M. Sc., received the Special Prize of the Ministry of Science and Higher Education and the Special Prize of the British Council in the competition FameLab in Poland – edition 2013.

Dr Stanislaw Kwieciński became the Lecturer of the Year 2012 of Children's University, for his lecture entitled "How does the Physicist help the Doctor?".

Dr Jadwiga Mazur, and Assoc. Prof. Krzysztof Kozak – received the PAU award in 2013 for their book: "The world of physics. Guide for secondary schools. Primary range", by M. Fiałkowska, J. Kreiner, M. Godlewski, S. Godlewski, K. Kozak and J. Mazur, published by ZamKor, Krakow 2012.

Fig. 2 *Paweł Janowski, Jerzy Grębosz and Andrzej Horzela performing in "Physics – The Largest Spectacle of the Universe" – Małopolska Reasercher's Night, 2013.*

ANNEXES

I. LIST OF PROJECTS
REFERRENCED IN RESEARCH HIGHLIGHTS

[102] **THE ZEUS EXPERIMENT AT HERA ACCELERATOR, (DESY, HAMBURG)**, J. Chwastowski, J. Figiel, K. Olkiewicz, P. Stopa, L. Zawiejski, D. Szuba, A. Galas, B. Pawlik

[103] **THE H1 EXPERIMENT AT HERA ACCELERATOR (DESY, HAMBURG)**, L. Görlich, S. Mikocki, G. Nowak, J. Turnau, E. Łobodzińska, I. Milcewicz-Mika, P. Sopicki

[104] **THE BELLE EXPERIMENT AT THE KEK B-FACTORY**, A. Bożek, J. Brodzicka, P. Kapusta, Z. Natkaniec, W. Ostrowicz, M. Rożańska, J. Stypuła, K. Adamczyk, O. Grzymkowska, J. Wiechczyński

[105] **THE AUGER COSMIC RAY EXPERIMENT**, H. Wilczyński, B. Wilczyńska, D. Góra, P. Homola, J. Pękala, J. Stasielak, N. Borodai, Cz. Porowski

[106] **NEUTRINO PHYSICS AND SEARCHES FOR DARK MATTER**, A. Zalewska, A. Dąbrowska, M. Szarska, K. Cieślik, D. Stefan, A. Szelc, T. Wąchała, P. Karbowniczek, M. Batkiewiz, M. Harańczyk, P. Kryczyński

[107] **THE ATLAS EXPERIMENT AT THE CERN LARGE HADRON COLLIDER (LHC)**, B. Wosiek, A. Olszewski, A. Trzupek, K. Woźniak, M. Turała, P. Malecki, J. Turnau, L. Görlich, E. Górnicki, A. Kaczmarska, K. Korcyl, A. Moszczyński, J. Olszowska, M. Wolter, P. Brückman de Renstrom, J. Chwastowski, Z. Hajduk, E. Banaś, B. Kisielewski, W. Iwański, E. Stanecka, K. Słowikowski, D. Derendarz, Pa. Malecki, R. Staszewski, B. Żabiński, M. Trzebiński, A. Zemła, J. Knapik

[108] **THE LHC-b EXPERIMENT AT LHC (CERN)**, M. Kucharczyk, T. Lesiak,G. Polok, M. Witek, J. Wiechczyński, A. Florek, B. Florek, J. Garwoliński, P. Morawski, A. Dziurda, S. Kukulak, B. Rachwał, M. Chrząszcz, R. Grzymkowski, M. Zdybał

[109] **DESIGN AND CONSTRUCTION OF THE LUMINOSITY DETECTOR PROTOTYPE FOR THE e+e– LINEAR COLLIDER (ILC) AND R&D FOR XFEL**, L. Zawiejski, A. Moszczyński, B. Pawlik, K. Oliwa, W. Wierba, W. Daniluk, E. Kielar, D. Bocian, B. Krupa

[110] **THEORY AND PHENOMENOLOGY OF FUNDAMENTAL INTERACTIONS INCLUDING EXPERIMENTAL RESULTS IN PARTICLE PHYSICS**, M. Jeżabek, K. Zalewski, S. Jadach, M. Jeżabek, M. Skrzypek, Z. Wąs, A. van Hameren, K. Kutak, A. Kusina, M. Sławińska, P. Stokłosa, O. Gituliar, O. Shekhovstova

[111] **ASTROPHYSICAL AND COSMOLOGICAL ASPECTS OF PARTICLE PHYSICS**, M. Kutschera, S. Kubis, Ł. Bratek, J. Niemiec, J. Jałocha-Bratek, D. E. Alvarez Castillo

[112] **ALGEBRAIC METHODS OF QUANTUM PHYSICS**, A. Horzela, P. Błasiak, K. Górska, P. Bochnacki

[113] **THE STAR EXSPERIMENT AT THE RHIC AKCCELERATOR (since 2012) (BNL, USA)**, J. Turnau, B. Pawlik

[114] **THE SUPERb EXSPERIMENT AT CABIBBO LAB (TOR VERGATA, ITALY)**, T. Lesiak, J. Wiechczyński

[115] **GAMMA-RAY ASTRONOMY**, J. Niemiec, M. Dyrda

[201] **MECHANISM OF NUCLEAR REACTIONS, AND MESON PRODUCTION IN HADRON COLLISIONS**, A. Budzanowski, B. Czech, M. Kistryn, E. Kozik, K. Pysz, G. Kamiński, S. Kliczewski, P. Kulessa, A. Kozela, W. Kantor, J. Łukasik, P. Pawłowski, W. Karcz, R. Siudak, R. Wolski, B. Czech

[202] **EVOLUTION OF NUCLEAR STRUCTURE WITH TEMPERATURE, SPIN AND ISOSPIN**, R. Broda, P. Bednarczyk, B. Fornal, M. Kmiecik, W. Krolas, K.H. Maier, A. Maj, K. Mazurek, W. Męczyński, T. Pawłat, J. Styczeń, J. Wrzesiński, M. Krzysiek, M. Niewiara, M. Cieplicka, M. Ciemała, Ł. Iskra, M. Matejska-Minda, S. Myalski, B. Szpak

[203] **STRUCTURE AND DYNAMICS OF MENY BODY SYSTEMS**, A. Szczurek, A. Adamczak, P. Czerski, J. Jakiel, J. Okołowicz, T. Srokowski, W. Schäfer, A. Cisek, M. Kłusek, P. Lebiedowicz, R. Maciuła, G. Kubasiak

[204] **RELATIVISTIC ION INTERACTIONS AT SPS AND LHC ENERGIES – THE NA49 AND ALICE EXPERIMENTS**, M. Kowalski, A. Rybicki, E. Gładysz-Dziaduś, J. Figiel, Ch. Mayer, A. Matyja, I. Sputowska, A. Cyz,

[205] **THE PHOBOS EXPERIMENT AT THE BNL-RHIC ACCELERATOR (in 2011)**, B. Wosiek, A. Trzupek, K. Woźniak, A. Olszewski

[206] **DEVELOPMENT OF THE THEORY OF PARTICLE PHYSICS IN CONNECTION WITH RESULTS OF NEW EXPERIMENTS**, W. Broniowski, A. Białas, P. Bożek, T. Chmaj, W. Florkowski, K. Golec-Biernat, R. Kamiński, L. Leśniak, P. Żenczykowski, M. Cerkaski, A. Staśto, B. Ziaja-Motyka, M. Chojnacki, A. Jarosz, E. Lewandowska, R. Ryblewski, I. Wyskiel-Piekarska, S. Zając, V. Nazari

[207] **RESEARCH AND DEVELOPMENT RELATED TO THE NEW DETECTION METHODS IN NUCLEAR PHYSICS**, A. Maj, A. Czermak, J. Grębosz, M. Zięblińśki, B. Fent, B. Czech, B. Szpak, M. Jastrząb, B. Sowicki, A. Szperłak

[208] **EKSPERIMENTS OF NATIONAL CYKLOTRON LABORATORY**, A. Maj, B. Fornal, M. Kmiecik, P. Bednarczyk, A. Kozela, W. Męczyński

[301] **STUDIES ON STRUCTURE AND DYNAMICS OF CONDENSED MATTER (MOLECULAR CRYSTALS, LIQUID CRYSTALS, MAGNETS, etc.) BY MEANS OF NEUTRON SCATTERING TECHNIQUES AND COMPLEMENTARY METHODS**, J. Janik, M. Massalska-Arodź, T. Wasiutyński, M. Bałanda, A. Budziak, J. Krawczyk, Z. Łodziana, A. Pacyna, R. Pełka, W. Zając, P. Zieliński, P. M. Zieliński, M. Krawczyk, M. Gałązka, E. Juszyńska-Gałązka, M. Czapla, N. Osiecka, M. Jasiurkowska, , Ł. Kolek, T. Rozwadowski, G. Lewińska, S. Mazur, M. Fitta (Makarewicz), P. Sobieszczyk, P. Konieczny, M. Majka

[302] **STUDIES OF CONDENSED MATTER USING NUCLEAR SPECTROSCOPY METHODS – POSITRON ANNIHILATION TECHNIQUES**, E. Dryzek, J. Dryzek, P. Horodek, S. Lewicka,K. Siemek,M. Sarnek

[303] **NUCLEAR MAGNETIC RESONANCE (NMR) METHODS IN STUDIES OF STRUCTURE AND MOLECULAR DYNAMICS IN SOLIDS**, J. Hennel, Z. Lalowicz, Z. Olejniczak, A. Birczyński, A. Szymocha, G. Stoch, M. Noga

[304] **RESEARCH OF STRUCTURE AND LATTICE DYNAMIC OF CRYSTALS AND NANOMATERIALS BY COMPUTATIONAL METHODS**, K. Parliński, P. Jochym, J. Łażewski, A. Oleś, P. Piekarz, A. Siegel, M. Sternik, M. Litwiniszyn

[401] **PHYSICS OF COMPLEX SYSTEMS – INTERDISCIPLINARY ASPECTS**, S. Drożdż, A. Górski, J. Kwapień, P. Oświęcimka, S. Gworek, M. Forczek, A. Kulik, I. Grabska

[402] **EXPERIMENTAL, THEORETICAL AND NUMERICAL RESEARCH ON THE INTERACTION OF NUCLEAR RADIATION WITH VARIOUS MEDIA**, U. Woźnicka, K. Drozdowicz, B. Gabańska, J. Dankowski, D. Dworak, G. Tracz, A. Igielski, A. Kurowski, Wł. Janik, U. Wiącek,

[403] **NEUTRONS AND ASSOCIATED PARTICLES DETECTION METHODS FOR D-D AND D-T PLASMA DIAGNOSTIC – RESEARCH FOR ITER PROGRAMME (TASK PERFORMED FOR EURATOM ASSOCIATION)**, U. Woźnicka, K. Drozdowicz, J. Dankowski, D. Dworak, B. Gabańska, A. Igielski, A. Kurowski, G. Tracz, D. Twaróg, U. Wiącek, Wł. Janik, M. Gajewski

[404] **RADIATION AND ENVIRONMENTAL BIOLOGY – RETROSPECTIVE BIOLOGICAL DOSIMETRY OF THE ENVIRONMENTAL EXPOSURES – STUDY OF RADIOSENSITIVITY AND DNA REPAIR EFFICIENCY**, A. Cebulska-Wasilewska, A. Panek, J. Adamczyk, J. Miszczyk

[405] **MAGNETIC RESONANCE IMAGING (MRI) AND LOCALIZED SPECTROSCOPY (MRS) IN BIOMEDICAL RESEARCH**, W. Węglarz, A. Krzyżak, P. Kulinowski, S. Kwieciński, T. Skórka, K. Kalita (Majcher), M. Noga, U. Tyrankiewicz, T. Banasik, S. Heinze-Paluchowska, B. Tomanek, K. Jasiński, B. Błasiak, A. Młynarczyk, P. Rosicka, W. Rutkowski, Ż. Bartel, M. Jabłońska, K. Byk, A. Osiak, W. Piędzia, G. Stoch, G. Woźniak

[406] **STUDIES OF VARIABILITY OF BIOLOGICAL AND ENVIRONMENTAL SYSTEMS AND OTHER COMPLEX STRUCTURES**, A. Hrynkiewicz, W. Kwiatek, M. Lekka, J. Lekki, A. Wiecheć, E. Dutkiewicz, Z. Stachura, T. Pieprzyca,Z. Szklarz, J. Wiltowska-Zuber, K. Tkocz, J. Szlagor, O. Klymenko, J. Bielecki, J. Kowalska, B. Frączek-Błachut, J. Czapla, E. Lipiec, S. Prauzner-Bechcicki, K. Pogoda, W. Piędzia

[407] **DEVELOPMENT AND APPLICATION OF THE TRACERS' MEASUREMENT METHODS TO THE ENVIRONMENTAL PHYSICS, HYDROGEOLOGY AND MEDICINE**, I. Śliwka, J. Faber, B. Grabowska-Polanowska, I. Grombik-Suwała, J. Najman, P. Mochalski, M. Skowron, J. Bielewski,

[408] **DEVELOPMENT OF THE ISOTOPIC METHODS BASED ON THE APPLICATION OF AIC-144 CYCLOTRON FOR NUCLEAR MEDICINE AND ANALYTICAL CHEMISTRY (in 2011),** B. Petelenz, E. Ochab, M. Szałkowski, B. Wąs

[409] **DEVELOPMNETS OF RADIOCHEMICAL METHODS FOR BASIC RESEARCH, MEDICINE, ENVIRONMENTAL STUDIES AND INVESTIGATION OF CONCENTRATION OF RADIOACTIVE ELEMENTS**, W. Mietelski, R. Kierepko, E. Łokas, E. Tomankiewicz, P. Zagrodzki, D. Borowicz, J. Jurkowski, M. Szałkowski, B. Wąs, B. Petelenz, E. Ochab, B. Kubica, R. Misiak, M. Stobiński, M. Bartyzel, K. Brudecki, K. Kleszcz, K. Szarłowicz, P. Janowski, A. Wójcik, M. Brożek, M. Miecznik

[409] **DEVELOPMNETS OF RADIOCHEMICAL METHODS FOR BASIC RESEARCH, MEDICINE, ENVIRONMENTAL STUDIES AND INVESTIGATION OF CONCENTRATION OF RADIOACTIVE ELEMENTS**, K. Kozak, J. Mazur, M. Janik, H. Hovhannisyan, D. Grządziel, M. Mroczek, T. Zdziarski,

[410] **LUMINESCENT DOSIMETRY IN MEASUREMENTS OF IONIZING RADIATION**, P. Bilski, B. Marczewska, P. Olko, I. Lipeńska, M. Puchalska, B. Obryk, M. Kłosowski, U. Sowa, M. Budzanowski, R. Kopeć, W. Gieszczyk, A. Twardak, A. Piaskowska, M. Sądel, A. Szumska

[411] **THIN FILMS, COATINGS AND NANOMATERIALS ENGINEERING**, M. Marszałek, M. Kąc, A. Kulińska, A. Dobrowolska, B. Rajchel, J. Jaworski, J. Kwiatkowska, K. Suchanek, Ż. Świątkowska-Warkocka, A. Zarzycki, M. Mitura-Nowak, S. Maranda, W. Kowalski, P. Strączek, A. Strzała, M. Krupiński, M. Kulij, Y. Zabila, A. Verbytska, A. Maksimenka, A. Grzymkowska, A. Karczmarska, M. Perzanowski

[412] **RADIOBIOLOGICAL ASPECTS OF ION RADIOTHERAPY/ THE USE OF PROTON BEAMS OF PROTEUS C235 CYCLOTRON FOR RESEARCH IN THE FIELD OF RADIATION PHYSICS, RADIOBIOLOGY AND PROTON RADIOTHERAPY (in 2013)**, M. Waligórski, P. Olko, J. Dąbrowska, D. Adamczyk, M. Korcyl, L. Grzanka, J. Gajewski, L. Malinowski, W. Męczyński

[413] **DEVELOPMENT AND CLINICAL APPLICATION OF PROTON EYE RADIOTHERAPY**, P. Olko, J. Swakoń, B. Michalec, T. Cywicka-Jakiel, T. Chorwacik, U. Sowa, T. Kajdrowicz, T. Nowak, M. Ptaszkiewicz, L. Stolarczyk, Ł. Góra, A. Czaderna, M. Liszka, M. Kłosowski, M. Boberek, G. Mierzwińska, I. Lipeńska

[501] **CONSTRUCTION OF DETECTORS AND RESEARCH INFRASTRUCTURE FOR PHYSICS EXPERIMENTS AND RELATED DISCIPLINES**, J. Adamek, M. Bednarski, J. Błocki(url.), D. Bocian, P. Borowiec, J. Chodak, J. Chorążak, B. Czech, B. Dąbrowski, M. Despet, M. Duda, A. Florek, B. Florek, W. Gaj, J. Garwoliński, J. Godlewski (url.), K. Grzybek, O. Grzymkowska, L. Hajduk, P. Jurkiewicz, J. Kantorski, D. Karolczyk, K. Kasprzak, E. Kielar, W. Kochański, L. Kolwicz-Chodak, A. Kotarba, J. Kotuła, A. Krawczyk, K. Krzysik, J. Ludwin, R. Łuszczak, W. Maciocha, A. Marendziak, J. Michałowski, K. Myalski, Sz. Myalski, S. Olek (url.), T. Ostrowicz, D. Partyła, B. Prochal, R. Pyzioł, M. Rachwalik, J. Rafalski, R. Romanow, A. Seweryn, M. Sienkiewicz, M. Skiba, P. Skóra, M. Sowiński, M. Stodulski, Z. Sułek, J. Szkutnik, I. Świerblewska, J. Świerblewski, H. Świerk, M. Tałach, W. Tałach, R. Tarczoń, M. Tier, P. Topolski, J. Wcisło, M. Wiencek, R. Wiertek, D. Wojas, T. Wojas, O. Woźnicka, J. Zbroja, P. Ziółkowski, A. Zwoźniak, P. Żychowski

[502] **MODERNIZATION AND ADAPTATION OF THE AIC-144 CYCLOTRON FOR THE EYE MELANOMAS TREATMENTS AND FOR PRODUCTION OF THE RADIOISOTOPES**, J. Sulikowski,K. Daniel, K. Guguła, G. Janik, A. Sroka, P. Bogdali, R. Cieślik, R. Grzybek,B. Lipka, A. Koczot, J. Molęda, H. Michałowski, T. Norys, W. Pyzioł, M. Ruszel, B. Sałach, R. Tarczoń, M. Sumera, L. Włodek

[503] **IMPLEMENTING OF MAGNETOHYDRODYNAMIC WATER TREATMENT (MWT) METHOD AND FILTRATION IN THE MAGNETIC FIELD METHOD**, M. Kopeć

[504] **RESEARCH AND DEVELOPEMENT OF ACCELERATORS AND ACOMPANYING TECHNIQUES (TIARA)**, P. Malecki

[505] **THE USE OF PROTON BEAMS OF PROTEUS C235 CYCLOTRON FOR RESEARCH IN THE FIELD OF RADIATION PHYSICS, RADIOBIOLOGY AND PROTON RADIOTHERAPY – cyklotron section (in 2013)**, K. Daniel, K. Guguła, G. Janik, A. Koczot, K. Suder, Ł. Kamiński, M. Matłaszek, T. Kajdrowicz, M. Bakoniak, R. Kos, A. Tekieli, D. Kędzierska, A. Kozera

[601] **COMPUTING DEVELOPMENT AND MAINTENANCE**, Z. Natkaniec, M. Kopaczewski, G. Pernach, W. Wajda, M. Wąsik, B. Żabiński, J. Wiertek, P. Wójcik, M. Gać, P. Dziewoński, P. Lechowicz

[602] **ORGANIZATION OF SCIENTIFIC CONFERENCES; POPULARIZATION OF SCIENCE**

[702] **INTERNATIONAL POST-GRADUADE STUDY COURSE**

II. UE PROGRAMS, CONSORTIA, NATIONAL NETWORKS

A. European Community Framework Programs

7. Framework Program (FP7)

I. Projects in which IFJ PAN was/is involved as a contractor:

[E1] Program: CAPACITIES – Research Infrastructures
Project: *"SPIRAL2 Preparatory Phase "* (**SP2PP**) Combination of CP & CSA (2007–2012);

Coordinator: GANIL, France

[E2] Program: CAPACITIES – Research Infrastructures
Project: *"Design of a pan-European Infrastructure for Large Apparatus studying Grand Unification and Neutrino Astrophysics"* (**LAGUNA**) CP Design Study (2008–2011);

Coordinator: Eidgenossische Technische Hochschule (ETH), Switzerland

[E3] Program: CAPACITIES – Research Infrastructures
Project: *"Design of a pan-European Infrastructure for Large Apparatus studying Grand Unification, Neutrino Astrophysics and Long Baseline Neutrino Oscillations"* (**LAGUNA-LBNO**) (2011-2014);

Coordinator: Eidgenössische Technische Hochschule Zürich, Switzerland

[E4] Program: COOPERATION – Space
Project: *"Human Model MATROSHKA for Radiation Exposure Determination of Astronauts"* (**HAMLET**) (2008–2011);

Coordinator: German Aerospace Center, Cologne, Germany

[E5] Program: COOPERATION – NMP
Project: *"Single Molecule Workstation"* (**SMW**) (2008–2011)

Coordinator: TILL I.D. GmbH, Germany

[E6] Program: PEOPLE – IRSES – International Research Staff Exchange Scheme
Project: *"Magnetic Resonance Methods Development and Applications for Life Sciences"* (**EuroCanMRI**) (2009–2012)

Coordinator: IFJ PAN, Poland

[E7] Program: CAPACITIES – Research Infrastructures
Project: *"European Coordination for Accelerator Research and Development"* (**EuCARD**) (2009–2013)

Coordinator: CERN, Switzerland

[E8] Program: CAPACITIES – Research Infrastructures
Project: *"Union of Light Ion Centers in Europe"* (**ULICE**) (2009–2013)

Coordinator: Fondazione Centro Nazionale di Adroterapia Oncologica (Fondazione CNAO), Italy

[E9] Program: CAPACITIES – Research Infrastructures
Project: *"European Nuclear Science and Applications Research"* (**ENSAR**) (2011–2014)

Coordinator: Management group based in GANIL, France

[E10] Program: CAPACITIES – Research Infrastructures
Project: *"Test Infrastructure and Accelerator Research Area"* (**TIARA**) (2011–2013)

Coordinator: CEA, France

[E11] Program: CAPACITIES – Research Infrastructures
Project: *"Advanced European Infrastructures for Detectors at Accelerators"* (**AIDA**) (2011–2015)

Coordinator: CERN, Switzerland

[E12] Program: Fusion for Energy (F4E) – European Union's Joint Undertaking for ITER and the Development of Fusion Energy F4E-FPA-327 (PMS-DG)
Project: *Diagnostics Design and Development of the Radial Neutron Camera (RNC) and Radial Gamma-Ray Spectrometer (RGRS) for ITER* (2013–2014)

II. Projects to which IFJ PAN contributes, but is not a signatory to the contract:

[E13] Program: PEOPLE – Marie Curie Initial Training Network
Project: *"Marie Curie Training Network on Particle Detectors"* (**MC-PAD**) (2008–2012);

Coordinator: CERN, Switzerland

[E14] Euratom Research and Training Program on Nuclear Energy
Association between the European Atomic Energy Community (**EURATOM**) *and the Institute of Plasma Physics and Laser Microfusion (IPPLM) in the field of nuclear energy with the priority thematic area fusion energy"* (2009–2013)

Polish Coordinator: IPPLM, Warsaw, Poland

[E15] Program: CAPACITIES – Research Infrastructures
Project: *"Integrated non-CO_2 Greenhouse Gas Observation System"* (**INGOS**) (2011–2015)

Coordinator: Stichting Energieonderzoek Centrum Nederland

[E16] Program: Coordination – ERA-NET
Project: *"Deepening and broadening of astroparticle physics European coordination"* (**ASPERA-2**) (2009–2012)

Polish Coordinator: The National Centre for Research and Development

[E17] Program: **NUPNET** – ERANET for nuclear physics infrastructures (2009–2012)

Polish Coordinator: The National Centre for Research and Development

[E18] Program: PEOPLE – Marie Curie Initial Training Network
Project: *"Advanced Particle Phenomenology in the LHC area"* (**LHCPhenoNet**) (2012–2014)

Coordinator: Agencia Estatal Consejo Superior de Investigaciones Cientificas

6. Framework Program (FP6)

I. Projects in which IFJ PAN was/is involved as a contractor

[E19] Program: Marie Curie Research Training Network
"Crust to Core: the Fate of Subducted Material" **(c2c)** (2007–2011)

Coordinator: Universität Bayreuth, Germany

II. Projects to which IFJ PAN contributed, but was not a signatory to the contract

[E20] Marie Curie Research Training Network RTN
"Polarized Helium Lung Imaging Network" **(PHeLINet)** (2007–2011)

Coordinator: Université Claude Bernard Lyon 1

B. Other international programs

[E21] Advanced Gamma Tracking Array for Nuclear Spectroscopy
Project: *"4π gamma tracking spectrometer"* **(AGATA)** (2005–2015)

[E22] Norwegian Financial Mechanism and the European Economic Area Financial Mechanism
Project *"Investigation of properties of a proton beam for radiotherapy of eye melanoma including treatment of pediatric patients"* (2008–2011)

[E23] Laboratoire européen associée (LEA) *"The Collaboration COPIN-GANIL on physics of exotic nuclei"* **COPIGAL** (2008–2011) and (2012–2015)

[E24] Collaboration IN2P3/CNRS, GANIL-SPIRAL2 (Caen), INFN, COPIN, IFN-HH (Bucharest)
Project: **FAZIA** – *"Four p A and Z Identification Array Demonstrator Phase"* (2011–2015)

[E25] Project: PARIS – „Proton Array for studies with RadioactiveIon and Stable beams" – (2006 – unlimited)

[E26] Program: Space Life Sciences and Space Science – ISS Combined Radiation Dosimetry Package inside Columbus module on ISS
Project: *"Dose Distribution inside ISS"* **(DOSIS)** (2008–2011)

Coordinator: German Aerospace Center, Cologne, Germany

[E27] European Science Foundation **ESF**
Program: Research Networking Programs in Physical and Engineering Sciences
Project: *"The New Physics of Compact Stars"* **(CompStar)** (2008–2013)

[E28] Forschungszentrum Julich GmbH, **COSY-111** (faze II); *Development of the PID method based on the dE/dx measurement for the Straw tube Tracker* (for PANDA experiment) (phase II) (2009–2012) and (phase III) (2012–2014)

[E29] European Cooperation in the Field of Scientific and Technological Research **COST** – MPNS Action MP 0601: *Short Wavelength Laboratory Sources* (2008–2011)

[E30] European Cooperation in the Field of Scientific and Technological Research **COST** – BMBS Action TD 1002: *European network on applications of Atomic Force Microscopy to NanoMedicine and Life Sciences* (2010–2014)

[E31] European Cooperation in the Field of Scientific and Technological Research **COST** – MPNS Action MP 0903: *Nanoalloys as advanced materials: from structure to properties and applications* (**NANOALLOY**) (2011–2014)

[E32] European Cooperation in the Field of Scientific and Technological Research **COST** – MPNS Action MP 1203: *Advanced Spatial and Temporal X-Ray Metrology* (2012–2014)

[E33] Program **NATO** Science For Peace And Security Programme; Collaborative Linkage Grant NATO CBP.NUKR.CLG 984305 *"Development of the thin-film and film-crystal combined scintillators based on the rare earth-doped silicates"* (2011–2013)

[E34] Agreement on cooperation in research on Fusion Energy Development – contribution to IPP Greifswald W7-X construction;
Task 1, 2 (2009–2012) *Staff delegation for the construction work*

[E35] Agreement on cooperation in research on Fusion Energy Development – contribution to IPP Greifswald W7-X construction
Task 3. *Manufacturing 30 polichromators*; (2009–2011)

[E36] Agreement on cooperation in research on Fusion Energy Development – contribution to IPP Greifswald W7-X construction
Task 4. *Development and manufacturing MSGC-detectors with read-out electronics for the W7-X C/O-Monitor diagnostics* (2011–2012)

[E37] Cooperation Agreement between DESY and IFJ PAN; Work Program for individual *subtasks for FLASH and XFEL* (2009–2012)

[E38] *In-kind contribution to the European XFEL Facility construction* (2010–2015)

[E39] Collaboration Agreement No. K 1598/AT
Quality Assurance Support during LHC Shutdowns; (QAS) (2009–2010)

[E40] Collaboration Agreement No. KE1818/TE/LHC
Participation of HNINP (IFJ PAN) in the consolidation of the Electrical Quality Assurance equipment of the LHC Machine (2011-2012)

[E41] Collaboration Agreement No. KE1884/TE
Collaboration in the field or re-organization of the documentation of the magnet system of the SPS complex and its experimental areas at CERN (2011–2014)

[E42] Collaboration Agreement No. KE2058, No. KE2059, No. KE2060,
Participation of HNINP (IFJ PAN) in the Electrical Quality Assurance during Long Shutdown 1 of the LHC (2013–2014)

[E43] Collaboration Agreement No. KE2061,
Participation of HNINP (IFJ PAN) in the Vacuum Quality Assurance for the Consolidation of the LHC superconducting splices during 1st Long Shutdown of the LHC (2013–2014)

[E44] MoC-CERN-CLIC-2013: *Memorandum on Cooperation for the CLIC Detector and Physics Study* (2013–...)

[E45] Polish-Swiss Research Programme project: *Ion mobility in lightweight compounds for energy storage* (2011–2014)

[E46] IAEA project: *Retrospective biological dosimetry at low and high dose of radiation and radioiodine impact on individual susceptibility and health risk* (2012–2013)

[E47] ZIBJ Dubna Project: *Modernization and preparation of the AIC-144 cyclotron for medical applications (hadron radiotherapy)* (2010–2012) and (2013–2015)

[E48] ZIBJ Dubna Project: *Project and construction of systems for optimization of performance LAR cyclotron at ZIBJ and AIC-144 cyclotron at IFJ PAN* (2010–2012)

[E49] ZIBJ Dubna Project: *Neutron study of the solid state structure and dynamics(2009–2014)*

[E50] ZIBJ Dubna Project: *Manufacturing of the semicondutor detectors* (2010–2012)

[E51] ZIBJ Dubna Project: *Construction of the joint Krakow-Dubna detector cluster for high energy gamma-ray detection based on the novel LaBr3 scintillators - an apparatus for studies of exotic nuclei* (2010–2014)

[E52] ZIBJ Dubna Project: *Zero degree spectrometer for ACCULINNA-2* (2013–2015)

[E53] ZIBJ Dubna Project: *Experimental studies at the U400M cyclotron beams in collaboration between Polish Institutes and JINR* (2013–2015)

[E54] International Visegrad Fund Project: *Harmonization of determining the radiation dose of the population originating from radon, in V4 countries* (2012)

C. Consortia

International consortia

The Institute is a partner in international consortia connected with our participation in the EU Framework Program projects and international projects listed above.

We also participate in two other international consortia:

[K1] ACC – XFEL Accelerator Construction Consortium- 2010–2015 In-kind contributions

[K2] BELSWENI-ILL – Collaboration of Belgian, Swedish and Polish scientists in the field of neutron scattering at the High Flux Reactor in Grenoble

The Institute participates in 29 national scientific consortia

Ten of them are coordinated by IFJ PAN:

[K3] National Consortium for Hadron Radiotherapy

[K4] COPIN – National Consortium for the scientific collaboration with France IN2P3 Institutes

[K5] ILLPL – Consortium of Polish scientific and educational establishments – carrying out research with the use of neutron beams and instrumentation of Institute Laue-Langevin, Grenoble

[K6] PAN-AKCENT – National Consortium of the Institutes of Polish Academy of Sciences

[K7] National Consortium of the radioactive isotopes innovative applications

[K8] IONMED – Cracow Research Center for Ion Engineering

[K9] National Consortium "Research and development in the field of technology for nuclear controlled fusion"

[K10] SuperB-PL – National Consortium for SuperB Collaboration

[K11] ALICE-PL – National Consortium for ALICE Experiment at the LHC at CERN

[K12] LHCb-PL – National Consortium for LHCb Experiment at the LHC at CERN

Other Consortia:

[K13] Atomic Center „CeAt"

[K14] Consortium of Advanced Technologies for Natural Resources, Hydrocarbons and Renewable Energy SUPERGO

[K15] IZATEM – Interdisciplinary Center for Advanced Medical Technologies

[K16] IOITOB Interdisciplinary Center for Innovative Techniques of Biomedical Imaging

[K17] National Consortium "FEMTOFIZYKA" (PhemtoPhysics)

[K18] National Consortium "XFEL-POLSKA"

[K19] National Consortium "Polski Synchrotron" (Polish Synchrotron)

[K20] National Consortium for HESS Experiment

[K21] National Cyclotron Laboratory (NLC)

[K22] National Consortium "Cherenkov Telescope Array"

[K23] Joint Laboratory for Isotope Geochemistry

[K24] National Consortium "Neutrina – ICARUS T600"

[K25] National Consortium "Neutrina – T2K"

[K26] National Consortium "PL-STAR"

[K27] Marian Smoluchowski Cracow Consortium: "Materia – Energia – Przyszłość" (Matter – – Energy – Future)

[K28] National Consortium ISOTTA (ISOTope Trace Analysis)

[K29] Polish Consortium „QUEST" for the research project "Study of quantum spin correlations of relativistic electron pairs" financed by the National Science Centre (NCN) – collaboration with Technische Universität Darmstadt

[K30] Consortium Polish Particie Physics

[K31] National Consortium NMR-Rocks for the research project Development of innovative NMR methods and their applications to evaluation of petrophysical properties of oil-rich rocks in Poland" financed by the National Centre for Research and Development (NCBiR).

D. Thematic Networks

International Networks

[S1] AIRCLIM-NET – International Thematic Scientific Network for Problems of Air Pollution and Climate Change

[S2] HadroNet – Central European Network on Hadrontherapy Technology

[S3] ENLIGHT – The European Network for LIGht ion Hadron Therapy

[S4] Non-Governmental International Scientific Network – The Radon Center

[S5] ASPERA 2 ERA-NET: AugerNext and ISOTTA

[S6] NuPNET Era-NET – GANAS – GAmma detection with New Advanced Scintillators

The Institute carries out research within 23 Thematic National Networks

Five of them are coordinated by IFJ PAN:

[S7] POLTIER – National Consortium of Scientific Network "Polish calculation system for experiments at LHC"

[S8] Polish Network "Neutrons-Emission-Detection"

[S9] Polish Network of Nuclear Methods for Geophysics

[S10] Polish Network of Radiation Protection and Nuclear Safety

[S11] MatFun – National Centre for synthesis and characterization of functional materials

Other Networks:

[S12] BIONAN – Molecular mechanisms of interactions in biological nano-systems and in biologically active systems modified by nano-compounds

[S13] Pharmacological and Genetical Protection and Cytoprotection in Pathologies of Central Nervous System

[S14] FiTAL – Polish Network for Physics and Technology of High Energy Linear Accelerators

[S15] Physics and Chemistry for Medicine

[S16] Cracow Center of Physico-Chemical Research for the Environment Protection

[S17] National Scientific and Educational Network of Radiochemical Laboratories

[S18] LUMDET – Scientific Network for Luminescence Detection of Ionizing Radiation

[S19] MANAR – New Layered Materials with Controlled Architecture and Functionality (until 2012)

[S20] Well logging Geophysics – Numerical Modeling and Comprehensive Interpretation (until 2011)

[S21] NanoMedPL Research Network – Modern applications in nano-medicine and nano-technology

[S22] Polish Network for Astroparticle Physics

[S23] Polish Network of Flavor Physics

[S24] Polish Neutrino Network

[S25] Polish Network of the Project "Cherenkov Telescope Array"

[S26] Research Network "Physics of Relativistic Ions"

[S27] Polish Nuclear Physics Network

[S28] Polish Network for the strategic research project "Technologies supporting the development of safe nuclear power" financed by the National Centre for Research and Development (NCBiR). Research Task 6 "Development of methods to assure nuclear safety and radiation protection for current and future needs of nuclear power plants".